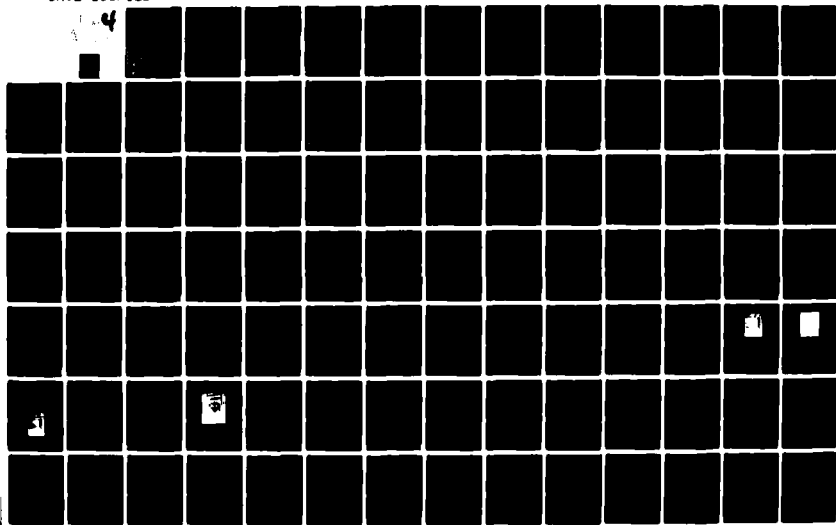


AD-A098 167

HUGHES AIRCRAFT CO CULVER CITY CA ELECTRO-OPTICAL AN--ETC F/G 9/5
MANUFACTURING METHODS AND TECHNOLOGY FOR ELECTROMAGNETIC COMPON--ETC(U)
DEC 80 E R BUNKER, J R ARNETT, J L WILLIAMS DAAK40-78-C-0271
FR-80-76-1254R-VOL-1 NL

UNCLASSIFIED



AD A 098 I 67

LEVEL *4*

2
B.S.

REPORT NO. FR-80-76-1254R
HAC REF. NO. D8712

DTIC
APR 24 1981
C

PROJECT NO. R-783372
(Contract DAAK40-78-C-0271)

VOLUME I

MANUFACTURING METHODS AND TECHNOLOGY FOR ELECTROMAGNETIC COMPONENTS

PHASE I

Prepared for: U.S. Army Missile Command
Redstone Arsenal, AL 35809

AEROSPACE GROUPS

HUGHES

HUGHES AIRCRAFT COMPANY
CULVER CITY, CALIFORNIA

DTIC FILE COPY

DISTRIBUTION STATEMENT 1
Approved for public release;
Distribution Unlimited

S/C
409084

81 4 24 040

DISPOSITION INSTRUCTIONS

**DESTROY THIS REPORT WHEN IT IS NO LONGER NEEDED. DO NOT
RETURN IT TO THE ORIGINATOR.**

DISCLAIMER

**THE FINDINGS IN THIS REPORT ARE NOT TO BE CONSTRUED AS AN
OFFICIAL DEPARTMENT OF THE ARMY POSITION UNLESS SO DESIGNATED
BY OTHER AUTHORIZED DOCUMENTS.**

TRADE NAMES

**USE OF TRADE NAMES OR MANUFACTURERS IN THIS REPORT DOES
NOT CONSTITUTE AN OFFICIAL ENDORSEMENT OR APPROVAL OF
THE USE OF SUCH COMMERCIAL HARDWARE OR SOFTWARE.**

HUGHES

HUGHES AIRCRAFT COMPANY

AEROSPACE GROUPS
CULVER CITY, CA 90230

In Reply Refer To:
81-76-06990/D8712

22 April 1981


SUBJECT: Distribution of the Final Report for Contract
DAAK40-78-C-0271, Manufacturing Methods and
Technology for Electromagnetic Components

TO : Defense Documentation Center
Camerson Station
Alexandria, Virginia 22314

1. Enclosed is your copy of the 2-volume report on "Manufacturing Methods and Technology for Electromagnetic Components" which covers in greater detail the information presented at the Government Industry debriefing held 28 October 1980 at Hughes, Culver City. The purpose of this meeting was to give an overview of the information assembled during this two-year program, note the major findings, point out possible breakthroughs in reliability improvement, and review possible new technologies. The hope was expressed that recipients would delve into this final report, with the intent of implementing appropriate technologies into their operations to obtain higher reliability, lower cost electromagnetic components for missile systems, space projects, and commercial applications. If done effectively, it is believed that a quantum jump in the reliability of these components would be forthcoming, which would benefit all concerned.

2. Questions of a technical nature should be directed to Mr. E. R. Bunker at the above letterhead address, Building 12, Mail Station V128. Contractual questions should be addressed to the undersigned at the above letterhead address, Building 6, Mail Station C137. They may be reached at Area Code 213-391-0711, Extension 4954 or 7075 respectively.

HUGHES AIRCRAFT COMPANY


J. E. Neff
Manager, Contracts
Technology Support Division

JEN:mfh
Enclosure: As Noted

19. Continued

Core banding
 Fine magnet wire joining
 Magnet wire stripping
 Transformer molding

Silicone molds
 Liquid injection molding (LIM)
 Wire insulation damage detector

20. Continued

Over 40 encapsulation thermo setting compounds for high reliability components were tested and evaluated. Two compounds were selected, one optimum for low stress applications, the other for high voltage, corona free applications. Cure times are main limitation of production rates, pointing up a need for faster cure time materials of at least an order of magnitude.

Winding techniques included establishing parameters for damage of fine wire windings on square bobbins, and a method of continuously monitoring insulation integrity of magnet wire during winding operations for both toroid, and bobbin/stick winders. Use of spot bonding instead of mylar tape to hold windings in place during the winding operation was developed to eliminate voids caused by the tape during encapsulation/potting.

Using a centrifuge for 5 to 10 minutes to remove bubbles from a poured transformer, then curing at room pressure showed promise over the conventional pressure cure at 500 psi for the required cure time and temperature.

High voltage gradient estimation and control to achieve corona-free encapsulation was investigated. Various methods of establishing conductive surfaces for faraday shielding of molded bobbins were evaluated. Molds for casting void free bobbins were made. Various methods of terminating fine (AWG 36-44) and ultra fine (AWG 45-56) wire in coils to intermediate AWG 36 leads were investigated, including soldering with conventional tin-lead, and tin free solders, laser welding, crimping, conductive adhesives, etc.

A method of discharge welding of "C" core bands under tension, without clips, to achieve a low profile, and eliminate solder creepage was demonstrated.

Accession for		<input checked="checked" type="checkbox"/>
NTIS GRI&I		<input type="checkbox"/>
DTIC TAB		<input type="checkbox"/>
Unannounced		
Justification		
By		
Distribution/		
Availability Codes		
Avail and/or		
Selling		
Dist		
A		

Report No. FR-80-76-1254R
HAC Ref. No. D8712

(6) MANUFACTURING METHODS AND TECHNOLOGY
FOR ELECTROMAGNETIC COMPONENTS.

VOLUME I.

PHASE I.

(11) December 1980

(11) E. R. Bunker, Program Manager
J. R. Arnett, Principal Investigator
J. L. Williams, Principal Investigator

Electro-Optical and Data Systems Division
AEROSPACE GROUPS
Hughes Aircraft Company • Culver City, California

FOREWORD

This is Volume I of a two-volume set covering the work done October 1978 - October 1979 in investigating, evaluating and implementing techniques for the manufacture of low cost, high reliability magnetic components for missile system applications. The Executive Summary, conclusions and recommendations, and the work statement are in this volume, but cover both volumes. Each volume has its own table of contents, list of illustrations and tables, references, and appendices. In addition, Volume II has cost data estimates and implementation efforts to date.

EXECUTIVE SUMMARY

The purpose of the present MM&T program is to investigate, evaluate, and implement techniques for the manufacture of low cost, highly reliable electromagnetic components for missile systems applications. The emphasis is on "implement", through a continuing program to rapidly disseminate this information to electromagnetic component manufacturers with the purpose of assisting them to produce lower cost, more reliable products. The Phase I of this program, reported in this document and designated as Volume I, was concerned with two tasks: improving the manufacturing methods of potting/encapsulation, and investigating the winding techniques of electromagnetic devices. The three remaining tasks, Phase II, reported in Volume II, were: interconnection techniques, tooling, and structural parts. It is anticipated that the combined results of these five tasks will implement improved manufacturing methods for electromagnetic components so that a significant payback in manufacture and life cycle costs of present and future missile systems, due to lower production costs, higher process yield, and improved reliability will be obtained.

METHODS OF POTTING/ENCAPSULATION

An in-depth investigation of over 40 encapsulation compounds was made to identify those which would have the optimum parameters for encapsulation or potting of electromagnetic components for missile applications. Proposed values of 36 parameters were established, against which each compound was evaluated. In many cases data was not available from the vendor, so tests were made to obtain the required information to facilitate comparison. One of the most critical parameters is the glass transition

temperature of the resin, below which many materials exhibit a rapidly rising compressive stress. Such stresses applied to strain sensitive cores during temperature cycling can adversely affect the functional response of magnetic components. A direct measurement of these stresses, ranging as high as 6000 psi at -40°C , was made using pressure calibrated mercurial thermometers. A two-step process, using a soft material first to cushion the core from the stresses generated by the final material, was investigated. This method showed some reduction, but was not comparable to the low stress materials evaluated.

As would be expected, no one resin was a universally ideal encapsulation material. Trade-offs of parameters and properties are required for each application. The five materials which were judged to have the most acceptable combination of parameters, including compressive stresses of less than 200 psi at the lowest temperatures, were: Epon 825 with HV hardener; Scotchcast 255; Eccoseal 1218; Hysol C-60 and Hysol C15-015. As an example of the trade-offs only, the Epon 825/HV was corona-free during high voltage tests; the other four had varying degrees of corona present. On the other hand, for low voltage applications under 250 V peak, some of the others had more optimum parameters. The information reported in this section would assist the designer in making the proper selection of encapsulating material for a high reliability magnetics application, and also help the manufacturer in setting up the proper processing and handling procedures to produce a cost effective, reliable part.

CONTROLLED WINDING TECHNIQUES

This task addressed four areas: wire handling, contamination, solenoid and transformer coil (bobbin) winding, and toroidal coil winding. The obvious observation that, in order to produce a reliable component, the materials being used must be of highest quality, is doubly true for the wire used in winding electromagnetic components. The wire handling and contamination investigation concluded that spools of wire, especially the fine and ultra-fine gauges, should be encased at all times in foam plastic protective enclosures, and inserted into plastic bags, except when wire is being removed at the winding station. The smaller sizes of wire are especially

susceptible to damage from dropping which damages the spool, objects striking the wire, interfering with the unwinding process. Exposure of the unprotected spool to contaminants of any kind, either airborne or liquid splashes, or handling without gloves will degrade the encapsulation process. Yet it was interesting to note that no such precautions were taken in any facility that was visited. In most cases the spools of wire were stacked in open stockroom areas without any protection whatever.

An analysis of the tension factors involved in winding many layers of ultra-fine wire on square bobbins, followed by fabrication of actual coils using normally accepted tension figures, revealed a cumulative wire and insulation deformation effect which apparently has not been reported in the literature. Using accepted tension levels of the industry which are calculated to stress the ultra-fine wire well under its elastic limit, a buildup of internal radial pressure (IRP) at the corners of the bobbin was sufficient to compress the insulation tightly together, eliminating all voids; also, plastic deformation and flow of the copper occurred. Slippage or cleavage planes of groups of conductors through the winding was also seen in sectioned coils. The analysis showed that the factors involved were the winding tension, wire diameter, number of layers, and initial radius of curvature of the corners of the bobbin. Tensions less than 42 percent of rated were required to prevent this damage. Rounding the corners of the bobbin sufficiently will reduce the IRP and achieve a damage-free winding. No problem exists if a round bobbin is used at standard winding tensions.

A hidden source of wire damage was also uncovered in the toroidal winding investigation. Realizing that a certain amount of skill is required of winding personnel in positioning the toroid so that the shuttle does not scrape the insulation from the windings already on the toroid, a method of detecting this possible damage was proposed. An alarm circuit was developed which would detect a momentary electrical contact between the shuttle and the wire it carried. For high reliability components it is proposed that tripping of the alarm during winding would be cause for rejection, thus saving the cost of further manufacturing a defective part.

An additional benefit of the device was found to be a continuous monitoring of wire insulation integrity, not before possible. Conventional QA acceptance of fine wire is to take a few feet off the end of the spool and perform the requisite tests, assuming that this is representative of wire quality throughout the spool, which may or may not be true. During the development of the circuit, while winding toroids, the alarm was tripped several times with no obvious contact of the shuttle and the windings. Since the wire being used was from an old spool, it was scrapped and a new spool substituted; the problem went away. When the cause was finally pinpointed as probably due to defective wire, it has been discarded so was not available for confirmation.

When toroidal windings were being made for the MM&T program, another anomaly was encountered, in that the alarm would trip randomly. Since this time the wire insulation quality was nominal, the cause was traced to the shuttle ring itself. The split in the shuttle ring which accommodates the toroidal core was found to scuff the insulation of the fine wire during the loading and subsequent winding operation to the extent that not only was the insulation penetrated, but sometimes a notch was made in the copper itself. A small piece of tape placed across the split prior to loading of wire corrected the problem, which apparently is not done in usual practice or required in general winding specifications.

From the above it is concluded that such a monitoring device used on all toroidal winders would improve the reliability and reduce costs by early detection of damage and localization of problems for all sizes of wire.

In conjunction with the bobbin and toroidal winding investigations, a study of the various methods of wire tension control was made. Such devices have been in use for many years, with no new approaches found applicable to fine wire. Also included is a suggested check list for setting up a toroidal winder for fine wire winding.

INTERCONNECTION TECHNIQUES

Five different areas were covered in this task, namely, stripping of wire insulation; techniques for joining ultra fine coil wires to intermediate lead wires; size requirements for intermediate leads; techniques for terminating ultra fine wire; radii of connections as a function of operating voltage including methods of making low cost, reliable connections in high voltage components.

A survey of the various methods to remove magnet wire insulation, which included heat, abrasive, laser, and chemical, was made and compared. No clear cut method of insulation removal was found that did not have significant disadvantages.

A method investigated, which appeared very promising at first, was the removal of the insulation by a stream of abrasive particles propelled by a small air blast, which removed insulation readily, including the high temperature ML materials. Initial tests, run on large wire sizes, showed an effective removal of insulation without eroding the copper conductor itself. Nozzles were designed to impinge fine wire on all sides so that it would not have to be rotated to completely remove the insulation; however, adverse effects on solderability and mechanical properties caused further work to be discontinued.

Various techniques for connecting fine and ultra fine magnet wires to intermediate lead wires were investigated. As a general rule, wire sizes smaller than AWG 36 should not be routed through encapsulation materials for any great distances, because the thermal expansion of the material can cause breakage. The normal procedure is that after winding a fine wire or ultra fine wire coil, the insulation is removed and an intermediate lead wire soldered in or otherwise connected and the resulting joint taped down on the winding. The intermediate wire then goes to the terminals to connect to the outside world.

Since tin-lead solders are capable of dissolving fine copper wire during the soldering operation, other solder formulations were investigated. Also other methods of achieving a low resistance joint was investigated, such as welding, laser welding, crimping, and the use of conductive adhesive materials. The conclusion was that careful control of all soldering

parameters, including soldering temperature, time, and size of the iron, would allow joints to be made with fine wire without significant dissolution, using conventional tin-lead solders.

During encapsulation of high voltage transformer windings, extensive care is taken to prevent the occurrence of voids, which are a source of corona, causing progressive degradation of the insulation material. It is also considered imperative to eliminate any sharp points which may occur in the high voltage gradient regions. What has not been appreciated previously, is that a sharp point in the high voltage winding can have a high enough voltage gradient to actually create voids in insulation where none originally existed. Once this void is created, the insulation begins to fail progressively, forming "trees." It was found that using diagonal cutters or scissors in cutting fine wire, the resultant sharpness of the cut increases the voltage gradient into the region where voids can be generated with only a moderate amount of high voltage applied to the winding. Caution must be especially taken in the termination of fine wire to the intermediate lead wire interface. A method of solder balling or putting a conductive sphere over the joint to control the gradient was investigated.

TOOLING AND EQUIPMENT FOR ENCAPSULATION

This task addressed three areas: evaluate equipment and tooling to encapsulate devices with the processes developed in the basic program; determine the feasibility of automatic mixing and metering equipment; implement a continuous process for potting and encapsulation. A multiwinding high voltage toroid with some windings using fine wire, and a high voltage biased, two-coil inductor with a C-core were selected from missile programs as being typical components. Depending on the quantities involved, various molding systems were investigated, ranging from low production of a few hundred per month to high production of ten thousand or more per month. A major constraint in the design of the molds was that it was to minimize hand labor in the finishing, and that the mold was to provide the outer surface of the component, as potting cups or covers were to be used. With the small and medium production runs, slush-type molds of low melting temperature metals, which could be melted down and recast, and silicone

rubber molds, were developed. The normal cure process requires these molds to be placed in a pressure vessel and held at 500 psi for 16 hours to eliminate voids. The silicone rubber molds allowed the substitution of a 5 to 10 minute centrifuging immediately after pouring to displace the bubbles, then cure in a simple temperature chamber instead of a pressure chamber for 16 hours. Another approach involved the use of aluminum molds of simple construction which would allow the encapsulation material to be introduced under vacuum, then pressurized at 500 psi and then the mold would be disconnected and placed into the temperature chamber. Each mold was its own pressure vessel. For high production rates using technology in other industries, a liquid injection mold (LIM) process was investigated for both the dual coil conductor and the toroid. Acceptable parts with a minimum of hand labor, very consistent in quality, were obtained, but the production rate was limited by the long cure time of the Epon-825/HV hardener used. A material with a faster cure time, meeting all of the other parameters required, would greatly enhance this method of encapsulation.

Automatic mixing and metering equipments were investigated and typical equipment obtained to evaluate operation in low-to-medium production operations. This would substitute for the hand labor usually used in mixing up batches of encapsulation material prior to pouring. The equipment evaluated allowed the resin and hardener to be maintained under vacuum, introduced into the mold through a mixer which caused mixing to take place at the point of entry. Temperature blankets allowed the materials to be maintained at a high temperature to facilitate pouring by reducing the viscosity.

STRUCTURAL PARTS

This task investigated four areas as follows: shielded bobbins for high voltage transformers; thermoplastic and thermosetting plastics for coil supports; anchoring of windings within transformer coils; and C-core assembly techniques. The use of fine and ultra fine wires in high voltage windings increases the maximum voltage gradients in the encapsulation materials. Controlling the spacings of such wires which have high voltage differences is difficult, consequently, the use of electrostatic conductive

shields is employed in the construction of the bobbin. A typical high voltage bobbin will have a low potential or ground electrostatic shield on the outer surfaces with an insulated, but also conductive, shield on the inner surfaces where the high voltage winding is located. In this manner, location of the separate wires is not critical in controlling the voltage gradients being developed.

In high reliability transformer design, thermoplastic materials are rarely used because of their tendency to soften at the higher temperatures to which the component is subjected, either during testing or actual operation. Some of the newer, high temperature thermoplastic materials, such as Ryton, which has a softening point in excess of 525⁰F, were evaluated. Typical square bobbins of this material were obtained and windings made. Another requirement in the specification was that no softening of such thermoplastic material would occur when the terminals swaged in it would be soldered to. This was not found to be possible as the softening could not be prevented by any acceptable soldering technique. The problem could be eliminated by a pulse type welding, but this seemed to add additional complications which overshadowed any advantages of using thermoplastic materials.

It is accepted practice to use small pieces of mylar tape to anchor windings at the end of each layer or at various stages during the winding operation. The presence of such tapes in a winding provides stress points in the encapsulation which can cause it to crack under thermal cycling, the possibility of entrapment of air producing voids at critical parts in the winding, and a lack of adhesion of the encapsulation material to the tape itself. To provide an acceptable method of anchoring windings without using tape, several quick-setting, adhesive materials were investigated. These included hot-melt, ultraviolet curing and anerobic types. It was found that these provided an acceptable substitute for the tape when the operator became used to the technique.

Conventional banding operations of C-cores assembled into windings on bobbins or sticks, which have been encapsulated prior, uses a metal clip and a soldering operation to anchor the band. By means of welding an auxiliary pull tab on the band, a method of welding was developed which required no clip and no soldering operation. The pull tab and excess band lengths are

then cut off after welding resulting in a low profile of only twice the thickness of the banding strap material.

IMPLEMENTATION

Part of the implementation effort at the end of Option 1 was the holding of a government/industry debriefing on 28 October 1980 at Hughes-Culver City. The purpose of this meeting was to give to all attendees an overview of the information assembled during this 2-year MM&T program; note the major findings, point out possible breakthroughs in reliability improvement, and review new technologies. It was hoped that this presentation would encourage those attending to delve into this final report for the complete story. Becoming acquainted with this information would allow them to take back to their organizations, hopefully with the intent of implementing appropriate portions of this technology into their operations so that higher reliability, lower cost electromagnetic components for missile systems, space projects, and commercial applications would be forthcoming in the immediate future. If this is done effectively a quantum jump in component reliability and cost reduction would be obtained which would be beneficial to all concerned.

A summary of the conclusions and recommendations given in both volumes is given below:

TASK 1 - POTTING/ENCAPSULATION TECHNIQUES

- a) There is no universally ideal encapsulation material. Trade-offs of parameters and properties are required for each application.
- b) A standard set of test conditions to obtain the required data for new resins should be established to allow comparison with existing materials for high reliability applications, especially for determination of electrical properties. Mechanical and thermal properties are covered fairly well by ASTM procedures.
- c) A major source of failure in encapsulated magnetic components wound with fine wire is breakage of the leads between the coil and the terminals caused by thermal expansion of the resin. Intermediate leads of AWG 36, or larger, should always be used.
- d) Pressure sensitive magnetic cores and other fragile electronic components require low stress potting/encapsulation techniques and materials. Quantitative measurements of stress as a function of temperature are needed to properly evaluate a material.

- e) A method of hydrostatically stressing small magnetic components to 10,000 psi was developed. Ferrites, MPP, and tape wound cores were exposed to this pressure level, with surprisingly small effects. Subsequent tests showed that unbalanced rather than isotropic stresses altered significantly the magnetic properties.
- f) Conap EN-9, Conap EN-9-OZR, Uralane 5753, RTV 615, RTV 619, RTV 627, and RTV 655 showed less than 200 psi at -40°F, with no apparent glass transition temperature reached.
- g) The use of a high stress material over a low stress encapsulant to reduce the overall stress generated was partially successful, but was far from the 200 psi arbitrary limit selected as acceptable.
- h) For high voltage applications, Epon 825/HV was the only material that showed zero corona level. Scotchcast 255 and Eccoseal 1218 had high corona levels at the same applied voltage, although their dielectric strength was sufficient to prevent short-term breakdown.

TASK 2 - WINDING TECHNIQUES

- a) All spools of magnet wire intended for high reliability magnetics should be stored and transported with rigid foam plastic covers, in turn covered with a plastic bag to prevent mechanical damage and contamination.
- b) Shuttle type toroidal winders should be modified to allow the use of an electrical short detector between the shuttle ring and the wire being wound on the toroidal core. This serves the dual purpose of detecting insulation damage during winding or faulty insulation on the wire itself.
- c) The short detector can also be used to monitor insulation integrity during winding of bobbins or sticks on manual or automatic machines, if an electrical connection can be made to the wire end on the wire spool.
- d) For high reliability applications, the usual QA procedures of approving a spool of fine wire by inspection and analysis of a few feet from the beginning is not considered adequate.
- e) Insulation and even conductor deformation may occur when fine wire is wound at rated tension on square bobbins due to stress build-up at the corners.

TASK 3 - INTERCONNECTION TECHNIQUES

- a) Investigation of wire stripping technique shows that no method of insulation removal from magnet wire, especially in the fine ultrafine gauges, has a clearcut advantage over the others, especially for high temperature polyimide (ML) materials.
- b) Insulation removal with the CO₂ laser showed promise with the larger wire sizes, but further work is required for application to fine wire gauges in a production environment.
- c) Removal of insulation by abrasive particles driven by an air blast was effective for the larger wire sizes, but further work needs to be done in nozzle design and abrasive materials to obtain a clean, solderable surface.
- d) Wire sizes smaller than AWG 36 should be joined to intermediate leads AWG 36 or larger, then taped or anchored to the winding, so that the intermediate lead interfaces with terminals for connection to the outside world.
- e) Careful control of soldering parameters using conventional tin-lead solder produced the most reliable joints between copper intermediate leads and fine wire gauges, when compared with all other methods of joining.
- f) Reduction of voltage gradients in encapsulation compounds by conductor placement, solder balling, conductive shields, radii selection, and interface geometries will reduce possibility of long-term degradation of insulation integrity in high voltage components.

TASK 4 - TOOLING AND EQUIPMENT FOR ENCAPSULATION AND POTTING OF ELECTROMAGNETIC DEVICES

- a) Individual molds, designed as a pressure vessel up to 500 psi, can accommodate both pouring in vacuum and cure of encapsulant under pressure for low production quantities.
- b) Slush molds and molds fabricated from RTV silicone rubber can be used for low production quantity if they are poured in a vacuum chamber and cured in a pressure vessel at 500 psi.
- c) As an alternative to the pressure vessel, the silicone molds, after pouring in vacuum, may be centrifuged for 5 to 10 minutes to remove the trapped air, then cured in an oven.
- d) Use of the centrifuge, instead of the pressure chamber, appeared to obtain an equally void free encapsulation of low voltage components; the CIV for high voltage components was higher for the pressure cured samples than the centrifuged ones.
- e) Various sizes of automatic mixing equipment, which automatically mix the resin and hardener on demand, are available to accommodate any production rate.

- f) Liquid injection molding (LIM) techniques show promise for large production quantities with proper mold design and selection of materials.
- g) Decreases in the cure time or "green strength" time of present encapsulation materials, when the encapsulated component may be removed from the mold for a post-cure, will increase the production rate and decrease the cost correspondingly.

TASK 5 - STRUCTURAL PARTS

- a) Electrostatic shields sprayed on bobbin surfaces after molding enable better process control with less problems than integral shields positioned in the mold cavity prior to molding.
- b) A high resistance coating for bobbin shields can be employed without requiring a gap, which is necessary for low resistance materials because of the shorted turn effect.
- c) High temperature thermoplastic bobbin materials were not considered acceptable for high rel components because of brittleness, and softening of the region around the swaged or bonded terminals during soldering.
- d) Anchoring of wires during winding operations with quick-set adhesive rather than mylar tape facilitates void free encapsulation.
- e) Welding rather than soldering straps during C-core banding operations eliminates solder creep problems.

VOLUME I

CONTENTS

1.0	INTRODUCTION	1-1
2.0	STATEMENT OF WORK	2-1
3.0	EVALUATION OF POTTING AND ENCAPSULATION MATERIALS AND TECHNIQUES	3-1
3.1	Vendor Data Survey	3-2
3.2	Outgassing Data	3-17
3.3	Process Evaluation	3-19
3.3.1	Viscosity Determination of Selected Materials	3-21
3.3.2	Process Evaluation of Low Stress Embedment Materials	3-23
3.4	Low Stress Embedment Techniques and Materials	3-24
3.4.1	Fine Wire Assembly Techniques	3-25
3.4.2	Selection of Materials	3-26
3.4.3	Relative Material Costs	3-27
3.4.4	Test of Materials	3-27
3.4.5	Embedment Pressure Measurement Investigation	3-44
3.5	Electrical and Environmental Testing of Hi-Rel Candidate Materials	3-66
3.5.1	Hydrolytic Stability Testing	3-75
3.5.2	Electrical and Mechanical Testing of Saturable Reactors Encapsulated with Hi-Rel Candidate Materials	3-80
3.5.3	High Voltage Transformer Model Testing	3-102
3.5.4	High Voltage Transformer Results and Conclusion	3-117

CONTENTS (Continued)

4.0	CONTROLLED WINDING TECHNIQUES	4-1
4.1	Wire Handling	4-1
4.1.1	Spool Packaging Styles	4-1
4.1.2	Wire Damage Modes	4-1
4.1.3	Evaluation and Recommendations	4-2
4.2	Contamination	4-5
4.2.1	Cleanliness of "As Received" Wire	4-6
4.2.2	Effects of Solvents	4-10
4.2.3	Effects of Humidity	4-14
4.2.4	Effects of Salt Spray	4-14
4.2.5	Outgassing	4-16
4.2.6	Effect of Hydrochloric Acid Vapor	4-19
4.2.7	Effects of Sulfuric Acid Vapor	4-21
4.2.8	Effect of Vibration	4-21
4.2.9	Conclusions	4-23
4.3	Solenoid and Transformer Coil Winding	4-24
4.3.1	Winding Machine Set-up	4-24
4.3.2	Coil Design and Winding Tension	4-25
4.4	Toroidal Coil Winding	4-33
4.4.1	Wire Size and Controlled Winding Techniques	4-33
4.4.2	Winding Machine Set-up	4-38
4.4.3	Winding	4-39
4.4.4	Multi-Filar Wire Winding	4-41
4.4.5	Dynamic Measurement of Wire Damage	4-43
4.4.6	Recommendations	4-50
4.5	Installation of Insulation Damage Detector on Coil Winders	4-53
4.5.1	Toroidal Winder Modification	4-55
4.5.2	Bobbin Winder Modification	4-55

CONTENTS (Continued)

5.0	REFERENCES	5-1
6.0	APPENDICES	6-1
Appendix 6.1	Paper: Wire Deformation in Ultra-Fine Wire Coils	6-3
Appendix 6.2	Paper: Low Stress Potting for Stress Sensitive Magnetic Cores	6-21
Appendix 6.3	Paper: High Reliability Potting Materials for Use in Missile Systems	6-51

LIST OF ILLUSTRATIONS

Figure		Page
3-1	Fine Wire Test Assembly	3-25
3-2	Pressure Pot	3-30
3-3	Header	3-31
3-4	Thermometers Ready for Bonding to Headers	3-33
3-5	Pressure Calibration of Thermometer	3-34
3-6	Three Stages in Test Sample Preparation	3-35
3-7	Mold	3-36
3-8	Encapsulated Thermometers in Temperature Chamber	3-38
3-9	Scotchcast 255 Stress vs Temperature, Thermometer Method	3-47
3-10	Scotchcast 9 Stress vs Temperature, Thermometer Method	3-48
3-11	URALANE 5753 Stress vs. Temperature, Thermometer Method	3-49
3-12	URALANE 5753 Stress vs. Temperature, Thermometer Method Average of 3 Samples	3-49
3-13	RTV 615 Stress vs. Temperature, Thermometer Method	3-50
3-14	RTV 655 Stress vs. Temperature, Thermometer Method	3-51
3-15	RTV 627 Stress vs Temperature, Thermometer Method	3-52
3-16	RTV 619 Stress vs. Temperature, Thermometer Method	3-53
3-17	Conap EN-9 Stress vs Temperature, Thermometer Method	3-55

LIST OF ILLUSTRATIONS (Continued)

Figure		Page
3-18	Conap EN-90ZR Stress vs Temperature, Thermometer Method	3-56
3-19	Core Tensile Stress Measurement	3-59
3-20	Inductance vs Temperature for No. 52 Ferrite Core, Unpotted and Potted in Conap EN-9	3-61
3-21	Conap EN-9 Stress vs Temperature, Four Sensors	3-62
3-22	Inductance vs Temperature for No. 51 Ferrite Core, Unpotted and Potted in Conap EN-90ZR	3-63
3-23	Conap EN-90ZR, Stress vs Temperature, Four Sensors.	3-64
3-24	Inductance vs Temperature for No. 53 Ferrite Core, Unpotted and Potted in Scotchcast 255	3-65
3-25	Scotchcast 255 Stress vs Temperature, Three Sensors	3-67
3-26	Inductance vs Temperature for Ferrite No. 54 Unpotted and Potted in Scotchcast 255/RTV 619	3-68
3-27	Scotchcast 255/RTV 619 Stress vs Temperature	3-69
3-28	Inductance vs Temperature for Ferrite Core No. 55 Unpotted and Potted in Scotchcast 255/RTV 627	3-70
3-29	Scotchcast 255/RTV 627, Stress vs Temperature, Two Sensors	3-71
3-30	Inductance vs Temperature for Ferrite Core No. 56 Unpotted and Potted in Scotchcast 255/Epolene C/AC 617	3-72
3-31	Scotchcast 255/Epolene C/AC 617 Stress vs Temperature, Two Sensors	3-73
3-32	Saturable Reactor Used for Electrical Tests	3-74
3-33A	SEM Photograph of Scotchcast 255 Corrosion Area	3-83
3-33B	SEM Photograph of Eccoseal 1218 Corrosion Area	3-84
3-33C	SEM Photograph of Epon 825/HV Corrosion	3-85
3-33D	SEM Photograph of Hysol C-60 Corrosion.	3-86
3-33E	SEM Photograph of Hysol C15-015 Corrosion	3-87
3-34A	EDAX Scan of Scotchcast 255	3-83
3-34B	EDAX Scan of Eccoseal 1218 Corrosion Area	3-84

LIST OF ILLUSTRATIONS (Continued)

Figure	Page
3-34C EDAX Scan of Epon 825/HV Corrosion Area	3-85
3-34D EDAX Scan of Hysol C-60 Corrosion	3-86
3-35A SEM Photograph of Scotchcast 255 Corrosion After Temperature Cycling	3-89
3-35B SEM Photograph of Eccoseal 1218 Corrosion After Temperature Cycling	3-90
3-35C SEM Photograph of Epon 825 (HV) Corrosion After Temperature Cycling	3-91
3-35D SEM Photograph of Hysol C-60 Corrosion After Temperature Cycling	3-92
3-35E SEM Photograph of Hysol C15-015 Corrosion After Temperature Cycling	3-93
3-36A No Ions Detected During EDAX Scan	3-89
3-36B EDAX Scan of Corrosion After Temperature Cycling . . .	3-90
3-36C EDAX Scan of Epon 825 (HV) Corrosion After Temperature Cycling	3-91
3-36D EDAX Scan of Hysol C-60 Corrosion After Temperature Cycling	3-92
3-36E EDAX Scan of Hysol C15-015 Corrosion After Temperature Cycling	3-93
3-37 Mechanical Shock Test Fixture	3-101
3-38A Longitudinal Cross Sections of Part Potted with Scotchcast 255	3-103
3-38B Longitudinal Cross Sections of Part Potted with Eccoseal 1218	3-104
3-38C Longitudinal Cross Sections of Part Potted with Epon 825	3-105
3-38D Longitudinal Cross Sections of Part Potted with Hysol C-60	3-106
3-38E Longitudinal Cross Sections of Part Potted with Hysol C15-015	3-107
3-39 TWT High Voltage Transformer	3-108
3-40 Spurious Resonance Frequency-Schematic	3-112

LIST OF ILLUSTRATIONS (Continued)

Figure		Page
3-41	Typical Gain vs Frequency Curve	3-113
3-42	Volt-Second Support Test - Schematic & Waveforms . . .	3-114
3-43	Intrawinding Insulation Test - Schematic	3-115
3-44	Interwinding Insulation Test - Schematic	3-116
4-1	Typical Particulate Contamination Greater Than 100 μ in Longest Diameter (26x)	4-9
4-2	Typical Particulate Contamination Less Than 100 μ in Diameter (26x)	4-9
4-3	Undamaged Insulation After Salt Spray Test (625x)	4-15
4-4	Typical Salt Crystal Contamination on Tested Wire (625x)	4-15
4-5	Insulation and Contaminant After Salt Spray Test (600x)	4-16
4-6	EDAX Spectrum of Region X2. The Bare Insulation at X2 Gives an EDAX Which Shows: Na - 1.2 EV, Al - 1.6 EV (the Substrate), Cu - 8.0 EV	4-17
4-7	EDAX Spectrum of Region X1. The Crystal at X1 Shows the Same Pattern as is Seen in Figure 4-6, Plus: Cl - 2.6 EV, Cu - 8.0 EV (Stronger Reaction)	4-17
4-8	HCl Test Apparatus	4-19
4-9	Vibration Test Apparatus	4-23
4-10	Magnet Wire Insulation Damage Detector - Schematic . .	4-44
4-11	Toroidal Wire Insulation Damage Detector - Block Diagram	4-45
4-12	Nick in Wire, Due to Shuttle Gap Flexing and Slicing (50x)	4-47
4-13	Nick in Wire, Due to Shuttle Gap Flexing and Slicing (190x)	4-48
4-14	EDAX, at Point X ₁ on Figure 4-12, Showing Normal Light Element Composition of the Insulation Material . .	4-48
4-15	EDAX, at Point X ₂ on Figure 4-12, Showing Bare Copper in the Slice	4-49
4-16	EDAX, at Point X ₃ on Figure 4-12, Showing Presence of Oil (Si, S, Cl, K, Ca, Fe) on the Sliced Portion of the Insulation	4-49
4-17	Conventional Roller Configuration	4-51

LIST OF ILLUSTRATIONS (Continued)

Figure		Page
4-18	Modified Roller Configuration	4-51
4-19	Wire Damage Detector Circuit Board	4-54
4-20	Toroidal Winder Modification	4-56
4-21	Closeup, Showing Shuttle Grounding Brush	4-56
4-22	Sketch of Grounding Brush	4-57
4-23	Bobbin Winder Wire Damage Detector - Block Diagram . .	4-58

LIST OF TABLES

Table		Page
3-1	Model Parameters	3-3
3-2	Material Evaluation of Prospective Embedment Compounds Based on Vendor Supplied Data	3-4
3-3	Material Rating	3-12
3-4	Test Results of Selected Materials	3-14
3-5	Comparison of Electrical Parameters	3-18
3-6	Outgassing Data Per HP626 and NASA TND-8008 for 40 Materials	3-20
3-7	Pot Life and Total Working Time	3-22
3-8	Materials Cost	3-27
3-9	Pressure Sensitive Core Data	3-41
3-10	Test Inductor Data	3-43
3-11	Material-Test Method Matrix	3-45
3-12	Hydrolytic Stability of Materials-Test Results	3-77
3-13	Hydrolytic Stability of Encapsulated Transformers	3-79
3-14	EDAX Ion Detection Data	3-95
3-15	Tensile Shear Strength	3-96
3-16	Electrical Properties of Encapsulated Reactors	3-97
3-17	Effects of Encapsulation Materials on Interwinding and Stray Capacitances	3-99
3-18	Mechanical Shock Testing Program	3-101
3-19	High Voltage Transformer Test Results	3-109
3-20	Interwinding Insulation Test	3-118

LIST OF TABLES (Continued)

Table		Page
4-1	Process Damage Modes	4-4
4-2	Identification of Wire Samples	4-7
4-3	Statistical Particle Count	4-8
4-4	Solvent Susceptibility - Acetone Test	4-11
4-5	Solvent Susceptibility - Freon TF Test	4-12
4-6	Solvent Susceptibility - Isopropyl Alcohol Test	4-13
4-7	Outgassing Testing Results	4-18
4-8	Acid Test - Hydrochloric Acid	4-20
4-9	Acid Test - Sulfuric Acid	4-22

1.0 INTRODUCTION

This document, consisting of Volumes I and II, covers the effort to investigate, evaluate, and implement techniques for the manufacture of low cost, highly reliable electromagnetic components for missile systems applications. The Phase I effort, Volume I, concentrated on improving the manufacturing methods of potting, encapsulation, and winding of electromagnetic devices. Volume II, the follow-on phase, designated as Phase II, had the objective to investigate interconnection techniques, tooling and structural parts. Implementation of the combined results of the Phase I and Phase II efforts will hopefully improve manufacturing methods for electromagnetic components so that a significant payback in manufacture and life cycle costs of missile systems due to lower production costs, higher process yield, and improved reliability will be obtained. The information to be obtained will also contribute to the manufacturing of certain types of electromagnetic devices with significantly reduced sizes and weights which will further reduce the cost of the missile systems.

The "implementation" part of this project during the basic effort was the dissemination of information to accomplish the above objectives to those vendors who are manufacturing magnetic components for missile systems on an "as you go" basis rather than waiting until the project is completed. This approach had two definite advantages. First, and most obvious is that the earlier such information becomes available, the sooner it can be incorporated into the manufacturing processes and the beneficial results obtained. The second and not so obvious result is that contact with the vendors during the course of the project results in a useful dialogue between the MM&T project personnel and the vendors allowing an exchange of information on their problem areas and other considerations, resulting in increased understanding

of the overall problems involved. A list of attendees and the program at the debriefing held 28 October 1980 at Hughes Aircraft Company, Culver City is given in Table 12-1, Volume II.

2.0 STATEMENT OF WORK

Phase I was divided into two tasks as described below.

Task 1. Evaluation and Implementation of Potting and Encapsulation Techniques

- a. Evaluate the processes and materials presently used to encapsulate high voltage magnetic components to determine the optimum material to use to produce a low cost process which will provide void-free potting with high yield and high reliability. Materials and processes selected shall be capable of operating under the environmental conditions normally encountered in missile systems.
- b. Investigate methods and materials to provide low-stress potting and encapsulation of stress sensitive components such as those containing pressure sensitive cores, or miniature components using ultra-fine wire.
- c. The processes and materials selected shall be documented in process specifications. The capability of the materials to withstand the applicable environmental conditions shall be demonstrated by subjecting representative components incorporating these materials to electrical, mechanical and environmental tests.

Task 2. Implementation of Controlled Winding Techniques

- a. Determine the effect of handling techniques on ultra-fine wires (wire sizes AWG 40 to 54). Determine the effect of various contaminants on the wire and its insulation. Investigate and implement methods of storage and usage which will eliminate problems related to the handling of ultra-fine wires.
- b. Implement controlled techniques for winding of fine wire on toroidal transformers. Determine limits of wire sizes using presently available toroidal winding machines to produce reliable devices. Investigate techniques for single-strand and bifilar winding of toroidal transformers under controlled wire tension.

- c. Implement methods to wind solenoidal coils and transformers under controlled tension. Determine the required wire tension as a function of coil shape and size, thickness and type of coil insulation, wire size and winding speed. Investigate the feasibility of dynamic tension control to provide better control of wire tension.

Phase II was divided into three tasks as described below.

Task 3. Interconnection Techniques

- a. Implement safe, reliable and low cost techniques for the stripping of high temperature insulation from magnet wire. Mechanical, thermal and chemical methods shall be considered. The method selected shall not produce nicks or scratches in the wire which would reduce the reliability of the devices, and shall not reduce the bare copper diameter of the wire.
- b. Implement techniques for terminating ultra-fine wire. Establish the requirements for intermediate leads in miniature devices as a function of wire diameter. Determine and implement techniques for soldering ultra-fine wire which will not result in embrittlement of the fine wire or in dissolution of the wire into the solder. Determine the feasibility of welded connections in devices using ultra-fine wire.
- c. Investigate techniques for connecting coil wires to lead wires which do not rely on soldered connections. Crimp-type connections and welded connections shall be compared to those of soldered connections.
- d. Implement methods of making low cost, reliable connections in high voltage components. These connections must result in corona-free operation of the components. The required radii of the connections shall be tabulated as a function of the operating voltage.

Task 4. Tooling and Equipment for Encapsulation and Potting of Electromagnetic Devices

- a. Evaluate the equipment and tooling required to encapsulate transformers and inductors with the materials and processes developed under 3.3.1.
- b. Determine the feasibility of using automatic mixing and metering equipment.
- c. Implement a continuous process for potting and encapsulation to replace the present batch-oriented process.

Task 5. Structural Parts

- a. Evaluate techniques for low-cost production of internal field control and electrostatic shields for high voltage transformers. The use of molded, machined or formed shields shall be considered. The reliability of the selected technique shall be tested under applicable environmental conditions.
- b. Implement techniques for anchoring of windings within transformer coils. Methods to be investigated are to include adhesive bonding, spot bonding or the use of cuffed (folded) insulation. The structural integrity of coils constructed by the methods selected shall be evaluated by electrical tests, X-ray inspection, and by dissection of test coils.
- c. Investigate and implement the use of bobbins and coil-forms in which the terminations form an integral part of the coil support. The characteristics of thermoplastic and thermosetting plastics shall be studied to determine which materials are most suited for the structural parts of subminiature devices. The material selected shall not produce stresses on the cores or magnet wire used and shall maintain its structural integrity under all environmental conditions. If terminations are molded into the structural parts the plastic material surrounding the terminal shall not soften or deteriorate under soldering during installation.
- d. Implement new techniques for assembly of "C" cores (cut tape-wound cores). The resulting technique shall not depend on solder for structural integrity. The use of welded banding straps shall be investigated. If welded straps are used, weld schedules, band materials and electrode materials shall be determined. The possibility of using mechanical means of securing the cores shall also be determined. The techniques to be considered include wedging, snap lock or clinching types. The resulting technique must be adaptable to low weight, low profile assemblies. The assembly technique selected shall be evaluated by shock and vibration testing of transformers using the improved technique.

3.0 EVALUATION OF POTTING AND ENCAPSULATION MATERIALS AND TECHNIQUES

Over the past 40 years a multiplicity of plastic or elastomeric resins have been developed for encasing magnetic components for electrical insulation, heat transfer and protection from environmental conditions and mechanical damage. Many of these materials exhibit radically different properties depending on the composition of the hardening agent, and the processing used. The specific application imposes multitudinous constraints on the material properties such as, but not limited to; outgassing, viscosity, weight, cure time, adhesion, stability, cost, and pot life. Selection of an "optimum" material for a specific application requires detailed knowledge of both the available materials and their properties and the constraints of the application itself.

This section reviews various materials and their properties to determine an optimum material to use to produce a low cost process with high yield and high reliability, and capable of operating under environmental conditions normally encountered in missile systems. In addition methods and materials to achieve low stress potting and encapsulation of pressure sensitive magnetic components or miniature components using fine wire are reported. Methods of measuring actual stresses quantitatively are described in detail.

For purposes of clarity the various terms such as potting encapsulation, embedment, etc. are defined here.

Embedment — a process by which circuit components are encased in a dielectric material. It includes both potting and encapsulation.

Potting — an embedment process in which the container (can) used in embedment remains as part of the completed assembly.

Encapsulation — an embedment process in which the resin is cast in removable molds.

Impregnation — a process by which the interstices of components (such as coils) or assemblies are filled with resin, usually by means of a vacuum-pressure cycle.

Casting, Molding — processes by which plastic parts are formed from a liquid resin which is solidified in a mold from the liquid state.

Conformal Coating — a coating which generally follows the contours of the assembly, providing resistance to mechanical shock and environmental conditions.

In the sections following of this document the term "embedment" will be used instead of "potting and encapsulation". In places where potting or encapsulation are specifically intended, then the appropriate designation will be used.

3.1 VENDOR DATA SURVEY

Each vendor contacted sent data on his entire product line of embedment materials. From all of these products lists the forty most applicable materials were included in a table of relevant materials/processes parameters. These parameters listed in Table 3-1 provide a model for comparison of the materials, in some cases their desired values are given. It should be noted that many of the parameters have no numerical value so qualitative ratings are given instead. In other cases a preferred value and sometimes a limiting value are shown. These cases allow latitude for engineering judgement to be made.

The assumption is made, where a definite figure is stated, is that a high voltage or other extreme operational environment is involved. A more benign environment would allow some latitude in these cases also. Some of the parameters, which are starred^(*), were considered important and had sufficient manufacturer's data to be used in the actual selection process.

Table 3-2 gives the manufacturer's data for the various material and process parameters. In many cases no data (ND) was given. In many other cases the data was given, but with differing test methods or conditions. An example of differing test conditions is the dielectric constant measurement. The frequency used varied from 60 Hz to 1.0 GHz. In some materials the dielectric constant may vary significantly over this range of frequencies. This example is not to detract from the data's authority, but is simply to

TABLE 3-1. MODEL PARAMETERS

Parameter	Value
1. Mix Ratio*	prefer 3:1 maximum 5:1
2. Mix Ratio Sensitivity	low
3. Pot life*	20 minutes minimum
4. Cure cycle	short
5. Viscosity*	1000 maximum at pouring temperature
6. Specific gravity	low
7. Moisture sensitivity	low
8. Ease of Cleanup	easy
9. Exotherm of reaction	low
10. Shrinkage*	≤1%
11. Byproduct hazards	few of low severity
12. Dielectric Strength*	≥400 Volts/mil
13. Dielectric Constant*	prefer <4 maximum <6
14. Dissipation Factor*	prefer <0.05 maximum <0.1
15. Volume Resistivity*	>10 ¹² Ω-cm
16. Cured form	semirigid to semiflexible
17. Service temperature range*	-55°C to 125°C or wider
18. Hardness*	80 shore D maximum
19. Mechanical Shock Resistance	high
20. Tear resistance	high
21. Adhesive strength	high
22. Mechanical Vibration Resistance	high
23. Thermal Shock Resistance	high
24. Outgassing Resistance	low (See Table 3-6)
25. Thermal Conductivity*	>3.4 x 10 ⁻⁴ $\frac{\text{gcal}}{\text{sec}} \text{ cm}^2/\text{°C}$
26. Heat Capacity	high
27. Flame Resistance	high
28. Soldering heat resistance	high
29. Moisture Absorption*	<0.2%/1 day
30. Hydrolytic Stability	must be stable
31. Chemical Solvent Resistance	high
32. Chemically inert to coil materials	inert
33. Fungus Resistance	non-nutritive
34. Repair Ease	Easy to repair
35. Automatic Mixing	
36. Thermal Expansion (cured)*	≈17.0 x 10 ⁻⁶ /°C maximum 100 x 10 ⁻⁶

TABLE 3-2. MATERIAL EVALUATION OF PROSPECTIVE EMBEDMENT COMPOUNDS BASED ON VENDOR SUPPLIED DATA

Parameters	Conthane EN-9	Conthane EN-10 (11)	Conepoxy Y1000/07	Conepoxy IM145	Conepoxy RN1600	R7521	R7501	Epoxy/D400	Epoxy/T403	Epoxy/D230
Mix Ratio	100:17.5	100:37	100:75	1 Component	100:26	100:1.5	100:1.5	100:50	100:40	100:35
Mix Ratio Sensitivity	Med - High	Low	Low	-	Medium	High	High	Low	Low	Low - Med
Pot Life	30 min @ 25°C	30 min @ 25°C	105 min	16h @ 60°C	30 min	14 days @ 60°C	14 days @ 60°C	300 min	320 min	240 min
Sugg. Cure Time	8h @ 100°C	16h @ 80°C	2h @ 60°C	2.3h @ 120°C + 4h @ 155°C	3h @ 140°C	15h @ 150°C	15h @ 150°C	2h @ 80°C + 3h @ 125°C	2h @ 80°C + 3h @ 125°C	2h @ 80°C + 3h @ 125°C
Viscosity, cps	6800 @ 25°C	5500 @ 25°C	3500 @ 25°C	1400 @ 25°C 280 @ 60°C	120,000 @ RT 1600 @ 80°C	2200 @ RT 300 @ 60°C	150 @ RT	500 @ 25°C	1360 @ 25°C	400 @ 25°C
Specific Gravity	1.0	0.97	1.05	1.18	1.7	1.13	1.11	0.97	0.98	0.95
Moisture Sensitivity	High	High	Moderate	High	Moderate	Moderate Air Sensitive	Moderate Air Sensitive	ND	ND	ND
Ease of Cleanup	Tol, MEK Xylene	Tol, MEK Xylene	ND	ND	ND	ND	ND	Toluene	Toluene	Toluene
Exotherm of Reaction	55°C @ 0.5 lb	55°C @ 0.5 lb	ND	ND	ND	ND	ND	ND	125°C @ 1.0 lb	208°C @ 1.0 lb
Shrinkage %	1.15	1.19	1.5	2.1	1.4	ND	ND	ND	ND	ND
Hazards	No	No	No	No	No	No	No	No	No	No
Diel. Strength V/ml	610	710	ND	ND	375	350	350	487	514	479
Diel. Constant	3.03 @ 100 Hz	3.1 @ 100 Hz	3.9 @ 100 Hz	3.8 @ 1 KHz	4.35 note 1	2.85 note 1	2.95 note 1	4.01 @ 1 KHz	4.14 @ 1 KHz	4.1 @ 1 KHz
Diag. Factor	0.031 @ 100 Hz	0.027 @ 100 Hz	0.009 @ 100 Hz	0.011 @ 1 KHz	0.020 note 1	0.002 note 1	0.003 note 1	0.009 @ 1 KHz	0.01 @ 1 KHz	0.011 @ 1 KHz
Volume Resistivity ohm-cm	3.42 x 10 ¹⁵	4.3 x 10 ¹⁵	3 x 10 ¹³	7.1 x 10 ¹²	2 x 10 ¹⁴	5 x 10 ¹⁵	7 x 10 ¹⁵	3.0 x 10 ¹⁶	1.7 x 10 ¹⁶	1.6 x 10 ¹⁶
Cured Form	Flexible	Flexible	Semiflex	Semiflex	Semiflex	Rigid	Rigid	Semiflex	Rigid	Semiflex
Service Temp. Range, °C	-70 to 135	-70 to 135	to 80	ND	-55 to 155	to 250	to 250	ND	ND	ND
Hardness, Shore	85(A)	75(A)	60(D)	80(D)	55(D)	ND	ND	80(D)	87(D)	79(D)

ND = No Data

(Notes: 1. Test frequency not given.)

Continued next page)

(Table 3-2 continued)

Parameters	Conathane EN-9	Conathane EN-10 (11)	Conepoxy Y1000/07	Conepoxy IM1145	Conepoxy RN1606	R7521	R7501	Epoxy/D400	Epoxy/T403	Epoxy/D230
Mech. Shock	ND	ND	ND	ND	ND	ND	ND	ND	ND	ND
Tear Resist.	275-310 psi (Die C)	140-180 psi (Graves)	ND	ND	ND	ND	ND	ND	ND	ND
Adhesive Strength	20 lb/in.	ND	ND	ND	ND	ND	ND	4.7 lb/in.	4.7 lb/in.	5.6 lb/in.
Mech. Vibration	ND	ND	ND	ND	ND	ND	ND	ND	ND	ND
Thermal Shock	Passes 10 cycles -70°C to 135°C	Passes 10 cycles -70°C to 135°C	ND	ND	ND	ND	ND	5 of 10 passed 10 -20°C to 140°C	7 of 10 passed 10 -20°C to 140°C	Passes 10 -20°C to 140°C
Thermal Conductivity	ND	ND	ND	ND	6.5×10^{-4}	3.67×10^{-4}	3.7×10^{-4}	ND	ND	ND
Heat Cap.	ND	ND	ND	ND	ND	ND	ND	ND	ND	ND
Flame Resist.	No ignition after 55 amp test	ND	ND	ND	Extinguished in 35 sec	ND	ND	ND	ND	ND
Soldering Heat	ND	NQ	ND	ND	ND	ND	ND	ND	ND	ND
Moisture Absorption	0.57% - 24 days	ND	0.20% - 1 day	ND	0.17% - 1 day	ND	ND	ND	ND	ND
Hydrolytic Stability	Good	Good	ND	ND	ND	ND	ND	ND	ND	ND
Chemical Solvent	See Cleanup	See Cleanup	Insensitive to solvents	ND	ND	ND	ND	ND	ND	ND
Chem. Inert to Coll Mtls.	ND	ND	ND	ND	ND	Yes	Yes	ND	ND	ND
Fungus Resistant	Non-nutrient	Non-nutrient	ND	ND	ND	ND	ND	ND	ND	ND
Repair Ease	ND	ND	Not easy to repair	ND	ND	ND	ND	ND	ND	ND
Automatic Production	Difficult	Difficult	Difficult	Possible	Difficult	ND	ND	ND	ND	ND
Thermal Expansion cm/cm °C	ND	ND	ND	ND	115×10^{-6}	125×10^{-6}	150×10^{-6}	ND	ND	ND

(Continued next page)

(Table 3-2 continued)

Parameter	RTV11/DBT	RTV60/DBT	RTV611	RTV614	RTV615	RTV655	RTV670	RTV627	Epocast 202	Scotchcast 255
Mix Ratio	500:1	500:1	10:1	10:1	10:1	10:1	10:1	1:1	100:15	2:1
Mix Ratio Sensitivity	High	High	Medium	Medium	Medium	Medium	Medium	Low	Medium	Low
Pot Life	2-4h @ 25°C	2-4h @ 25°C	1.5h @ 25°C	4h @ 25°C	4h @ 25°C	4h @ 25°C	5h @ 25°C	2h @ 25°C	16-20h @ 25°C	4h @ RT
Suggested Cure Time	24-36h @ 25°C	24-36h @ 25°C	12-24h @ 25°C	1h @ 100°C	1h @ 100°C	1h @ 100°C	1h @ 125°C	1h @ 100°C	16h @ 60°C	2h @ 120°C
Viscosity cps Room Temp.	12,000	50,000	12,000	500	3500	4800	5000	1600	4000	23,000
Specific Gravity	1.18	1.47	1.18	0.97	1.02	1.02	1.06	1.39	1.18	1.56
Moisture Sensitivity	ND	ND	ND	ND	ND	ND	ND	ND	Shortens Shelf Life	ND
Ease of Cleanup	MEK, TCE	MEK, TCE	MEK, TCE	MEK, TCE	MEK, TCE	MEK, TCE	MEK, TCE	MEK, TCE	ND	ND
Exotherm of Reaction	0	0	0	0	0	0	0	0	ND	ND
Shrinkage %	0.2 - 0.6	0.2 - 0.6	0.2 - 0.6	0.2 - 0.6	0.2 - 0.5	0.2 - 0.6	0.2 - 0.6	0.2 - 0.6	1.11	ND
Hazards										
Diel. Strength V/mil	500	500	500	500	500	500	500	500	350	375
Diel. Constant	3.6 @ 100 Hz	3.6 @ 100 Hz	3.6 @ 100 Hz	3.0 @ 100 Hz	3.0 @ 100 Hz	3.0 @ 100 Hz	2.8 @ 100 Hz	3.4 @ 100 Hz	4.8 @ 60 Hz	5.9 @ 100 Hz
Disa. Factor	0.019 @ 100 Hz	0.020 @ 100 Hz	0.019 @ 100 Hz	0.001 @ 100 Hz	0.001 @ 100 Hz	0.001 @ 100 Hz	0.001 @ 100 Hz	0.001 @ 100 Hz	0.036 @ 60 Hz	0.05 @ 100 Hz
Volume Resistivity ohm-cm	6×10^{14}	1.3×10^{14}	6×10^{14}	1×10^{15}	1×10^{15}	1×10^{15}	4×10^{15}	1×10^{15}	4.8×10^{14}	1×10^{15}
Cured Form	Rubbery	Rubbery	Rubbery	Gel Like	Rubbery	Rubbery	Rubbery	Rubbery	Semirigid	Semiflex
Service Temp. Range	-60 to 204°C	-60 to 204°C	-60 to 204°C	-60 to 204°C	-60 to 204°C	-115 to 204°C	-60 to 204°C	-60 to 204°C	ND	-55 to 130°C
Hardness, Shore	45(A)	60(A)	45(A)	Penetrates 5 MM	45(A)	45(A)	70(A)	45(A)	83(D)	72(D)

(Continued next page)

(Table 3-2 continued)

Parameter	RTV11/DRT	RTV10/DRT	RTV8111	RTV619	RTV615	RTV655	RTV670	RTV627	Epocast 202	Scotchcast 255
Mech. Shock	ND	ND	ND	ND	ND	ND	ND	ND	ND	7.75 lb
Tear Resist kg/cm	3	7	3	ND	4	4	6	4	ND	ND
Adhesive Strength	Low	Low	Low	Low	Low	Low	Low	Low	ND	High
Mech. Vibration	ND	ND	ND	ND	ND	ND	ND	ND	ND	ND
Thermal Shock	ND	ND	ND	ND	ND	ND	ND	ND	ND	Pass 10 cycles -55 to 130°C
Thermal Conductivity g cal/sec cm ² °C	7×10^{-4}	7.4×10^{-4}	7×10^{-4}	4.5×10^{-4}	4.5×10^{-4}	4.5×10^{-4}	4.5×10^{-4}	4.5×10^{-4}	4×10^{-4}	4×10^{-4}
Heat Cap.	ND	ND	ND	ND	ND	ND	ND	ND	ND	ND
Flame Resist	No	No	No	No	No	No	No	Yes	ND	Pass UL-94 (V-0)
Soldering Heat	ND	ND	ND	ND	ND	ND	ND	ND	ND	ND
Moisture Abs.	ND	ND	ND	ND	ND	ND	ND	ND	0.4%/1 day	0.45%/10 day
Hydrolytic Stability	Yes	Yes	Yes	Yes	Yes	Yes	Yes	Yes	ND	Yes
Chemical Solvent	ND	ND	ND	ND	ND	ND	ND	ND	ND	ND
Chem. Inert. to Coil Mat.	ND	ND	ND	ND	ND	ND	ND	ND	ND	ND
Fungus Resist	ND	ND	ND	ND	ND	ND	ND	ND	ND	ND
Repair Ease	ND	ND	ND	ND	ND	ND	ND	ND	ND	ND
Automatic Production	No	No	Yes	Yes	Yes	Yes	Yes	Yes	Yes	Yes
Thermal Exp. cm/cm °C	26.0×10^{-6}	110×10^{-6}	250×10^{-6}	330×10^{-6}	270×10^{-6}	270×10^{-6}	270×10^{-6}	220×10^{-6}	ND	ND

(Continued next page)

(Table 3-2 continued)

Parameters	Scotchcast 235	Scotchcast 280	Scotchcast 281	Scotchcast 5237	Eccoseal 63	Stycast 62	Epon 825/1HV	EM & Cumm W-67	Eccoseal 1207	Eccoseal 1218
Mix Ratio	1:2 Low	2:3 Low	2:3 Low	3:4 Low	100:1 High	100:1 High	100:18 Mod.	100:85 Low	100:2 High	100:70 Low
Mix Ratio Sensitivity										
Pot Life	18 Min @ 120°C	20 min @ 120°C	21 min @ 120°C	15 min @ 60°C	7 day @ 25°C	7 day @ 25°C	25 min @ 67°C	1 month @ 25°C	8h @ 50°C	3h @ 50°C
Sage. Cure Time	2h @ 120°C	2h @ 120°C	2h @ 120°C	1h @ 95°C	18h @ 85°C	18h @ 85°C	4h @ 125°C	4h @ 125°C + 16h @ 175°C	4h @ 71°C + 1h @ 177°C	12h @ 125°C
Viscosity cps	250 @ 76°C	350 @ 76°C	48,000 @ 23°C	20,000 @ 23°C	ND	ND	4,000 @ 23°C	250 @ 25°C	150 @ 50°C	500 @ 50°C
Specific Gravity	1.1	1.08	1.43	1.35	0.95	1.05	1.15	ND	ND	1.2
Moisture Sensitivity	ND	ND	ND	ND	ND	ND	ND	High	ND	ND
Ease of Cleanup	ND	ND	ND	ND	ND	ND	ND	ND	ND	ND
Exotherm of Reaction	ND	ND	ND	ND	ND	ND	ND	ND	ND	ND
Shrinkage %	ND	ND	ND	ND	ND	ND	ND	ND	ND	ND
Hazards	ND	ND	ND	ND	ND	ND	ND	ND	ND	ND
Diel. Strength, V/mil	325	375	375	370	500	500	400-500	450	450	ND
Diel. Constant	4.25 @ 100 Hz	4.07 @ 100 Hz	4.03 @ 100 Hz	5.0 @ 100 Hz	2.4 @ 100 Hz	2.6 @ 100 Hz	3.81 @ 1 KHz	3.3 @ 1 KHz	3.5 @ 1 GHz	3.7 @ 60 Hz
Dis. Factor	0.07 @ 100 Hz	0.008 @ 100 Hz	0.032 @ 100 Hz	0.08 @ 100 Hz	0.005 @ 100 Hz	<0.0015 @ 100 Hz	0.004 @ 1 KHz	0.006 @ 1 KHz	0.015 @ 1 GHz	0.025 @ 60 Hz
Volume Resistivity ohm/cm	2.9 x 10 ¹⁴	10 ¹⁵	10 ¹⁵	10 ¹⁵	10 ¹⁶	10 ¹⁶	3 x 10 ¹²	10 ¹⁵	10 ¹⁶	10 ¹⁵
Cured Form	Semiflex	Semiflex	Semiflex	Semiflex	Semiflex	Semiflex	Semiflex	Semiflex	Semiflex	Semiflex
Service Temp. Range °C	-55 to 125	-55 to 155	-55 to 155	-55 to 125	-55 to 190	-55 to 150	-55 to 125	up to 230	up to 177	-100 to 175
Hardness, Shore	55(D)	65(D)	65(D)	80(D)	ND	ND	80(D)	ND	ND	40(D)

(Continued next page)

(Table 3-2 continued)

Parameters	Scotchcast 235	Scotchcast 280	Scotchcast 281	Scotchcast 5237	Eccoseal 63	Stycast 62	Epon 825/HV	EM & Cumm W-67	Eccoseal 1207	Eccoseal 1218
Mech. Shock	7.75 lb ball	7.75 lb ball	7.75 lb ball	5 lb ball	ND	ND	ND	ND	ND	ND
Tear Resist.	ND	ND	ND	ND	ND	ND	ND	ND	ND	ND
Adhesive Strength	ND	ND	ND	ND	ND	ND	ND	ND	ND	ND
Mech. Vibration	ND	ND	ND	ND	ND	ND	ND	ND	ND	ND
Thermal Shock	pass 10 cycle -55 to 130°C	fail, 10 cycle -55 to 130°C	pass, 10 cycle -55 to 130°C	pass, 10 cycle -55 to 130°C	ND	ND	pass, 10 cycle -55 to 130°C	ND	ND	ND
Thermal Conductivity $\frac{\text{Btu-in}}{\text{sq. ft. sec } ^\circ\text{C}}$	4×10^{-4}	5.3×10^{-4}	12×10^{-4}	ND	ND	ND	ND	ND	ND	5×10^{-4}
Heat Cap.	ND	ND	ND	ND	ND	ND	ND	ND	ND	ND
Flame Resist.	ND	ND	ND	Passes UL94-V1	ND	ND	ND	ND	ND	ND
Soldering Heat	ND	ND	ND	ND	ND	ND	ND	ND	ND	ND
Moisture Abs.	0.92%/240h	0.52%/240h	0.32%/240h	0.78%/240h	ND	ND	ND	ND	0.2%/24h	0.2%/240h
Hydrolytic Stability	ND	No	No	Yes	ND	ND	Yes	ND	ND	ND
Chem. Solvent	ND	ND	ND	ND	ND	ND	ND	ND	ND	ND
Chem. Inert to Coll Mat.	ND	ND	ND	ND	ND	ND	ND	ND	ND	ND
Fungus Resistant	ND	ND	ND	ND	ND	ND	ND	ND	ND	ND
Repair Ease	ND	ND	ND	ND	ND	ND	ND	ND	ND	ND
Automatic Production	Yes	Yes	Yes	Yes	Yes	Yes	No	Yes	Yes	Yes
Thermal Expansion cm/cm °C	ND	ND	ND	ND	ND	ND	51×10^{-6}	ND	ND	ND

(Continued next page)

(Table 3-2 continued)

Parameters	GF707	GF702	Hysol CH5-015	Hysol C-60	Hysol HD3501	Hysol E204A/9816	M&T E204A/9652	Uralane 5753	Conathane EN-2	Conathane EN-90/R
Mix Ratio	100:1	100:1	7:3	2:3	100:30	100:15	100:50	100:20	100:90	100:17.5
Mix Ratio Sensitivity	High	High	Low	Low	Mod	Mod-High	Low	Mod-High	Low	Mod-High
Pot Life	25 min @ 118°C	25 min @ 118°C	90 min @ 99°C	3-9h @ 75°C	35 min @ 25°C	2h @ 65°C	3.5h @ 25°C	35 min @ RT	20 min @ 25°C	30 min @ 25°C
Spec. Cure Time	1-4h @ 163°C	6-10h @ 180°C	6h @ 125°C	16-24h @ 125°C	3h @ 60°C	2h @ 65°C	3h @ 65°C	8h @ 95°C	4h @ 60°C	24h @ 60°C
Viscosity, cps	1000 @ RT	1000 @ RT	200 @ 90°C	300 @ 75°C	600 @ 25°C	2600 @ 25°C	6000 @ 25°C	ND	ND	ND
Specific Gravity	1.1	1.1	1.15	1.15	1.15	1.1	1.1	ND	1.0	1.0
Moisture Sensitivity	ND	ND	ND	ND	ND	Mod.	Mod.	Mod.	High	High
Ease of Cleanup	ND	ND	ND	ND	ND	ND	ND	ND	Conap S-8	Xylene, MEK TOL
Exotherm of Reaction	ND	ND	90°C/200g	0.0	190°C/200g	ND	ND	ND	0.0	55°C/227g
Shrinkage %	ND	ND	2.8	2.8	0.6	ND	ND	3	0.31	1.0
Hazards	ND	ND	SPICL2	SPICL2	SPICL5	ND	ND	ND	MOCA base	ND
Diel. Strength V/mil	500	500	350	350	ND	395	395	350	645	610
Diel. Constant	1.97 @ 60 Hz	5.4 @ 60 Hz	3.8 @ 100 Hz	4.0 @ 100 Hz	4.96 @ 100 Hz	4.2 @ 100 Hz	4.0 @ 100 Hz	3.6 @ 1 KHz	5.7 @ 100 Hz	3.3 @ 100 Hz
Diss. Factor	0.004 @ 60 Hz	0.03 @ 60 Hz	0.03 @ 100 Hz	0.038 @ 100 Hz	0.007 @ 100 Hz	0.012 @ 100 Hz	0.020 @ 100 Hz	0.021 @ 1 KHz	0.123 @ 100 Hz	0.031 @ 100 Hz
Volume Resistivity ohm-cm	10 ¹¹	10 ⁶	3 x 10 ¹⁴	7 x 10 ¹⁴	4 x 10 ¹⁴	2.6 x 10 ¹⁴	1 x 10 ¹⁴	5 x 10 ¹⁵	3.1 x 10 ¹³	3.4 x 10 ¹⁵
Cured Form	Semirigid	Semiflex	Semiflex	Semiflex	Semiflex	Rigid	Semi-Rigid	Flex	Flex	Flex
Service Temp. Range °C	-55 to 180	-55 to 180	-55 to 125	-55 to 125	-40 to 125	ND	ND	-55 to 125	-65 to 130	-70 to 135
Hardness, Shore	ND	ND	60(D)	60(D)	75(D)	88(D)	75(D)	55-65(A)	69(A)	85(A)

(Continued next page)

(Table 3-2 concluded)

Parameters	GE707	GE702	Hysol C15-015	Hysol C-60	Hysol HD3501	M&T E204A/9816	M&T E204A/9652	Uralane 5753	Conathane EN-2	Conathane EN-902R
Mech. Shock	ND	ND	ND	ND	ND	ND	ND	ND	ND	ND
Tear Resist	ND	ND	ND	ND	ND	ND	ND	130 lb/in	110 lb/in	275-310 psi
Adhesive Strength	ND	ND	ND	ND	20 lb/in	ND	ND	30 lb/in	ND	20 lb/in
Mech. Vibration	ND	ND	ND	ND	ND	ND	ND	ND	ND	ND
Thermal Shock	ND	ND	ND	ND	ND	ND	ND	ND	ND	Pass 10 cycles -55 to 130°C
Thermal Conductivity $\frac{\text{g cal}}{\text{sec cm}^2 \text{ } ^\circ\text{C}}$	ND	3.4×10^{-4}	4.5×10^{-4}	4.5×10^{-4}	ND	4.8×10^{-4}	4.4×10^{-4}	ND	3.5×10^{-4}	ND
Heat Cap.	ND	ND	ND	ND	ND	ND	ND	ND	ND	ND
Flame Resist.	ND	ND	ND	ND	ND	1.5 in/min	1.1 in/min	ND	ND	No ignition 55 ADC
Soldering Heat	ND	ND	ND	ND	ND	ND	ND	ND	ND	ND
Moisture Abs.	ND	ND	0.51%/7 day	0.84%/7 day	0.43%/1 day	0.16%/1 day	0.31%/1 day	3.0%/1 day	ND	0.5%/24 day
Hydrolytic Stability	ND	ND	ND	ND	ND	ND	ND	ND	ND	ND
Chem. Solvent	ND	ND	ND	ND	ND	ND	ND	ND	ND	ND
Chem. Inert to Coil Mat.	ND	ND	ND	ND	ND	ND	ND	ND	ND	ND
Fungus Resistant	ND	ND	ND	ND	ND	ND	ND	Non Nutrient	ND	Non Nutrient
Repair Ease	ND	ND	ND	ND	ND	ND	ND	ND	ND	ND
Automatic Production	No	No	Yes	Yes	Yes	No	Yes	Yes	Yes	Yes
Thermal Expansion $\text{cm/cm } ^\circ\text{C}$	ND	220×10^{-6}	190×10^{-6}	ND	54×10^{-6}	98×10^{-6}	140×10^{-6}	250×10^{-6}	ND	ND

point out that further testing by the user at the condition of interest is considered necessary.

Table 3-2, tabulation of the manufacturer's data, provides a side by side comparison of 40 materials; the materials themselves, together with specific designations of hardeners used where alternate choices existed, are listed in Table 3-3. Taking into account differences in vendors' measurement techniques, Table 3-3 gives an estimate of the relative suitability of the 40 encapsulation materials.

The assessment of the relative merit of the various materials was done using the thirteen starred parameters in Table 3-1. Each parameter was given equal weight in the selection process. The range of values varied

TABLE 3-3. MATERIAL RATING

Score	Material
11	Hysol C-60 ¹ , Hysol C-15-015 ¹
10	Eccoseal 1218 ¹ , Scotchcast 280 ¹
9	Eccoseal 1207, Epon 825/HV ¹ , RTV-11, RTV-60, RTV-627, RTV-8111, Scotchcast 235 (237) Scotchcast 255, Scotchcast 281
8-1/2	RN1600
8	Conathane EN-2, Conathane EN-9, Conathane EN-9-0ZR, Conathane 10, E204A/9652, R7501, R7521, RTV 619 Epoxy/D400
7-1/2	R9-2039
7	Conepoxy IM1145, Conepoxy Y1000/07, Eccoseal 63, Eccoseal W67, GE 707, RTV 615, RTV 655, RTV 670, Stycast 62, Uralane 5753, Epoxy/0230, Epoxy/T403
6-1/2	E204A-9816
5-1/2	Epocast 202, Scotchcast 5237
4	GE 702
¹ Top five materials chosen initially.	

from four to eleven, with the average value 7-1/2 and the median of 8. Table 3-3 gives the list of the materials and their values in order of merit. The top five materials were chosen initially for evaluation of their specific gravity, hardness, thermal conductivity, degradation temperature, glass transition temperature, coefficient of thermal expansion, moisture absorption, shrinkage, dielectric constant, dissipation factor and volume resistivity.

Subsequent data from the literature showed that Scotchcast 280 was hydrolytically unstable, so Scotchcast 255 was added to the final list because it ranked very well on the model. At the same time 702 and 707, two solventless polyester varnishes, were added to the list because of their low material cost, although they were rated rather low in Table 3-3.

The tests were designed to achieve two goals: (1) test all the materials under the same conditions, (2) obtain data that was not available from the manufacturers. Test results are shown in Table 3-4, with specific test procedures and summary of results as follows. Paragraph numbers refer to items in Table 3-4.

2. Specific gravity: Specific gravities of the samples were determined at ambient temperatures in accordance with Fed. Std. 406-5011 (water displacement method).

Results: The specific gravity of all test materials with the exception of Scotchcast 255 (s. g. 1.51), ranged from 1.06 to 1.17, and were acceptably close to the manufacturers' values.

3. Hardness: Hardness of the test materials was determined per Fed. Std. 406-1083 at ambient temperature.

Results: Epon 825, Hysol C15-015, Hysol C60, Scotchcast 255, and Scotchcast 280 test materials had hardness within the acceptable limits. Eccoseal 1218 test material had a very low hardness value compared to the manufacturer's specification.

4. Thermal conductivity: The thermal conductivity measurements of the test materials were conducted at 95°C under 5.2 kg (11.5 lbs.) loading using a Colora thermoconductometer. Dow Corning 200 dielectric fluid was used throughout the determinations to improve surface contact of the samples.

Results: Eccoseal 1218, Epon 825, Hysol C15-015, Hysol C60, and Scotchcast 280 test materials showed reasonable thermal conductivity values; Scotchcast 255 test material had a much higher thermal conductivity (9.7×10^{-4} cal. cm/sec. cm²°C) compared to the

TABLE 3-4. TEST RESULTS OF SELECTED MATERIALS

Test Material Evaluation	Eccoseal 1218	EPON 825 With HV Hardener (HMS 16-157b, Type I)	GE 702	GE 707	Hysol C15-015	Hysol C60	Scotchcast 255	Scotchcast 280
1. Curing Schedule (Note 1)	17 hrs. at 120°C (250°F)	16 hrs./70°C (160°F) and 4 hrs./120°C (250°F)	16 hrs. at 120°C (250°F)	4 hrs. at 163°C (325°F)	16 hrs./70°C (160°F) and 6 hrs./120°C (250°F)	17 hrs. at 120°C (250°F)	3 days at 70°C (160°F)	16 hrs./70°C (160°F) and 2 hrs./120°C (250°F)
2. Specific Gravity (Note 2)	1.06	1.17	1.17	1.15	1.17	1.13	1.51	1.10
3. Hardness (Shore D) (Note 3)	10	83	60	75	55	45	70	55
4. Thermal Conductivity (Cal. cm/sec.cm ² °C (Note 4))	6.2×10^{-4}	5.9×10^{-4}	4.8×10^{-4}	4.8×10^{-4}	5.9×10^{-4}	4.8×10^{-4}	9.7×10^{-4}	5.5×10^{-4}
5. Degradation Temperature (°C) (Note 5)	Starts around 250	250 to 280	Starts around 280	Around 225	250 to 300	275 to 300	Around 250	250 to 300
6. Glass Transition Temperature (°C) (Note 5)	-15	Near 250	Near 25	50	40	25	Near 35	35 to 40
7. Coefficient of Thermal Expansion (in/in/°C) Above Tg (Note 5)	433×10^{-6} (25 to 75°C)	172×10^{-6} (150 to 250°C)	256×10^{-6} (50 to 125°C)	208×10^{-6} (75 to 225°C)	249×10^{-6} (50 to 250°C)	246×10^{-6} (25 to 100°C)	172×10^{-6} (55 to 70°C)	246×10^{-6} (50 to 250°C)
8. Moisture Absorption (%) (Note 6)	0.40	0.17	0.27	0.27	0.31	0.33	0.12	0.15
9. Shrinkage (%) (Note 7)	1.73	0.37	1.03	2.87	0.07	(Note 9)	0.37	1.87
10. Dielectric Constant (Note 8)	3.99	3.98	(Note 10)	(Note 10)	3.84	(Note 9)	3.26	3.24
11. Dissipation Factor (Note 8)	0.083	0.011	(Note 10)	(Note 10)	0.05	(Note 9)	0.017	0.037
12. Volume Resistivity (Ohm, cm) (Note 8)	1.6×10^{15}	6×10^{15}	(Note 10)	(Note 10)	1×10^{15}	(Note 9)	1.3×10^{15}	8×10^{15}

NOTES: 1. Curing of the test materials was performed by Electromagnetic Group (76-31-21)

2. Per FED. STD. 406-5011
3. Per FED. STD. 406-1083
4. Using Colora Thermoconductometer
5. Using DuPont Thermal Analyzer
6. Per ASTM D570: Modified
7. Per ASTM D2566: Modified
8. Refer to report for method and technique
9. Resin material not available at this time.
10. Test material did not lend itself to testing (see report)

manufacturer's specified value (4.5×10^{-4} cal.
cm/sec. cm²°C).

5. Degradation temperature: The degradation temperature of the test materials was determined by Thermal Gravimetric Analysis (TGA), Thermal Mechanical Analysis (TMA), and Differential Scanning Calorimetric (DSC) techniques using a DuPont thermal analyzer.

Results: All test materials appeared to decompose very readily at approximately 350°C. Starting decomposition temperatures of the test materials are shown in Table 3-4.

6. Glass transition temperature (Tg): The glass transition temperatures (Tg) of the test materials were determined by TMA techniques using a thermal analyzer.

Results: Epon 825 test material showed the highest Tg (150°C), Eccoseal 1218 test material exhibited a low Tg (-15°C), and others had Tg near 20°C to 50°C.

7. Coefficient of thermal expansion (CTE): The CTEs of the test materials were determined by TMA techniques.

Results: Eccoseal 1218 test material expanded most; Epon 825 and Scotchcast 255 test materials expanded the least. Other test materials expanded moderately (200 to 250×10^{-6} in/in °C).

The CTEs at temperatures lower than the Tg for all test materials are shown below:

• Eccoseal 1218	89×10^{-6} in/in °C	(-175 to -25°C)
• Epon 825	65×10^{-6} in/in °C	(+25 to +125°C)
• GE 702	69×10^{-6} in/in °C	(-150 to 0°C)
• GE 707	69×10^{-6} in/in °C	(-125 to +50°C)
• Hysol C15-015	159×10^{-6} in/in °C	(0 to +25°C)
• Hysol C60	91×10^{-6} in/in °C	(-125 to +25°C)
• Scotchcast 255	54×10^{-6} in/in °C	(-175 to +25°C)
• Scotchcast 280	—	—

8. Moisture absorption: The moisture absorption was determined by twenty-four (24) hour immersion per ASTM D570. One sample of each material was cast, cured, machined to a thickness of one-eighth (1/8) inch and a diameter of two (2) inches, and subjected to the test procedure at ambient temperature.

Results: All test materials absorbed less than 0.4 percent moisture by weight.

9. Linear shrinkage: The linear shrinkage of the test materials was determined in a manner similar to ASTM D2566. The procedure used differs from the ASTM method in a few respects. The mold used was aluminum and three (3) inches long instead of ten (10) inches long stainless steel, as specified in the document. Mold release agents were used rather than Teflon film to prevent adhesion of the resin material to the mold. The results obtained are listed in Table 3-4.

Electrical properties determinations: The electrode arrangement used for dielectric constant, dissipation factor, and volume resistivity was a standard air dielectric variable capacitor with its plates fully meshed. Use of these electrode configuration offered several advantages: test specimens are easily produced, the encapsulation is more representative of the end use, the sample is not altered by fabrication to size or electrode processing steps, errors produced in measurement of sample geometry are eliminated, and calculation of dielectric constant is greatly simplified.

- 10, 11. Dielectric constant and dissipation factor: The measurements were made at 1 kHz using a General Radio 1608A Impedance Bridge. The dielectric constant was obtained as the ratio of the capacitance after encapsulation to the capacitance before encapsulation. The dissipation factor reported is that associated with the encapsulated capacitance.
12. Volume resistivity: Using the same sample as was used for the dielectric constant and dissipation factor, the volume resistivity was determined. A volume resistance was measured with a General Radio 1230A DC Amplifier and Electrometer. From the capacitance and dielectric constant, an effective electrode term was calculated. The product of the volume resistance and the effective electrode term gave the volume resistivity.

The electrical testing techniques used were not successful with GE 702 and GE 707 resins. These resin systems, which are designed for dip coating applications, produced such an exotherm when cured in the bulk (300 ml) required by the test apparatus that, on cooling, the material cracked severely and meaningful measurements could not be made. Hysol C60 was not available for this portion of the testing program because of a vendor error.

The electrical measurements reflect the physical state of the wired resin system at the time of test under a specific environment. The material's prior history; temperature, test frequency and many other factors have an effect on measurements of this type. When the electrical measurements were made here, these factors were known; however, the particular conditions

existing during the manufacturers' tests are not known. Variances caused by sample processing, molecular polarizability and test conditions are probable causes for the differences between the manufacturer's data and Table 3-4. In an attempt to resolve the discrepancies, measurements of dielectric strength by ASTM D-149, dielectric constant, and dissipation factor by ASTM D-150, and volume resistivity by ASTM D-257, and the results tabulated in Table 3-5 for comparison. The two inch diameter, 0.1 inch thick disc samples were prepared using the manufacturers instructions or the applicable Hughes Process Specification.

Comparison of the results for the four electrical measurements shows in most cases reasonable agreement considering the small number of samples run, with the exception of the ASTM D-257 volume resistivity values. It would appear that the ASTM sample holder had surface leakage resistivity which bypassed the sample under test, giving the 10^{13} ohm-cm readings.

The conclusion from the physical parameter study of the selected materials is that Epon 825 with HV hardener appears from its physical parameters to be the most promising. When a resin is to be used as an embedment material for electromagnetic components, the dominant considerations must be the reliability and favorable behavior under the functioning environment, with economic considerations secondary.

3.2 OUTGASSING DATA

The outgassing properties of the materials were the subject of a survey of the NASA and Hughes Aircraft Company data on all 40 materials. An understanding of the test methods used to simulate outgassing is required if the data submitted on these materials is to be used correctly in evaluating the suitability of a material for a given engineering application.

Outgassing is measured in the laboratory by heating a sample under vacuum for a specified amount of time and collecting the volatile condensable material (VCM) in some manner. The total weight loss (TWL) in percent and amount of VCM collected are the parameters used to evaluate the suitability of a material for a given application where outgassing is a concern.

Hughes Aircraft Company process specification HP6-26 describes an outgassing test method and apparatus. In this test the VCM is collected in a

TABLE 3-5. COMPARISON OF ELECTRICAL PARAMETERS

	Dielectric Strength			Dielectric Constant			Dissipation Factor			Volume Resistivity		
	Vendor	1st Test	ASTM D-149	Vendor	1st Test	ASTM D-150	Vendor	1st Test	ASTM D-150	Vendor	1st Test	ASTM D-257
Epon 825	400-500	Note 1	530	3.81	3.98	4.0	0.004	0.011	0.008	3×10^{12}	6×10^{15}	4.3×10^{13}
Hysol C-60	350	Note 1	486	4.0	Note 2	4.4	0.038	Note 2	0.04	7×10^{14}	Note 2	3.9×10^{13}
Hysol C15-015	350	Note 1	496	3.8	3.84	4.1	0.03	0.05	0.054	3×10^{17}	1×10^{15}	3.5×10^{13}
Scotchcast 255	375	Note 1	495	5.9	3.26	3.9	0.05	0.17	0.37	10^{15}	1.3×10^{15}	4×10^{13}
Eccoseal 1218	ND	Note 1	515	3.7	3.99	3.4	0.025	0.083	0.27	10^{15}	1.6×10^{15}	4.9×10^{13}
Note 1: Dielectric strength data not done in 1st test.												
Note 2: Material not available in time for test.												

qualitative manner. A total percent weight loss of 1.0 percent or more and/or a visual observation that the amount of VCM appears as a medium or heavy deposit on the collection surface is cause for rejection of the sample.

In recent years ASTM E595 (77) has become the standard outgassing test method. This test allows quantitative determination of the amount of VCM outgassed by a material, and is currently performed at White Sands Test Facility per NASA TND-8008 (1975). There are no pass/fail criteria with this method, material acceptability being determined for a specific engineering application. Data obtained from this test is published in NASA document JSC 08962, Rev. R. The Hughes compilation of data per HP6-26 and these NASA documents were the sources used in the data search.

Outgassing data on 20 of the 40 materials is listed in Table 3-6. Data is not available on the remaining materials. Factors such as cure cycle parameters, unreacted components, low molecular weight constituents and preconditioning of the sample before testing will affect the result of the test. Only the last parameter is explicitly included in the table. Because of these variables the tables should be used only as a guide for material selection, any program needing low outgassing materials should test the proposed materials/processes for their specific environmental requirements.

After the testing and evaluation of physical parameters was completed five materials were selected for continuing evaluation of other properties based on the preferred properties given in Table 3-1. Those materials selected were Hysol C-60, Hysol C15-015, Epon 825 (HV), Scotchcast 255 and Eccoseal 1218.

3.3 PROCESS EVALUATION

The physical properties of a resin system greatly influence the application process selected. A resin system with a moderately high vapor pressure either should not be used in vacuum impregnation or should have an excess of the high vapor pressure material initially to offset the losses during application. In general it is good policy to use low vapor pressure systems in vacuum impregnation and the higher vapor pressure systems for embedding. Viscosity, pot life, specific heat, thermal conductivity, and heat of exotherm all interact to affect the temperature of application and the batch size. The

TABLE 3-6. OUTGASSING DATA PER HP626 AND
NASA TND-8008 FOR 40 MATERIALS

Material	TWL (%)	VCM (%)	Reference	Preconditioning	
				Time (Hours)	Temp (°C)
GE 702	-	-	-	-	-
RTV 11	0.91	0.55	NASA	24	150
RTV 60	0.69	0.54	NASA	24	150
RTV 8110	-	-	-	-	-
RTV 619	1.30	0.50	NASA	24	25
RTV 615	1.01	0.77	NASA	24	150
RTV 616	1.41	0.66	NASA	1	100
RTV 670	1.25	0.59	NASA	1	125
RTV 655	2.72	1.27	NASA	24	150
RTV 627	-	-	-	-	-
Epocast 202	-	-	-	-	-
Scotchcast 255	-	-	-	-	-
Scotchcast 280	0.48	0.14	NASA	24	121
Scotchcast 281	0.35	0.02	NASA	12	100
Scotchcast 235	6.20	0.31	NASA	6	95
Scotchcast 237	-	-	-	-	-
Scotchcast 5237	-	-	-	-	-
Scotchcast 9	3.74	1.16	NASA	24	66
Eccoseal 63	-	-	-	-	-
Stycast 62	-	-	-	-	-
R 7501	-	-	-	-	-
Epon 825/HV	0.51	Trace	HP6-26	16	25
Eccoseal W-67	-	-	-	-	-
Eccoseal 1207	0.226	Light	HP6-26	-	-
Eccoseal 1218	2.04	0.35	NASA	12	125
GE 707	-	-	-	-	-
Hysol C15-015	1.45	0.10	NASA	16	100
Hysol C60	1.01	0.11	NASA	24	88
Hysol C9/H2-3561/ PC 1224	0.50	0.00	NASA	24	25
E204A/9816	-	-	-	-	-
E204A/9652	-	-	-	-	-
Uralane 5753 (A/B as 1/5 BW)	1.01	0.02	NASA	14	38
Conathane EN2	-	-	-	-	-
Conathane EN9	0.44	0.00	NASA	0.5	RT
Conathane EN9-07R	-	-	-	-	-
Conathane EN11	0.38	0.01	NASA	24	50
Conepoxy Y-1000/07	-	-	-	-	-
Conepoxy IM 1145	-	-	-	-	-
RN1600	-	-	-	-	-
R 7521	-	-	-	-	-

five materials: Scotchcast 255, Hysol C15-015, Hysol C-60, Eccoseal 1218 and Epon 825 (HV) were tested for pot life both with and without external heating to maintain the pouring temperature.

3.3.1 Viscosity Determination of Selected Materials

The systems were warmed to the following temperatures prior to mixing:

Hysol C-15-015	90°C
Hysol C-60	75°C
Epon 825 (HV)	75°C
Scotchcast 255	70°C
Eccoseal 1218	50°C

The first viscosity tests involved mixing the resins at the above temperatures and the viscosity readings taken without additional heating. The second viscosity test involved mixing the resin at the above temperatures and maintaining those temperatures during the test. Both sets of data are plotted in Table 3-7 for comparison. The Pot Life (PL) and the Total Working Time (TWT) is defined as the time intervals when the viscosity become twice and four times the initial value, respectively.

With the exception of the Epon 825 (HV) resin, the continuous heating of the resin reduces the viscosity and lengthens the pot life and the total working time. In the case of the Epon resin systems the hot viscosity is an order of magnitude lower than the unheated resin. Further work on the viscosity of the Epon 825 (HV) system determined that heating the resin 50 minutes at 75°C was necessary before the resin increased its viscosity to 1000 cps. However, if the resin was heated for more than 50 minutes, it started to noticeably exotherm. Reducing the temperature to between 55°C and 60°C should provide a longer pot life, with an increased viscosity for this material.

The vapor pressure data from the manufacturer's data and the manufacturer's suggested applications divide the materials into two groups: the embedding resins and the vacuum impregnating resins. Scotchcast 255,

TABLE 3-7. POT LIFE AND TOTAL WORKING TIME

Material	Without Additional Heating		With Additional Heating	
	Elapsed Time, min	Viscosity, cps	Elapsed Time, min	Viscosity, cps
Hysol C15	0	3,500	0	200
	35	7,000 Pot Life	152	400 Pot Life
	75	14,000 Total Working Time	175	800 Total Working Time
Epon 825 (HV)	0	3,500	0	75
	35	7,000 Pot Life	30	150 Pot Life
	60	14,000 Total Working Time	32	300 Total Working Time
Hysol C-60	0	650	0	150
	20	1,300 Pot Life	85	300 Pot Life
	45	2,600 Total Working Time	185	600 Total Working Time
Scotchcast 255	0	1,400	0	1,500
	11	2,800 Pot Life	105	3,000 Pot Life
	22	5,600 Total Working Time	175	6,000 Total Working Time
Eccoseal 1218	0	500	0	300
	55	1,000 Pot Life	95	600 Pot Life
	165	2,000 Total Working Time	180	1,200 Total Working Time

Hysol C60 and Hysol C15-015 are the embedding resins, while Epon 825 (HV) and Eccoseal 1218 are impregnation resins.

3.3.2 Process Evaluation of Low Stress Embedment Materials

The materials selected for the low stress embedment study from a processing standpoint were Conap EN-9, Conap EN9-OZR, Conap EN-11, Uralane 5753, Scotchcast 255, Scotchcast 9, RTV 615, RTV 619, RTV 627 and RTV 655. This processing study was done simultaneously with the pressure calibrated thermometer method of measuring embedment stresses as described in 3.4.4.1. All were processed according to the cognizant Hughes Process document, when one existed, otherwise to the manufacturer's instructions. Each of these materials was judged according to the ease of use in a production application. The areas of importance considered were; mix ratio, degassing ease, and excess material removal. As considered in the vendor data survey, 3.1, the materials with numerically small mix ratios, e.g., 3:2, 1:1, 5:1 or even 10:1 were easier to measure than products with a mix ratio of 17.5:100. When a small amount was needed materials with mix ratios of 1:1 or 3:2 were easier to mix accurately than a mixture of 10:1 ratio. RTV 627 and the Scotchcast epoxies were the easiest to mix.

In general, the silicone rubbers were the easiest mixtures to degas; the epoxies were the next, and the urethanes were the hardest.

Removal of excess material (flash) or that required to expose and repair an embedded assembly is of serious concern when evaluating a resin for production applications. A good, practical simulation of this is the recovery of the fragile thermometers embedded in the material after temperature cycling is completed.

The silicones, as a group, were the easiest from which to remove excess material. The medium hardness, clear silicones, RTV 655 and 615, were the easiest overall for this process, with a utility knife as the only tool required. The transparency of the cured resin allowed the technician to see where the thermometer bulb was located so that the process proceeded rapidly without fear of damage. The RTV-627 had nearly the same hardness as the RTV 615 and should therefore be removed from the bulb with the same ease, but the opacity of the RTV 627 required the

technician to exercise more care when removing the cured material so that the thermometer would not be damaged. The RTV 619 was so soft and sticky that mold release coated aluminum molds adhered to the cured resin more strongly than did the resin to the thermometer or even to itself. To successfully encapsulate the pressure calibrated thermometer with RTV 619, it was necessary to use a teflon sheet as a mold liner. Based on this experience the RTV 619 should only be used for potting applications where the mold remains as part of the final assembly.

The epoxy parts permitted small amounts of excess material to be removed using only a utility knife. For removing large amounts of epoxy a soldering iron and a knife was used to heat up and dig out the material. Obviously, the process was very slow and laborious.

The urethanes were, in many respects, just as difficult to remove excess material as the epoxies. Instead of the soldering iron heating up the resin so that it could be dug out with a knife, as with the epoxies, the urethane material melted resulting in the additional complication of the fumes given off by the molten urethane containing cyanogen so that a special fume hood was needed.

All of the materials evaluated have their advantages and their drawbacks. All of these materials can be cured using several different schedules which usually can be selected so that production costs and schedules can be optimized.

3.4 LOW STRESS EMBEDMENT TECHNIQUES AND MATERIALS

The embedment of devices with pressure sensitive cores, and small devices using fine wire is a serious problem. Devices using cores of ferrite, powdered iron, and to a lesser extent, Fe-Ni and Si-Fe exhibit characteristic inductance changes when the cores are stressed by the encapsulating material. Transformers with bobbin type windings are encapsulated with a teflon insert where the core should be. This insert is removed after curing and the core, either "C" type or stacked, is inserted and strapped in position. This procedure eliminates the pressure upon the core, but the extra manufacturing steps increase the cost.

Also toroidal designs can not be constructed in this manner because the core is one piece rather than two parts which can be strapped together.

At present, the toroidal cores are placed within an aluminum protective case to remove the stress from the core. This case adds weight, bulk, and cost to the finished product. The breakage of very fine wire wound devices often is due to the thermal expansion differential between the wire and the embedding material.

3.4.1 Fine Wire Assembly Techniques

The fine wire assembly problem was investigated using fine wires strung between two posts across a mandrel in order to eliminate stress concentration as shown in Figure 3-1. Further analysis of the test specimen showed that the geometry effects were so much larger than any material effects, so, at best, the latter would be second order from the test data obtained. It is recommended that single strand lead-out wires smaller than 36 AWG not be used. Any number of alternate methods may be used, such

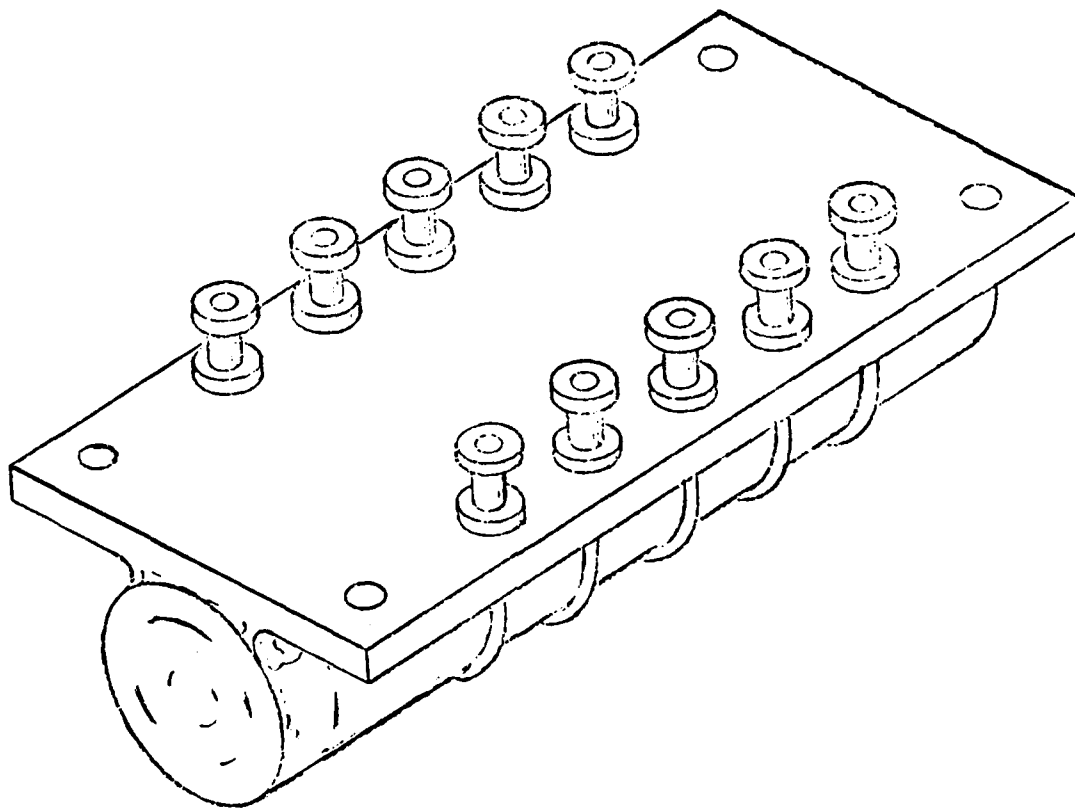


Figure 3-1. Fine wire test assembly.

as twisted multiple strand self leads, reinforced multiple twisted leads or intermediate wires of 36 AWG or larger

3.4.2 Selection of Materials

Ten prospective potting compounds were chosen from an original field of over forty materials shown in Table 3-2. These included: Conap EN-9, EN-9-QZR, EN-11; General Electric RTV-615, RTV-619, RTV-627, RTV-655; Scotchcast 9, 255; Uralane 5753. Hartel 17024 GA was added as a promising material for encapsulation after Table 3-2 was completed. These compounds include urethanes, silicone rubbers, and epoxies. Some of these materials are presently being used and therefore provide a base line with which to compare the other materials in fine wire and pressure sensitive core applications. The materials were first evaluated for electrical parameters, followed by a further selection process using the mechanical, thermal and physical parameter data available.

For low embedment stress, the important parameters are: low shrinkage during cure, low glass transition temperature, low hardness and low coefficient of thermal expansion. Some of these properties are in opposition to one another, so that an engineering tradeoff is needed. Although moisture absorption and outgassing parameters were of secondary import, the materials lacking hydrolytic stability were rejected without further study. The thermal requirements for the candidate materials was that each be capable of passing a thermal cycling test of at least ten cycles over a temperature range of -55°C to 130°C . The various parameters given above are to assure this result.

Mechanical requirements for embedment of pressure sensitive core/ fine wire magnetic devices are two fold: (1) the material must support and protect the device, (2) the material must not exert sufficient pressure to change the electromagnetic characteristics of the device over the required temperature range. The requirements of hydrolytic stability, outgassing and moisture absorption provide assurance of physical integrity under adverse environmental conditions.

3.4.3 Relative Material Costs

Comparative cost of the various materials have been obtained. Table 3-8 shows unit package cost estimated material and cost for a gallon of mixture.

TABLE 3-8. MATERIALS COST

Material	Available Package Size						Cost per Gallon (Est)
	9 1/2 lb	10 lb	12 lb	18 lb	20	22 lb	
EN-9							
EN-9-OZR	\$37.25						\$37.25
EN-11			\$44.00				\$29.33
RTV-615		\$103.40					\$82.72
RTV-619		\$108.90					\$87.12
RTV-627						\$102.08	\$51.04
RTV-655		\$162.00					\$129.60
SC-9					\$95.60		\$47.80
SC-255				\$65.52			\$36.40
Hartel				\$103.60			\$51.80

3.4.4 Test of Materials

In order to compare the pressures exerted by the subject encapsulation materials on a magnetic component, the material stresses must be measured as a function of temperature. No standard procedure or equipment is available to make these measurements. Embedment of small pressure transducers in the test material and then temperature cycling is the obvious approach, but usually is not considered practical. Because the transducers are expensive, they must be recoverable from the embedment without damage, which is a major operation with the harder materials. The shape

and size of existing transducers are not representative of the magnetic components being potted or encapsulated.

Previously, several investigators have measured the pressure exerted by the potting compounds on embedded parts by the novel approach of using pressure calibrated mercury thermometers: namely, Dewey and Outwater (Ref. 5.2), Isleifson, Swanson (Ref. 5.3) and Bunker and Kloeze-man (Ref. 5.4). The advantages of the thermometer approach are: simplicity, low cost, inscribed serial no's, small size of the pressure sensing element (the bulb), extreme linearity of calibration, and elimination of temperature effects by subtraction of thermocouple readings. Disadvantages are fragility, non-electrical readout and temperature range limitations. Consequently, the unaltered thermometer approach described in Ref. 5.3, 5.4 was selected by Hughes to evaluate the various low stress embedment materials individually, and in combination for anticipated greater stress reduction. For example, an otherwise satisfactory embedment material that exerted a high stress on magnetic components embedded in it, might have such stress alleviated by a dip or conformal coat of a softer material.

To eliminate the disadvantages of the thermometer method, but still use the available pressure and temperature calibration facilities, Hughes fabricated small inductors with pressure sensitive cores. It was thought that such inductors could be calibrated individually by measuring their inductances as a function of temperature and pressure separately. It was expected that embedment of these inductors in the various materials being investigated would then give a measure of the embedment stresses being generated by subtracting out the temperature effects.

Both methods are reported in this section, but the thermometer method was found to be much more successful than the pressure sensitive inductor, which now is realized requires more effort and time to perfect the method than was available on this program.

3.4.4.1 Pressure Calibrated Thermometer Approach

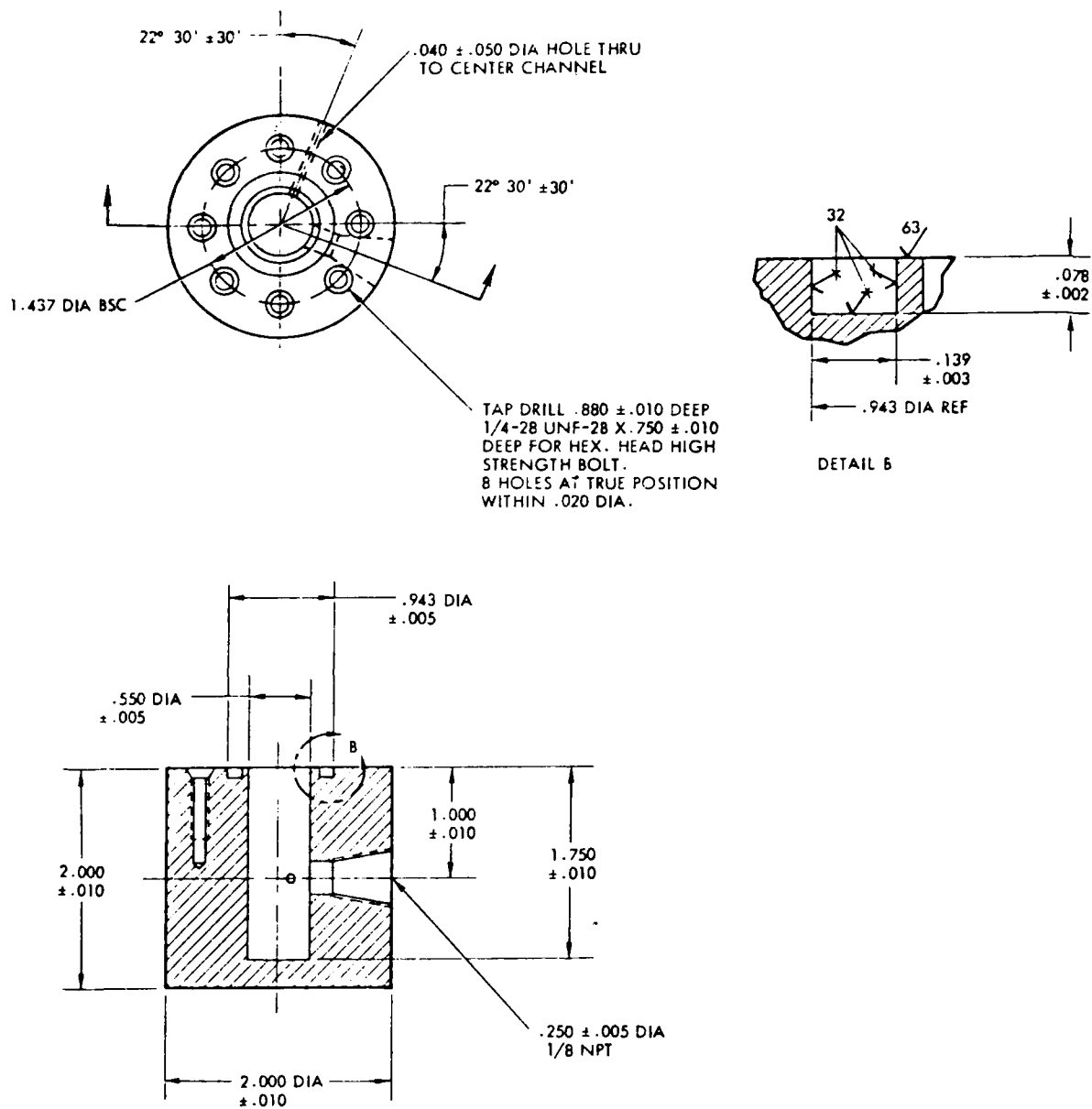
Because of the general unfamiliarity of the method of using pressure calibrated mercury thermometers, a complete step by step procedure which

was followed by Hughes is given, including dimensioned sketches of the specially fabricated parts.

A pressure pot and headers were initially fabricated to the dimensions shown in Figures 3-2 and 3-3 respectively. The pressure pot drawing shows one 1/4 in. diameter hole with a 1/8-in. female pipe thread on the side which is the hydraulic fluid inlet. Subsequently, two more identical holes were drilled at 120° to this hole so that inductors in the pot can be electrically connected to external measuring equipment, and a thermocouple to measure the hydraulic oil temperature, both used with 1/8 in. pipe plugs modified with insulated wires passing through them.

The 1/8 in. female pipe thread in the header serves two purposes. First, installing a pipe plug in the header allows the hydraulic system to be proof tested to its maximum pressure. Second, the cavity in the header serves as a conical-shaped enclosure for the material used to bond the thermometer to the header. Under pressure calibration, the material in the header flexes outward wedging the bonding material against the thermometer and header so as to seal against leaks. After calibration, the header serves as a mount and cover plate for the mold used to contain the encapsulating material undergoing tests.

Instead of using a pressure intensifier or a deadweight tester directly, both of which were not available, it was decided to use the hydraulics laboratory pressure gauge, calibrated with the Hughes Secondary Standards pressure calibration procedures and equipment. In reference (4), a method of using a Polaroid camera to photograph the readings of the various thermometers through the window, and correcting for parallax to obtain the data at each chamber temperature was discarded in favor of direct visual readings in the interest of simplifying the experimental procedure, since the accuracy of a dead weight tester in the calibration procedure was not available. Because of greater than anticipated spreads of data points in the final analysis it is recommended for future work that the dead-weight tester and photographic readout be reinstated.



NOTES - UNLESS OTHERWISE SPECIFIED:

1. REMOVE ALL BURRS AND SHARP EDGES .003 MIN - 0.010 MAX
2. MACHINED FILLET RADIUS 0.010
3. AISI 416 SS, QQ-5-763B

Figure 3-2. Pressure pot.

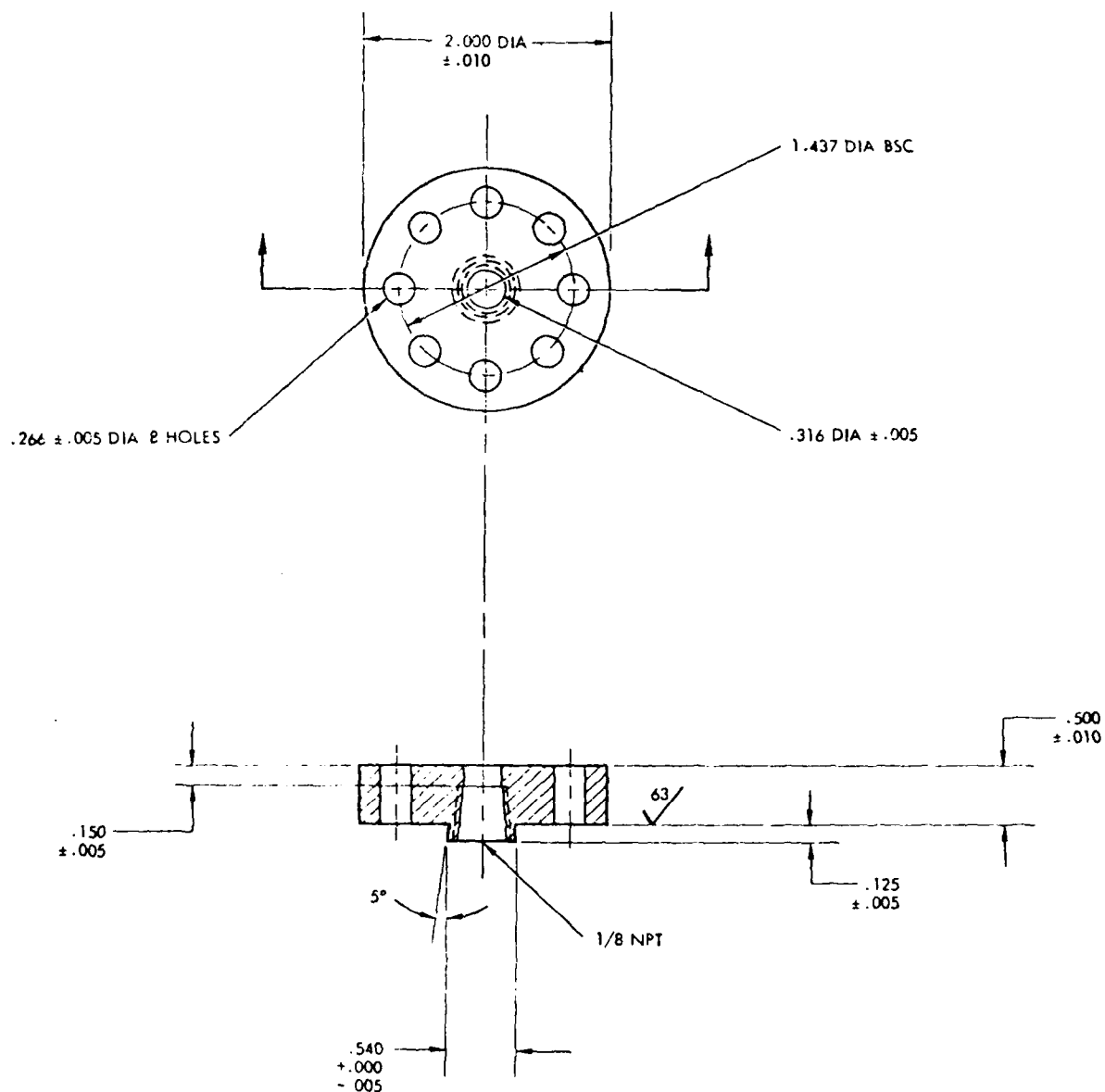


Figure 3-3. Header.

A. MOUNTING OF THERMOMETERS

The thermometer is mounted in a header which serves both as a cover for the pressure pot, and an end for the mold. A detailed, proven technique is given step by step below.

1. Equipment Required for Mounting

The following equipment is required for mounting of the thermometers:

- a. Thermometers -40°F to $+220^{\circ}\text{F}$, 1°F graduations
- b. Headers (aluminum).
- c. Polyethylene syringe - Biggs No. 10.
- d. Balance scale for weighing EC 1614 (Triple Beam Balance, Western Scale Company).
- e. Mounting stand.
- f. EC 1614 (3M Company), Parts A and B or equivalent.

2. Procedure for Mounting

The following steps detail the procedure followed in mounting thermometers into the header:

- a. Thoroughly clean the header and thermometer, in order to remove any surface dirt and/or grease.
- b. Set up a mounting stand to hold the header perpendicular to the thermometer while bonding the thermometer to the header. A photograph of the mounting stand with thermometers and headers ready for bonding is shown in Figure 3-4.
- c. Prepare 10 g of EC 1614 (3M Company), using 5 g of Part A and 5 g of Part B.
- d. Combine Parts A and B and blend thoroughly until a creamy yellow substance is obtained.
- e. Ensure that the header and thermometer are at room temperature 21°C (70°F) when the EC 1614 is applied.
- f. Record the serial number of the thermometer for identification purposes.
- g. Place the thermometer through the center hole in the header, allowing from $3/4$ in. to 1 in. of the bulb end to protrude through the bottom side of the header.
- h. Apply the EC 1614 so that it fills the space between the thermometer and header, leaving no air bubbles, with about a $1/4$ -in. fillet on both the top and bottom of the header.
- i. Allow the EC 1614 to cure at room temperature for 24 h before calibration.

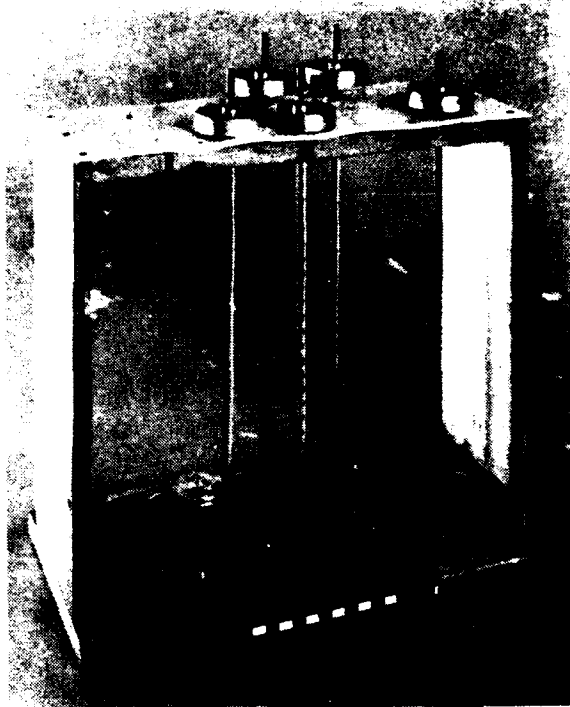


Figure 3-4. Thermometers ready for bonding to headers.

B. CALIBRATION OF THERMOMETERS

The objective of the calibration phase of this procedure is to determine the pressure coefficient of the thermometer in psi per °F. Figure 3-5 shows the pressure pot and thermometer connected to the hydraulic test setup.

1. Equipment Required

- a. Thermometer bonded to header.
- b. Pressure calibration setup.

2. Procedure

- a. Mount thermometer and header with its O-ring, on the pressure pot which is then connected to the calibration setup and tighten bolts finger-tight. Refer to Figure 3-5.
- b. Bleed air out of the system by operating the manual hydraulic pump slowly until air-free oil seeps out under the header, and then tighten the bolts to seal the pressure pot.
- c. Take readings of thermometer readings in steps of 1000 psi from 0 psi to 7,000 psi, and return to 0 psi.



Figure 3-5. Pressure calibration of thermometer.

- d. Average the thermometer readings for each up and down 1000 psi increments to balance out temperature effects, then subtract the thermometer reading at 0 psi from all to get ΔT .
- e. Plot ΔT as a function of applied pressure, and draw a straight line through these points. The slope of this line gives the pressure calibration of the thermometer in psi per $^{\circ}F$.

C. PREPARATION OF TEST SAMPLES

Following calibration, the thermometer is left in the header which serves as a part of the mold for the embedment compound. The header also serves to distribute the stresses on the glass stem of the thermometer so as to minimize breakage during handling and encapsulation. From the references it was found, that removing the thermometers from the headers and embedding them alone in the encapsulant material resulted in excessive breakage, both from handling as well as from stresses exerted on the stem where the thermometer emerged from the material.

The mold is designed to produce a 1-in. diameter standard configuration of test material is shown in Figure 3-7. A photograph of the three major stages in test sample preparation

are shown in Figure 3-6. A thermocouple is embedded near the bulb to indicate when the sample reached temperature equilibrium with the chamber. Three samples were used for each material in order to detect erratic data which can be due to defective sample, poor adhesion, or a broken thermometer bulb.

1. Equipment Required for Preparation of Test Samples

- a. Thermometer and header.
- b. Mold (aluminum).
- c. Embedment material.
- d. Thermocouple.
- e. Release agent (Miller and Stephenson Chemical Company S-122 Fluorocarbon or equivalent).
- f. Zinc chromate primer (Sprayon Products, No. 611 Green or equivalent).
- g. Masking tape.
- h. Thermofit tubing.

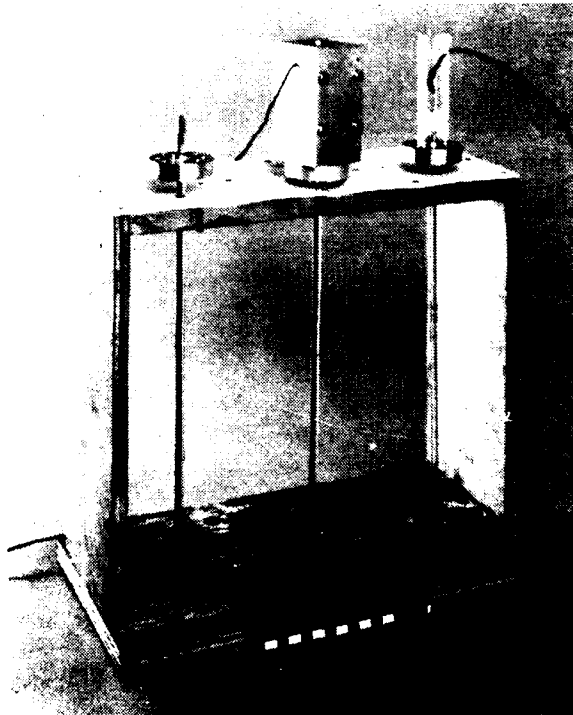
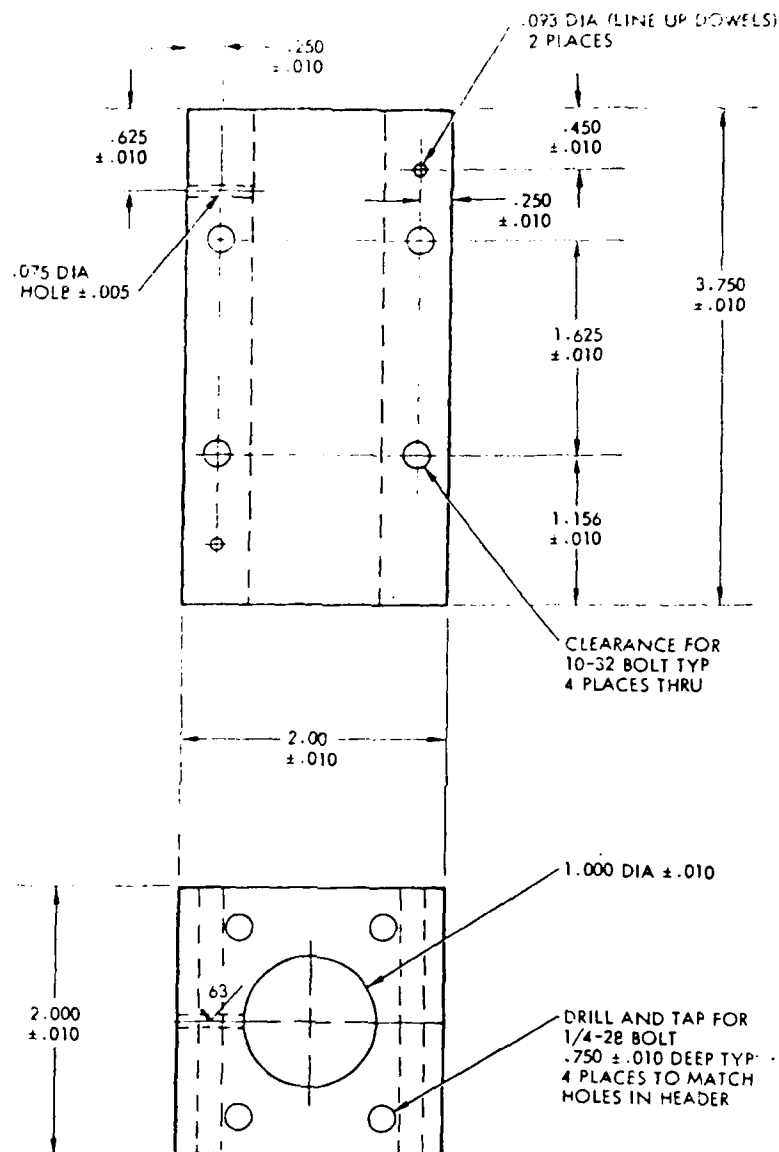


Figure 3-6. Three stages in test sample preparation.



NOTES - UNLESS OTHERWISE SPECIFIED:

1. REMOVE ALL BURRS AND SHARP EDGES .003 MIN - .010 MAX
2. MACHINED FILLET RADIUS .010
3. POLISH INSIDE OF 1.000 DIA HOLE, MATCHING EDGE MILLED TO GOOD FIT.
4. MATERIAL - 6061-T6 ALUMINUM

Figure 3-7. Mold.

2. Procedure for Preparation of Test Samples

- a. Thoroughly clean the mold, thermometer, and header surfaces to remove any surface dirt/or grease.
- b. Mask the thermometer bulb and apply a coat of zinc chromate primer to the header, to ensure that a good bond to the encapsulant will occur.
- c. Spray the interior of the mold, not the header, with a release agent.
- d. Mount the header and thermometer to the mold together with the thermocouple to be embedded. The thermocouple junction should be 1/32 in. to 1/16 in. from the bulb with the tie lead wire at a greater distance from the bulb. Use Thermofit tubing to protect the thermocouple wires emerging from the embedment material.
- e. Pour the embedment material to be tested into the mold and allow it to cure in accordance with material specifications.
- f. After the embedment material has cured, remove the mold from the material, header, and embedded thermometer.

D. EMBEDMENT PRESSURE MEASUREMENT PROCEDURE

This section covers the techniques used at Hughes Aircraft Company to obtain the internal pressures generated by the encapsulating material as a function of temperature. A number of test specimens prepared in accordance with 3.4.4.1 were placed in the temperature chamber which had a window in the door. The samples were arranged so that each can be clearly seen through this window as is shown in Figure 3-8. As mentioned before the photographic method to read out the data at the various temperature points would have been of advantage because of increased accuracy of reading and the use of Polaroid photographs establishes a permanent record which can be referred to at a later date.

1. Equipment Required for Embedment Pressure Measurements

- a. Oven (Missimers, -125°F to 425°F, Model No. FT2-100 x 350 or equivalent).
- b. General Radio GR1633-A or equivalent.
- c. Embedded thermometers.

2. Procedure for Embedment Pressure Measurement

- a. Place the test specimens (thermometer, thermocouple, header, and embedment material) into the test oven on a foam rubber cushioned holding fixture.



Figure 3-8. Encapsulated thermometers in temperature chamber.

- b. Connect each test specimen thermocouple to the bridge, just before making a reading (unless a multichannel chart recorder is used).
- c. Take temperature readings for each of the embedded thermocouples, for each of the bulbs, as well as for the oven as the oven temperature is varied in 40°F increments as follows:

<u>FROM</u>	<u>TO</u>
Ambient	220°F
220°F	-40°F
-40°F	Ambient

- d. Allow 30 min between readings to enable the oven to stabilize or for the temperature difference between the embedded thermocouple and the oven thermocouple to be less than 5°F.
- e. Determine the pressure on the bulb by calculating the difference between the thermometer bulb temperature reading and the embedded thermocouple reading, and multiplying by the pressure coefficient of the thermometer.
- f. Plot the temperature (°F) of the embedded thermocouple versus the pressure (psi) on the bulb.
- g. After completion of the test, disconnect the thermocouples and remove the embedment material from the bulb so that the thermometer can be reused.

E. EMBEDMENT ADHESION AND REMOVAL

The use of a tapered lip on the header gave extra surface area to which the embedment material could adhere. In only one case was there adhesion problems. The ETV 619 adhered more strongly to the mold-released aluminum molds than it did to the glass thermometer. The use of a thin teflon sheet to line the mold allowed the resin to remain attached to the glass thermometer when the mold was removed.

Another problem was encountered in attempting to remove tested embedment material from the thermometer bulb so that the mounted and calibrated thermometer could be reused. The technique finally arrived at for removing the tested material consists of removing the major portion of the material either with an Exacto knife alone or in conjunction with a soldering iron. The use of a grinder or a lathe was considered inappropriate because the tested materials were too soft. The remainder of the material was removed with an epoxy stripper. The major portion of the material has to be removed before the epoxy stripper was used or the expansion of the material would usually break the thermometer at the stem.

3.4.4.2 Pressure Sensitive Core Approach

A major effort of this program is the selection of materials and processes to achieve stress-free embedment of magnetic components, because many core materials are sensitive to stresses. Extensive precautions in manufacture and handling are taken by manufacturers to eliminate stress effects on core materials by coating them with a soft material, or enclosing them in non-magnetic boxes or enclosures. Based on this information, it was proposed that inductors using pressure sensitive cores could be used to measure the stresses generated by embedment materials, if they could be suitably calibrated with inductance as a function of pressure. This could be accomplished with the pressure pot used to calibrate the thermometers described in 3.4.4.1. An additional benefit would be the direct measurement of the effects of mechanical stress on the core. All core manufacturers warn of the deleterious effects on the magnetic properties of stressing the core, but none have any experimental data or quantitative results to show.

Pressure calibrated inductors could overcome the major disadvantages of the thermometers namely, fragility, limited temperature range, and non-electrical readout. Some of the advantages of the thermometers would still be retained; i.e., low cost, even smaller size. The temperature limits of core magnetic materials range from the Curie point on the high end to cryogenic on the low. A simple inductance bridge would be used as the readout.

Samples of three different types of toroidal core materials considered to be very stress sensitive, some in different sizes, were obtained as listed below in Table 3-9. The only size limitation was that the completed inductor must fit in the 0.55 in. dia hole in the pressure pot.

The plan to use these inductors as stress measuring devices or transducers in various embedment materials was as follows: To calibrate these inductors it is necessary to determine both the pressure-inductance and temperature-inductance curves. Embedding an inductor in a test material, curing it in accordance with applicable specifications, then

TABLE 3-9. PRESSURE SENSITIVE CORE DATA

Material Type	Mfgr.	Mfgr. Designation	Size			Total Quantity	μ at 25°C	Curie Temp
			ID	OD	Th			
Ferrite Note 1	TDK	H5B2T	2 mm	4 mm	1 mm	4	8,000	136°C
	TDK	H5B2T	3 mm	6 mm	1.5 mm	4	8,000	
	TDK	H5B2T	4 mm	8 mm	2 mm	4	8,000	
MPP (moly-permalloy powder)	Magnetics, Inc.	55031-M4	0.156 in.	0.310 in.	0.125 in.	4	60	460°C
	Magnetics, Inc.	55038-M4	0.200 in.	0.400 in.	0.156 in.	4	160	
Fe-Ni 49 Square-mu wound core Note 2	Magnetic Metals	CC433U4602	0.375 in.	0.438 in.	0.125 in.	15	35,000	480°C
Note 1. Parylene coated								
Note 2. Uncased								

temperature cycling it and measuring the inductance. The difference between the inductance measured in the test material and the inductance of the unpotted device at that same temperature, should, from the pressure-inductance curve, give the stress being exerted on the test inductors by the material.

In order to determine if the change of inductance with pressure is a function of the inductance itself, two different inductances were wound on the ferrite and Moly Permalloy Powder (MPP) cores using, in all cases, AWG 32 wire. The minimum inductance was one layer, perfect lay, on the cores. The maximum, on the other hand, was winding as many turns as possible on the core by hand, resulting in essentially zero I.D. Because of the larger OD of the Fe-Ni cores, only the minimum inductance was wound, as the larger one would not fit into the pressure pot.

Also, the inductance values are a function of the inductance bridge driving voltage. Measurements of inductance vs driving voltage at 1 kHz were made. It was found that, for all inductors, as the driving voltage was increased from zero, the inductance would increase to a peak value. A further increase in drive voltage would cause the inductance to decrease, and continue decreasing until third harmonic distortion occurred in the drive voltage, as the core saturated. Further increase in drive would cause the inductance curve to flatten out, then, in some cases increase slightly. It was not known at which drive level the inductor would be most sensitive to pressure levels, so runs at different drive voltages were made with the inductors in the pressure pot. Percentage-wise, it was found that there was not much difference, so the sinusoidal drive voltage which gave the peak inductance was used in all cases, since this made it easier to measure with the inductance bridge.

A summary of the inductors wound for the embedment tests reported in inductance values and average changes in inductance with temperature/pressure is shown in Table 3-10. This table shows several interesting features. The number of turns has no significant effect on the change of inductance with pressure; the percentage change is the same. Ferrite cores show a negative or decreasing inductance with pressure, while the MPP cores have a positive characteristic, although much less. The Fe-Ni cores

TABLE 3-10. TEST INDUCTOR DATA

Core Material	Size	No. Turns AWG 32	Qty.	Normal Inductance, mH	$\Delta L/10K$ psi avg.	$\Delta L/^{\circ}F$ Avg.			Coil S/N
						-37 $^{\circ}$ to +40 $^{\circ}$	+60 $^{\circ}$ to +160 $^{\circ}$	+200 $^{\circ}$ to +240 $^{\circ}$	
Ferrite	2-4-1	20	2	0.458	-53.8%	+0.28%	-0.054%	-0.41%	1, 2
		36	2	1.66	-50.5%	-0.57%	-0.30%	-0.90%	51, 52
Ferrite	3-6-1.5	34	2	2.21	-30.5%	+0.24%	-0.10%	-1.13%	3, 4
		90	2	15.9	-36.2%	+0.31%	-0.13%	-3.11%	53, 54
Ferrite	4-8-2	44	2	5.25	-57.8%	+0.25%	-0.23%	-1.48%	5, 6
		140	2	49.3	-54.1%	+0.27%	-0.071%	-0.12%	55, 56
MPP	031	50	2	0.066	+2.3%	No Significant Change			1, 2
	031	120	2	0.367	+3.8%				3, 4
MPP	038	64	2	0.350	+10.6%	No Significant Change			5, 6
	038	200	2	3.42	+10.2%				7, 8
Fe-Ni	433	120	14	6.88-10.0	No Significant Change	Data Very Scattered ~0.16%			1-16

show no significant change in inductance with pressure. In the case of temperature, MPP cores exhibit zero temperature coefficient simplifying the reduction of data for encapsulated or potted inductors. However, the small percentage change with pressure compared to ferrite imposes more stringent requirements on the measuring equipment.

An unexpected result was the lack of pressure effects on the Fe-Ni coils. This wound core material is from a family of materials considered extremely sensitive to stress; consequently, they are inserted in core boxes by the vendor to prevent any possible stresses during winding and embedment. Perhaps it is unequal or non-isotropic stress that the core is sensitive to as contrasted to the isotropic stresses created by hydrostatic pressures in the pressure pot. In other words, the damping effects of oil at high pressures on the magnetostriction of the iron-nickel cores are not significant.

3.4.5 Embedment Pressure Measurement Investigation

Results of both the pressure calibrated thermometer method and the pressure sensitive core method of measuring the embedment stresses as a function of temperature for selected low stress encapsulation materials are reported in this section. As mentioned before, the parameter which has the most significance for low stress embedment materials is the glass transition temperature. Above this temperature most materials exert average stresses less than 100 psi; below the stress increases markedly as the material becomes harder and usually more brittle. Obviously, then, low stress materials should have glass transition temperatures lower than the lowest to be encountered by the embedded component.

It appears that the curves are more understandable and representative from the thermometer data than the pressure sensitive inductances, notwithstanding the disadvantages of the thermometer over the inductance. Further work needs to be done with the pressure sensitive inductors to account for the erraticity and excessive values of compressive stresses calculated before confidence can be established with this method. A possible explanation of the high values of stress obtained are given in 3.4.4.2.

The materials tested with both methods are summarized in Table 3-11, which gives the number of samples run. In the plotted curves following, individual points of each run are shown as triangle (Δ), square (\square), or diamond (\diamond), respectively, and the average of the points at a given temperature as circles (\circ). If the points are close together, then the average points are not shown:

TABLE 3-11. MATERIAL-TEST METHOD MATRIX

Material	Test Methods Used			
	Thermometer	Fe-Ni Core	Ferrite Core	MPP Core
RTV615	3	1		1
RTV619	3	1		1
RTV627	3	1		1
RTV655	3	1		1
CONAP EN-9	3	1	1	1
CONAP EN-90%R	3	1	1	1
CONAP EN-11	3			
URALANE 5753	3	1		1
Scotchcast 255	3	1	1	
Scotchcast 9	2			
Scotchcast 255 + RTV619		1	1	
Scotchcast 255 + RTV627		1	1	
Scotchcast 255 + EPOLENE C/AC617		1	1	

3.4.5.1 Thermometer Pressure Measurement Results

The differences between the thermocouple readings and the embedded thermometer readings were calculated, and multiplied with the thermometer calibration factor of $67 \text{ psi}/^{\circ}\text{F}$ which was characteristic of nearly all thermometers. To show the spread in the data the pressure exerted on the embedded thermometer as a function of temperature by Scotchcast 255 is plotted for three samples separately in Figure 3-9. First of all, it is obvious that the samples exerted increasingly high stresses as the temperature was decreased. Second, there is an appreciable scatter of points, and third, some of the points are negative, which would appear that the material is in tension rather than in compression. Careful analysis and comparison with previous results by one of the authors (Bunker) indicates that the scatter and negative points are due to inaccuracies in the readings; and compounding the error of the difference when the two numbers are nearly equal. Considering that the scatter is random, then averaging the three sets of points at each temperature should balance out some of the errors. The curve drawn in Figure 3-9 represents the average.

Extending the tangent to this rapidly rising line back, results in intersection of the x-axis between 85°F and 95°F , which is defined as the glass transition temperature. The value using the Dupont Thermal Analyzer is 35°C , or 95°F . This is remarkable agreement between two totally different determination techniques, providing confidence for the use of thermometers as pressure gauges.

Scotchcast 9 also passes through its glass transition temperature of approximately 60°F , as can be seen from its graph of pressure as a function of temperature in Figure 3-10.

All of the points from three samples of Uralane 5753 are plotted in Figure 3-11 showing the scatter and lack of any trend. Averaging the readings at each temperature and replotting gives a somewhat better picture in Figure 3-12. No glass transition temperature is observable at the low end, but it appears that a gradual increase is taking place at the high end, which is also the case with RTV 615, Figure 3-13, and RTV 655, Figure 3-14.

RTV-627 shows no such rise at either end as plotted in Figure 3-15. The points are close enough that a plot of the average is not needed to observe the trend. The same is true for RTV 619, Figure 3-16.

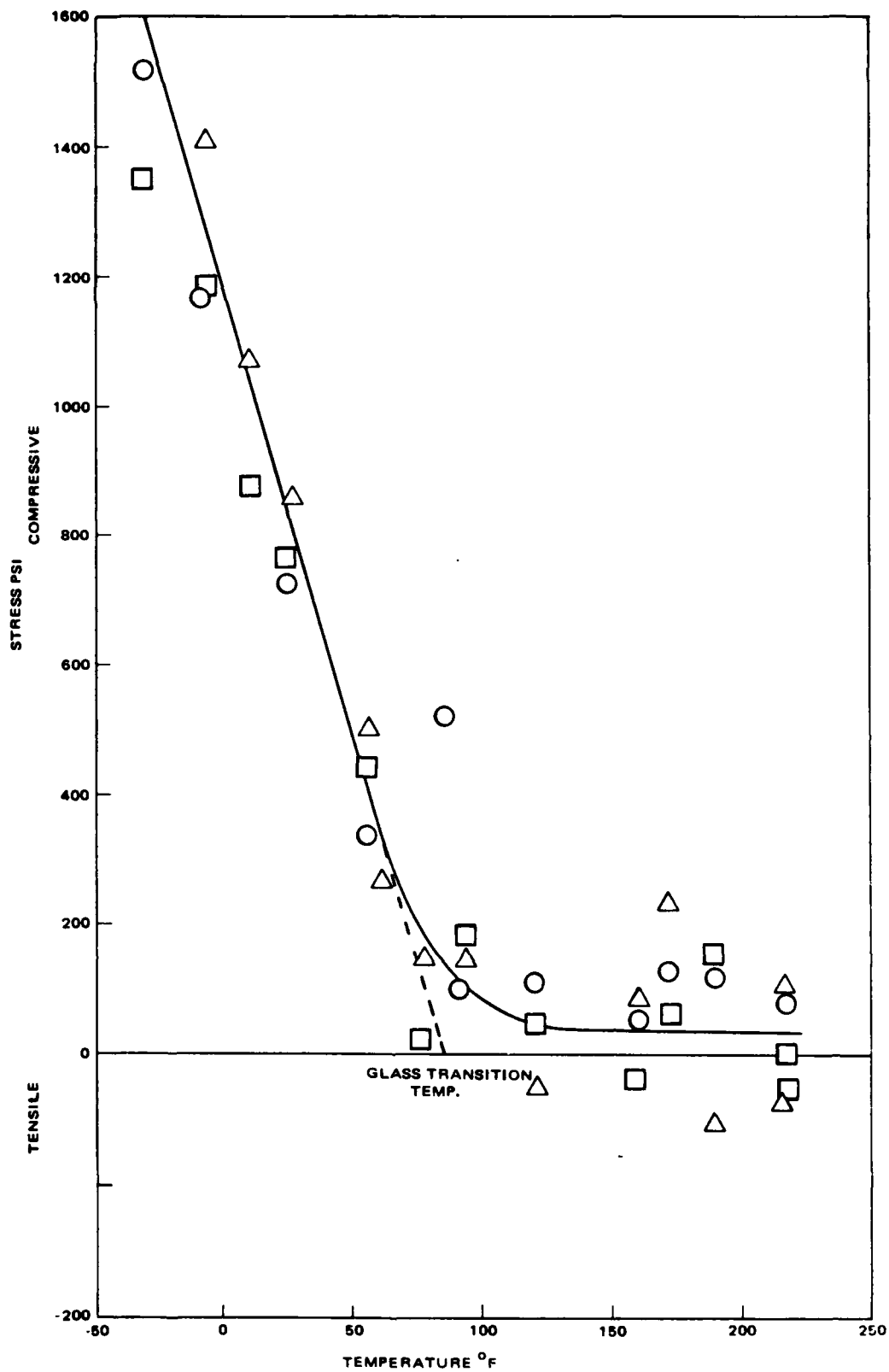


Figure 3-9. Scotchcast 255 stress vs temperature, thermometer method.

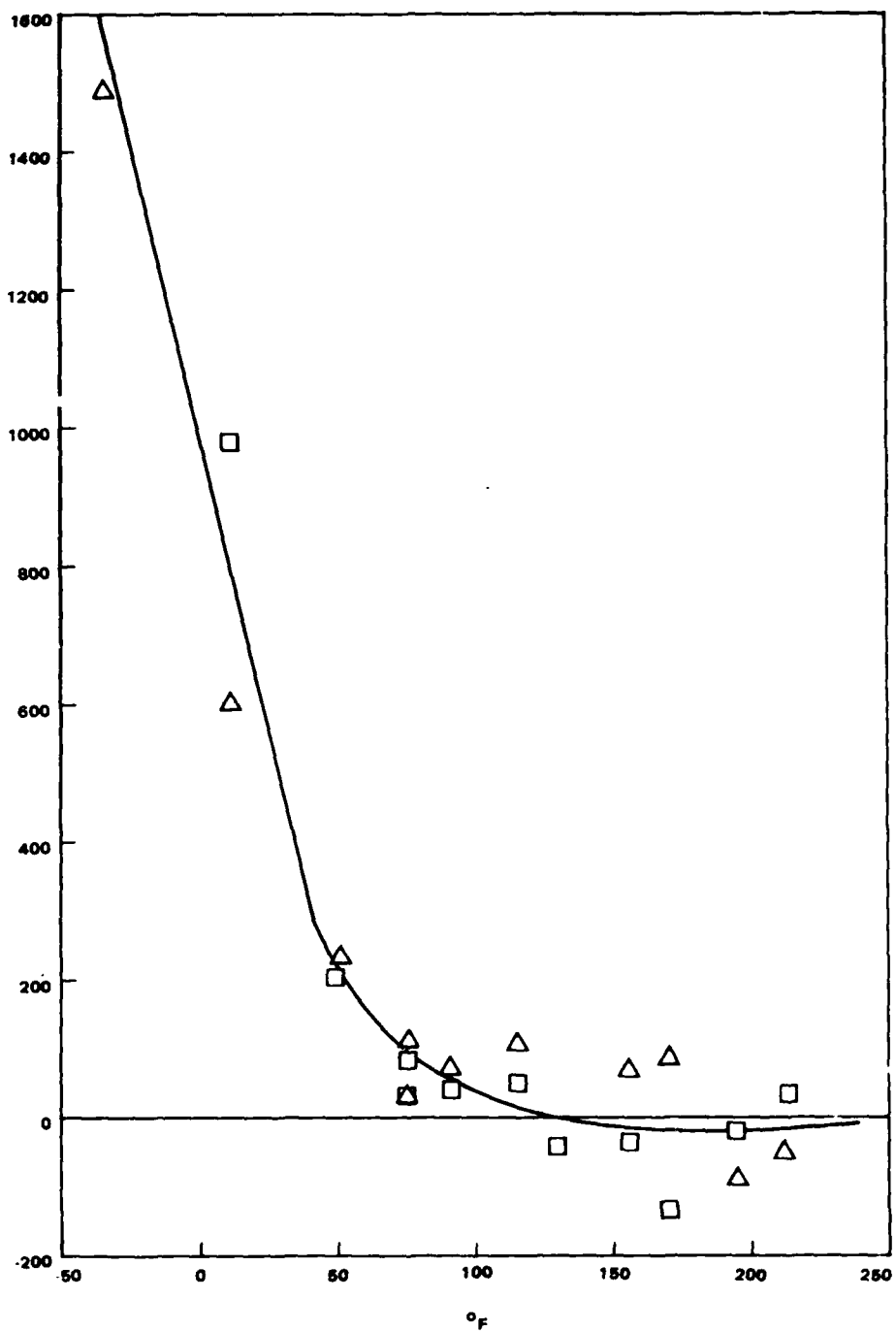


Figure 3-10. Scotchcast 9 stress vs temperature, thermometer method.

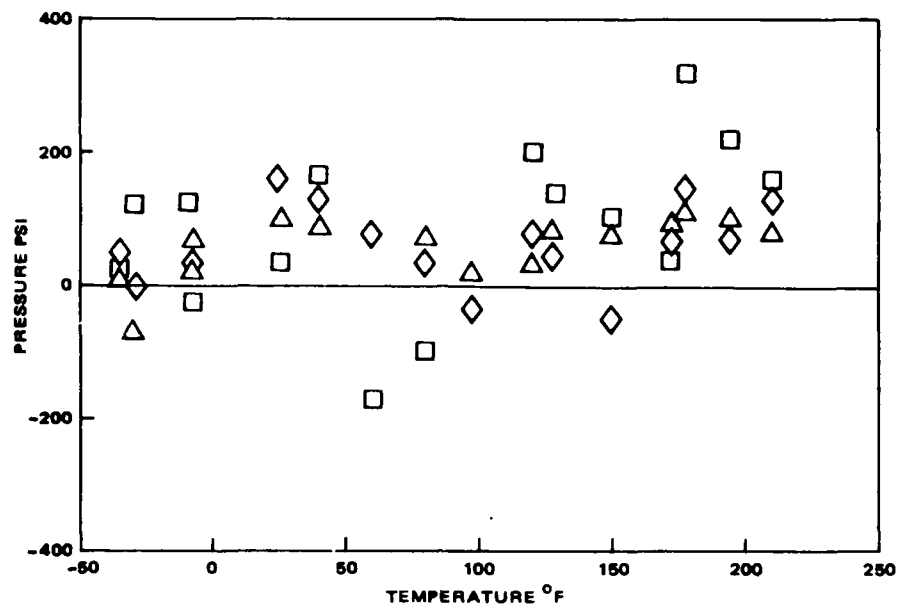


Figure 3-11. URALANE 5753 stress vs. temperature, thermometer method

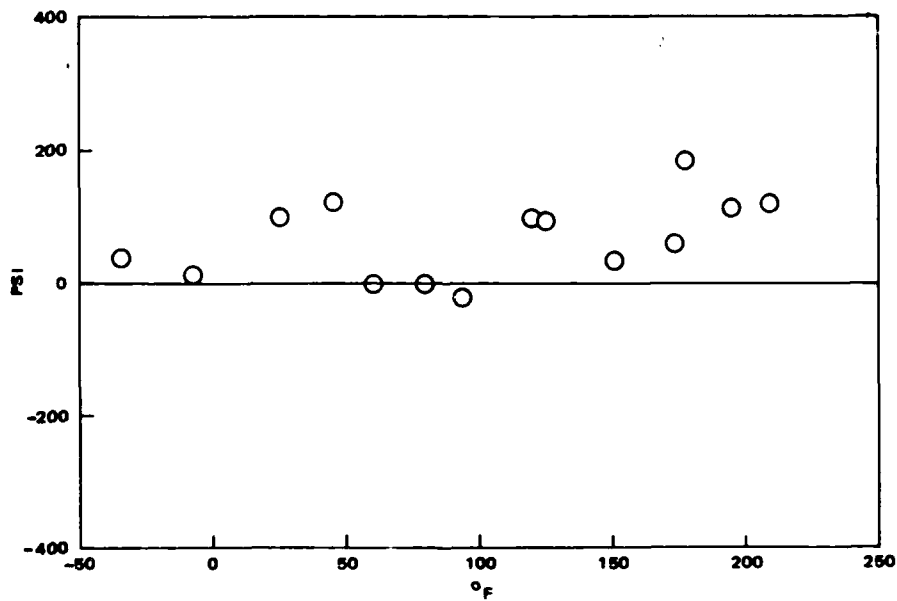


Figure 3-12. URALANE 5753 stress vs. temperature, thermometer method, average of 3 samples.

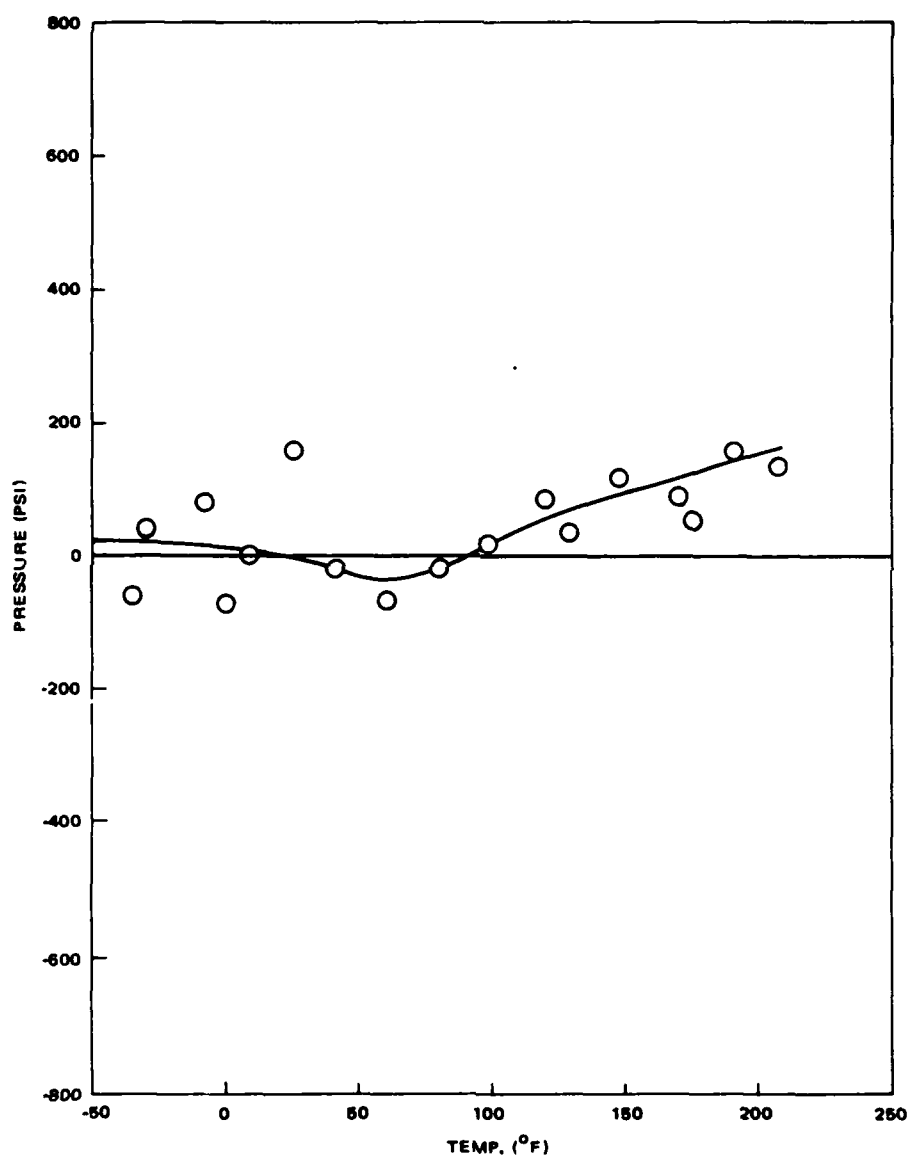


Figure 3-13. RTV 615 stress vs temperature, thermometer method.

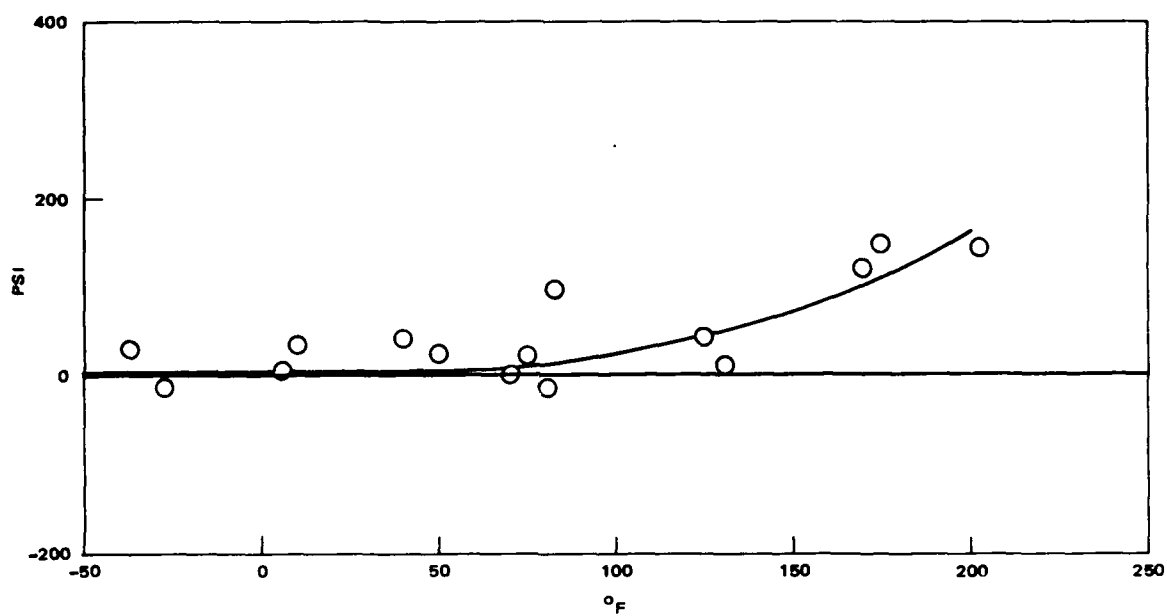


Figure 3-14. RTV 655 stress vs temperature, thermometer method.

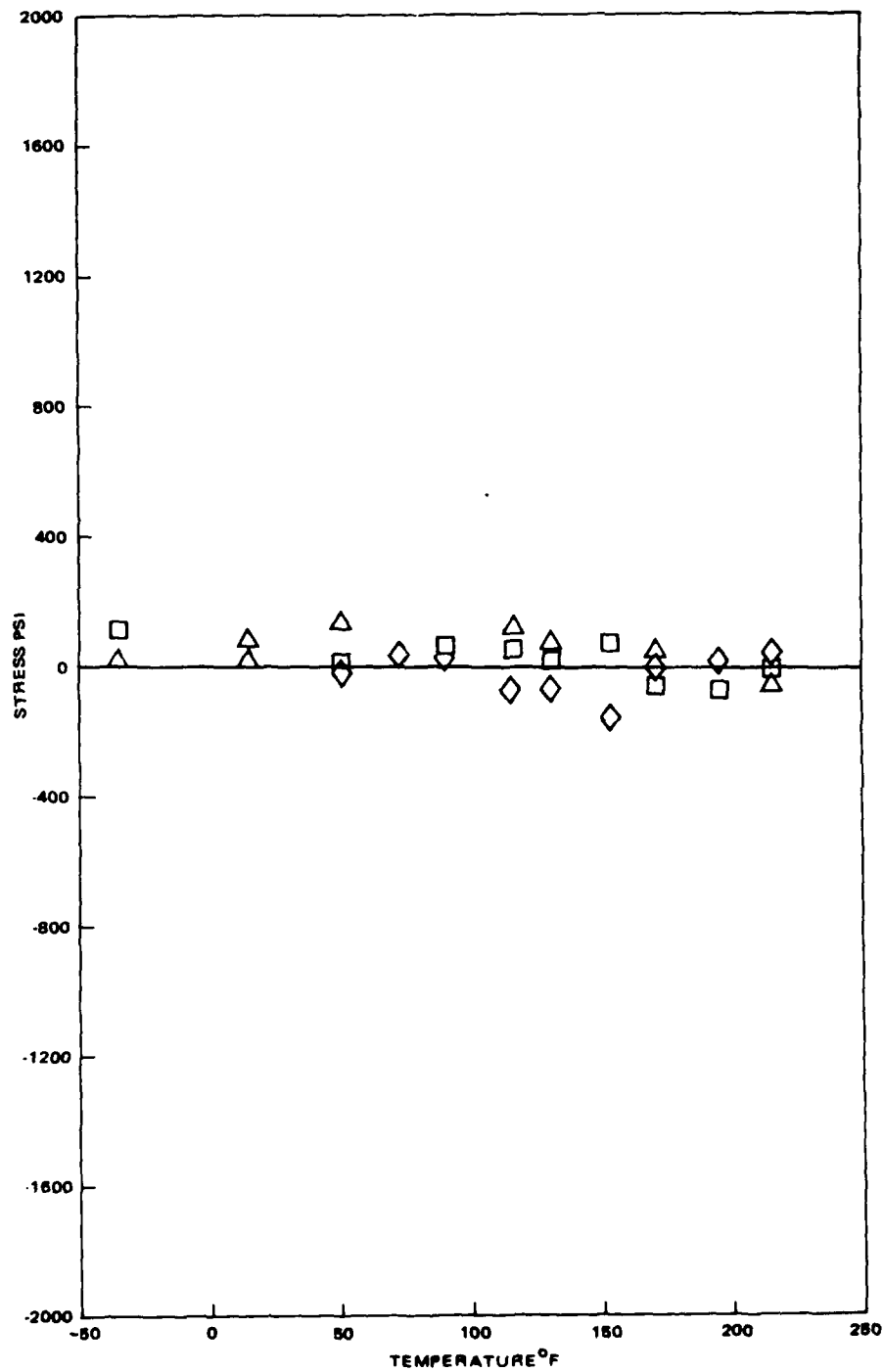


Figure 3-15. RTV 627 stress vs temperature, thermometer method.

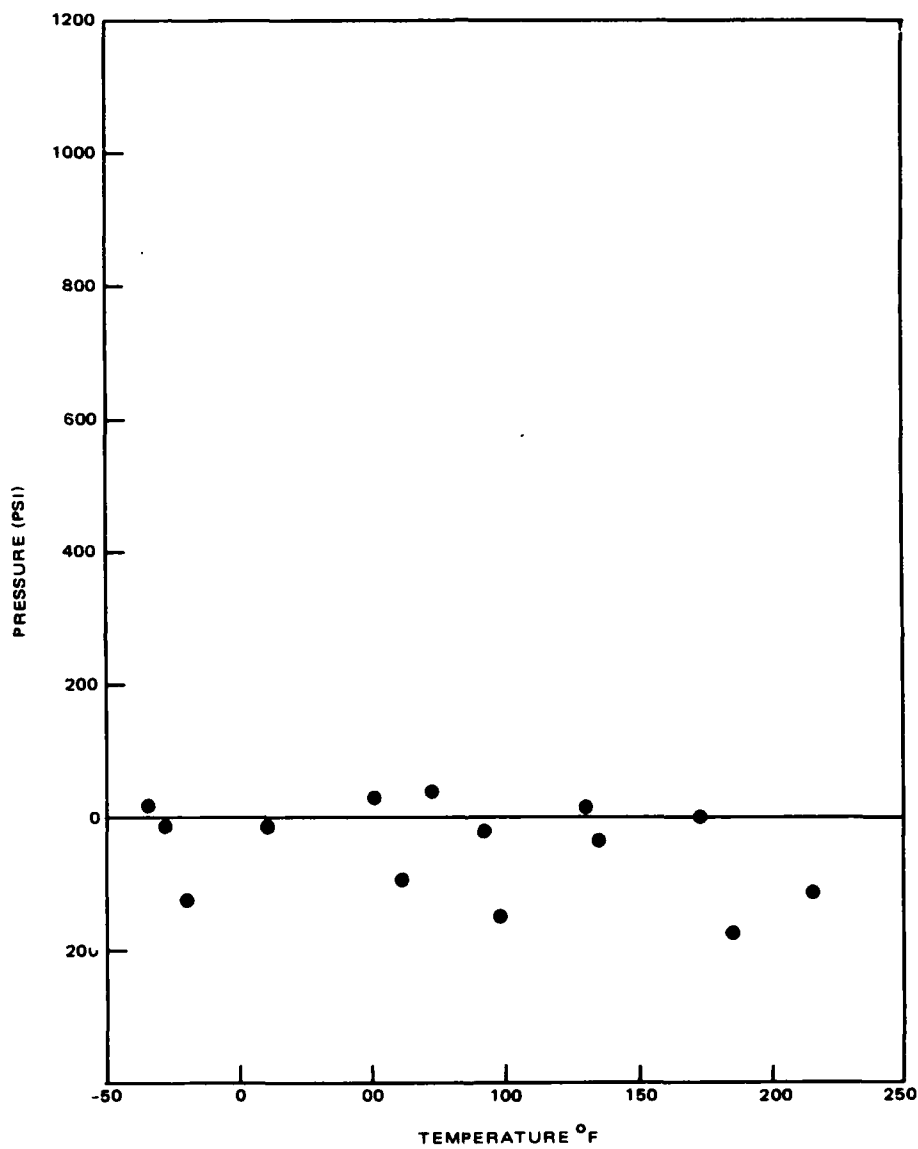


Figure 3-16. RTV619 stress vs temperature, thermometer method.

Conap EN-9 and Conap EN-90ZR both show a rise at the low temperature end, Figure 3-17, and 3-18 respectively, probably indicating a glass transition point.

From the embedded thermometer tests candidate materials and processes for low stress potting were selected. It was decided that the candidate materials shall have a maximum stress of less than 200 psi. The basis for this figure is somewhat arbitrary, based on the rationale that the percentage change of inductance from 0 psi to 1 K psi is usually less than 1/2 the change from 1 K psi to 2 K psi. Also noted is the experimental observation that it takes more than 200 psi to note any observable change of inductance value from the zero psi value.

This requirement eliminated Conap EN-11 and Scotchcast 9. Scotchcast 255 would also have been eliminated except that a two step embedment was planned, with a soft material as the first stage, and with this epoxy for the second stage. It seemed desirable to combine the qualities of a good epoxy with those qualities of a silicone or a polyethylene wax. In the test Scotchcast 255 is used alone as a control to show how much less stress is exerted on the coil by the two step potting process than by the Scotchcast 255 alone. The materials included in the low stress embedment study are shown in Table 3-11.

3.4.5.2 Inductor Pressure Measurement Results

Using the low stress materials selected from the thermometer tests inductors were potted as shown in Table 3-11. Although the responses of the Fe-Ni cores to pressure were disappointing, and as mentioned before thought to be due to the isotropic pressure environment, so it was thought that these might be responsive to non isotropic stresses in the embedment compounds. Accordingly 11 of these inductors were potted in various materials as shown in Table 3-11 to be compared with ferrite or MPP inductors.

Since Scotchcast 255 is a favorite material, but one with a significant increase in pressure below its glass transition temperature, several test inductors were coated with a softer material, it was hoped, would provide a cushioning effect which could be evaluated quantitatively. Two of these

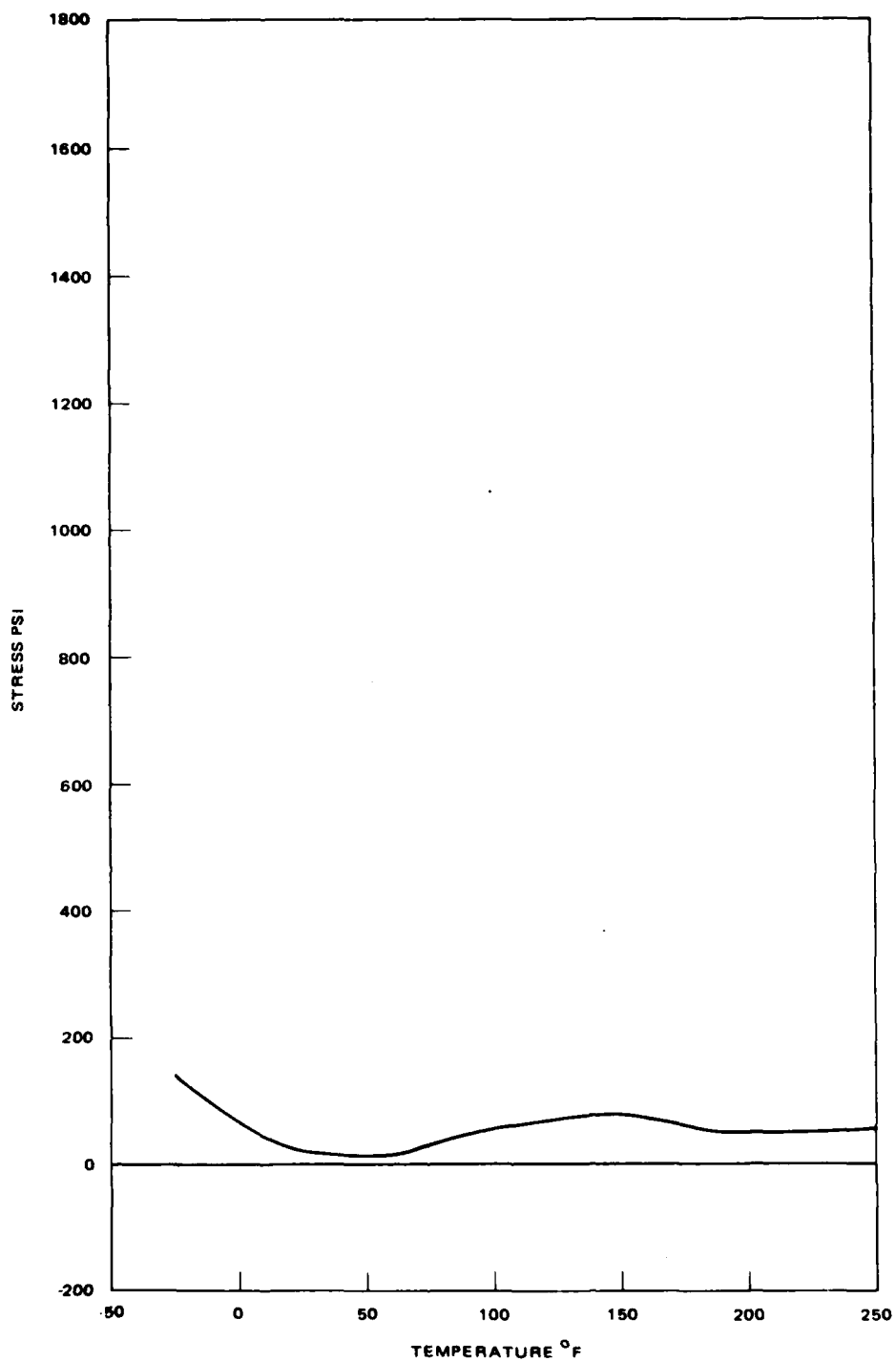


Figure 3-17. Conap EN-9 stress vs temperature, thermometer method.

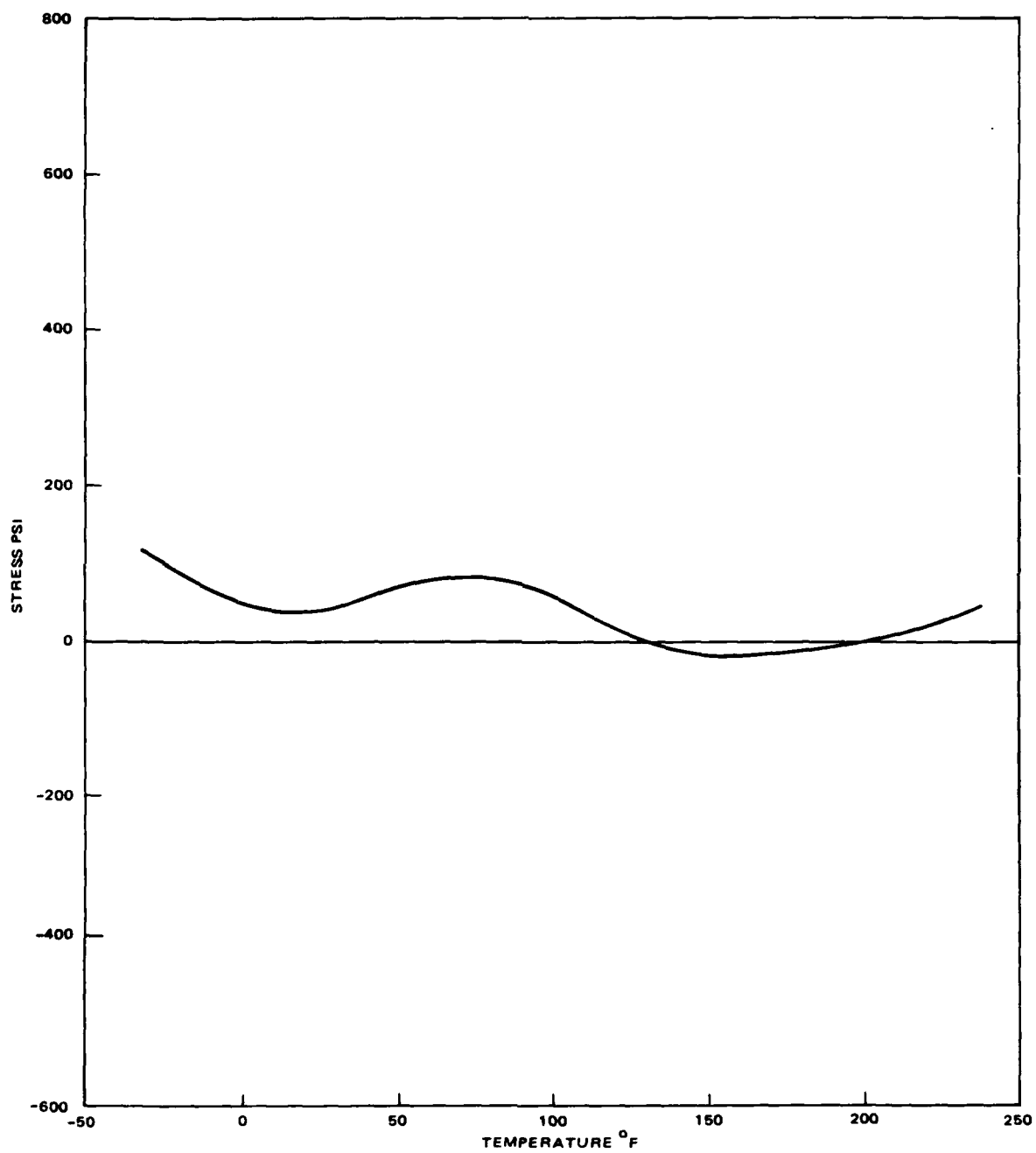


Figure 3-18. Conap EN-90ZR stress vs temperature, thermometer method.

cushioning materials were RTV 619 and RTV 627, previously evaluated in their own right as embedment materials. The third was Epolene C/AC617, a polyethylene wax with a melting point of 250°F.

Plastic potting cups 3/4 in. dia x 3/4 H were used for potting the various inductors. In all cases the inductor axis was perpendicular to the cup axis. Materials were mixed and cured in accordance with applicable manufacturers' or Hughes specifications.

The processes used for each embedment were those suggested by the manufacturer, except that all materials requiring a cure were placed in an oven at 190°F overnight. The silicones chosen required only one to two hours at this temperature to cure; however it was convenient to place all of the materials in the oven at the same time and to remove them from the oven at the same time. The two-material potting processes required extra time for the second cure.

After the cures were completed, the potted inductors were temperature cycled between -50°F to +250°F in most cases. At various temperatures, when the samples stabilized, the inductance and Q values were taken at the voltage input to the inductance bridge used before for each group of inductors during calibration.

The data reduction process was relatively straightforward. For each material sample, the temperature vs measured inductance curve was drawn. Referring to the temperature-inductance calibration of the unpotted inductor, the inductance was subtracted from the potted curve. The remaining inductance was then a function of the stress being generated on the inductor by the potting material. Comparing this value for each temperature with the pressure inductance calibration curve gives the pressure being generated on the inductor at that temperature. In the case of the MPP cores, which had essentially zero temperature characteristic, this procedure was greatly simplified, as the values for pressure from the calibration curve can be read directly. The Fe-Ni cores, which showed no pressure effects were included anyway to see if anything would happen.

The results were somewhat confusing as well as disappointing. Following the above procedure for both the ferrite and MPP core resulted in

enormous values of stress, far greater than any material could withstand. Tensile stresses were indicated in temperature regions where compressive stresses would be expected.

The excessive values of stresses were reduced somewhat by the assumption that, at the cure temperature of 200°F (250°F for the Scotchcast 255-Epolene C/AC617 combination) there should be no stress on the embedded inductor. This conclusion follows from the fact that embedment stress is due to the difference between the temperature expansion coefficients of the solid potting material and the inductor core. While the material is liquid, no stress can exist, which is assumed to continue on into the cured material at the cure temperature of 200°F. In all curves plotted, the potted curve is translated so that the inductances at 200°F are equal; i.e., the difference is zero.

It is recognized that, instead, another mechanism may exist to explain the stresses measured at the cure temperatures; for example, shrinkage of the potting material after curing. Another explanation could be an unnoticed change in the measuring technique or equipment.

Temperature runs of materials with potted Fe-Ni cores showed some change in inductance, so a simple test jig was made to apply non-isotropic stresses to the remaining unpotted inductors. This was done by hanging the inductor on a support, and adding weights to a weight pan to apply a force across it. Knowing the cross-sectional area of the core, the psi value vs inductance can be determined and plotted. Figure 3-19 shows a sketch of the method.

Reduction of data and comparison of the results of the ferrite cores to the others and to the thermometer method showed unbelievably high pressure values, in some cases 30 K psi and higher. A careful investigation and analysis results in one possible explanation that the pressure pot method is not an adequate means of pressure calibration of pressure sensitive cores, because of the isotropy of the applied hydraulic stresses. In support of this some of the unpotted ferrite cores were stressed on the test jig used on the Fe-Ni inductors described above, with interesting results.

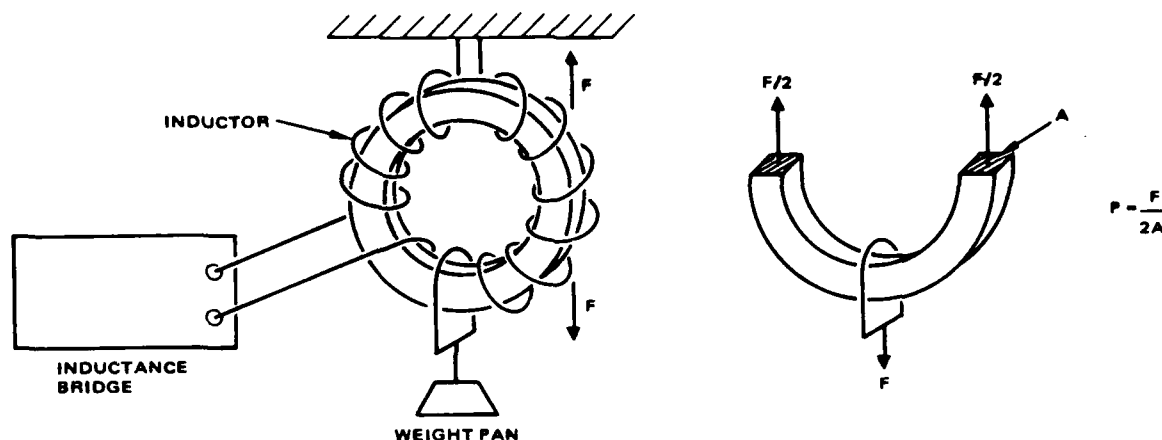


Figure 3-19. Core tensile stress measurement.

Ferrite core S/N 6, 4 mm x 8 mm x 2 mm, wound with 1 layer of AWG 32 wire had a nominal inductance of 5.45 mH. Applying a force, F , of 850 gms max (1.87 lb) reduced the inductance to 4.72 for a percentage change of

$$\frac{4.72 - 5.45}{5.45} \times 100 = -13.4\%.$$

Taking into account the cross-sectional area over which this force acts, results in a stress of 151 psi.

Referring to the data for S/N 6 in the pressure pot, there was a -57.8 per cent change in inductance at 10 Kpsi. Assuming a linear relationship then the pressure pot stress to obtain the same percentage change as the tensile stress is

$$\frac{10 \times 13.4\%}{57.8\%} = 2.3 \text{ K psi.}$$

for a ratio of $2.3/0.15 = 15.3$. In other words, an unbalanced tensile stress has a 15.3 times greater effect on the inductance change than the compressive isotropic stress.*

*At this point in time, an old report (Reference 5.6) was found in the literature, in which the experimenters reported similarly high stress values using a ferrite core in a specially designed micro pressure transducer, which was calibrated hydrostatically. Having no means of checking such as the thermometer method, they accepted their results at face value.

To see what effect occurred with the MPP cores, S/N 8 was exposed to a 900 gm force with absolutely no change in inductance. Since these cores showed an increase in inductance with pressure, this was just opposite to the ferrites. At first this was surprising, but investigation of the method of fabrication of the MPP cores showed that this was reasonable. Great care is taken to select magnetic Permalloy powders with a spectrum of Curie temperatures so that a flat or zero permeability change with temperature is achieved. Since pure Permalloy has a rising temperature coefficient, various powders with different Curie points are employed for core materials. As the temperature is raised, the Curie points of certain mixes are exceeded which results in them becoming non-magnetic, increasing the effective air gaps between the still magnetic particles which offsets their rising permeability values. Hydrostatically stressing an MPP core compresses these air gaps slightly, resulting in a rising inductance curve which was observed. On the other hand, a tensile stress across the core would lengthen some gaps and compress others, resulting in a net zero effect.

Results and comments on the data obtained for various materials/ combinations using the potted inductors, and including, where available, thermometer pressure data are given below. Because of the various assumptions made above, the data quantitatively is open to question; however, since conditions under which measurements were made are presumed identical, cross comparisons of the various materials/ combinations should be of value. The temperature and PSI stress scales are identical in all graphs, which facilitates comparison. Above the temperature axis the stress is compressive, below tensile. The single material samples are covered first, followed by the combinations.

The Conaps EN-9 and EN-90ZR were the only materials to have their stresses measured by all 4 pressure sensing devices. For the EN-9, Figure 3-20 compares the potted ferrite inductor with the unpotted. Taking the difference in inductance, converting it to psi stress from the pressure pot calibration and dividing it by the factor obtained from the tensile test method, the ferrite curve in Figure 3-21 is obtained. The potted MPP and Fe-Ni temperature vs stress curves are also shown, together with the

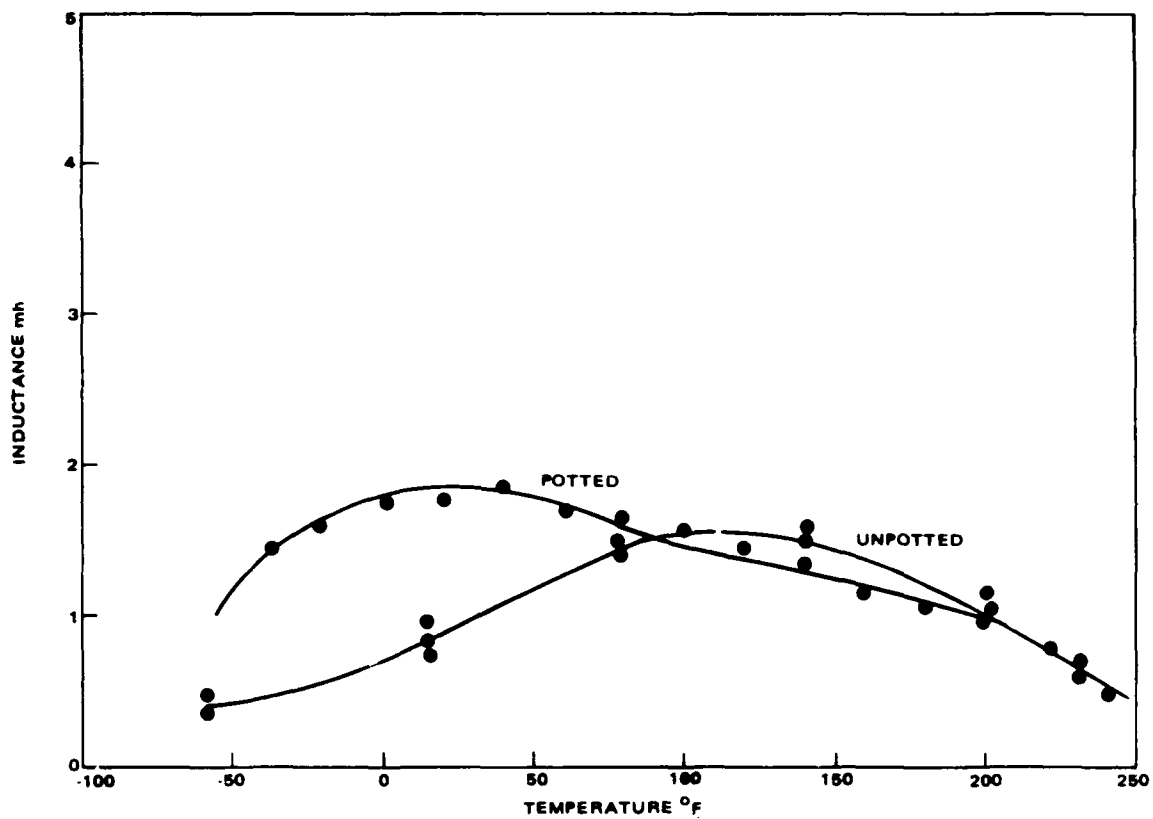


Figure 3-20. Inductance vs temperature for No. 52 ferrite core, unpotted and potted in Conq EN-9.

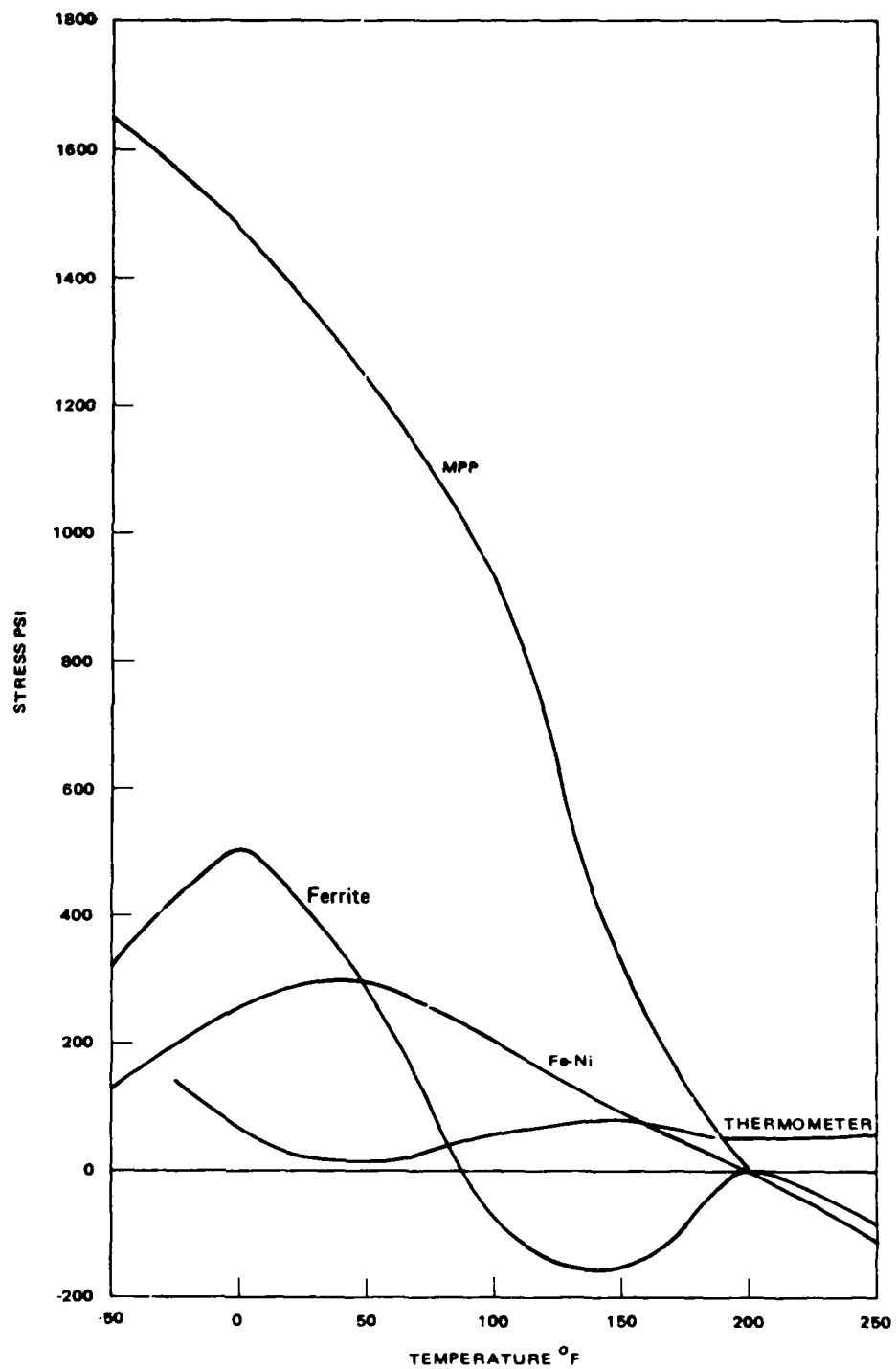
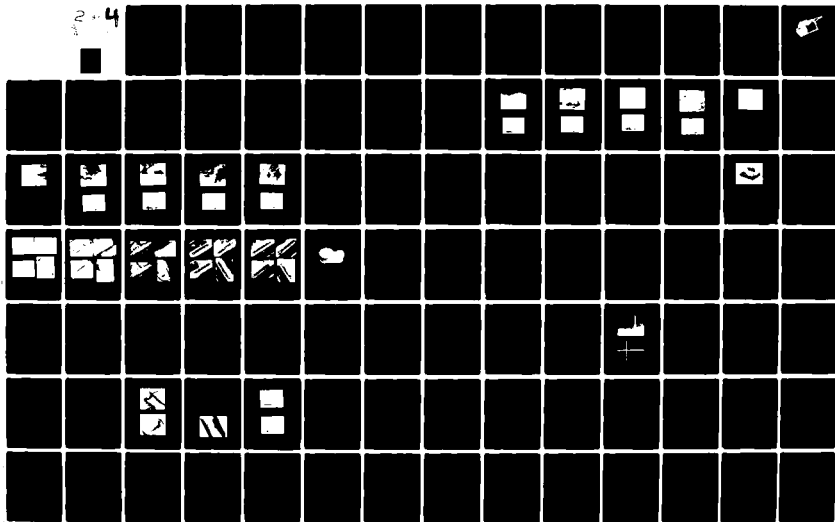


Figure 3-21. Conap EN-9 stress vs temperature, four sensors

AD-A098 167 HUGHES AIRCRAFT CO CULVER CITY CA ELECTRO-OPTICAL AN--ETC F/G 9/5
MANUFACTURING METHODS AND TECHNOLOGY FOR ELECTROMAGNETIC COMPON--ETC(U)
DEC 80 E R BUNKER, J R ARNETT, J L WILLIAMS DAAK40-78-C-0271
UNCLASSIFIED FR-80-76-1254R-VOL-1 NL

24



thermometer for comparison. As can be seen, the ferrite and Fe-Ni curves show some similarity to the thermometer curve, even to the extent of possibly anticipating a rise in stress due to a possible glass transition point indicated by the thermometer. There is no obvious reason for the MPP curve to take off as it does, and similar curves occur with the other tests.

The temperature vs inductance curve for ferrite core No. 51 unpotted, and potted in Conap EN-90ZR, is shown in Figure 3-22 which is very similar to the previous Figure 3-20. With the MPP core a little better behaved, the 4 curves in Figure 3-23 are very close to those in Figure 3-21, and the same comments hold.

Ferrite core No. 53 potted, and unpotted, temperature vs. inductance curves are shown in Figure 3-24 for Scotchcast 255.

As mentioned above, pressure pot calibration of the ferrite cores resulted in exaggerated values of internal stresses, so the 15.3 factor obtained

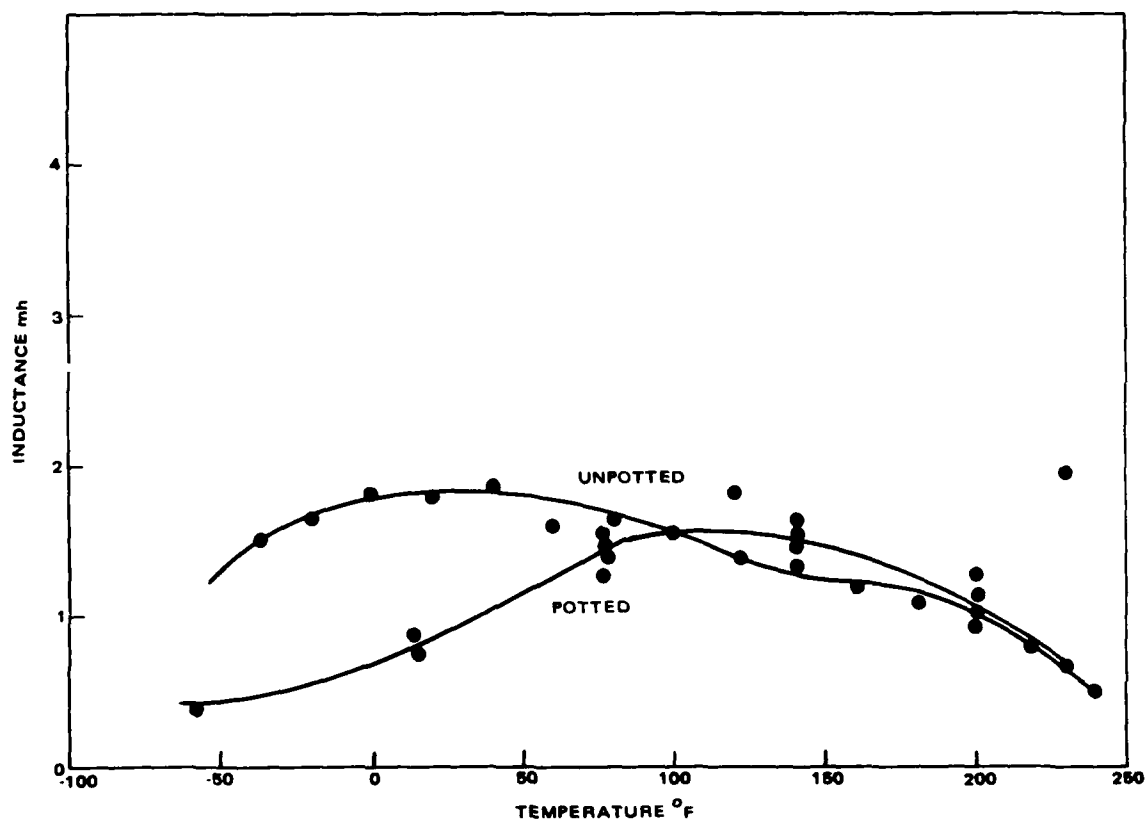


Figure 3-22. Inductance vs temperature for No. 51 ferrite core, unpotted and potted in Conap EN-90ZR.

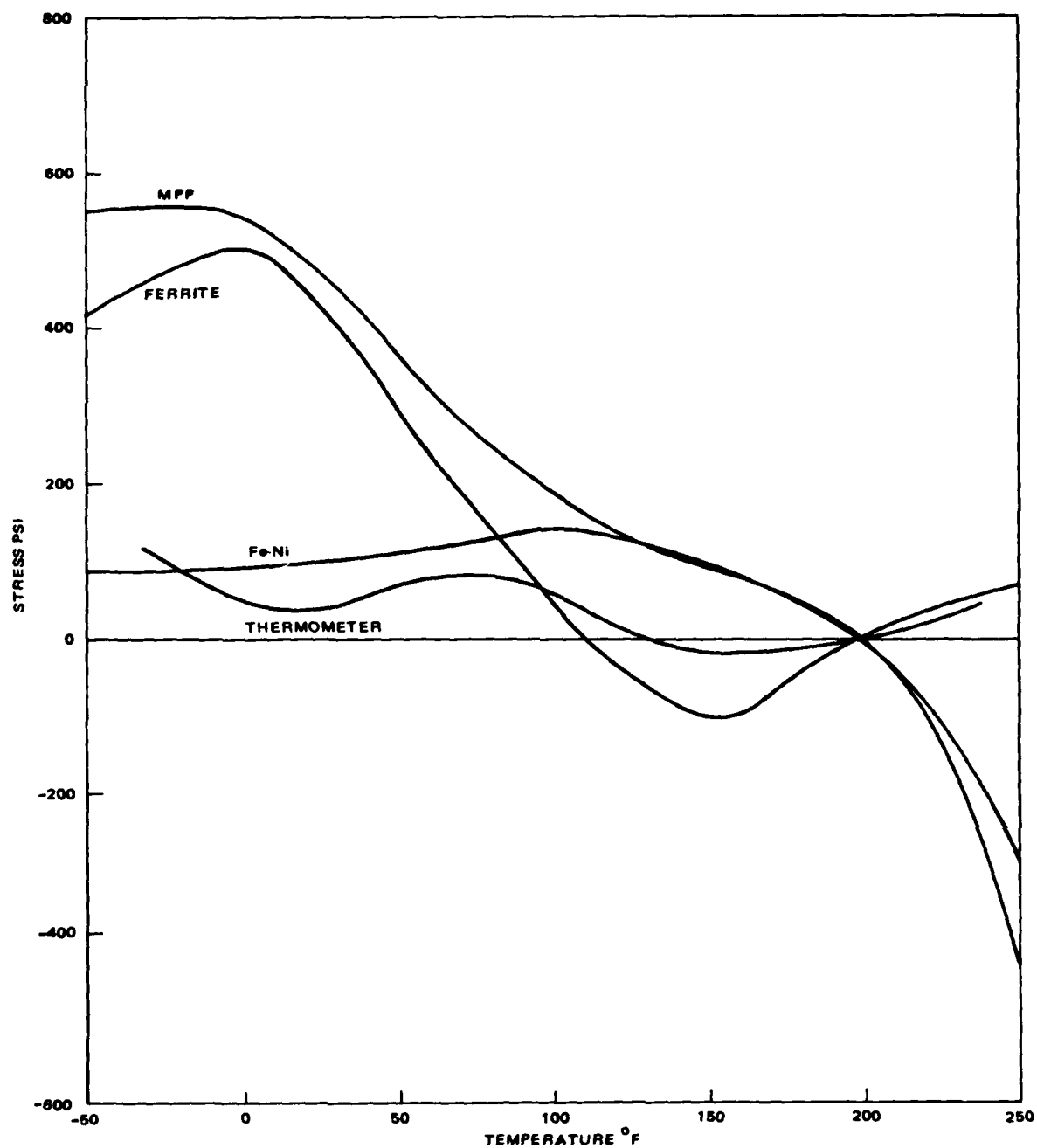


Figure 3-23. Conap EN-90ZR, stress vs temperature, four sensors.

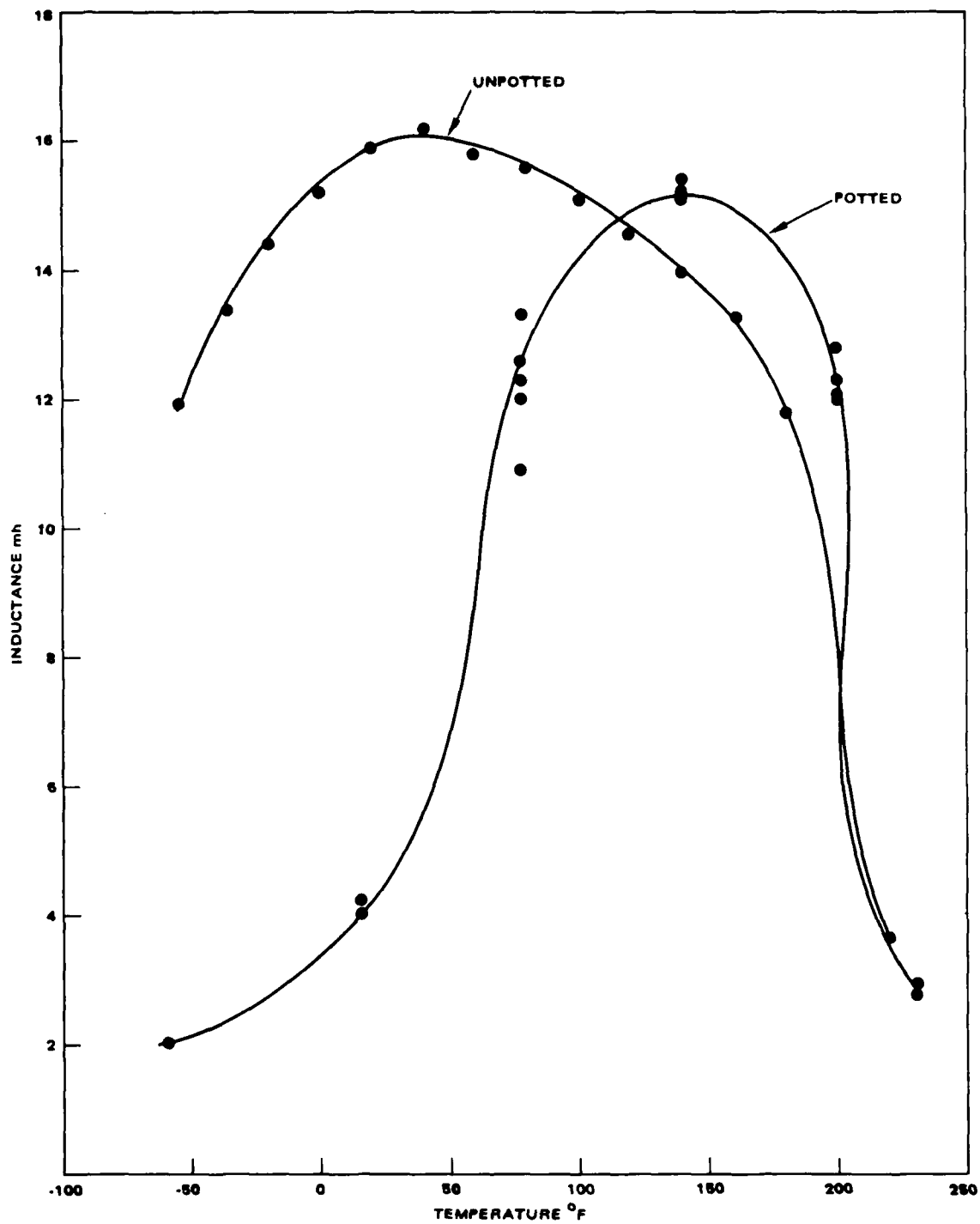


Figure 3-24. Inductance vs temperature for No. 53 ferrite core, unpotted and potted in Scotchcast 255.

from the tensile stress method in Figure 3-19 was substituted and plotted in Figure 3-25. Also plotted is the thermometer curve from Figure 3-9 for comparison. A potted Fe-Ni inductor shows a constant tensile stress for most of the temperature range, which is not understood at this time using a calibration factor from the test setup in Figure 3-19. The thermometer and ferrite curves agree in showing a rapid rise as the temperature decreases past the glass transition temperature. The reason for the abrupt change in direction of the ferrite curve at -50°F is not explained, but seems to be typical in almost all data.

The temperature vs. inductance curve for ferrite core No. 54 before and after potting in a Scotchcast 255/RTV 619 combination is shown in Figure 3-26. It is obvious that the differences in inductances at each temperature are much less than in the previous example of Scotchcast 255 alone, Figure 3-24. Figure 3-27 compares the curves of both ferrite and Fe-Ni core inductors. The ferrite curve, when compared with Figure 3-25, shows a significant reduction in stress at temperatures below the glass transition point. The Fe-Ni inductor shows a small, nearly constant compressive stress. Whether this is due to the different sample, or to the core material is not known.

Similar curves for Scotchcast combinations with RTV 627, ferrite No. 55, and Epolene C/AC 617, ferrite No. 50, are shown in Figure 3-28, and Figure 3-30. Stress-temperature curves are shown in Figure 3-29, and Figure 3-31 respectively, with the same general results. Of the 3 initial materials, the Epolene does the most to reduce the stress, but as can be seen in Figure 3-31, the curve is a long way from the 200 psi acceptance limit.

3.5 ELECTRICAL AND ENVIRONMENTAL TESTING OF HI-REL CANDIDATE MATERIALS

The electrical and environmental testing of candidate materials and processes seek to determine how well these compounds meet end product and manufacturability requirements. The ideal material was considered at the beginning as a material that degassed quickly, had a viscosity below 1000 centipoise at the pouring temperature, had a low surface tension, and cured thoroughly at a relatively low temperature. It also should enable a designer to meet the electrical, material, and environmental end product

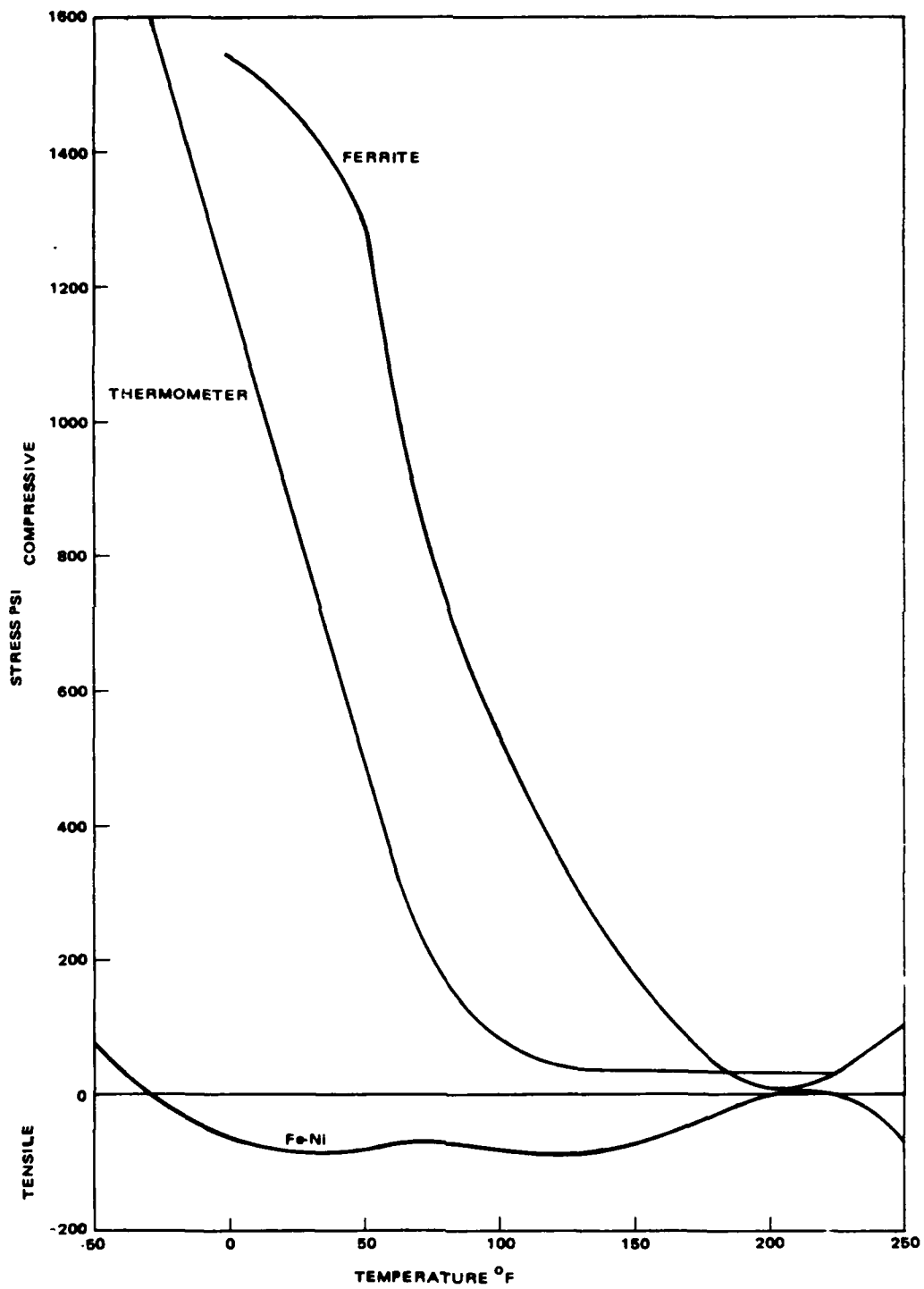


Figure 3-25. Scotchcast 255 stress vs temperature, three sensors

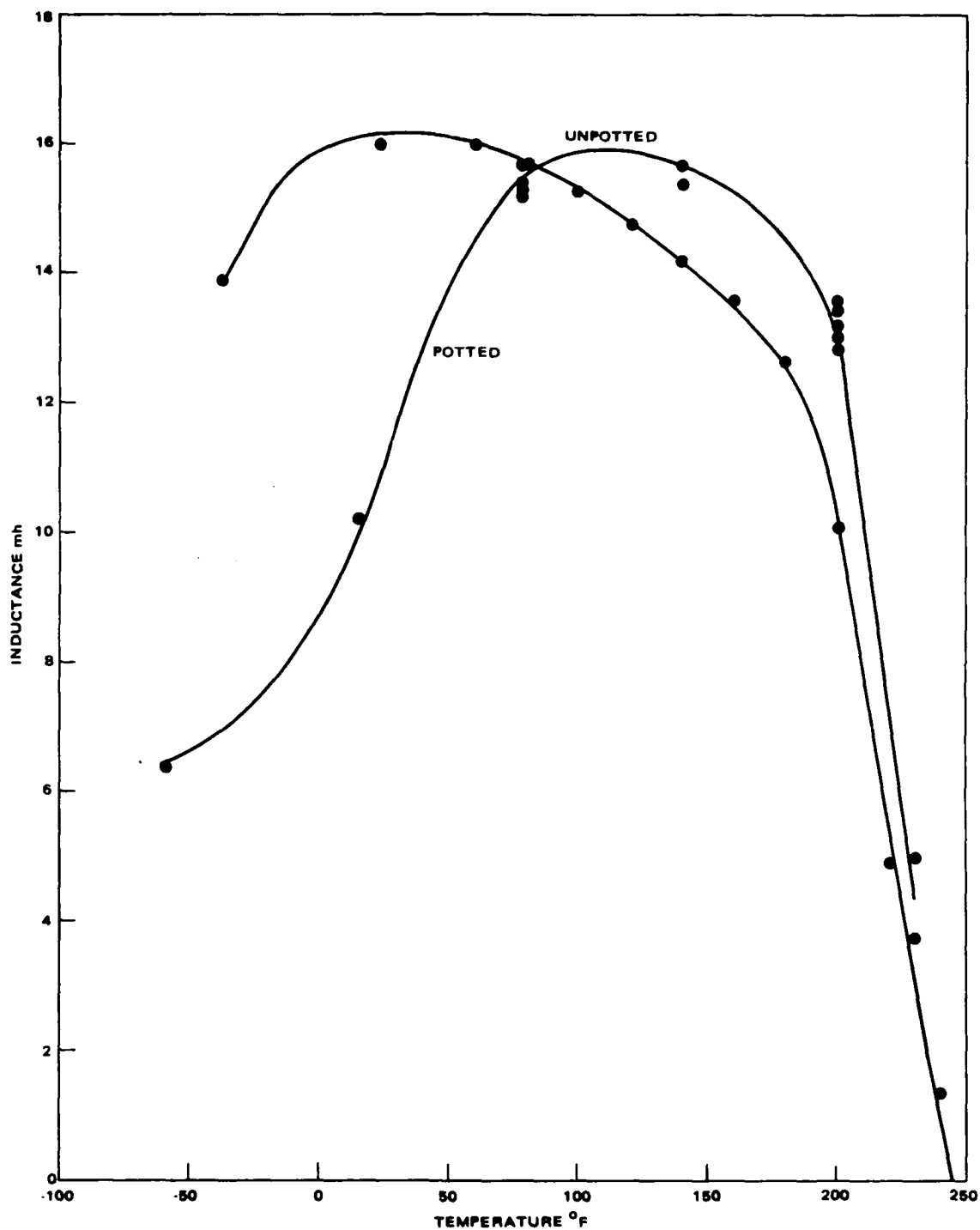


Figure 3-26. Inductance vs temperature for ferrite No. 54 unpotted and potted in Scotchcast 255/RTV 619.

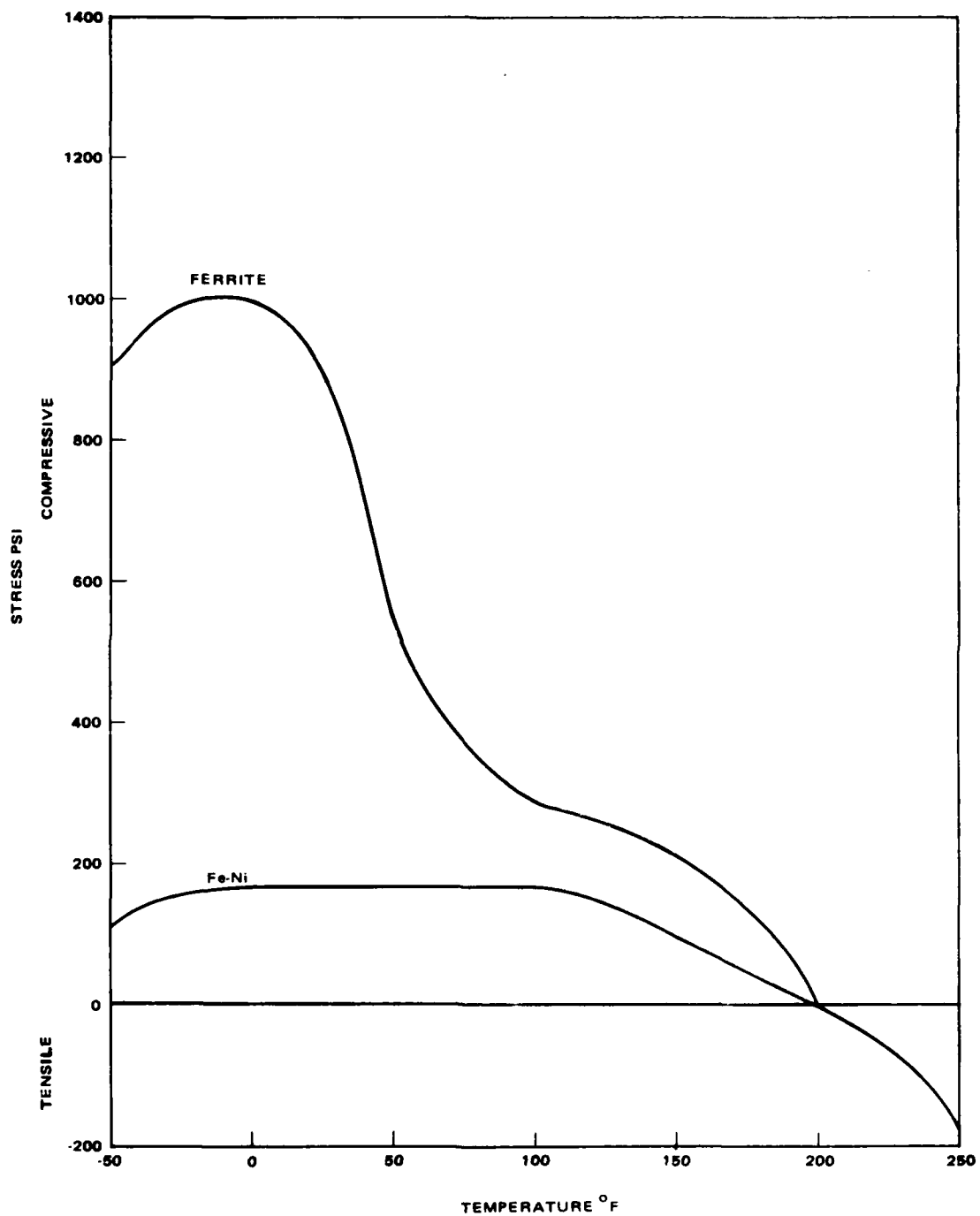


Figure 3-27. Scotchcast 255/RTV 619 stress vs temperature.

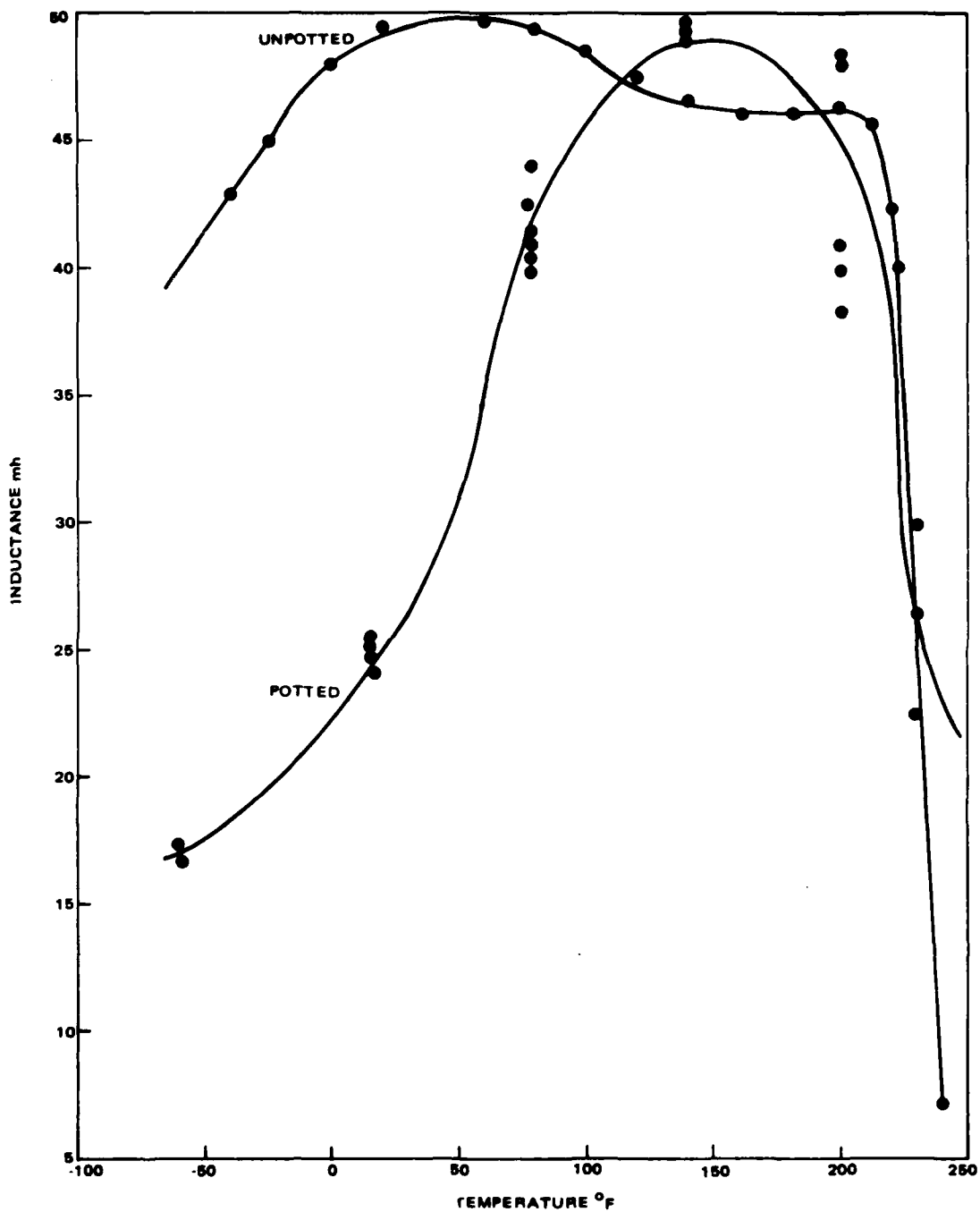


Figure 3-28. Inductance vs temperature for ferrite core No. 55 unpotted and potted in Scotchcast 255/RTV 627.

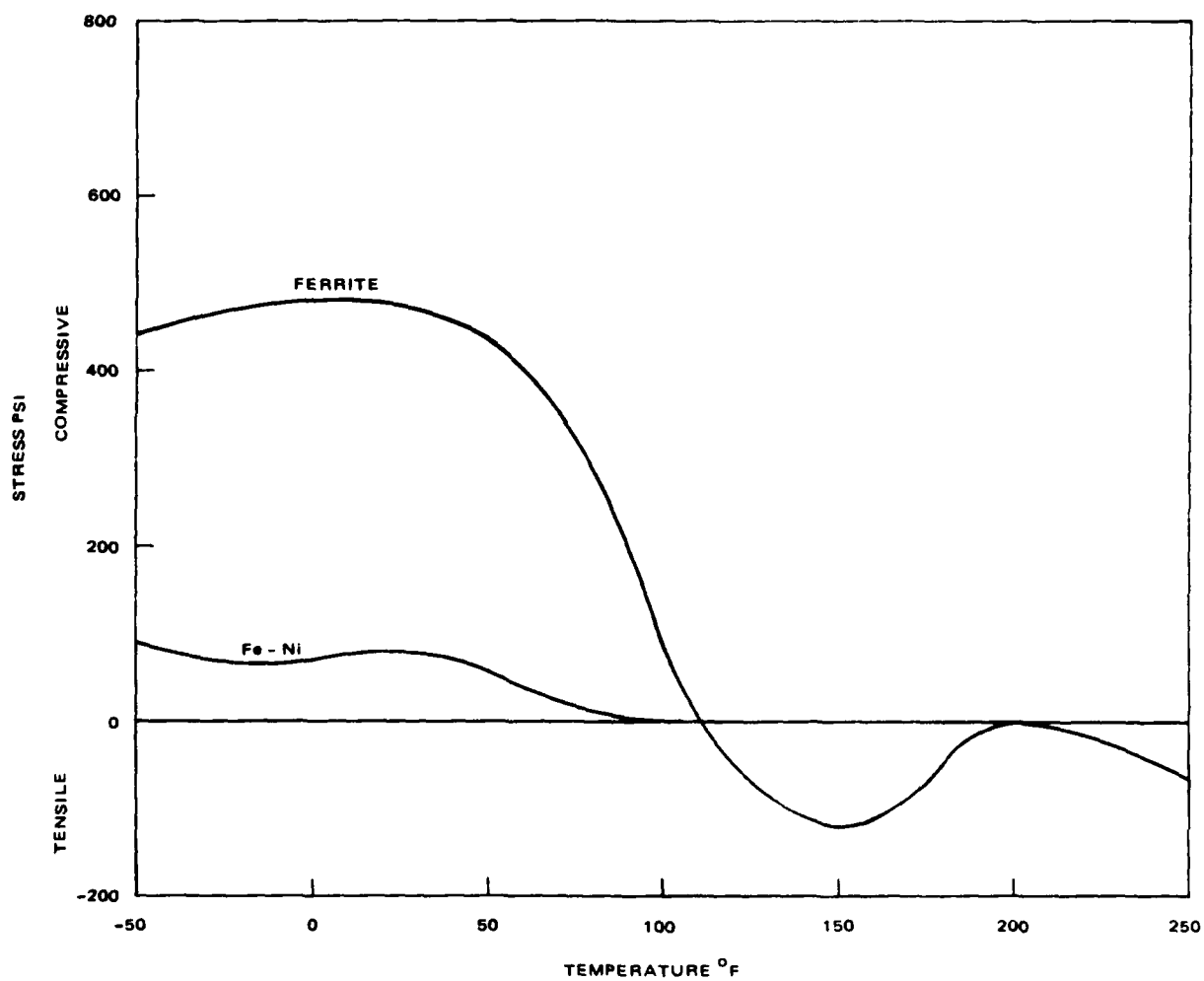


Figure 3-29. Scotchcast 255/RTV 627, stress vs temperature, two sensors.

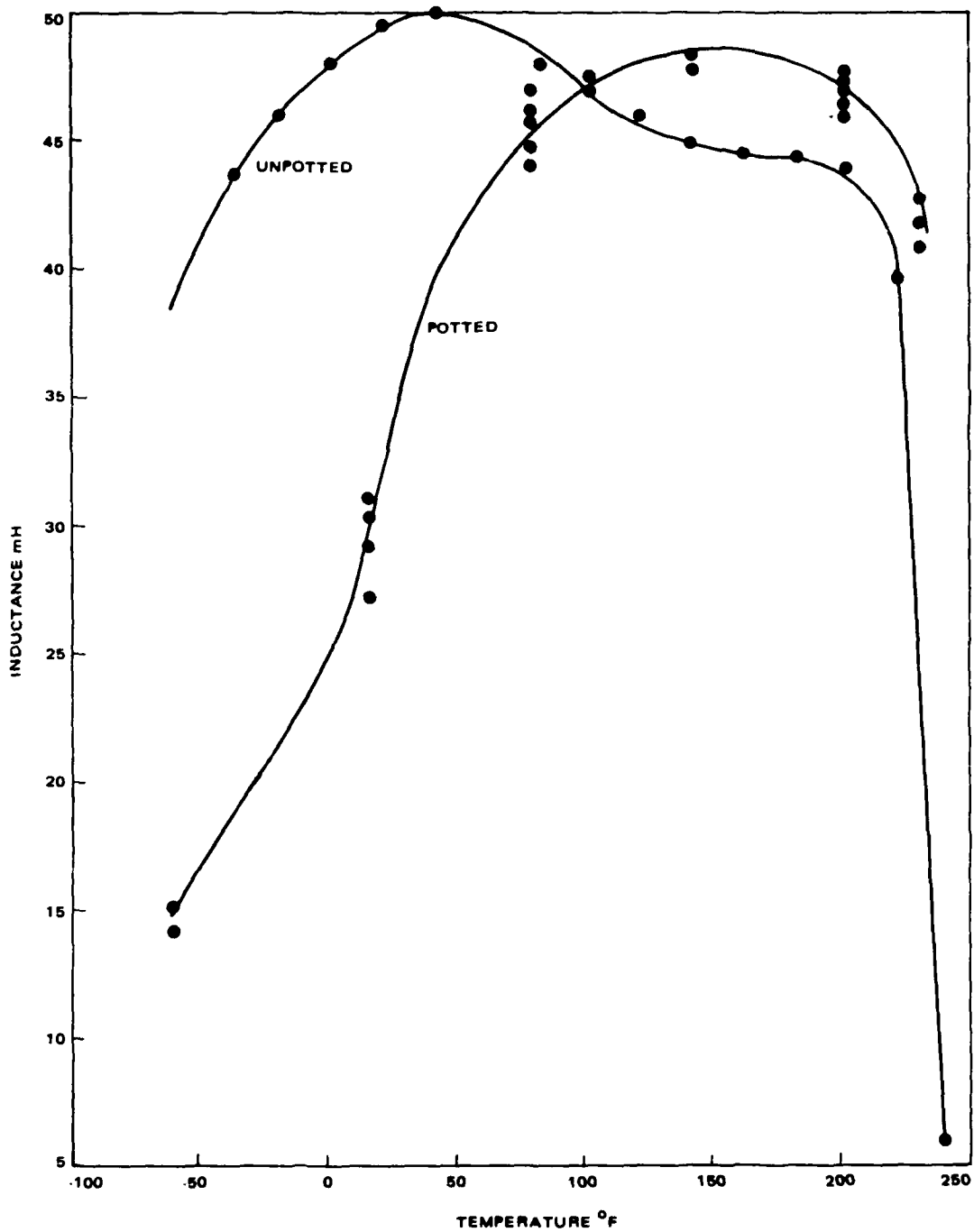


Figure 3-30. Inductance vs temperature for ferrite core No. 56 unpotted and potted in Scotchcast 255/Epolene C/AC 617.

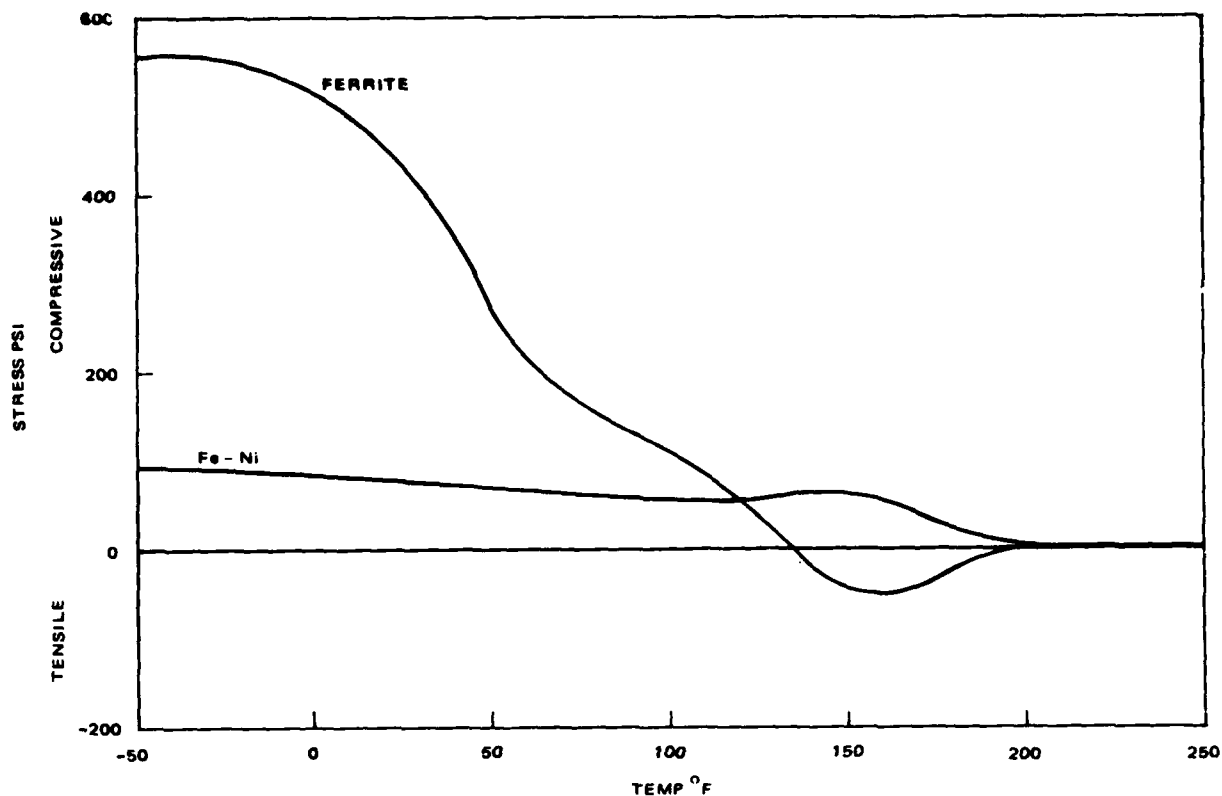


Figure 3-31. Scotchcast 255/Epolene C/AC 617, stress vs temperature, two sensors.

criteria found in MIL-T-27D, MIL-I-16923G and MIL-S-23586, as appropriate. In the present case the material must be reliable under extremes of humidity, temperature, vacuum, electric field, and mechanical abuse.

This section shows the results of a series of electrical, mechanical and environmental tests. Some of the tests were of short duration, such as resistance to soldering heat. Others were, by nature, long duration, the most extreme example being the hydrolytic stability tests.

Twenty saturable reactors of a typical design for a missile application designated as "Type X82141 Alternate" were fabricated in order to test the candidate potting materials in a real world environment. Figure 3-32 shows this device after a typical encapsulation operation.

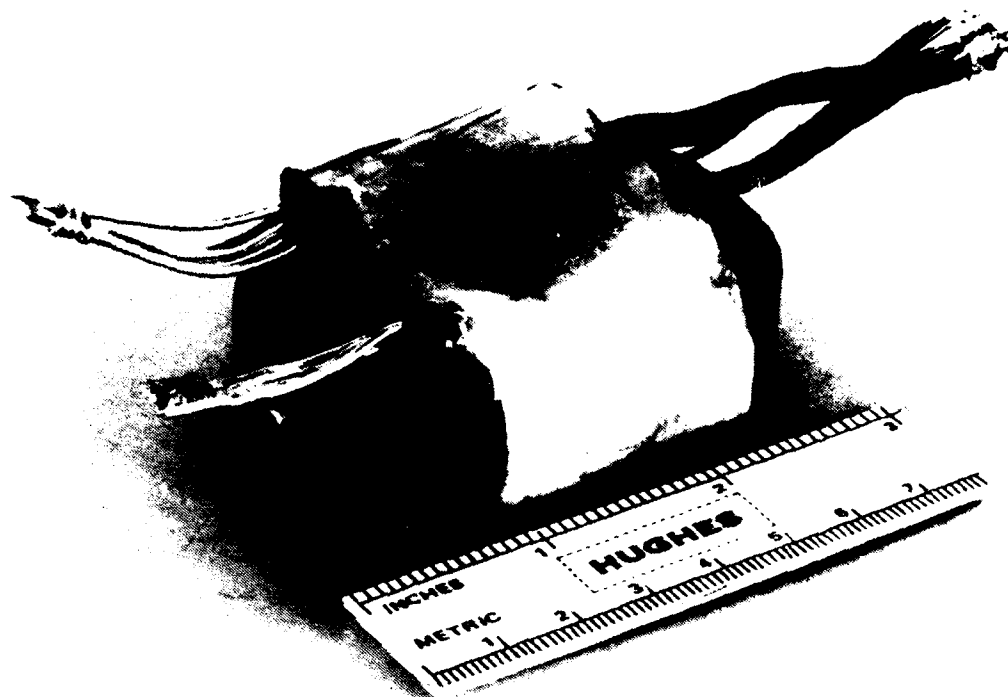


Figure 3-32. Saturable reactor used for electrical tests.

Thirteen tests were done using these reactors:

1. Hydrolytic stability of electrical parameters .
2. Excess material removal.
3. Visual before and after thermal cycling.
4. Resistance to soldering heat.
5. Corrosion susceptibility before and after temperature cycling.
6. Dielectric strength before and after temperature cycling.
7. Leakage inductance before and after temperature cycling.
8. Inductance, with and without dc bias, before and after temperature cycling.
9. DC resistance before and after temperature cycling.
10. Temperature cycling, +10 cycles, -55°C to 130°C .
11. Adhesion of material to part after temperature cycling.
12. Mechanical shock.
13. Cross section of part to determine extent of voids.

3.5.1 Hydrolytic Stability Testing

The hydrolytic stability test was divided into three parts: Hydrolytic stability of the high reliability materials, listed in 3.3.1, hydrolytic stability of the low stress embedment materials, in 3.3.2 and electrical parameter testing of the saturable reactor coils undergoing hydrolytic stability testing are included. In all three cases, the samples were maintained at an ambient temperature of 71°C and 95 percent relative humidity.

Samples two inches in diameter and about 1/2 inch thick were prepared for the first two hydrolytic stability tests. The hardness of each sample was measured at the start of the 120 day period, and repeated at various intervals. Two samples of each material were maintained in the humidity chamber and two samples were retained as controls. The results are shown in Table 3-12.

The third test utilized saturable reactors as electrical test vehicles. The inductance, leakage inductance, self resonant frequency, turns ratio and D.C. resistance were measured at the start, at 30 days, and at 60 days.

The results are shown in Table 3-13. The boundary between hydrolytic stability and instability is ultimately the reversion of the solid embedment into a liquid form. It is difficult to give a reversion boundary using only a hardness test, because moisture absorption also causes a hardness decrease. In general, a hardness decrease combined with an infrared determination of the soluble constituents in the sample provides the necessary information for a reasonable determination. The solvent must dissolve the monomers without attacking the polymers, so obviously the choice of solvent will depend on the system studied. The hardness of the samples (excluding Eccoseal 1218 and Hysol C-60, which had fully reverted) had varied from a 22 point increase due to further polymerization for Uralane 5753, to a 33 point decrease for GE702, since the test started in February. Eight of 16 materials in the study have varied by only five points or less in the same time period. A reduction of ten points in hardness was not considered a significant change in the material. The GE 702 which had the 33 point hardness reduction, was considered a significant change.

Further testing is required to determine conclusively if reversion was indeed occurring in materials which had a significant hardness reduction.

		Trade Name	GE707		GE702		Scotchcast 9		Scotchcast 255		RTV611
		Shore Gauge	"D"		"D"		"D"		"D"		"A"
Hydrolytic Stability Tests	25°C, 50% R.H.	Specimens Prepared	1	2	1	2	1	2	1	2	1
		Hardness after 0 days exposure	75	75	65	70	70	70	75	75	38
		Hardness after 28 days exposure	75	80	70	70	78	78	80	80	38
		Hardness after 56 days exposure	75	77	70	70	78	78	77	79	37
		Hardness after 84 days exposure	75	76	70	70	80	80	80	80	38
		Hardness after 120 days exposure	80	80	70	70	80	80	78	76	43
	71°C, 95% R.H.	Specimens Prepared	3	4	3	4	3	4	3	4	3
		Hardness after 0 days exposure	75	78	70	70	70	70	75	75	37
		Hardness after 28 days exposure	80	80	55	52	65	65	70	68	46
		Hardness after 56 days exposure	80	80	45	47	65	67	70	71	45
		Hardness after 84 days exposure	80	80	38	34	65	65	70	71	47
		Hardness after 120 days exposure	80	80	35	37	65	66	68	68	47

1

TABLE
OF

RTV615	RTV627	Conap EN-9	Conap EN9-0ZR	Conap EN-11	Epon 825 w/D400	Epon 825 W/T403	Eccoseal 1218	Hysol C60	
"A"	"A"	"D"	"D"	"A"	"D"	"D"	"A"	"D"	
1 2	1 2	1 2	1 2	1 2	1 2	1 2	1 2	1 2	
38 37	63 65	36 36	36 38	65 63	73 72	65 65	51 52	40 42	
38 38	63 66	40 40	38 40	62 62	78 78	80 75	51 53	41 42	
37 37	64 65	40 40	38 40	70 70	76 75	75 77	55 55	40 40	
38 40	65 65	40 40	38 40	65 67	77 75	75 76	55 55	42 43	
43 43	67 65	40 41	39 40	75 75	77 73	75 76			
3 4	3 4	3 4	3 4	3 4	3 4	3 4	3 4	3 4	
37 37	65 64	36 37	36 36	63 62	75 75	74 70	52 52	40 40	
46 46	63 65	38 38	34 35	60 60	70 75	80 80	33 35	32 32	
45 45	64 65	36 37	32 31	65 64	75 74	80 80	Reverted	12 13	
47 47	65 65	35 35	30 31	60 62	72 73	80 80	-----	Reverted	
47 47	70 72	35 35	30 31	65 65	72 75	80 80			

Conap EN-9 taken 2-15-79.

TABLE 3-12. HYDROLYTIC STABILITY
OF MATERIALS-TEST RESULTS

	Hysol C15		Epon 825 w/H. V.		Uralane 5753	
	"D"		"D "		"A"	
	1	2	1	2	1	2
42	55	55	82	80	51	50
42	60	60	85	80	61	65
40	57	59	82	81	68	69
43	58	59	82	83	70	68
	60	60	85	82	75	75
	3	4	3	4	3	4
0	52	53	83	82	50	50
2	53	55	83	83	67	67
	55	55	81	82	66	66
	52	54	85	83	65	66
	50	52	83	84	72	72

TABLE 3-13. HYDROLYTIC STABILITY OF ENCAPSULATED TRANSFORMERS

	Inductance ¹ , μH		Leakage Inductance ² , μH	Self Resonant Frequency ³ , MHz	Ratio	D.C. Resistance, ohms	
	w/20 ADC	w/o ADC				1-2	3-4
EPON/825 w/HV							
Days 0	189	207	0.5	38.0 ⁴	0.99774	0.00736	0.0297
30	184	208	0.5	27.4	0.99664	0.00721	0.0290
60	185	211	0.55	26.2	0.99975	0.0083	0.029
Scotchcast 255							
Days 0	187	214	0.58	38.0 ⁴	0.99661	0.00720	0.0287
30	178	203	0.45	27.4	0.99670	0.00713	0.0284
60	180	206	0.55	27.0	0.99890	0.0075	0.028
Eccoseal 1218							
Days 0	188	214	0.53	38.0 ⁴	0.99821	0.00729	0.02920
30	182	207	0.40	29.1	0.99724	0.00713	0.0285
60	182	208	0.55	26.8	0.99955	0.0075	0.029
Hysol C-60							
Days 0	187	216	0.75	33.8 ⁴	0.99697	0.00755	0.02930
30	180	209	0.65	24.2	0.99574	0.00711	0.0286
60	182	212	0.75	22.8	0.99865	0.0074	0.029
Hysol C15-015							
Days 0	190	216	0.60	38.0 ⁴	0.99784	0.00737	0.02942
30	183	212	0.50	28.6	0.99644	0.00719	0.0285
60	185	216	0.62	26.4	0.99865	0.0074	0.029

¹ 17 vrms, 20 kHz, with and without 20 ADC measured across 1-2.² Measured across 3-4 with 1-2 shorted.³ Self resonant frequency with 1-2 shorted.⁴ Self resonant frequency before encapsulation.

However, during the embedment material selection and initial testing process, GE 702 was eliminated. For this reason expenditure of funds needed to chemically analyze these samples for reversion products could not be justified.

Electrical test parameters, such as inductance, leakage inductance, turns ratio, and DC resistance, showed no difference in the reverted (Eccoseal 1218, Hysol C-60) samples. As can be seen from Table 3-13, there is a significant decrease in self resonant frequency after encapsulation, due to the higher dielectric constant of the material introduced. Pouring off the liquified compound still leaves appreciable material between the wires due to surface tension and adhesion; consequently, the pre-encapsulation self resonant frequency is not attainable.

These test results eliminated from the high reliability encapsulation list two materials, Eccoseal 1218 and Hysol C-60, leaving three remaining resins, Hysol C15-015, Scotchcast 255, and Epon 825 with HV hardener, still under consideration.

3.5.2 Electrical and Mechanical Testing of Saturable Reactors Encapsulated With Hi-Rel Candidate Materials

Four of the saturable reactors shown in Figure 3-32, were encapsulated with each of the five resin systems. These reactors are representative of high reliability electromagnetic components for missile applications. All parts were constructed in exactly the same manner. Each material was used in the manner suggested by the manufacturer or applicable Hughes document.

3.5.2.1 Removal of Excess Material

All encapsulated parts in the material matrix were heated to 125°C in order to soften the cured resin prior to removal. All parts were removed from the matrix using Exacto knives, utility knives, screw-drivers, hammers, chisels, and grinders.

Hysol C15-015, Hysol C60 and Eccoseal 1218, all took less than 30 minutes total time to break out the parts from the matrix and clean off excess encapsulant (flash) from the part. The only tools used on these parts were a screwdriver and an Exacto knife with a large blade. The consistency of the cured resin systems at 125°C was quite similar to a gum eraser.

Scotchcast 255 was much more difficult to remove from the matrix and to trim to the drawing dimensions. The resin system even at 125°C was quite tough. The parts were removed from the matrix carefully using a hammer and chisel. The blows had to be carefully aimed and reasonably light since the resin system is opaque and a badly aimed blow could propagate a crack into the part. A heavy utility knife was used to remove the flash from the warm part. The trimming was tedious on the hot part; however trimming the parts cold was much more laborious. It took two hours to clean off the four parts, including the time needed to reheat each part to maintain it at the elevated temperature.

Epon 825 (HV) impregnated parts were also difficult to break out of the matrix. Removing the matrix between the parts was tedious because unreinforced Epon 825 is a hard brittle epoxy even at 125°C. Cracks in the unreinforced matrix could propagate through the fill holes in the polypropylene vacuum forms into the part if care was not exercised. Removing the flash from the parts was also time consuming as the unreinforced resin was next to the part. A hammer was used to break out the leads and a grinder used slowly and carefully to remove the flash next to the part. The total time needed to clean off these four parts was two hours.

Care is needed to design the mold if a permanent mold is used so that the excess material can be readily removed. Also, if a vacuum formed mold is used, care should be used in the heating and vacuum fitting to obtain as close a fit as possible.

3.5.2.2 Visual Inspection

After encapsulation, material removal, and after thermal cycling the parts were checked visually for cracks or other defects. Exposed areas of the magnetic core were found after cleaning off the excess material. No changes in these exposed areas were evident after the ten cycles between -55°C to 130°C. Various other tests also include visual observations; the results of these tests are found in their respective sections.

3.5.2.3 Resistance to Soldering Heat

One part from each lot was selected for this test. The insulation on the leads was removed up to within 1/4 in. of the part, the part was then dipped into the solder pot up to the start of the wire insulation. No cracking of the encapsulation material or delamination of the potting from the lead was noted.

3.5.2.4 Corrosion Susceptibility Before and After Temperature Cycling

One part of each lot was subjected to 48 hours in a salt spray chamber at 94°F, per MIL-STD-202 Method 101. The parts all showed corrosion damage where the cores were exposed. SEM photographs of corrosion damaged areas for each encapsulant are shown in Figures 3-33A-E. EDAX studies of these areas included as Figures 3-34A-D, showed that the damaged areas had high concentrations of metallic chlorides. In some cases phosphides and sulphides are also noted. These photographs show areas of corrosion of the core surface exposed to the environment due to breaks in the encapsulation.

The Scotchcast 255 photograph, Figure 3-33A, shows a nearly closed crack where the underlying core is partially exposed to the salt spray. The EDAX scan, Figure 3-34A, shows mostly ions due to the epoxy fillers; Al, Mg, Sb, Si and Ti, as well as Fe ions from the core, and Cl from the spray.

The Eccoseal 1218 photograph, Figure 3-33B, shows extensive rough, crusty, areas of the core iron, the result of the corrosive effect of the salt spray on the bare core. The respective EDAX scan, Figure 3-34B shows iron and small amounts of silicon in addition to the chloride ions.

The SEM photograph, Figure 3-33C, of the Epon 825 filled reactor shows small dark dots of corrosion. The EDAX scan of these small areas, Figure 3-34C shows Fe, Sn, Cl, S, P, and Si ions. The iron and silicon ions are mostly from the core material while the Cl, P, S and some iron are corrosion products from the salt spray.

The Hysol C-60 SEM photograph, Figure 3-33D, shows the core material surface that was fully exposed to the salt spray. The encrustation is similar in form to that on the Eccoseal 1218 encapsulated part. The EDAX scan, Figure 3-34D, of the encrusted area shows only iron and chlorine ions.

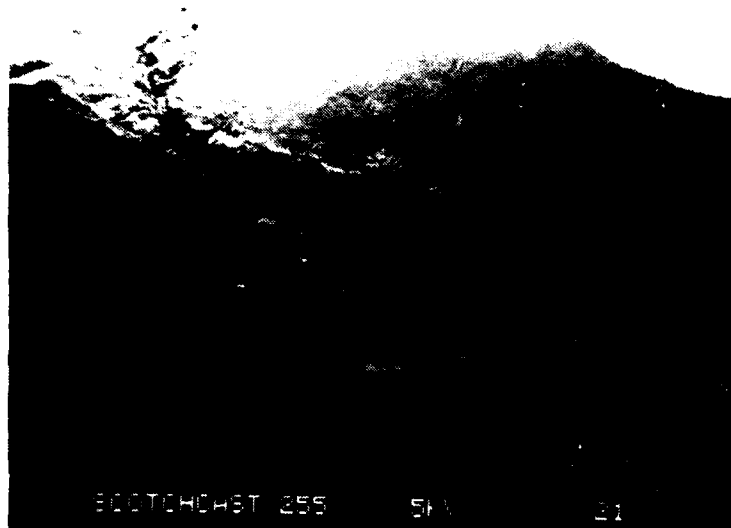


Figure 3-33A. SEM photograph of Scotchcast 255 corrosion area.

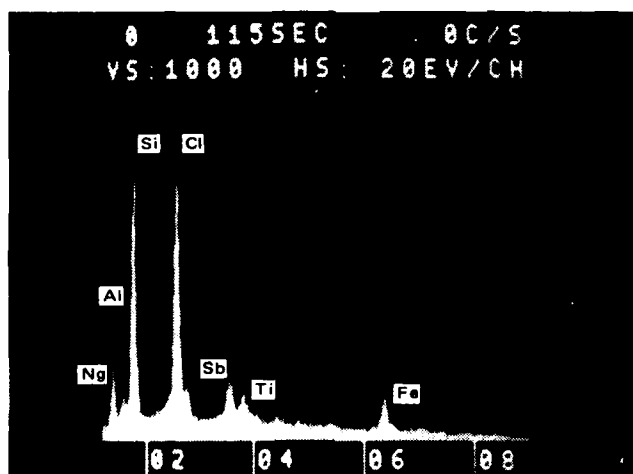


Figure 3-34A. EDAX scan of Scotchcast 255.

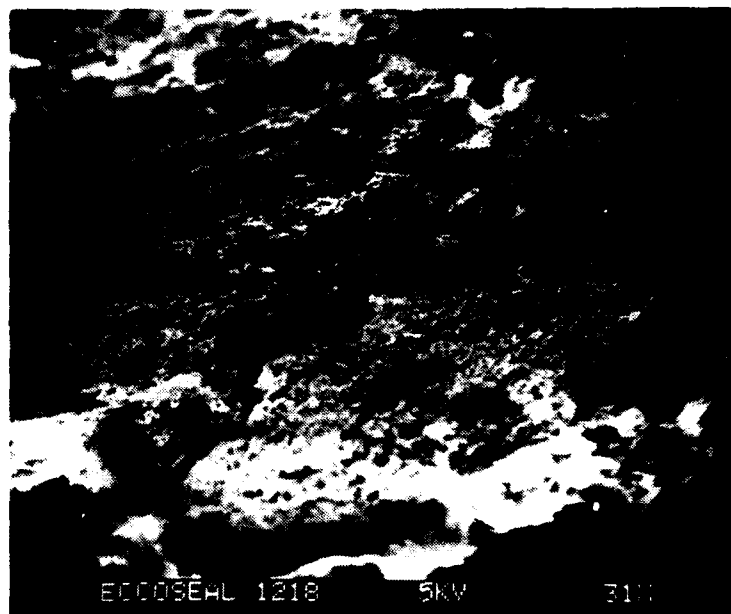


Figure 3-33B. SEM photograph of Eccoseal 1218 corrosion area.

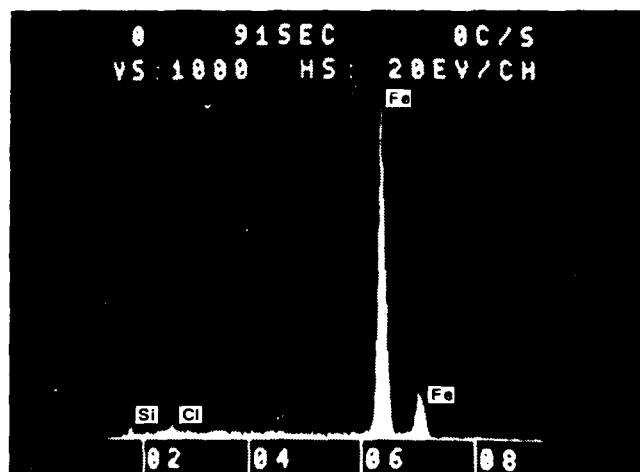


Figure 3-34B. EDAX scan of Eccoseal 1218 corrosion area.

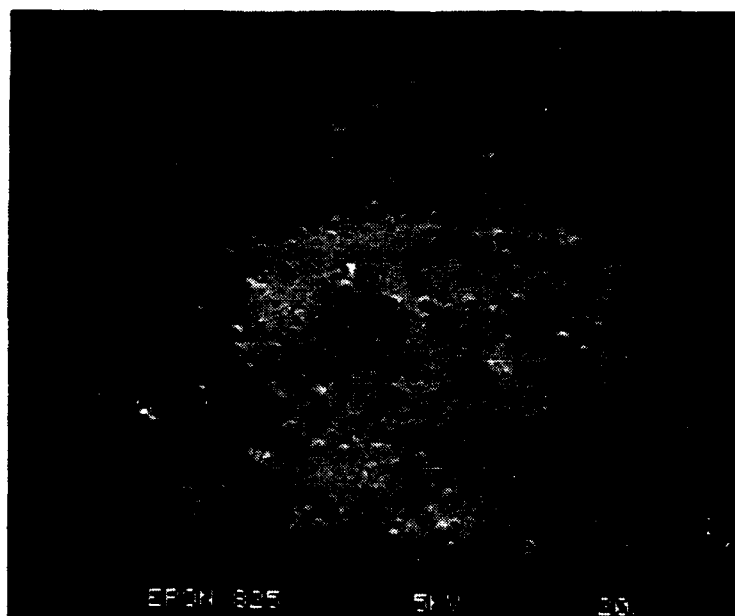


Figure 3-33C. SEM photograph of Epon 825/HV corrosion.

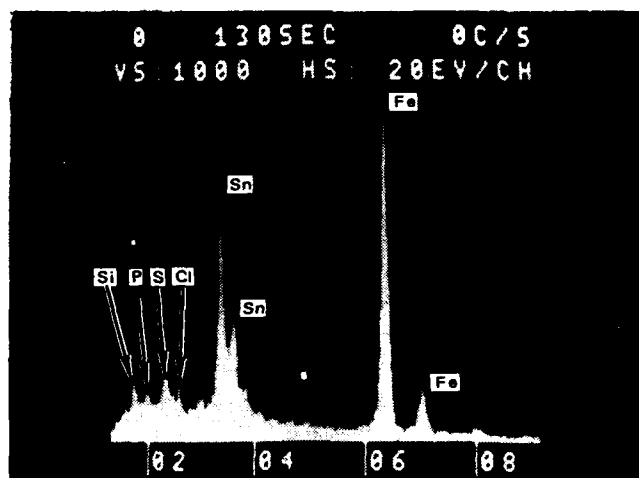


Figure 3-34C. EDAX scan of Epon 825/HV corrosion area.

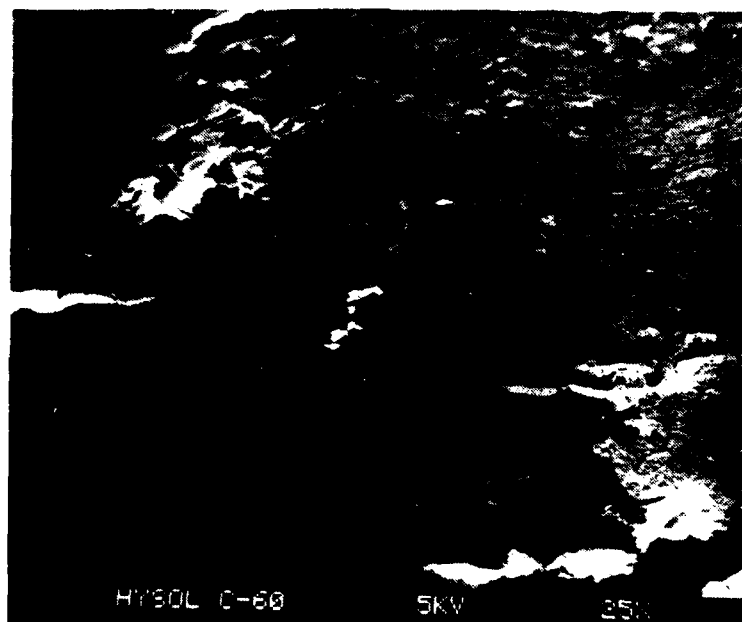


Figure 3-33D. SEM photograph of Hysol C-60 corrosion.

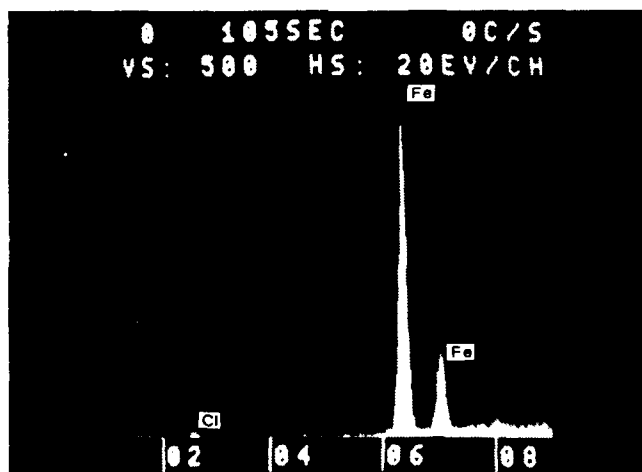


Figure 3-34D. EDAX scan of Hysol C-60 corrosion.



Figure 3-33E. SEM photograph of Hysol C15-015 corrosion.

The Hysol C15-015 SEM photograph, Figure 3-33E, shows the surface of the inductor. No cracks were found in the area of the core. The surface roughness shown is due to uneven trimming of the plastic. No ions were detected during the EDAX scan.

The inductors were next temperature cycled ten times from -55°C to 130°C . Dwelling at the lower temperature for two hours, and at the upper temperature for four hours, with the temperature change rate between these extremes of 3 to $6^{\circ}\text{C}/\text{min}$. SEM photographs and EDAX scans of the corrosion tested inductors were made after temperature cycling. With the exception of Hysol C15-015, the inductors had no deterioration in their surface after temperature cycling. Hysol C15-015 developed cracks in its surface because of the temperature cycling. Figures 3-35A-E and 3-36A-E show the actual SEM photographs and EDAX scans of the inductor's surfaces after temperature cycling.

Figure 3-34A shows a SEM photograph of the Scotchcast 255 corrosion after temperature cycling. Unaccountably the EDAX scan did not detect any ions.

The after-temperature cycling SEM scan of the Eccoseal 1218 encapsulated part is shown in Figure 3-35B. The companion EDAX scan of the Eccoseal impregnated part is shown in Figure 3-36B. The second scan shows small amounts of Si and P as well as the Cl and Fe found in the first EDAX scan. Since the Eccoseal 1218 was beginning to come loose from the core, the Si is clearly from the core. The origin of the P ions is subject to varying theories; corrosion by product from the salt spray, contamination between scans during temperature cycling or core material constituent. The quantity of phosphorous detected is so small that any or all of these may account for the amount found.

The SEM photograph of the corrosion areas in the Epon 825 encapsulated part is shown in Figure 3-35C. The area has small modules of corrosion rising above the base metal. The EDAX scan in Figures 3-36C shows Al, Si, P, Pb, Cl, Sn and Fe. These elements were also found in the previous EDAX scan, Figure 33C, prior to thermal cycling, so it can be assumed that these ions are either from the core or the salt spray.

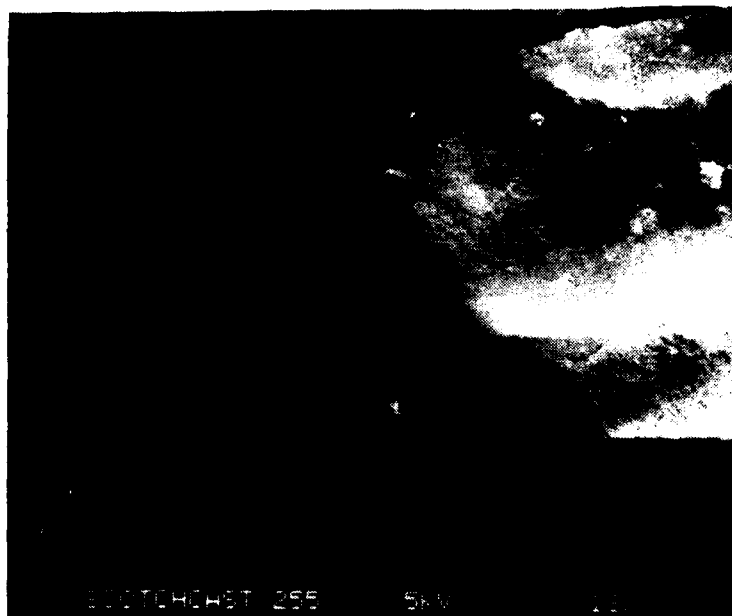


Figure 3-35A. SEM photograph of Scotchcast 255 corrosion after temperature cycling.

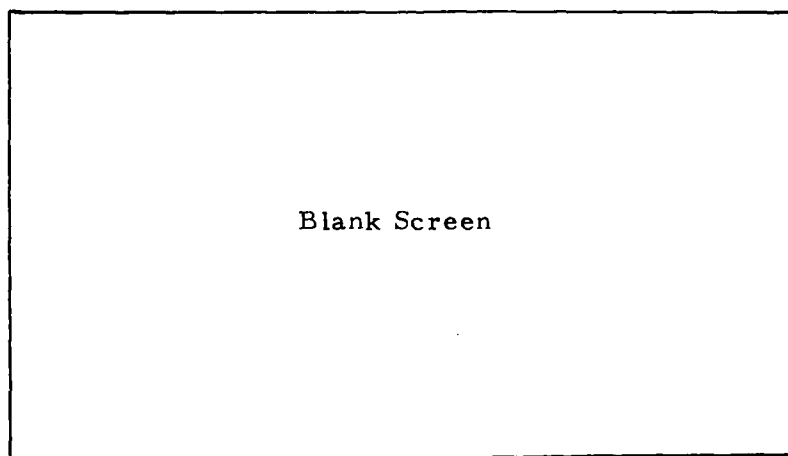


Figure 3-36A. No ions detected during EDAX scan.

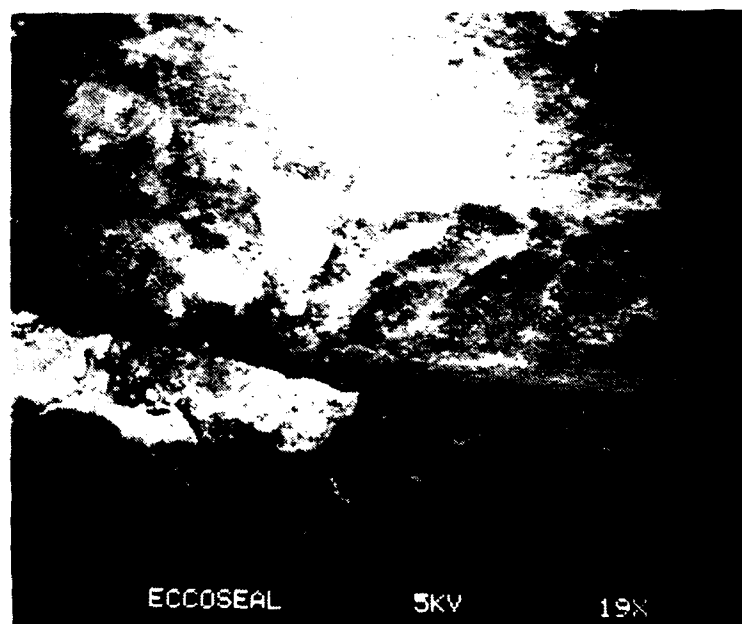


Figure 3-35B. SEM photograph of Eccoseal 1218 corrosion after temperature cycling.

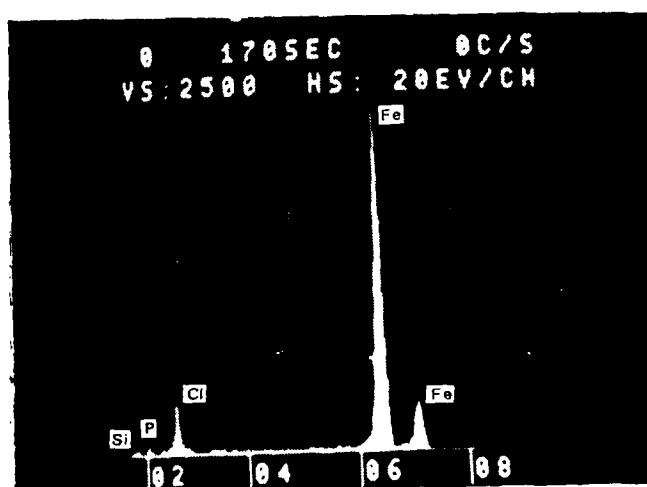


Figure 3-36B. EDAX scan of corrosion after temperature cycling.

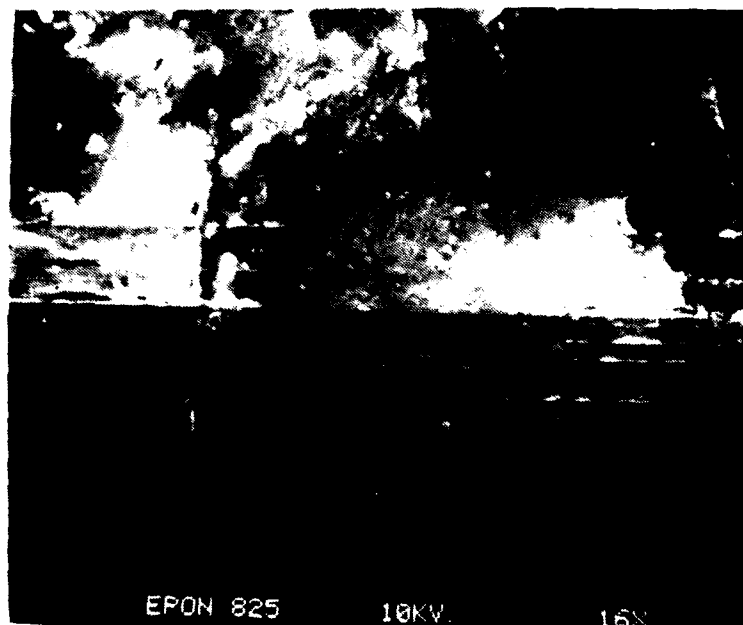


Figure 3-35C. SEM photograph of Epon 825 (HV) corrosion after temperature cycling.

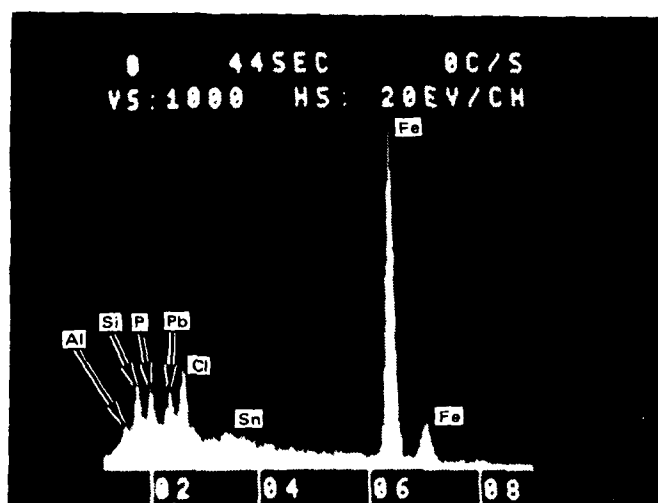


Figure 3-36C. EDAX scan of Epon 825 (HV) corrosion after temperature cycling.

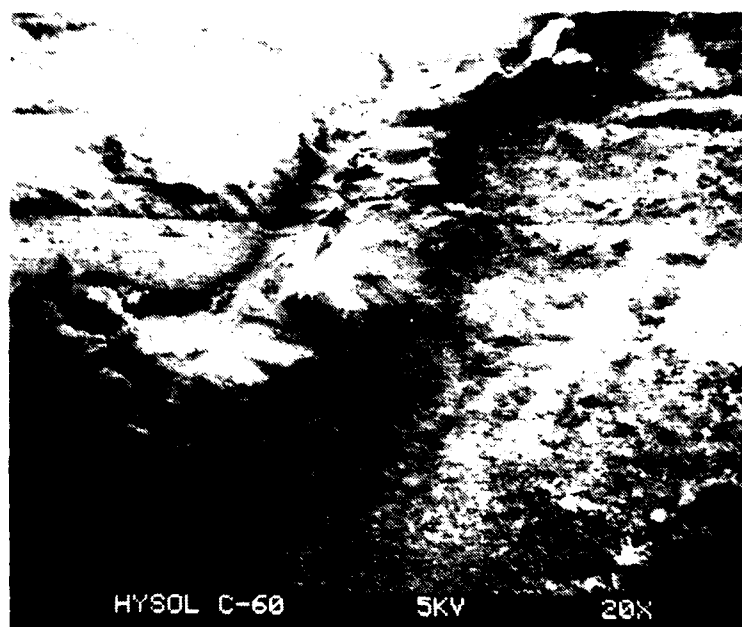


Figure 3-35D. SEM photograph of Hysol C-60 corrosion after temperature cycling.

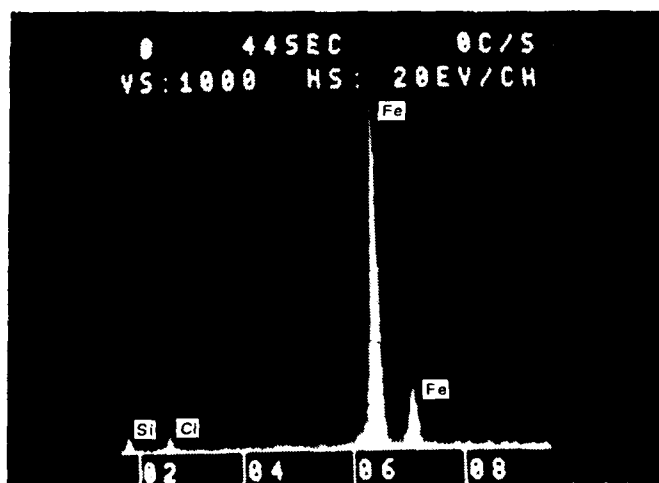


Figure 3-36D. EDAX scan of Hysol C-60 corrosion after temperature cycling.



Hysol C-15 10 KV 12X

Figure 3-35E. SEM photograph of Hysol C15-015 corrosion after temperature cycling.

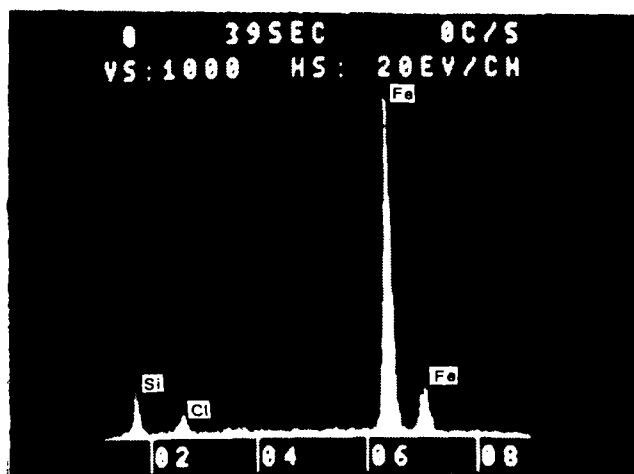


Figure 3-36E. EDAX scan of Hysol C15-015 corrosion after temperature cycling.

Figure 3-35D shows the scanning electron microscope photograph of the corrosion areas of the reactor potted with Hysol C-60. The temperature cycling has increased the damaged area and the intensity of damage. The EDAX scan, Figure 3-36D, shows Fe, Cl, and Si ions in the surface. The Si concentration is probably from the core.

The SEM photograph of the corrosion after temperature cycling on the Hysol C15-015 encapsulated part is shown in Figure 3-35E. It should be noted that a crack has occurred in the surface, probably due to the temperature cycling. The EDAX scan of this area is shown in Figure 3-36E, and it shows Fe, Si, and Cl ions. Table 3-14 shows a summary of all the EDAX data.

3.5.2.5 Adhesion of Encapsulation Material to Part After Temperature Cycling

As a part of the previous section, the adhesion of the 5 selected embedment materials were measured in accordance with ASTM D1002-72 except that 4 shear samples of each material were used to obtain average values.

Most epoxy resins adhere well to coil materials when they are clean, and most resins retain their adhesion during corrosion testing. Eccoseal 1218, as shown in Table 3-15 has the best tensile shear strength to clean surfaces of any material in this subtask. However, Eccoseal 1218 could easily be peeled off corrosion tested inductor surfaces with a fingernail. None of the other materials could be so easily removed from the inductor after the corrosion test.

3.5.2.6 Electrical Measurements of Parts Encapsulated with Selected Materials

Five electrical parameters of the reactor shown in Figure 3-32 were measured after initial inductor construction, after encapsulation, and after temperature cycling. These parameters were: inductance with and without bias current, leakage inductance, self-resonant frequency, DC coil resistance, and dielectric withstanding voltage. The testing methods conformed to the requirements of MIL-T-27D.

TABLE 3-14. EDAX ION DETECTION DATA

Material	Al	Cl	F	M	P	Pb	S	Sb	Si	Sn	Ti
Scotchcast 255	B A	B A	B A	B A	B A	B A	B A	B A	B A	B A	B A
Eccoseal 1218	X -	X -	X -	X -	- -	- -	- -	X -	X -	- -	X -
Epon 825/HV	- -	X X	X X	- -	- X	- -	- -	- -	X X	- -	- -
Hysol C-60	- X	X X	X X	- -	X X	- X	X X	- -	X X	X X	- -
Hysol C-15-015	- -	X X	X X	- -	- -	- -	- -	- -	- X	- -	- -
	-	- X	- X	- -	- -	- -	- -	- -	- X	- -	- -

X indicates presence of ions
 - indicates EDAX run made but no ions present
 B Before Temp Cycle
 A After Temp Cycle

TABLE 3-15. TENSILE SHEAR STRENGTH

Material	Sample Area	Tensile Shear Strength Average	Temperature/ Failure Type
Hysol C15-015	0.500 in ²	374 psi	R.T/ 100% adhesive
Eccoseal 1218	0.509	2599	R.T/ 100% cohesive
Epon 825/HV	0.515	1755	R.T/ 100% adhesive
Scotchcast 255	0.520	1135	R.T/ 60-80% cohesive
Hysol C-60	0.515	1995	R.T/ 100% cohesive

The results of the electrical tests are found in Table 3-16. The inductance values, shown in the first two columns, have only a 1 to 3 percent variance in value for all the encapsulation materials with the exception of Eccoseal 1218. The 1 to 3 percent variance in value can be partially accounted by the 1 percent test set accuracy and the use of two different test sets at different stages of the process. Also Kapton film is used to maintain the gap widths in the "C" cores, and any slight change in gap dimension would have significant effects on the inductance.

In the case of the Eccoseal 1218 the definite change in the inductance must be attributed to the encapsulation material. Plots of inductance as a function of time shows no discernible pattern for the other parts.

The variation of leakage inductances with respect to fabrication steps as shown in Table 3-16 is different for each material utilized. Only Hysol C-60 had a significant change as a result of encapsulation. However, a significant change in leakage inductance value occurred for all materials after temperature cycling. The leakage inductance also shows no common trend with fabrication step.

The self resonant frequency column clearly show that the impregnation material changes the stray capacitance of the inductor. This frequency measurement was made with the primary leads 1-2 shorted. The secondary coil can then be considered an inductor and a series resistor in parallel with

TABLE 3-16. ELECTRICAL PROPERTIES OF ENCAPSULATED REACTORS

Material	Time	Inductance ² , μH			Leakage ³ , μH	DC Resistance, ohms		Self Resonant Frequency, MHz (1-2 shorted)	Dielectric Withstanding Voltage ⁴ , vac rms	
		w/20 ADC	No I			1-2	3-4		(1+2) to (3+4)	(1+2+3+4) to Core
Scotchcast 255	1	181	213		0.65	0.0074	0.029	38	>300	>300
	2	185	214		0.65	0.00710	0.0282	26	>300	>300
	3	180	208		0.50	0.00695	0.0283	27.8	>300	>300
Epon 825	1	181	214		0.60	0.0073	0.029	38.0	>300	>300
	2	188	214		0.62	0.00724	0.0282	26.4	>300	>300
	3	182	211		0.75	0.00712	0.0290	24.4	>300	>300
Hysol C15-015	1	183	214		0.70	0.0072	0.029	38.0	>300	>300
	2	183	214		0.73	0.00710	0.0286	25.0	>300	>300
	3	181	204		0.58	0.00710	0.0290	23.9	>300	>300
Eccoseal 1218	1	191	212		0.70	0.0077	0.030	38.0	>300	>300
	2	198	218		0.69	0.00737	0.0292	29.0	>300	>300
	3	182	211		0.75	0.00712	0.0290	24.7	>300	>300
Hysol C-60	1	183	210		0.62	0.0071	0.029	33.8	>300	>300
	2	183	211		0.81	0.00723	0.02872	24.0	>300	>300
	3	185	211		0.52	0.00712	0.0290	30.0	>300	>300

¹ 1. Initial Construction, 2. After Encapsulation/Before Cycling, 3. After Cycling, temperature cycling was 10 cycles, -55°C to 130°C, 2 hours dwell time at bottom temperature, 4 hours dwell time at top temperature and 3-6°C/min between temperature extremes.

² 17 vrms, 20 kHz, with and without 20 ADC in winding 1-2.

³ Measured across 3-4 with 1-2 shorted.

⁴ Dielectric withstanding voltage measured.

a capacitor due to the ac resistance of the coil. In the case of the Scotch-cast 255, the leakage inductance was 0.65 μ H before and after encapsulation. The direct current resistance was 0.029 ohms. However, the self resonant frequency was 38 MHz before encapsulation and 26 MHz after wards.

Skin effect must be considered to find the ac resistance of the wire at the self resonant frequency. Curves relating the ratio R_{ac}/R_{dc} to $D\sqrt{f}$ are given in reference 1, page 130. The diameter, D of the wire is 0.032 inches, therefore, at 30 MHz, $D\sqrt{f}$ is 197. The multiplication ratio R_{ac}/R_{dc} is 19.6 and R_{ac} equals 0.57 ohms. Similarly for the resistance at 26 MHz the ac resistance is 0.46 ohms. The basic formula for the resonant circuit is $(2\pi F)^2 = 1/LC - R^2/L^2$. At 38 MHz $C = 27.0$ pf as wound; at 26 MHz $C = 57.6$ pf, the increase is due to the greater dielectric constant of the encapsulent.

The capacitance C between two parallel cylindrical conductors of length l spaced c apart and of diameter d , all in MKS units, equals in vacuum, (Ref 5).

$$C_o = \frac{\pi E_o l}{\cosh^{-1}(c/d)}$$

The error in using this formula for air can be neglected; however for embedment materials with dielectric constant E_r ,

$$C_r = \frac{\pi E_r E_o l}{\cosh^{-1} c/d}$$

Substituting values in the Equation for C_o we obtain:

$$C_o = \frac{\frac{.872 \times 10^{-9}}{36}}{\cosh^{-1} \frac{9.80 \times 10^{-4}}{8.13 \times 10^{-4}}}$$

If two materials of differing E_r fill the void between conductors, the resultant capacitance can be considered the result of two capacitors in series, each one filled with one of the dielectrics.

In the as-constructed state, the inductor has volumes filled with air and polyimide/polyamide insulations. The E_r of the polyimide is 3.1.

$$C_{\text{total}} = \frac{3.1 \times 1 C_0}{3.1 + 1} = 29.0 \text{ pf}$$

$$C_{\text{measured}} = 27.0 \text{ pf}$$

In the encapsulated state, the inductor has spaces filled with insulation and encapsulation material.

$$C_{\text{total}} = \frac{3.1 \times 3.87 C_0}{3.1 + 3.87} = 66.1 \text{ pf}$$

$$C_{\text{measured}} = 57.6 \text{ pf}$$

These capacitance values are remarkably close. The capacitance can be similarly calculated for the other materials. Table 3-17 gives the self resonant frequency before and after potting the capacitance calculated from the self resonant frequency and the theoretical capacitance.

TABLE 3-17. EFFECTS OF ENCAPSULATION MATERIALS ON INTERWINDING AND STRAY CAPACITANCES

Material	Frequency		Experimental Capacitance	Theoretical Capacitance
	Before	After		
Epon 825/HV	38.0 MHz		29.2 pf	29.0 pf
		26.4 MHz	58.6	67.5
Scotchcast 255	38.0		27.0	29.0
		26.0	57.6	66.1
Eccoseal 1218	38.0		25.	29.0
		29.0	43.6	62.1
Hysol C15-015	38.0		25.1	29.0
		25.0	55.5	67.9
Hysol C-60	33.8		35.7	29.0
		24.0	54.3	69.8

The dielectric withstanding voltage test was intended to locate any materials which failed to provide adequate dielectric strength between the coils and between the coils and ground. All of the coils passed this during all three test intervals; before potting, after potting, and after temperature cycling; apparently the insulation of the wire is sufficient to pass this test.

3.5.2.7 Mechanical Shock Testing

Ten of the saturable reactors, were mechanically shock tested using the test fixture in Figure 3-37. Five of the reactors had previously been electrically and corrosion tested; the other five had been electrically but not corrosion tested. All reactors were electrically good at the start of the mechanical shock test.

The purpose of this mechanical shock test was to determine which material best improved the mechanical integrity of the reactor and protected it from mechanical shock. The normal mechanical shock test of a part weighing 300+ grams generally is done at 100 to 200 g. Rarely the mechanical shock will be tested up to 400 g.

The test started at 100 g and increased by 100 g intervals until part rupture, or 3000 g acceleration, whichever came first. All ten parts were subjected to the entire test regimen of Table 3-18. No part had obvious external damage after 3000 g acceleration. The parts were then X-rayed in order to determine the extent of internal structural damage. Several of the reactor X-rays showed gray areas that could be due to mechanical damage to the core. These parts had their inductance measured in order to compare the before and after electrical values, in order to determine if the gray areas were structural changes in the device or photographic artifacts of some type.

All of the transformers, except one of the two parts encapsulated with Epon 825, showed a variation in electrical values within the test equipment error. The part encapsulated with Epon 825 was X-rayed from two directions in order to obtain a stereoscopic effect. The maximum separation that could be obtained using the high energy X-ray machine was a 30 degrees half angle. The photographs taken by this machine at maximum angle showed some stereoscopic effects, especially the leads to the outside world, using an oldtime stereoscopic viewer. With the X-ray pictures available, the depth of the grey areas could not be determined

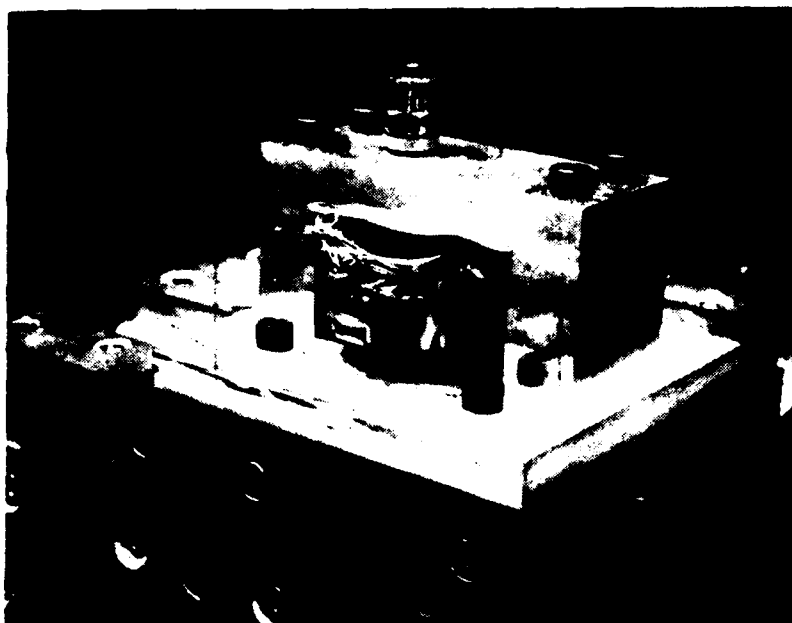


Figure 3-37. Mechanical shock test fixture.

TABLE 3-18. MECHANICAL SHOCK TESTING PROGRAM

Acceleration	Duration	Acceleration	Duration	Acceleration	Duration
100	7 msec	1100	0.5 msec	2100	0.2 msec
200	6 msec	1200	0.5 msec	2200	0.2 msec
300	3 msec	1300	0.4 msec	2300	0.2 msec
400	3 msec	1400	0.4 msec	2400	0.2 msec
500	2.8 msec	1500	0.4 msec	2500	0.2 msec
600	3 msec	1600	0.4 msec	2600	0.2 msec
700	2 msec	1700	0.4 msec	2700	0.2 msec
800	2 msec	1800	0.4 msec	2800	0.2 msec
900	2 msec	1900	0.3 msec	2900	0.2 msec
1000	0.5 msec	12000	0.2 msec	3000	0.2 msec

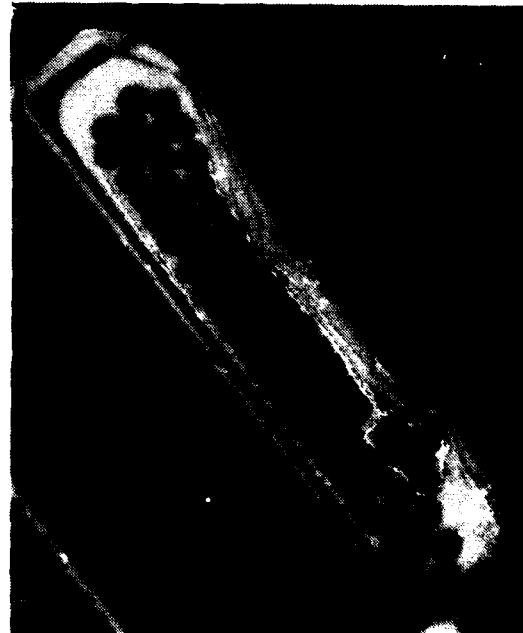
Further investigation showed that a half angle of 32 degrees was the minimum to obtain the three dimensional effect and a half angle of 45 degrees was needed to obtain quantitative stereographic information. Machines that could give a radiation cone this large with a movable head did not have sufficient energy to penetrate the core. From the rather disappointing results of the X-ray study it was decided that further efforts were not warranted. It must be concluded that one of the Epon 825 potted parts was damaged by the mechanical shock test regimen because the electrical parameters changed.

3.5.2.8 Cross Section of Part to Determine Extent of Voids

One reactor which had been encapsulated with each material was electrically tested and found to meet the design criteria. The parts were then temperature cycled from -55°C to $+125^{\circ}\text{C}$ ten times. A second electrical test of the reactors showed that no significant changes occurred. The parts were then cross-sectioned, polished, photographed, and shown in Figures 3-38A-E in longitudinal sections. The Epon 825, Scotchcast 255, and Eccoseal 1218 parts showed no voids or cracks in the encapsulation. The part potted with Hysol C15-015 shows extensive cracking in the coil areas. The C-60 part shows numerous voids as well as extensive cracking. All the parts were constructed in the same manner. Each part used the same amount of fiber glass filler, and the same bobbin and core. They differ only in the encapsulation techniques and materials used. Epon 825 with HV hardener cracks easily if it is not sufficiently reinforced. Since, as stated earlier, the Epon 825 parts showed no cracking, the cracks found in the Hysol epoxy encapsulated parts can only be due to the potting materials rather than the reinforcing and construction techniques used.

3.5.3 High Voltage Transformer Model Testing

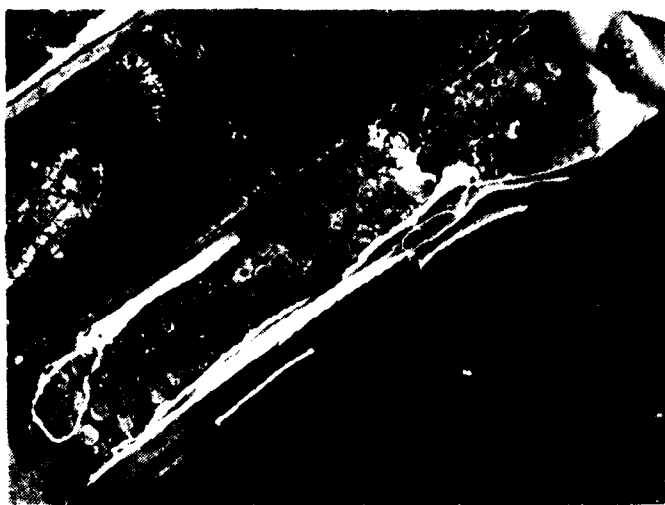
A typical high voltage TWT saturable core transformer design, Figure 3-39 was used as a test component for the five selected encapsulation materials. Each material was used to encapsulate two parts, so that a material might not be eliminated due to a simple construction error or other nonmaterial related problem. The test criteria included: excitation current, core loss, D.C. resistance of the windings, interwinding capacity, leakage inductance, spurious resonance frequency, dielectric strength, induced



Magnification: 2.5x

Comments: No voids or cracks
evident

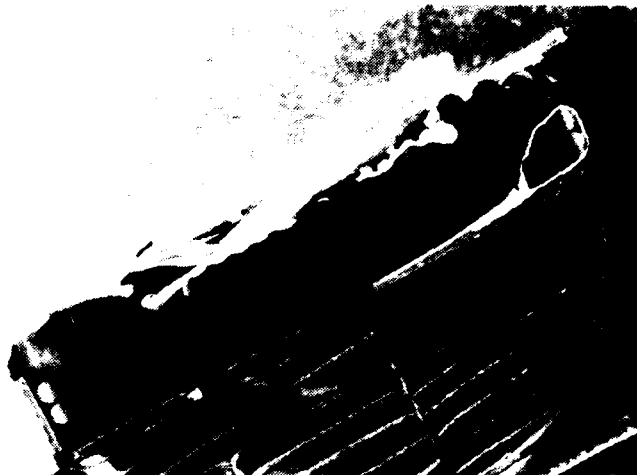
Figure 3-38A. Longitudinal cross sections of part potted with Scotchcast 255.



Magnification: 2.5x

Comments: No voids or cracks
evident

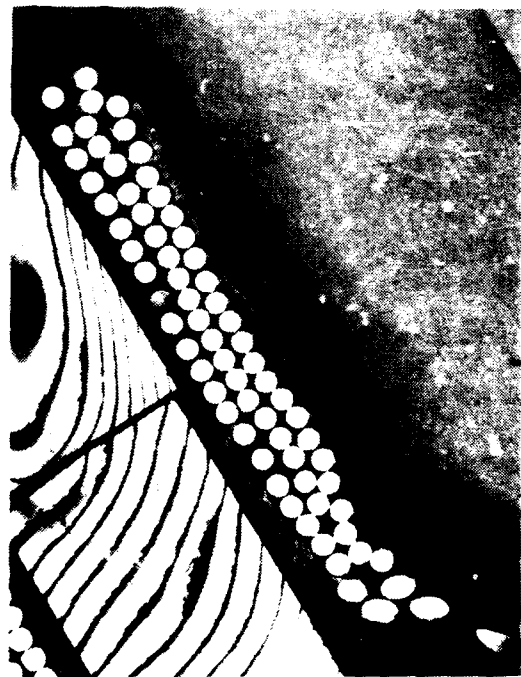
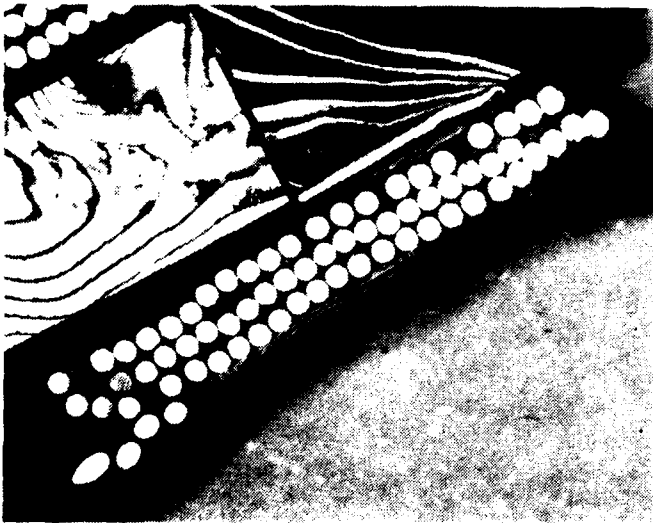
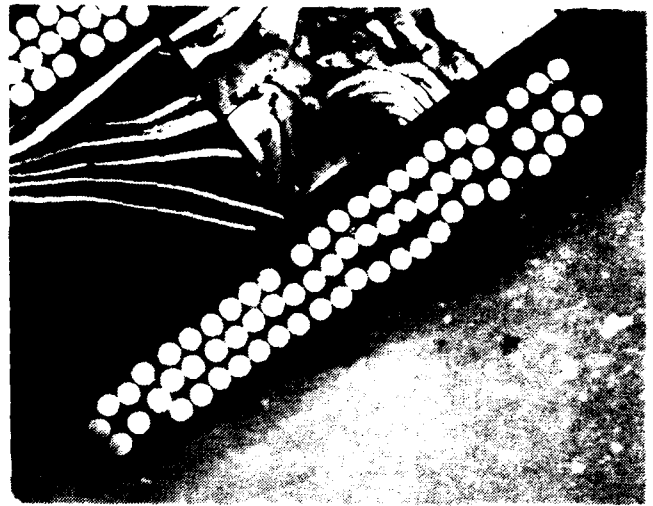
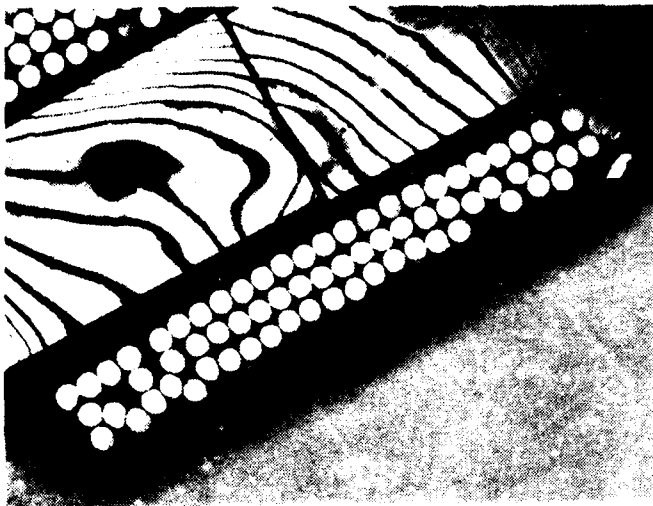
Figure 3-38B. Longitudinal cross sections of part potted with Eccoseal 1218.



Magnification: 2.5x

Comments: No voids or cracks
evident

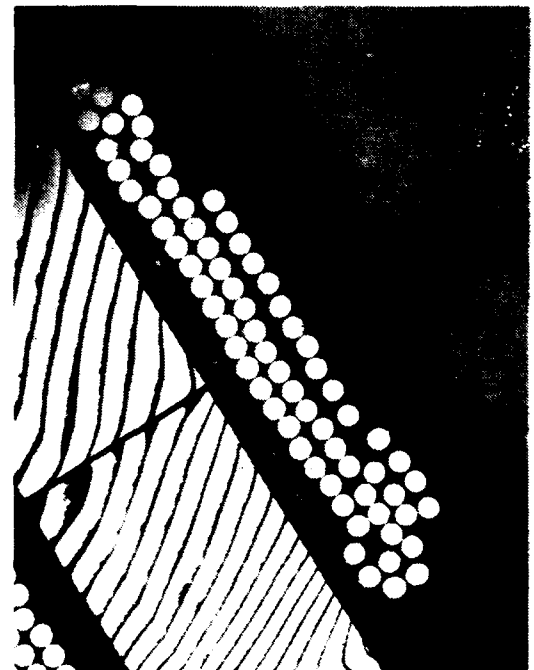
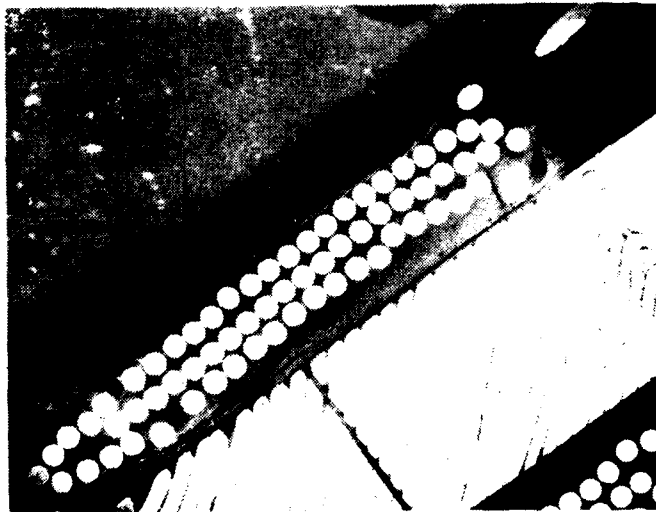
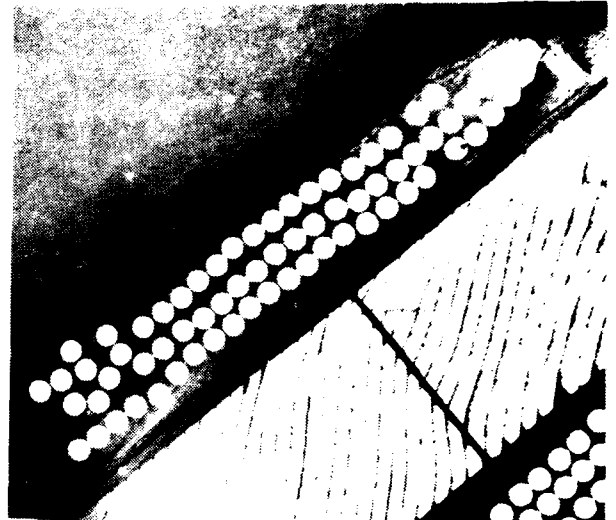
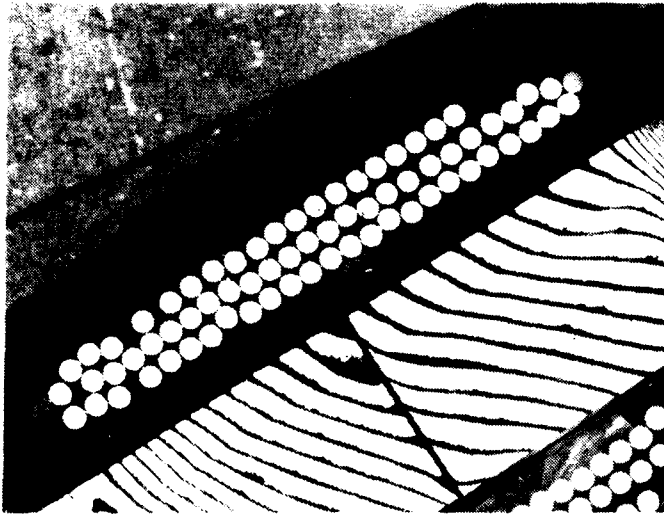
Figure 3-38C. Longitudinal cross sections of part potted with Epon 825.



Magnification: 2.5x

Comments: Note cracks and voids
in cross sections

Figure 3-38D. Longitudinal cross sections of part potted with Hysol C-60.



Magnification: 2.5x

Comments: No voids in cross section. There is extensive cracking

Figure 3-38E. Longitudinal cross sections of part potted with Hysol C15-015.

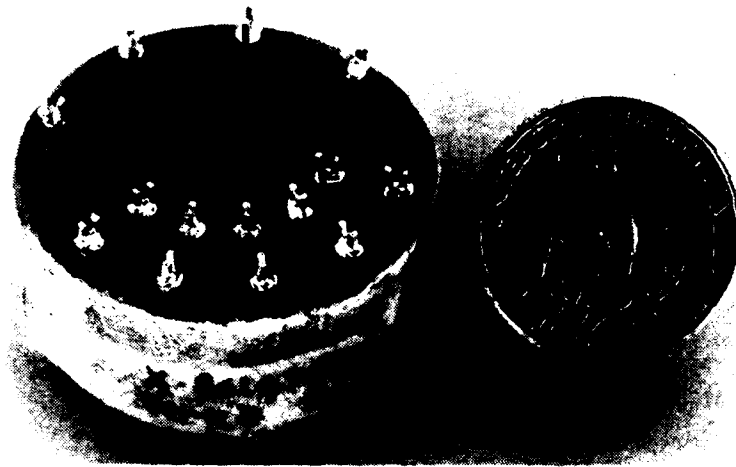


Figure 3-39. TWT high voltage transformer.

voltage, insulation resistance, volt-second support, intrawinding insulation weight and environmental seal. These tests cover the major magnetic and electric characteristics of the transformer. The data from these tests are shown in Table 3-19. The excitation current is the current developed in the primary when a given input signal is applied to the primary, with all other windings open.

3.5.3.1 Core Loss

In the present series of tests, 21 Vrms at 8 KHz was applied to the primary winding (1-2). The maximum excitation current for this design is 120 mA, which checks that the correct core was used or that the core is not damaged or cracked. The core loss is comprised of two components; hysteresis loss, the portion of the input dissipated into heat in altering the orientation of the magnetic poles, and eddy current loss, the I^2R losses within the core that occur from currents induced in the core from the varying magnetic flux. In effect, the core loss can be considered a resistance in series with the

TABLE 3-19. HIGH VOLTAGE TRANSFORMER TEST RESULTS

Part No.	Excitation Current $\leq 120\text{mA}$	Core Loss $\leq 60\text{mW}$	D. C. Winding Resistance					300 Vrms (@60 Hz (1-3) to all Others No Breakdown	300 Vrms (@60 Hz (4-6) to all Others No Breakdown	Dielectric Strength 3300 Vrms (@60 Hz (7-8) to all Others No Breakdown	2200 Vrms (@60 Hz (9-10) to all Others No Breakdown	850 Vrms (@60 Hz (11-14) to all Others No Breakdown
			1-3 $\leq 0.78\Omega$	4-6 $< 0.39\Omega$	7-8 $\leq 28\Omega$	9-10 $\leq 40\Omega$	11-14 $\leq 11\Omega$					
Epon 825/HV 1	88mA	0.27mW	0.645	0.282	223.8	318.3	93.8	OK	OK	OK	OK	OK
Epon 825/HV 2	89	0.271	0.650	0.271	228.0	323.0	95.9	OK	OK	Breakdown 500V	OK	Breakdown
Eccoseal 1218 3	76.8	0.29	0.641	0.276	220.0	310.2	92.3	OK	OK	OK	OK	OK
Eccoseal 1218 4	81.1	0.30	0.638	0.265	223.3	312.4	92.1	OK	OK	OK	OK	OK
Hysol C15-015 5	79.9	0.29	0.647	0.275	223.4	312.4	91.4	OK	OK	OK	OK	OK
Hysol C15-015 6	94.6	0.31	0.647	0.289	216.4	306.4	92.0	OK	OK	OK	OK	OK
Scotchcast 255 7	47.9	0.25	0.650	0.279	224.4	302.0	93.3	OK	OK	Breakdown	OK	Breakdown
Scotchcast 255 8	56.0	0.25	0.647	0.265	221.8	306.8	91.3	OK	OK	OK	OK	OK
Hysol C-60 9	81.9	0.25	0.642	0.281	226.2	310.8	93.4	OK	OK	OK	OK	OK
Hysol C-60 10	80.0	0.28	0.649	0.289	223.0	306.1	22.0	OK	OK	OK	OK	OK

(Continued next page)

(Table 3-19 concluded)

Part No.	Insulation Resistance				Voltage Second Support 2.3 to 3.1 Vrms	Intrawinding Insulation				Interwinding Insulation (in Freon)														Seal	Resin Viscosity at Pouring Temperature
	(1-3) To All Other Windings >10 ⁹ Ohms @ 500 Vdc	(4-6) To All Other Windings >10 ⁹ Ohms @ 500 Vdc	(7-8) To All Other Windings >10 ⁹ Ohms @ 500 Vdc	(9-10) To All Other Windings >10 ⁹ Ohms @ 500 Vdc		(11-14) To All Other Windings >10 ⁹ Ohms @ 500 Vdc	7-8	8-7	9-10	10-9	(18-7) to (11-21)		(4-5) to (6-9)		(10-11) to (12-13)		(9-10) to (12-23)		(4-5) to (7-8)		(11-12) to (13-14)				
											2.5 pC 0 Count	5 pC 0 Count	10 pC 0 Count	25 pC 0 Count	50 pC 0 Count	2.5 pC 0 Count	5 pC 0 Count	10 pC 0 Count	25 pC 0 Count	50 pC 0 Count	2.5 pC 0 Count	5 pC 0 Count	10 pC 0 Count		
Epon 825 1	OK	OK	OK	OK	2.63 Vrms	OK	OK	OK	OK	0	0	0	0	0	0	0	0	0	0	0	0	0	OK	75 cps	
Epon 825 2	OK	OK	7K Ω	OK	2.56	Shorted				Shorted														Leaks	75
Eccoseal 1218 3	OK	OK	OK	OK	2.65	Shorted, Breakdown 10V				8636	4778	5874	3261	1817	0	0	0	0	0	0	0	0	OK	300	
Eccoseal 1218 4	OK	OK	OK	OK	2.68	OK	OK	OK	OK	0	0	0	0	0	0	0	0	0	0	0	0	0	OK	300	
Hysol C15-015 5	OK	OK	OK	OK	2.63	OK	OK	OK	OK	3768	2059	786	0	0	0	0	0	0	0	0	0	0	OK	200	
Hysol C-15-015 6	OK	OK	OK	OK	2.63	OK	OK	OK	OK	4788	3906	3045	2928	2630	0	0	0	0	0	0	0	0	OK	200	
Scotchcast 255 7	OK	OK	5K Ω	OK	2.66	Shorted				Shorted														Leaks	1500
Scotchcast 255 8	OK	OK	OK	OK	2.63	OK	OK	OK	OK	0	0	0	0	0	0	0	0	0	0	0	0	0	Leaks	1500	
Hysol C-60 9	OK	OK	OK	OK	2.69	Corona in all tests				7780	13440	3609	354	233	0	0	0	0	0	0	0	0	OK	150	
Hysol C-60 10	OK	OK	OK	OK	2.63	Corona in all tests				6648	1323	275	20	10	0	0	0	0	0	0	0	0	OK	150	

primary. The core loss test for the test transformer used the same 21 Vrms, 8 KHz signal to the primary as noted above. The core loss should be 60 milliwatts maximum.

3.5.3.2 Winding Resistance

The D.C. resistance of the windings are proportional to the copper losses of the transformer. The values should be read using a Kelvin bridge or other instrument of similar accuracy. The maximum values of resistance are:

Winding	Ohms
1-2 = 2-3 =	0.387
4-5 = 5-6 =	0.196
8-7 =	282.0
9-10 =	402.0
11-14 =	117.0

3.5.3.3 Winding Capacitance

The interwinding capacitance is measured between (2, 3), (7, 8) and (9, 10) where the parenthesis encloses those pins which are shorted for the test. The maximum values of capacitance are:

(1, 2, 3) to (9, 10)	60 pf
(1, 2, 3) to (7, 8)	55 pf
(8, 7) to (9, 10)	40 pf

These measurements give the capacitances which are useful to integrate the device into the circuit.

3.5.3.4 Leakage Inductance

The leakage inductance is the inductance of the secondary windings when the primary coil is shorted.

A 1 volt rms signal at 10 KHz is placed on each secondary coil in turn. The maximum inductance for each coil in the transformer is:

$$L_{9-10} = 15 \text{ mH}$$

$$L_{8-7} = 12 \text{ mH}$$

$$L_{11-14} = 1 \text{ mH}$$

3.5.3.5 Spurious Resonance Frequency

The spurious resonance frequency is a frequency where the voltage response of the secondary coils exhibits greater than a 6 db resonant dip. The instructions only require the dip not be within a certain frequency range, but the data actually shows where the first dip occurs. The further away from this range this dip is, the lower are the leakage or stray capacitances.

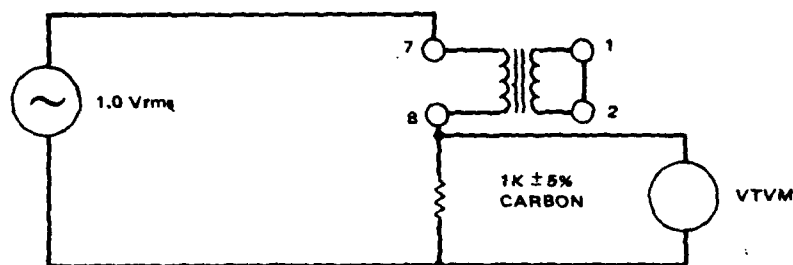


Figure 3-40. Spurious resonance frequency-schematic.

- Short winding 1-2, connect transformer in circuit of Figure 3-40 above, leave other windings open.
- Apply 1.0 VRMS $\pm 10\%$ to winding 7-8.
- Vary the frequency from 75.0 KHz to 350 KHz.
- If any resonance occurs in this frequency range determine the gain "A" per Figure 3-41 for each resonance. ("A" is measured at the back-swing of the response curve).
- There shall be no resonance in the range from 75.0 KHz to 350 KHz for which the gain "A" is greater than 6 db.
- Repeat b thru e above for winding 9-10.

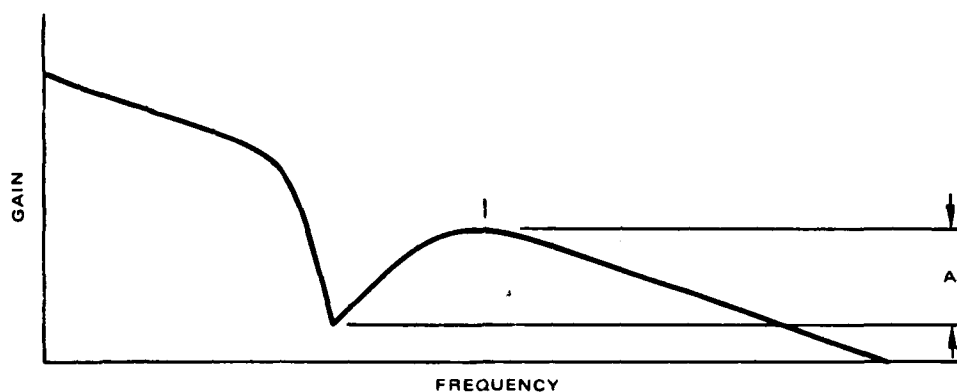


Figure 3-41. Typical gain vs frequency curve.

3.5.3.6 Dielectric Strength

The dielectric strength is measured according to the method outlined in MIL-T-27. This test is performed only after aging in the following manner:

3300 VRMS, 60 Hz between 8-7 and all other windings

2200 VRMS, 60 Hz between 9-10 and all other windings

300 VRMS, 60 Hz between 1-2-3 and all other windings/then 4-5-6 and all other windings

850 VRMS, 60 Hz between 11-14 and all other windings

The induced voltage test is performed as outlined in MIL-T-27 except a square wave instead of a sine wave at twice the operating frequency is used. The transformer is examined for evidence of continuous arcing, insulation breakdown and abrupt changes in input current. Any changes in input current and Q are also noted during this test. In the present test, 40 volt peak square wave of 16 KHz was applied to winding 1-2.

3.5.3.7 Insulation Resistance

The insulation resistance is measured at 500 volts d. c. in the following manner: 1-3, 4-6, 7-8, 9-10 and 11-14 to all other windings. The resistance shall be greater than 10^9 ohms.

The volt-second support test is a test of the coils to find the input voltage at which the core saturates.

The test diagram is shown in Figure 3-42 below. The test is performed by applying a certain voltage and measuring the current which is proportional to V_{Rpk} . The input signal is increased until V_{Rpk} is 3 times the original V_{Rpk} . The second V_{in} is recorded as the data.

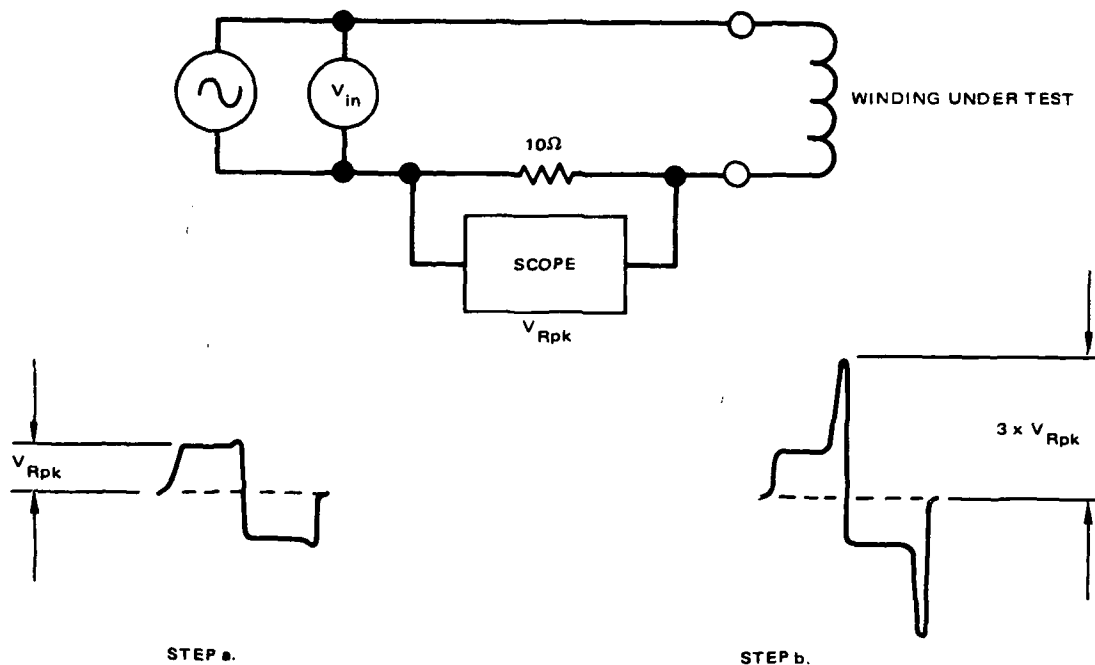


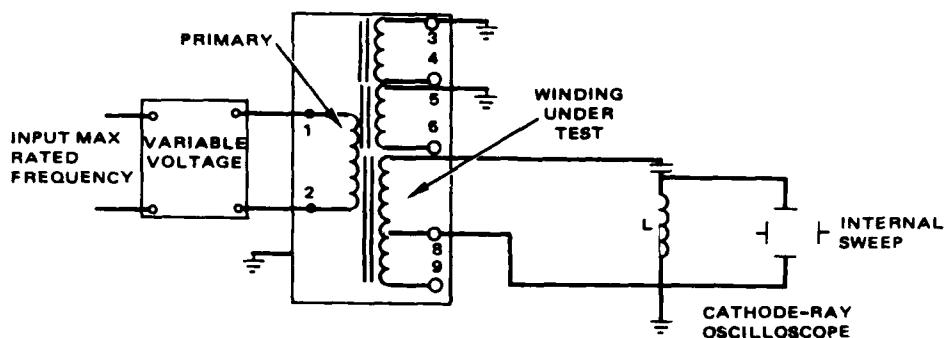
Figure 3-42. Volt-second support test-schematic and waveforms.

3.5.3.8 Intrawinding Insulation

The intrawinding insulation test uses circuit 1 of Figure 10 of MIL-T-27, shown as Figure 3-43. The test voltages were applied in the same manner as the dielectric withstanding voltage and the test voltage must be 130 percent of the working voltage. In the present design the working voltage is a 23.5V square wave so that a 21 volt RMS sine wave at 11 KHz gives the required signal. The test sequence is as follows:

- a. Test winding 8-7 by applying 21.0 VRMS, 11.0 KHz to winding 1-2 with No. 8 grounded.

- b. Test winding 8-7 by applying 21.0 VRMS, 11.0 KHz to winding 1-2 with No. 7 grounded.
- c. Test winding 9-10 by applying 21.0 VRMS, 11.0 KHz to winding 1-2 with No. 10 grounded.
- d. Test winding 9-10 by applying 21.0 VRMS, 11.0 KHz to winding 1-2 with No. 9 grounded.
- e. There shall be no corona present.



Circuit 1 - primary excited

- Notes:
1. When using circuits 1 and 2, ground the case of the transformer or inductor and all windings except that being tested.
 2. Legend for test circuits: C = 200 picofarad, mica capacitor, corona free L = RF choke, 20 to 30 millihenries inclusive, with a minimum Q of 50 at 100 Kilohertz, HV = high voltage source, corona free.
 3. Corona will be evident as a superimposed high-frequency oscillation on the basic power wave.

Figure 3-43. Intrawinding insulation test-schematic.

3.5.3.9 Interwinding Insulation

The interwinding insulation test is performed using a circuit equivalent circuit 2 of Figure 10, MIL-T-27. A schematic is shown as Figure 3-44

below. The voltages used are 130 percent of the working voltages. The notes for Figure 3-43 apply also to Figure 3-44.

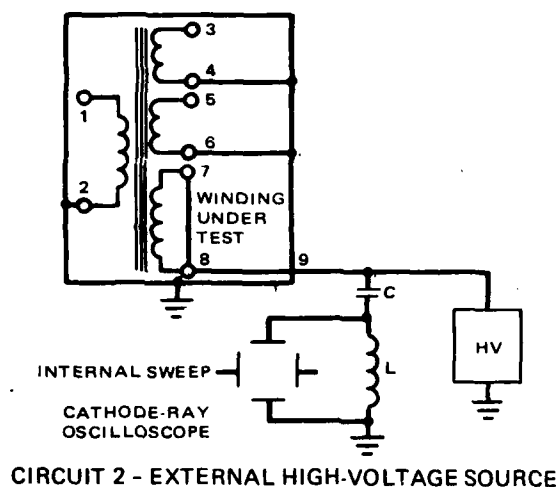


Figure 3-44. Interwinding insulation test-schematic.

The test procedure was as follows:

- a. Short all other windings before testing.
- b. The test will be a 30 second nonaccumulative count measured at five levels: 2.5 pC, 5 pC, 10 pC, 25 pC and 50 pC.
- c. Use 1700 VRMS at 60 Hz between (9 + 7) and (1 + 2 + 3 + 4 + 5 + 6 + 9 + 10 + 11 + 12 + 13 + 14).
- d. Use 900 VRMS, 60 Hz between (9 + 10) and (1 + 2 + 3 + 4 + 5 + 6 + 7 + 8 + 11 + 12 + 13 + 14).
- e. No corona shall be found.

3.5.3.10 Weight

The weight of the device is measured in order to confirm that the device will meet the customer's requirements. This is especially critical in missile and space applications where excess weight equates with reduced system performance. The maximum weight for this design is 2.2 ounces.

3.5.3.11 Seal Test

The seal test consists of placing the parts in a waterbath at $85^{\circ}\text{C} \pm 5^{\circ}\text{C}$. The part upon immersion must have a temperature less than 40°C . Leaks are detected by the presence of bubbles around the parts during immersion. The seal test may be repeated until the leak is corrected. In this test series the parts were only seal tested once with no repair work allowed.

3.5.4 High Voltage Transformer Results and Conclusion

The data from the high voltage transformer testing summarized in Table 3-19 supports these conclusions: The viscosity variations among the resins are over the range of 75 to 1500 cps and make no observable difference in the high voltage tests. The interwinding and intrawinding insulation tests, (corona tests) are more sensitive to overstress conditions than are the insulation resistance, and dielectric strength, or "high pot" tests. The parts encapsulated with Hysol C-60, and Hysol C15-015 had much higher intrawinding insulation test counts due to corona than did the good parts encapsulated with Epon 815/HV, Eccoseal 1218 and Scotchcast 255.

The uncured resin viscosity appears to have little to do with the electrical character of the finished part. The viscosity of the poured resin should affect the completeness of the encapsulants penetration into the windings. The higher viscosity and supposedly lower penetrating resins would have more voids and higher corona levels. In the viscosity range used in this test, 75 to 1500 cps, this phenomenon is not evident. Some parts that passed the dielectric strength test had a high level of corona. Those parts that had no corona also passed the dielectric strength test. The interwinding insulation data from Table 3-19 shows that the Hysol C15-015 and Hysol C-60 encapsulated parts consistently had corona present.

The inference is that these materials/processes allow the corona to initiate and maintain more easily than do the other materials. The other materials each did have one part fail due to high resistance breakdown. The other of each of these lots functioned perfectly.

A further test, an interwinding insulation test, was performed at 3300 volts AC at 60 Hz between (7-8) and the other pins. The results of this test are shown below in Table 3-20. Only the one good part of each material was available for test.

TABLE 3-20. INTERWINDING INSULATION TEST

Material	Interwinding Insulation (3300V AC at 60 Hz)				
	2.5 pC	5 pC	10 pC	25 pC	50 pC
Epon 825/HV	0	0	0	0	0
Scotchcast 255	9249	4826	6283	149	4024
Eccoseal 1218	19609	11933	14732	583	9824

The striking part of the results in Table 3-20 is that the Epon 825 impregnated part even at four times the design voltage had no corona. The Scotchcast 255 and Eccoseal 1218 encapsulated parts definitely showed large quantities of corona. This test also shows the greater sensitivity of the corona tests in comparison to the high-pot tests. From this test it can be concluded that for high voltage magnetic components Epon 825/HV tends to give the best results. The Scotchcast 255 and Eccoseal 1218 potted parts did meet the performance criteria; however they were apparently being used at or near the limits of their properties.

4.0 CONTROLLED WINDING TECHNIQUES

4.1 WIRE HANDLING

This section contains the data and conclusions on the effects of handling techniques on the fine and ultra-fine wires used in electromagnetic components. The term "fine" is defined as wire sizes from AWG 36 (0.005 inch dia) to AWG 44 (0.002 inch), and "ultra-fine" from AWG 45 (0.00176) to AWG 56 (0.00049). It has been reported that wires as small as AWG 63 (0.00022) are being used in production of electromagnetic components in some foreign countries. Unless specifically designated otherwise in the text, the term "fine" will include "ultra-fine" wire.

4.1.1 Spool Packaging Styles

The wire, which has been studied in this program, arrived in four different package styles listed below, in increasing order of protection.

- Style A The spool of wire protected by a sheet of heavy weight paper wrapped in one layer around the spool.
- Style B The same as Style A, with the spool, then placed in a pressboard box.
- Style C The same as Style A, with the spool, then tightly confined in a polystyrene container.
- Style D The same as Style A, with the spool, then confined in an hermetically sealed, impact resistant, rigid container.

4.1.2 Wire Damage Modes

Several ways to cause damage to the wire during handling and storage have been observed. Among the various damage modes are:

1. Breaking the spool which holds the wire (note: this can lead to the other damage modes).

2. Slicing or scraping the wire and/or insulation with fingernails or other sharp objects.
3. Creasing or extreme bending of the wire, thus causing physical and/or electrical weakness.
4. Damaging the insulation by melting it or causing embrittlement and cracking.
5. Striking the wire spool on one end, causing interior turns of wire to fall over exterior turns and making subsequent despooling of the wire impossible.
6. Contaminating the wire with dust, liquids, metal fillings, etc.
7. Marring the edge of the spool, thus causing the wire to be dragged across the marred surface during despooling and damaging the insulation.

4.1.3 Evaluation and Recommendations

Since the spooled wire is exposed to several different environments with varying risks of damage, the different packaging styles must be evaluated at each environment, with the following comments.

Style A packaging is sufficient to protect the wire after it reaches the end-use work station, providing there are no accidental blows, slices, scrapes or contamination which penetrate the paper shield. Style A protects the wire from all normal handling problems associated with the end-user work station. It does not give sufficient protection for typical shipping or bulk storage conditions.

Style B packaging is more effective than Style A, because it adds an extra layer of protection due to the pressboard box. Style B is sufficient for normal handling and storage at the Project Stores level.

Style C packaging appears to be sufficient to protect the wire during shipment and subsequent handling and storage at the end-user's facilities.

Style D packaging protects the wire even more efficiently than packaging Style C. In addition, Style D will protect the wire from all forms of contamination once the wire is sealed in the container, and from catastrophic accidents such as falling off a moving vehicle or being submerged in liquids.

Examining the costs versus benefits of the four packaging styles reveals that Styles A, B, and C provide increasingly better protection to the wire with little additional cost, estimated at less than 1 percent of the cost of the wire. Style D consists of a reusable container which can cost more than the wire it protects. In the event that the wire and container are stressed beyond what Style C is adequate protection for, the Style D container can protect the wire, even though it sustains considerable damage. Thus, the cost trade-off becomes whether it is less expensive to use and replace a spool of wire or to replace the Style D container. In most cases, the cost of using and replacing the Style D container is currently larger than the cost of replacing the spool of wire.

Table 4-1 consists of a list of processes through which the wire will pass, the damage modes which are typical during each process, and the packaging style which gives adequate protection to the wire. "Adequate protection" is defined as having no detectable damage to the wire or insulation throughout the manufacturing process. None of the packaging styles listed in Table 4-1, discussed in this paper or mentioned in any other available source, can protect the wire during usage. While the wire is being used, the only way to prevent contamination or damage is for the user to employ proper safeguards.

During usage, the wire can be accidentally damaged by several methods. First, and most commonly, the wire can be sliced, scraped, or creased by the fingernails of the users. Second, it can be contaminated by liquid, vaporous, or solid chemicals. Third, it can be overstressed, scraped, or broken during the winding process. Fourth, it can be hit by other objects or dropped, resulting in abrasions, slices, dents, etc. Thus, there exist a set of rudimentary handling guidelines which must be followed in order to protect the wire. The guidelines are:

1. The spool of wire should be held in a despooling container which protects the wire from accidental contacts with other objects and allows unhindered despooling of the wire.

TABLE 4-1. PROCESS DAMAGE MODES

Processing	Packaging Style	Damage Modes*
Manufacturer Shipment	Style C or better	1, 2, 3, 4, 5, 6, 7, 8
End User Receiving	Style C or better	1, 2, 4, 6, 7, 8
Storage	Style C or better	1, 2, 4, 6, 7, 8
Handling	Style C or better	1, 2, 4, 6, 7, 8
Project Stores	Style B or better	2, 4, 6, 8
Storage	Style B or better	2, 4, 6, 8
Handling	Style B or better	2, 4, 6, 8
Work Station	Style A or better	6, 8
Storage	Style A or better	6, 8
Handling	Style A or better	6, 8
<p>*Damage Modes</p> <ol style="list-style-type: none"> 1. Collisions at velocities greater than 10 mph. 2. Collisions at velocities less than 10 mph (a drop of approximately 3 feet). 3. Vibrations at greater than 1/4 g and 10 Hz (truck, train or airplane vibrations). 4. Use of sharp blades in immediate vicinity (unpacking shipping containers). 5. Thermal extremes ($T \leq 0^{\circ}\text{C}$, $T \geq 50^{\circ}\text{C}$) winter or summer temperatures). 6. Hand handling (fingernails, screw drivers, etc.). 7. Large scale contamination (rain, dust clouds, air pollution, etc.). 8. Small scale contamination (sweat, sneezes, dust, etc.). 		

2. The wire tension controls must be able to maintain the desired tension (within ± 10 percent) and must be periodically calibrated to ensure proper winding without overstressing the wire.
3. The edge of the spool, over which the wire is removed, must be inspected to ensure that it is not rough enough to damage the wire during the despooling.
4. The work area should not contain any exposed sharp edges, heat sources, chemicals, etc., which can accidentally damage the wire.
5. Spools of wire should be returned to their protective containers and storage areas whenever they are not in actual use.
6. The wire should not be handled with bare hands and should be handled as little as possible.

4.2 CONTAMINATION

There are many possible ways in which fine wire can be contaminated. It may be contaminated by particulates which could scrape the insulation or inhibit the component's potting or encapsulation material and thus decrease the reliability of the component.

The various tests employed are described briefly by paragraph number. Test 4.2.1 checked the condition of the wire as it was received from storage. The tests measured the amount of particulate contamination on the wire and the amounts of previous chemical contamination. Test 4.2.2 determined the effects of three solvents on the wires. The solvents selected were chosen on the basis that, even though the wire is usually not exposed to any solvent during its manufacturing process, the components in which the wire is used are often cleaned by one of the three solvents tested. Tests 4.2.3 and 4.2.4 are included to determine the effects of H_2O and salt spray on the wire because of the ever present moisture and sweat in any industrial environment. Test 4.2.5 was designed to determine the amount of volatile contamination which existed in the wire by putting the samples in a vacuum and allowing the volatiles to volatilize. Test Series 4.2.6 and 4.2.7 were used to determine the effects of HCl and H_2SO_4 on the wire. The acids chosen are both strong, readily available, and used in the industrial environment. Test 4.2.8 checked the effects of vibration, such as is experienced on an airplane or other vehicle during

transport, on single strands of stretched wire and on wire which has been wound around an object and is allowed to vibrate against the object and other strands of wire.

In each of the tests, the wire samples consisted of pieces of wire removed from their spools and subjected to the tests. Since each sample consisted of both insulation, the item to be tested, and copper, equations were developed which calculated the mass of the insulation, the exposed surface area of the insulation, and the insulation thickness for each sample. Thus, results are reported based upon insulation weight, the insulation surface area, or the insulation thickness, whichever is appropriate.

Each sample of wire has three methods of identification. First, there is identification based upon insulation type and thickness. Second, the samples are identified by the suppliers' designation. Third, an identification number has been assigned to each sample, summarized in Table 4-2. Each of the tables which report observed data have the wire samples segregated into categories which correspond to the insulation material. Thus, any observable trends can be seen for each insulation material as a group, rather than solely on the basis of the arbitrarily assigned identification number.

4.2.1 Cleanliness of "As Received" Wire

4.2.1.1 Particulate Contamination

Samples of wire were subjected to particulate contamination particle counts in accordance with ASTM 312. The results are shown in Table 4-3 where the percent of surface area covered by the particles has been calculated. The percentage of cover ranged from a minimum of 0.29 percent to a maximum of 1.20 percent. The particles can be separated into two distinct classes of contaminants. First, virtually all of the particles smaller than 100μ are irregular in shape and have been identified as non-metallic dust. Second, the particles larger than 100μ were mostly fibers of insulation. Photographs of the two categories of particle are shown in Figures 4-1 and 4-2.

TABLE 4-2. IDENTIFICATION OF WIRE SAMPLES

Insulation Material and Thickness (mils)	Supplier's Designation*	Identification Number
Heavy Nylon (.25)	43N130B2	J1463-57A
Heavy Nylon (.195)	45N130B2	J1463-57B
Heavy Polyurethane (.25)	44PT200K2	J1463-57C
Single Polyurethane (.85)	52S105T	J1463-57D
Single Polyvinyl Formal (.20)	40BZ105T	J1463-57E
Single Polyvinyl Formal (.10)	45F105T	J1463-57F
Heavy Polyvinyl Formal (.35)	40F105T2	J1463-57G
Single Nylon (.35)	34N130B	J1463-57H
Heavy Nylon (.35)	40N130B2	J1463-57I
Single Polyimide (.30)	35ML220M	J1463-57J
Heavy Polyimide (.40)	39ML220M2	J1463-57K
Single Polyimide (.15)	41PT180H	J1463-57L
Single Polyimide (.20)	40PT180H	J1463-57M
Heavy Polyimide (.40)	39PT200K2	J1463-57N
Heavy Polyimide (.35)	40PT200K2	J1463-57O
Single Nylon (.25)	42PT200K	J1463-57P
Single Polyimide (.55)	28T155L	J1463-57Q
Heavy Polyurethane (.30)	41S1052T2	J1463-57R
*The first two digits are the AWG size, the next one or two letters identify the insulation, the next four numbers and letters give the maximum temperature (°C), and the last number indicates: 2-heavy insulation, blank-single insulation.		

TABLE 4-3. STATISTICAL PARTICLE COUNT

Insulation Type	Sample Identification Number	Sample Surface Area (cm ²)	Particle Size Distribution (particles/cm ²)					% of Surface Area Covered by Particles
			5-10μ	10-25μ	25-50μ	50-100μ	>100μ	
Nylon	J1463-57A	9.39	282	234	156	23	6	0.57
	J1463-57B	12.27	159	110	77	22	4	0.36
	J1463-57H	9.52	611	393	315	41	15	1.17
	J1463-57I	6.26	367	224	199	26	5	0.63
	J1463-57P	7.52	272	220	212	22	6	0.64
Polyurethane	J1463-57C	8.60	837	221	315	35	11	1.00
	J1463-57D	2.35	221	137	68	9	4	0.29
	J1463-57R	7.11	295	219	134	40	8	0.68
Polyvinyl Formal	J1463-57E	7.64	746	289	274	39	9	0.94
	J1463-57F	12.21	274	168	110	21	5	0.45
	J1463-57G	6.83	476	234	234	40	7	0.81
Polyimide	J1463-57J	5.25	392	315	181	61	17	1.10
	J1463-57K	11.19	384	260	232	48	22	1.19
	J1463-57L	6.60	712	379	364	60	7	1.16
	J1463-57M	5.61	481	241	233	21	7	0.70
	J1463-57N	7.54	292	199	146	31	7	0.61
	J1463-57O	8.91	539	371	314	49	14	1.18
	J1463-57Q	8.48	893	554	259	58	13	1.20
$\% \text{ of surface area covered} = \sum_i \left(\frac{LL_i + UL_i}{2} \right)^2 Y_i \times 10^{-6} \%$ <p> LL_i = lower limit of i^{th} element UL_i = upper limit of i^{th} element (assume UL for over 100μ → 200μ) Y_i = particle count of i^{th} element </p>								



Figure 4-1. Typical particulate contamination greater than 100μ in longest diameter (26x).

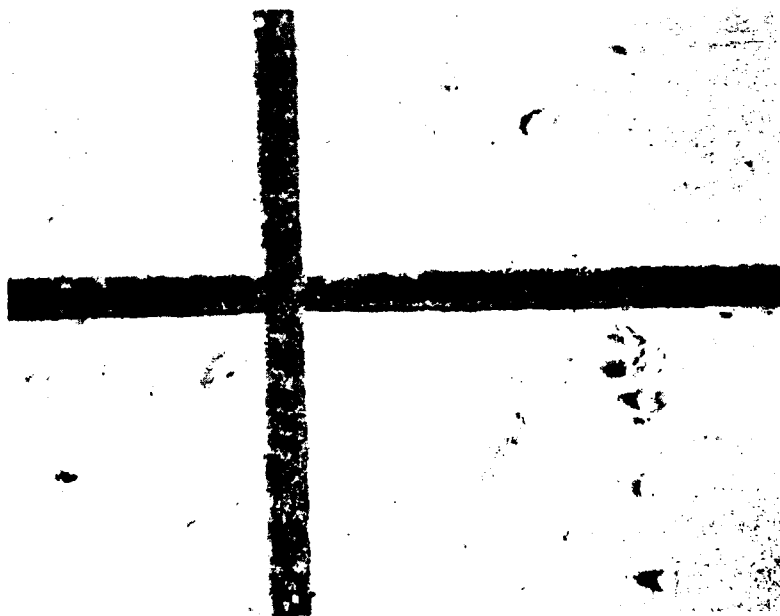


Figure 4-2. Typical particulate contamination less than 100μ in diameter (26x).

SEM photographs indicate that the particulate contamination does not have any adverse effect on the insulation as it is received from material stores. However, there is a possibility that the particles would contaminate the encapsulant or otherwise affect the components reliability after the wire is used. It has been observed that the particles do not adhere to the wire and are easily removed by felt pad friction tension devices or the normal vibration which the wire experiences during the winding process. Thus, existing particulate contamination does not appear to be significant.

4.2.1.2 Non-Volatile Residue (NVR) Contamination

Samples of the wire were washed in hexane and then the liquid was evaporated in a pre-weighted beaker. The beaker, containing non-volatile residue, was reweighed and the amount of NVR was determined. The NVR was then analyzed by infrared (IR) spectroscopy. Analysis of the resulting NVR yielded only slight traces of aliphatic hydrocarbons. Microphotographic inspection of the wire samples revealed no damage to the wire and insulation.

4.2.2 Effects of Solvents

Samples of the wire were immersed in approximately 50 milliliters of boiling solvent for one hour. NVR and IR analyses were conducted on this liquid to determine the amount and identity of material extracted from the wire into the solvent. In addition, the tested wire samples were examined under an optical microscope at 25X magnification for signs of physical damage.

Acetone, 1, 1, 2-trifluorotrichloroethane (Freon TF) and isopropyl alcohol were selected to test the effects of solvents on the insulations. These solvents are commonly found in laboratories, shops and industry and are used for cleaning components and other purposes.

The effects of the three different solvents are shown in Tables 4-4, 4-5, and 4-6.

Table 4-4 shows the effects of acetone (a ketone) on the test samples. The data indicates that, in general, the nylon, polyurethane and polyimide

TABLE 4-4. SOLVENT SUSCEPTIBILITY - ACETONE TEST

Insulation Type	Sample	Calculated Insulation Weight (mg)	NVR Weight (mg)	% of NVR vs. Initial Weight
Nylon	J1463-57A	76.91	7.1	9.2
	J1463-57B	92.35	1.8	1.9
	J1463-57H	40.98	0.8	2.0
	J1463-57I	70.07	1.5	2.1
	J1463-57P	67.27	0.6	0.89
Polyurethane	J1463-57C	81.01	0.8	0.99
	J1463-57D	79.70	9.5	11.9
	J1463-57R	68.97	1.9	2.8
Polyvinyl Formal	J1463-57E	45.93	32.7	71.2
	J1463-57F	43.25	7.2	16.6
	J1463-57G	76.50	15.4	20.1
Polyimide	J1463-57J	36.08	0.4	1.1
	J1463-57K	67.07	0.1	0.15
	J1463-57L	35.98	1.3	3.6
	J1463-57M	42.87	2.9	6.8
	J1463-57N	85.74	0.5	0.58
	J1463-57O	70.77	4.6	6.5
	J1463-57Q	28.31	0.2	0.71

TABLE 4-5. SOLVENT SUSCEPTIBILITY - FREON TF TEST

Insulation Type	Sample	Calculated Insulation Weight (mg)	NVR Weight (mg)	% of NVR vs. Initial Weight
Nylon	J1463-57A	74.32	0.1	0.13
	J1463-57B	85.55	0	0
	J1463-57H	38.00	0.4	1.1
	J1463-57I	71.58	0.2	0.28
	J1463-57P	67.57	0.4	0.59
Polyurethane	J1463-57C	77.82	0.7	0.90
	J1463-57D	81.24	2.5	3.1
	J1463-57R	84.78	1.3	1.5
Polyvinyl Formal	J1463-57E	45.17	0.3	0.66
	J1463-57F	36.47	0.7	1.9
	J1463-57G	78.57	0.6	0.76
Polyimide	J1463-57J	34.92	0.2	0.57
	J1463-57K	72.50	0.2	0.28
	J1463-57L	36.36	0.5	1.4
	J1463-57M	41.72	0.2	0.48
	J1463-57N	84.78	0.3	0.35
	J1463-57O	79.59	0.5	0.63
	J1463-57Q	27.87	0	0

TABLE 4-6. SOLVENT SUSCEPTIBILITY - ISOPROPYL ALCOHOL TEST

Insulation Type	Sample	Calculated Insulation Weight (mg)	NVR Weight (mg)	% of NVR vs. Initial Weight
Nylon	J1463-57A	75.83	5.9	7.8
	J1463-57B	65.00	1.3	2.0
	J1463-57H	37.31	0.7	1.9
	J1463-57I	65.97	1.1	1.7
	J1463-57P	66.72	0.7	1.0
Polyurethane	J1463-57C	77.88	0.7	0.90
	J1463-57D	79.59	8.8	11.1
	J1463-57R	75.65	2.3	3.0
Polyvinyl Formal	J1463-57E	38.12	24.7	64.8
	J1463-57F	48.03	4.8	10.0
	J1463-57G	70.84	9.1	12.8
Polyimide	J1463-57J	36.56	0.4	1.1
	J1463-57K	76.97	0.3	0.39
	J1463-57L	33.27	0.8	2.4
	J1463-57M	42.04	2.6	6.2
	J1463-57N	70.04	0.2	0.29
	J1463-57O	76.91	3.9	5.1
	J1463-57Q	28.65	0.1	0.35

insulations are resistant to acetone. However, the polyvinyl formal insulations are severely attacked by acetone. If acetone is to be considered for use as a cleaning solvent, then a careful study of the data should be undertaken to determine the least damageable insulation material that should be used.

Table 4-5 shows the effects of Freon TF on the test samples. The data indicates that there is little if any damage done to the insulation by Freon TF. The overall impression is that Freon TF would be a good choice as a cleaning solvent for all of the tested wires.

Table 4-6 shows the effects of isopropyl alcohol on the test samples. The effects of isopropyl alcohol are very similar to the effects of acetone on the wires. From the results, it is obvious that polyvinyl formal should not be exposed to either of these two solvents, and a careful examination of the remaining wires must be undertaken before exposing them to either isopropyl alcohol or acetone.

If a solvent is going to be used to clean any of these wires, the safest, all around solvent appears to be Freon TF. Both of the other solvents can result in drastic reductions in insulation thickness.

4.2.3 Effects of Humidity

The humidity test was conducted on samples of each wire in accordance with Method 10C of MIL-STD-202B. The samples were exposed to 85-95 percent relative humidity at a temperature cycle range of 25° to 65°C for 240 hours. At the end of the tests, the samples were examined by SEM. The SEM microphotographs revealed that there was no apparent damage to the insulation at magnifications up to 2400X.

4.2.4 Effects of Salt Spray

The sample wires were tested in accordance with Method 101 of MIL-STD-202. After exposure to a 5 percent salt spray at 95°C for 96 hours the samples were immersion rinsed in distilled water for 10 minutes. SEM examination revealed that while there was no apparent degradation of the insulation, Figure 4-3, the wire is unusable due to a buildup of salt crystals on the wire. (See Figure 4-4.)



Figure 4-3. Undamaged insulation after salt spray test (625x).

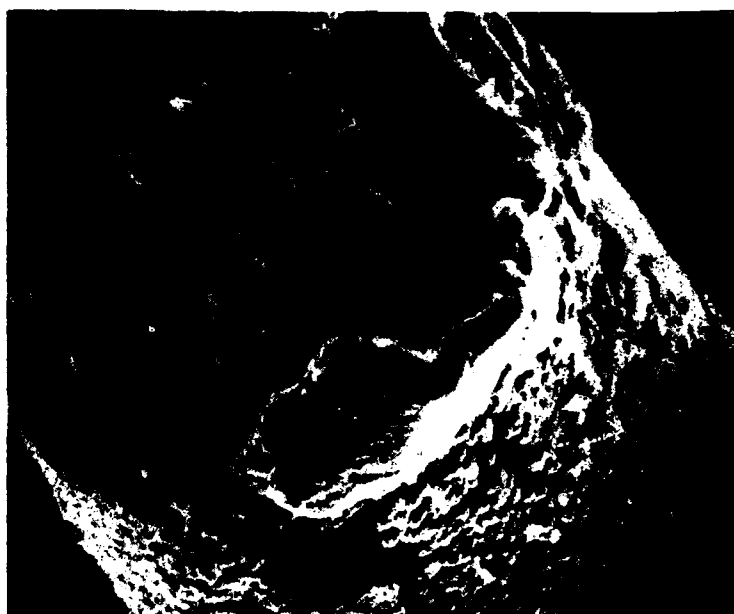


Figure 4-4. Typical salt crystal contamination on tested wire (625x).

Energy Dispersive X-ray (EDAX) spectra of particles along the wire, at points X1 and X2 (Figure 4-5) and near the cut ends indicate the presence of sodium, chlorine and copper (Figures 4-6 and 4-7). The fact that copper is found away from the cut end and that no pinholes were found in the insulation implies that a corrosion product may have been washed along the wire during the course of the test.

4.2.5 Outgassing

The outgassing test was conducted on wire samples in accordance with HP6-26, Class 1. The wire samples were exposed to a vacuum of 10^{-5} torr at 75°C for 96 hours. Data is available for the outgassing test on 15 of the wire samples. The results are listed in Table 4-7. There were no visible condensates for any of the wires tested. One of the wires, sample number J1463-57D (a polyurethane), exceeded the maximum acceptable limit of 1.00 percent outgassing. While the excess is only 0.01 over the limit and could be due to inaccuracy of measurement, the amount



Figure 4-5. Insulation and contaminant after salt spray test (600X).

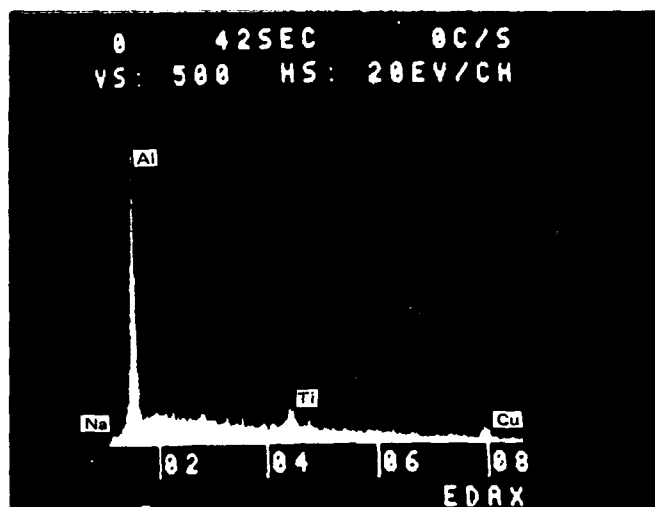


Figure 4-6. EDAX spectrum of region X2.
The bare insulation at X2 gives an EDAX
which shows: Na - 1.2 EV, Al - 1.6 EV
(the substrate), Cu - 8.0 EV

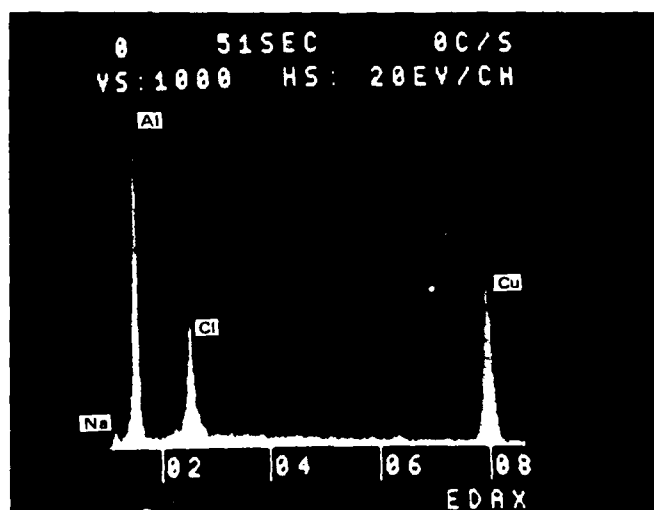


Figure 4-7. EDAX spectrum of region X1.
The crystal at X1 shows the same pattern
as is seen in Figure 4-6, plus: Cl - 2.6 EV,
Cu - 8.0 EV (stronger reaction)

TABLE 4-7. OUTGASSING TEST RESULTS

Insulation Type	Sample	Calculated Insulation Weight (mg)	Weight Loss (mg)	% of Weight Loss
Nylon	J1463-57A	36.06	0.1	0.28
	J1463-57B	23.43	0.2	0.85
	J1463-57H	34.73	0.2	0.58
	J1463-57I	42.11	0	0
	J1463-57P	29.72	0	0
Polyurethane	J1463-57C	29.09	0.1	0.34
	J1463-57D	29.17	0.3	*1.01
	J1463-57R	—	—	—
Polyvinyl Formal	J1463-57E	25.75	0.2	0.78
	J1463-57F	—	—	—
	J1463-57G	43.30	0.1	0.23
Polyimide	J1463-57J	30.54	0	0
	J1463-57K	—	—	—
	J1463-57L	16.76	0	0
	J1463-57M	26.62	0	0
	J1463-57N	45.83	0	0
	J1463-57O	43.16	0	0
	J1463-57Q	92.97	0	0
*Maximum acceptable limit = 1.0 percent				

indicates that the wire in question could have received an excessive amount of contamination or could have been manufactured improperly.

4.2.6 Effect of Hydrochloric Acid Vapor

The wire samples were suspended in a closed system with beakers containing a total of 100 milliliters of 0.01N HCl for 24 hours. The experimental apparatus is depicted in Figure 4-8.

The concentration of HCl in the atmosphere of the test system was calculated to be approximately 0.9 percent, which is several orders of magnitude greater than that in the atmosphere of the earth due to smog. The concentration is similar to that which would occur in a normally vented room in which opened, liquid HCl exists.

The results of the HCl test are given in Table 4-8. As can be seen, all of the wire samples, with the exceptions of J1463-57J and J1463-57M, have insulation thicknesses which are less than the design minimum requirement of insulation for the wires. The reason why two samples are still conforming to standards is that all calculations are based on minimum

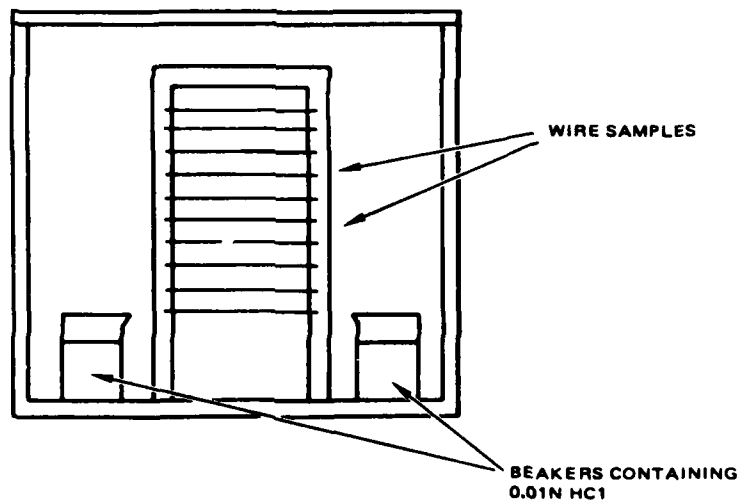


Figure 4-8. HCl test apparatus.

TABLE 4-8. ACID TEST - HYDROCHLORIC ACID

Insulation Type	Sample	Minimum Insulation Thickness Before Test mils	Measured Insulation Thickness After Test mils	% of Insulation Left After Contamination
Nylon	J1463-57A	0.40	0.260	65.0
	J1463-57B	0.30	0.263	87.7
	J1463-57H	0.50	0.229	45.8
	J1463-57I	0.60	0.340	56.7
	J1463-57P	0.20	0.163	81.5
Polyurethane	J1463-57C	0.40	0.262	65.5
	J1463-57D	0.10	0.0952	95.2
	J1463-57R	0.50	0.143	28.6
Polyvinyl Formal	J1463-57E	0.20	0.141	70.5
	J1463-57F	0.10	0.031	31.0
	J1463-57G	0.60	0.336	56.0
Polyimide	J1463-57J	0.40	0.098	24.5
	J1463-57K	0.60	0.296	49.3
	J1463-57L	0.20	0.064	32.0
	J1463-57M	0.20	0.204	102.0
	J1463-57N	0.60	0.274	45.7
	J1463-57O	0.60	0.315	52.5
	J1463-57Q	0.80	0.520	65.0

insulation thicknesses. This allows the two exceptional samples to have originally started the test with considerably more than the minimum insulation and thus end up with more than the minimum, after the test was completed.

The damage which HCl does to all of the tested wires indicates that, even at the low concentrations which normally occur in the atmosphere, the wire can become unusable after several months of storage. An important factor to consider is that the acid vapor attacks the insulation uniformly over its surface. Thus, a visual inspection of the wire will not reveal any pitting or holes in the insulation (unless actual drops of the acid reach the insulation). The only satisfactory check would be to actually measure the insulation thickness.

4.2.7 Effects of Sulfuric Acid Vapor

For this test, the wire samples were exposed to H_2SO_4 in the same manner as the previous HCl test. The test procedure consisted of suspending the samples for 96 hours in a closed system which contained 0.1 M H_2SO_4 . The results of this test are given in Table 4-9. With the exceptions of samples J1463-57E, J1463-57J, and J1463-57Q, all of the sample insulations were reduced to thicknesses which are considerably less than the required minimums.

All of the conclusions which were made about the effects of HCl are equally valid for H_2SO_4 . Thus, it is highly desirable to keep both acids, either vapor or liquid, away from the wires at all times.

4.2.8 Effect of Vibration

The vibration tests used the experimental apparatus depicted in Figure 4-9. The samples of wire were exposed to 60 Hz vibrations for 5 minutes and to 3000 Hz vibrations for 30 seconds. After the completion of the vibration portion of the tests, each sample of wire was examined at 25X magnification under an optical microscope and compared to untested wires. The conclusion which has been drawn from this test is that none of the wires were damaged by the test conditions.

TABLE 4-9. ACID TEST - SULFURIC ACID

Insulation Type	Sample	Minimum Insulation Thickness Before Test ($\times 10^{-4}$ inches)	Measured Insulation Thickness After Test ($\times 10^{-4}$ inches)	% of Insulation Left After Contamination
Nylon	J1463-57A	4.0	2.78	69.5
	J1463-57B	3.0	2.29	76.3
	J1463-57H	5.0	3.87	77.4
	J1463-57I	6.0	2.83	47.2
	J1463-57P	2.0	1.21	60.5
Polyurethane	J1463-57C	4.0	2.28	57.0
	J1463-57D	1.0	0.461	46.1
	J1463-57R	5.0	2.05	41.0
Polyvinyl Formal	J1463-57E	2.0	1.88	94.0
	J1463-57F	1.0	0.598	59.8
	J1463-57G	6.0	3.30	55.0
Polyimide	J1463-57J	4.0	2.59	64.8
	J1463-57K	6.0	3.15	52.5
	J1463-57L	2.0	0.880	44.0
	J1463-57M	2.0	1.40	70.0
	J1463-57N	6.0	2.98	49.7
	J1463-57O	6.0	2.33	38.8
	J1463-57Q	8.0	4.88	61.0

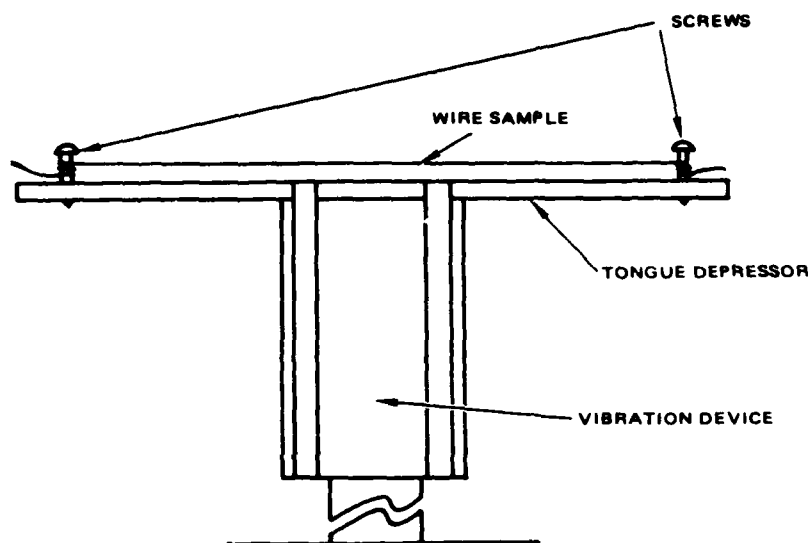


Figure 4-9. Vibration test apparatus.

4.2.9 Conclusions

The wire which has been studied during this portion of the MMT Program has been exposed to a typical cross-section of industrial contaminants. The results of the contamination indicate that the wire can be severely damaged by chemical reactions. To avoid damage to the wire, it should be protected from contamination and handled as outlined in the wire handling guidelines set forth in Section 4.1.

Even if the wire is properly handled and protected, there exists a strong possibility that prolonged storage can cause degradation of the insulation. Thus, stock piles of wire should be held at a minimum level and processed on a first in-first out basis. Inspections of long held wire should be conducted, just prior to usage, in order to confirm that the insulation is within specified tolerances. After the wire has been used in a component, all exposed wires within the component should be covered with a compatible conformal coating, or similar protection, in order to prevent deterioration of the wire during subsequent storage, handling, and use.

If the guidelines listed in Section 4.1 are followed, and the wire is maintained in an uncontaminated state, then it will remain usable and reliable. If the guidelines are not followed and/or the wire becomes contaminated, then the wire may be damaged and subsequently be unusable. The only way

to be reasonably certain that the wire meets all applicable tolerances is if the insulation thicknesses are measured before usage.

4.3 SOLENOID AND TRANSFORMER COIL WINDING

There are several factors which determine the ability to wind reliable solenoid and transformer coils. The major factors are: proper machine set-up and proper coil design. The relevant portions of each factor are discussed below.

4.3.1 Winding Machine Set-up

Before winding takes place, the operator must become thoroughly familiar with the winding equipment and the design requirements of the coil. The design requirements of the coil tell the operator what must be done, and the winding machine characteristics provide the means to do it. Thus, before winding begins, the operator will need to set the desired values for:

1. The total number of turns needed in the coil.
2. The width of the coil.
3. The number of turns per layer in the coil.
4. The winding tension for the wire in the coil.

4.3.1.1 Total Number of Turns

The total number of turns needed on the coil is determined by the electrical characteristics of the solenoid or transformer and is specified by the designer. Operators are responsible for making the coil to the specifications. Thus, the operators should set, and check, the turns-counter on the winding machine, before proceeding.

Setting the turns-counter is a simple task which can cause considerable trouble, if it is done improperly. The opportunities for error are limited, but, if the operator is unfamiliar with the winding equipment, and does not check the counter before and during operation, too few ("under-run"), or too many ("over-run"), turns of wire can be wound. If too many turns are wound, then the removal of excess turns can cause the wire in the coil to spring loose and the coil to be less than optimally wound. As a result, the operators should read and understand the specific winding machine's manuals and follow their procedures for preventing "over-run".

4.3.1.2 Coil Width

When winding coils which use bobbins, or coil forms, it is essential that the width of the bobbin (or form) be the same width that the machine is set to wind. This can be accomplished by setting the "throw", "run", or "width" adjustment on the winding machine. [Each machine should have a manual which explains this.]

If the "throw" of the machine is smaller than the width of the bobbin, then the wire will fall off the edge(s) of the coil and result in a coil with a bulge in its center. This is undesirable for many reasons (i. e., it can make the coil too large to fit in its allotted volume and/or cause cross-overs between turns of the wire). If the "throw" of the machine is larger than the width of the bobbin, then the edges of the coil will be thicker than the center, and many problems will develop (i. e., the wire can snag on the bobbin walls, over-flow the bobbin and/or the coil may become too large). Thus, careful attention should be paid to setting the "throw" of the machine.

4.3.1.3 Turns Per Layer

The number of turns per layer (commonly called "pitch") determines where each succeeding turn of wire is wound on the coil. It is determined by the overall thickness of the wire and should be adjusted according to the manuals provided by the winding machine manufacturer.

If the pitch is incorrect, then the machine might try to wind one turn directly over the preceding turn, causing cross-overs and undue build-up of the coil, or the coil could be wound with too few turns per layer, resulting in considerable wire cross-over. Both conditions can greatly reduce component reliability and should be eliminated.

4.3.2 Coil Design and Winding Tension

The determination of required winding tension, for use when winding ultra-fine wire, has two distinct aspects. First, the tension must be great enough to properly wind the wire. When winding coils, it is extremely important that the individual turns of wire are wound so that:

1. None of the turns collapse into the coil and cause a high potential difference between adjacent wires.

2. None of the wires are loose enough to allow cross-overs to develop and provide pressure points where the wires can penetrate through the insulation or cause severe, localized deformation of the wires.
3. The total coil is compact enough to allow it to fit in its allocated volume.

Second, the tension must be small enough so that the wire is not damaged during the winding process. There are two ways that damage can occur. It can be exhibited either as a break or necking down of the wire as it is being wound, or as a deformation of the wire, core, or bobbin, due to internal coil pressure.

During this investigation, several dozen coils have been analyzed and the effects of winding tension have been determined. Initially, many of the coils which were evaluated were selected from ultra-fine wire transformers which are currently being used in military products manufactured at Hughes Aircraft Company. These test coils were sliced apart, micro-polished and photographed using a scanning electron microscope (SEM).

Since the coils were manufactured by various sources and since they were already completed before the examination, the evaluations were based on existing specifications and were used as a control group for determining the current effects of winding tension. Subsequent to the examination of these existing coils, additional test coils were manufactured at Hughes Aircraft Company facilities, under various controlled winding tensions and winding speeds, which provided additional experimental data to establish a mathematical model for describing wire damage, correlated with:

1. The physical configuration of the coils, and
2. The winding tension, as a function of wire size.

The model provided a measure of what maximum winding tensions can be used for each wire size, for any particular coil configuration.

The results of this investigation are elaborated later in this paper and in Appendix 6.1 "Wire Deformation in Ultra-Fine Wire Coils". The conclusions which were reached are given both as an integral part of the explanation and as the last section of this report.

4.3.2.1 Optimal Winding Tension

The minimum tension with which it is possible to wind ultra-fine wire coils is a difficult, if not impossible, quantity to measure. Not only does it vary with the coil configuration, wire size and insulation, but it is also difficult to quantify any damage which is done. As a result, most manufacturers establish their minimums as being the maximum allowable tension (MAT). This is a realistic approach which results in properly wound coils, providing the winding actually takes place at or just below the MAT. The difficulties which arise occur only if the level of winding tension is improperly established or changes during the winding process.

The MAT is more easily quantified than the minimum winding tension, because wire damage which occurs due to excess winding tension is measurable, so an upper limit for winding tension can be established. A mathematical model has been developed which accurately predicts the MAT for any coil configuration and wire size. A description of the development of the model is contained in the paper in Appendix 6.1.

The mathematical model requires as input the minimum radius of bend for the wire as it is wound (R), the number of layers to be wound (L) and the diameter of the wire which will be used (D). Given this data, the MAT for winding the coil can be calculated from the model.

The model is:

$$\text{MAT (in grams)} = 5.91 \times 10^6 D^2 / \ell n \left\{ \frac{R + (L \cdot D)}{R} \right\} \quad (4-1)$$

Then, for the typical coils which are tested, the constants are:

$$R = 1.27 \times 10^{-2} \text{ inches at the corners of the bobbin}$$

$$L = 65 \text{ layers}$$

$$D = 1.11 \times 10^{-3} \text{ inches (AWG 49 wire)}$$

then,

$$\text{MAT} = 3.8 \text{ grams}$$

This winding tension is 42 percent of the manufacturers recommended winding tension. If 3.8 grams is used as the winding tension, then the Internal Radial Pressure (IRP) will be small enough to prevent damage to the wire. By setting the MAT at the tension computed using Equation (4-1), any wire deformation problems which may have occurred using the standard winding tension can be eliminated.

Alternatively, if Equation (4-1) provides a value for the winding tension which is too small to allow adequate winding control, then the equation can be modified to determine a design for coil configurations which will use a higher MAT. The typical results of using this modification of the model will be in the form of:

1. changing the wire size used,
2. changing the bending radius for winding the coil,
3. changing the number of layers in the coil.

In order to define what wire size will prevent damage, while using a greater winding tension, Equation (4-1) can be evaluated for a particular set of specifications. Thus, to find D, if one wants MAT to be equal to 9 grams, and all other factors to remain the same as in the previous example, Equation 4-1 becomes:

$$\text{MAT} = 9 \text{ grams} = 5.91 \times 10^6 \cdot D^2 / \ell n \left\{ \frac{R + (L \cdot D)}{R} \right\} \quad (4-2)$$

and

$$D = 1.90 \times 10^{-3} \text{ inches}$$

Therefore, in order to wind the coils at 9 grams, one must use size AWG 44 wire. This will cause the depth of the coil to increase (from 7.22×10^{-2} inches to 1.24×10^{-1} inches), thus increasing the overall outer dimensions of the coil by 1.04×10^{-1} inches. The increase in coil size may not be possible, and therefore, this optional way of reducing the coil's internal radial pressure might not provide a viable solution.

Another way to reduce wire damage by the IRP is to increase the radius of bend as the wire is wound around the corners of the bobbin. To determine the minimum bending radius, R , which can be used for the example coil, assuming all other factors remain the same, Equation 4-2 can be used, while looking for the value of R which will work. When this is done, R is found to be equal to 5.80×10^{-2} inches. Thus, if the bobbin corners are manufactured to have a radius greater than 5.80×10^{-2} inches, then the IRP will be sufficiently under control to allow reliable coils to be wound.

The third way to prevent damage to the wire within the coil is to reduce the number of layers, L , being wound. Again, using the previous examples and keeping all other variables fixed, the maximum allowable L can be determined ($L = 14$ layers). The value for L is only 21.5 percent of the original value and thus requires that the coil be 4.65 times as wide as originally planned. This increase in width cannot usually be tolerated.

As can be seen above, the solution to IRP control which provides the least amount of redesign is to round the corners of the bobbin rather than changing the wire size or the number of layers wound. If the corners of the bobbin are rounded to at least the value given by the model, then there will be relatively small, usually insignificant, changes in the resulting transformer characteristics along with an increase in component reliability.

One of the fallout benefits of the model, which has developed while checking the equation results, is that a modified form of the model can be used to easily evaluate existing coil designs. Since the expression $5.91 \times 10^6 \cdot D^2$ in Equation (4-1) defines the recommended winding tension for wire with a diameter of D , Equation (4-1) can be modified to become:

$$\text{Recommended winding tension/MAT} = \ln \left\{ \frac{R + (L \cdot D)}{R} \right\} \quad (4-3)$$

Because the coil should be wound at as high a tension as possible, without exceeding the recommended winding tension, it becomes desirable

to have the MAT equal the recommended value. Thus, Equation 4-3 can be reduced to:

$$1 = \ln \left\{ \frac{R + (L \cdot D)}{R} \right\} \quad (4-4)$$

and, further, the minimum allowable value for R can be derived as:

$$R \geq 0.582 \cdot L \cdot D \quad (4-5)$$

Thus, putting the values of R, L, and D into Equation (4-5) provides a binary-type evaluation rule for any coil. If Equation (4-5) is true, then the coil is properly designed. If this Equation is false, then the coil cannot be reliably wound at the recommended winding tension, and a redesign of the coil and/or winding specifications is strongly recommended.

This section has presented a mathematical model which can help the design engineer determine the maximum allowable tension (MAT) which should be used in winding copper wire coils. The model provides several suggested ways to decrease the probability that the wire will be damaged due to the winding tension/coil configuration combination. In addition, it provides a method for evaluating existing coil designs which has a simple GO/NO-GO result as to whether the design is satisfactory. If the MAT which can be derived from the model is used when winding coils, then there should no longer be any problems associated with the winding tension.

4.3.2.2 Dynamic Tension Control

Dynamic tension control, for winding wire, is the process of real time comparison between actual winding tension and desired winding tension and adjustment of the tensioning parameters so that the difference between the two tensions is zero. Thus, when actual winding tension is greater than the desired value, the dynamic tension control device will automatically reduce the winding tension. Conversely, if the actual winding tension is too low, there will be an automatic readjustment to increase the tension.

Dynamic tensioning can provide the additional control to winding parameters which is necessary to overcome one main problem associated with winding transformer coils. If static tensioning is used when winding rectangular coils, the tension on the wire increases as the wire is wound over the corners of the bobbin or coil form. Since the actual winding tension is extremely important during winding, the variations in tension, caused by winding over the corners of the bobbin, can result in damage to the wire in the coil and a reduction in reliability for the finished component. Therefore, dynamic tensioning could provide a significant advantage when winding high reliability coils.

There are currently two distinct types of dynamic tension devices available. The first type employs the use of a lever controlled dereeling brake which reacts to the small variations in wire tension by tightening or loosening the brake (thus, increasing or decreasing the tension). The other style of dynamic tension device uses a feed-back controlled servo-mechanism. There are advantages and disadvantages for both systems.

The advantages which the lever controlled dynamic tension devices have are: quick response rate (sufficient for handling the changes in tension due to winding around the corners of the bobbin), ease in set-up and calibration, and compact size. Its two major disadvantages are that the tension control is limited to a narrow range about its target tension and the spool of wire has considerable rotational inertia which can cause unallowable stress to be placed on the wire during fast starts and stops.

The narrow response range should not become a serious problem for the lever type dynamic tension device. The reason why no problems should arise is that under normal, acceptable operation, the wire tension would not exceed the range of the device. If the tension did suddenly exceed the limits, then, something else has gone wrong in the winding process. Thus, the lever type tension device would only mirror damage which had already occurred to the coil, and not initiate the problem.

There are two actions which can relieve the spool inertia problem. First, the wire could be purchased on smaller spools, thus reducing the mass. Second, the operating procedures could specify slow starts and stops

during the winding process. Eliminating quick starts and stops would be sufficient to overcome the inertia problem, even without using wire off a smaller spool.

The advantages of the feed-back controlled servo-mechanism dynamic tension devices are that they have a wide tension control response range and can have the necessary response rate to counteract tension changes at the corners of the bobbins. The disadvantages include relatively large size and complex operations.

The wide tension control response range, available with the servo-mechanism, provides the single most effective justification for using this type of device, rather than a lever-type dynamic tension control. The large response range will even allow the operator to reverse the direction of wind and remove turns from the coil, while maintaining the pre-selected tension on the wire. This is a distinct advantage over all other tension controls, providing the removal of wire is not necessitated by snags or improper winding where the wire has been sliced, creased, kinked, or otherwise damaged. Thus, it is a useful attribute of the tensioning device in cases where too many turns have been wound and the excess turns must be removed.

Both styles of dynamic tension devices will help eliminate the tension variations associated with winding around the corners of the bobbins. There remains a doubt as to whether any dynamic tension device is necessary for winding ultra-fine wire coils. This doubt stems from the research and findings which were previously done in the MMT program. Specifically, techniques have been developed which eliminate the damaging internal radial pressure found at bobbin corners, and thus, minimize the adverse effects due to wire tension variations due to winding around the corners. Reconfiguration of bobbin shapes and evaluation of internal radial pressure damage to the wire will overcome the problems discussed here. Thus, the additional large costs for servo-mechanism type dynamic tension devices may not be justified. The minimal extra expense for the lever-type devices seem to be justified by minor improvements in tension and winding control.

As a result of the investigation in this subtask, additional findings, and the use of new procedures developed in prior sections of the program, dynamic tension control can usually be adequately handled by means of the lever-type controls. As winding tension decreases (due to decreased size of wire) it may become necessary to use a servo-mechanical type dynamic tension control, however, that need will be beyond most available units, and, in the past, has required considerable modifications by the users to fit the particular circumstances.

4.4 TOROIDAL COIL WINDING

The single and bifilar toroidal winding technique subtask has built upon, and expanded the work from most of the other subtasks in this program. As a result, an attempt will be made to give a coherent representation of the techniques needed to wind ultra-fine wire toroidal transformers. The findings of this segment of the MMT program can be divided into two distinct areas:

1. Preparation for winding ultra-fine wire toroidal transformers.
2. Winding ultra-fine wire toroidal transformers.

Since this report considers both single and bifilar (or more) winding, it will be necessary to identify each type of winding separately. Fortunately, everything which applies to single strand winding also applies to bifilar winding. Thus, those comments which specifically apply to the bifilar (or trifilar, etc) winding will be included as NOTES and be enclosed in brackets [].

4.4.1 Wire Size and Controlled Winding Techniques

This paper contains the observations and conclusions which were made concerning the minimal wire sizes and control techniques for winding toroids. The minimum wire sizes are determined by the machinery and techniques used for winding the toroids. Thus, both topics are discussed at the same time and the conclusions are included at their logical position within the paper.

The wire size limitation for winding toroidal transformers is a function of the mechanical limitations of both the winding equipment and the wire. After carefully examining the various winding machines which are available and searching through the literature which described the winding machines which are currently being sold to the industry, a set of common, limiting winding machine mechanical factors has been identified and investigated. The results are given below. Likewise, the physical properties of available wire have been examined and are reported below.

Equipment exists which will wind toroidal transformers using AWG 50 (0.001 inch) wire even though industry tends to go only to AWG 48. This minimum wire size seems to be an almost arbitrary cutoff point since finer wire toroids can be wound with a corresponding increase in the number of components which are lost in the manufacturing process. The minimum size restriction is not a precise limit such as would exist if it were easy to wind AWG 50 and impossible to wind AWG 51. The difficulty in winding fine wire covers a continuum where each of the fine wire sizes is harder to wind than the size immediately larger. As a result, a dirty machine or an inexperienced, tired, or ill operator may not be able to wind AWG 44 and conversely, if everything works smoothly, wire finer than AWG 50 can be wound.

The winding machine mechanical factors which restrict usable wire size are:

1. Sudden pulls (jerks) on the wire during winding,
2. overall wire tension too great during winding, and
3. damaging the wire before and during winding.

The greatest number of problems during the winding operation are caused by sudden jerks on the wire as the slider snags on rough points along the shuttle or the wire is caught on burrs or "sticky" places on the machinery. There are three reasons why jerks can exist. First, the shuttle or slider can be damaged by nicks along the edges. Second, dirt or other contamination can get on the shuttle, slider, brush, or brush plate. Third, the slider lubrication can break down due to friction and heat and become inoperative.

If the shuttle or slider are damaged (as can be caused by dropping them or storing several of them together) or become contaminated, the smooth surfaces which must have a controlled friction during operation can cause the slider to slow down drastically and place an enormous tension on the wire. If this happens, the wire will almost certainly break. There are a few simple procedures which will prevent these problems. First, store the shuttles and sliders in separate, padded containers. Second, the winding machine should be covered when not in use and all parts which come into contact with either the wire or the slider should be thoroughly cleaned at regular periods or whenever the winding becomes difficult. (Note: The parts should be cleaned until there are no traces of dirt or contamination present. If there are still problems with winding, the shuttle, slider, brush, and brush plate should be examined for physical damage). Third, the lubrication should be constantly monitored, and cleaned and replaced at any time it appears to have become degraded. (Note: Lightweight non-silicon oil is a good lubricant for the slider, even though it breaks down relatively rapidly and must be replaced frequently. If there are no contamination restrictions, graphite lubricant can be used. Silicone oil should never be used because when it gets on the insulation it inhibits the cure of many encapsulants, and prevents adhesion to the wire.) Following the above procedures will greatly reduce or eliminate the probability of wire being overstressed and broken during the winding process.

The second factor which places limits on the minimum wire size is the overall tension control. Winding tension is controlled by a wire spring attached to the slider. As the slider travels around the shuttle, the spring places a controlled drag on it, thus causing the appropriate tension to be placed on the wire. The winding machine manufacturers produce a great number of different slider-spring combinations, each of which is designed for use with particular wire sizes (down to AWG 50 wire).

When working with ultra-fine wire, three problems develop. First, the sliders are relatively fragile and it is probable that the spring will become either too tight or too loose due to normal wear or bending of the wire. If this occurs, the winding tension can become so far out of specification that it becomes impossible to wind the toroid, even if all other parameters of the machinery/operator system are satisfactory. When the slider becomes

uncalibrated, the only reliable solution is to replace it. However, many experienced operators re-adjust the spring so as to "make-do" with the old slider. This procedure often results in breaking the wire, wasting time and materials, and eventually causes an overcompensating adjustment which causes the wire tension to be too small.

In addition to the fragility of the sliders causing unknown and damaging winding tensions, there are no available sliders for wires finer than AWG 50. It is possible to modify the lightest tension sliders to be able to handle finer wires, but the tension control becomes erratic if this is done and it is not practical to wind reliable toroids using this method. The obvious solution is to design new sliders capable of generating the small winding tensions necessary for wire finer than AWG 50.

The third mechanical factor which helps to limit the minimum wire size used in toroidal transformers is that AWG 51 and finer wire (as well as thicker wire) can become damaged or tangled during the shuttle loading operation. All of the precautions that are taken during the winding process must also be taken while loading the shuttle (since shuttle loading is a form of winding. Furthermore, since the shuttle must be unloaded, it is imperative that the wire be wound onto the shuttle in such a way that it can easily, be removed. This requires that the loading tension be great enough to wind the wire in layers, where the wire cannot become tangled by previous turns, and that the loading tension be small enough to prevent wire damage due to stretching. The proper tension (i. e. , 16, 000 psi) can be achieved by one of the readily available spring loaded tension devices which are commonly available in a coil winding facility.

The wire can also be damaged on the shuttle during loading and winding. Section 4.4.5 describes in detail the mechanism of damage. The sharp edges of the shuttle gap must be prevented from touching the wire while loading and winding. This can be done by placing a protective piece of mylar tape in the groove covering the edges before loading the shuttle. At the same time, care should be taken in aligning the shuttle drive rollers, in order to minimize the flexing of the shuttle.

The above mentioned type of wire damage was detected by means of a "black-box" which was developed to measure insulation damage during the winding process. It is recommended that this damage detector be used for all loading and winding of fine wire toroids to immediately indicate any insulation damage or defective wire insulation. The continuous monitoring of wire insulation integrity during the actual winding process overcomes the quality control problem of determining the quality of the wire inside the spool of wire by sampling the first few feet at the beginning.

In addition to the mechanical factors which tend to limit the sizes of wire which can be wound on existing machines, there are two additional factors which must be considered. First, fine wire is not always uniform in either wire diameter or in insulation thickness. At times the variations can exceed 10 percent of the "nominal" measurements. Since the winding tension is transmitted along the wire, a significant decrease in wire diameter can place a load on the wire which will cause damage. The only way to eliminate these non-uniformities is to specify tighter limits on the wire diameter to the manufacturer. The second non-mechanical factor concerns the experience of the winding machine operators and their ability to use the machinery properly.

At this time, a significant portion of the reliability problems have been traced to operator errors. The errors occur primarily from three causes: the operators either do not know the proper procedures and techniques, they do not realize the importance of following the winding specifications, or the design engineers have not adequately written the specifications for the part. All three of these error-producing factors can be solved by a concerted training effort aimed at insuring that both the operators and the design engineers know the appropriate techniques and capabilities of the winding machinery and that the engineers are able to and do inform the operators of the relevant specifications.

The above discussion has not specifically dealt with the problem associated with using what are known as "open shuttle toroid winders." The open shuttle winding machines use a completely different method for loading wire onto the shuttle but they face all of the same wire size and tension control limitations as the previously discussed "closed shuttle" machines. Their

primary advantage lies in the fact that they can be used for toroids with smaller residual inner diameters than can the standard models. While this advantage will help reduce the component size by allowing use of a smaller core, it also faces the same types of problems as the standard winding machine discussed above.

In conclusion, it can be said that current winding technology and machinery is capable of winding reliable toroidal transformers, as they are now designed, and is also capable of winding finer wire sizes than the industry now attempts. The reasons for wire size limitations are that many shops do not always have calibrated, reliable winding machines available and the probability that, as wire size decreases, minor operational errors will make the winding of ultra-fine wire extremely difficult, if not impossible. A combination of strict equipment maintenance and replacement of worn or damaged parts, along with a continual training and retraining of personnel, will improve the quality of all parts produced and provide the basis for working with wires which are smaller than are currently attempted.

4.4.2 Winding Machine Set-up

The first activity which must be done, when winding ultra-fine wire toroidal transformers, is to select the proper shuttle/slider combination for the specified core and wire size and inspect and clean the winding machine. The selection of the shuttle/slider combination can be governed by the recommendations made by the winding machine manufacturer. [Note: For bifilar winding, select a shuttle/slider combination which is capable of handling wire three AWG sizes larger than the wire used (i. e., tension control is directly proportional to the cross-sectional area of all of the wire strands being wound, and three AWG sizes is equivalent to doubling the area). Using this method, it is possible to reliably wind any number of strands and still use the proper winding tension.] (See Section 4.4.4.) Once the machine components are selected, the operator should clean all contamination from the sliding surfaces and inspect the edges for nicks or rough spots which can damage the wire. When these steps are properly executed, the next phase can begin.

After assembling the winding machine, load the wire on the shuttle (see Section 4.4.5). This must be accomplished not only without damaging the wire(s) which will be used during winding, but also in smooth, easily removed layers, in order to prevent damage when the wire(s) are wound on the core. [Note: For multi-strand winding, the wires should be loaded on the shuttle at the same time and as near to each other as possible. In this way, the various strands will be very nearly of the same length and will respond to subsequent winding tensions as a cable and almost as though they were a single strand. This will allow the use of higher tension sliders for winding and the subsequent ability to use finer wire than the machines normally wind.]

4.4.3 Winding

The winding process should begin with a measurement of the actual tension on the wire. After the shuttle is loaded, and the wire(s) looped over the slider, it is possible to measure the tension which is placed on the wire by the slider. Take the lead wire(s) for the transformer, attach to a tension gauge, and pull the wire(s) off the shuttle, just as is done during winding. The slider will slide along the rim of the shuttle and its resulting tension can be easily measured. By this activity, the tension can be checked and compared to the desired winding tension. If the tension is too great, or too small, a new slider can be attached to the shuttle and calibrated (operators with considerable experience have been known to bend the slider spring in order to adjust the tension to its proper value).

Once the tension has been calibrated, it is necessary to check several additional points. First, the core positioning should be checked to ensure that the shuttle/slider mechanism does not hit the core (or any turns of wire on the core) as it passes through during winding. At the same time, the core should also be checked for horizontal alignment (see Section 4.4.6). Second, the operator should make sure that the wire(s) come off the shuttle/slider properly. Third, the lead wire(s) should be the proper length and be positioned so that it (they) do not interfere with winding and is (are) not going to cause electrical problems due to being too close together. These checks are done visually and take very little time to examine and correct.

The actual winding of the transformer can now begin. The first step in winding is to check the counter (to ensure the proper number of turns are placed on the core), the winding direction, and the core rotation direction.

The winding should start slowly and build up to the maximum winding speed gradually. This prevents the sudden, starting jerk which occurs if the machine is turned on at the maximum winding speed. The operator should watch the wire build-up on the core and adjust the winding speed so that the turns are placed on the core in a controlled manner. If winding is too fast, the operator can miss seeing an improper turn and lose control of the process. While winding the transformer, it is extremely important that the shuttle/slider mechanism does not hit the wire already on the core. If a collision occurs, the wire and/or insulation can be sliced by the sharp edges on the shuttle/slider. This event drastically reduces the reliability of the transformer, even though it may not cause an immediate open-or short-circuit. As a result, the components may be able to pass all quality control tests regardless of the insulation and wire damage, and fail at a much later date, after it has been incorporated into the finished product. In order to detect any penetration of the insulation by the shuttle/slider, a "black box", which sounds an alarm any time the wire is short circuited to the machine, has been built. This alarm works very well (see Section 4.4.5).

As the winding process comes to a close, the operator should double check the number of turns placed on the core and make sure the target number of turns are actually placed in the transformer. Since the number of turns on the transformer is critical, the operators should be careful that they do not add or subtract turns as they prepare the last lead(s) and get ready to remove the finished coil from the machine.

After the winding has taken place, the leads should be located at their proper position and all of the wire should be fastened down, so that the turns cannot move out of their proper locations. Before removing the toroid from the machine, it is advisable that the wire tension be checked again to determine if it has changed significantly. Then the toroid can be removed from the winding machine and placed in a protective container for storage and transport to the next phase of the manufacturing process.

HUGHES AIRCRAFT CO CULVER CITY CA ELECTRO-OPTICAL AN--ETC F/G 9/5
MANUFACTURING METHODS AND TECHNOLOGY FOR ELECTROMAGNETIC COMPON--ETC(U)
DEC 80 E R BUNKER, J R ARNETT, J L WILLIAMS DAAK40-78-C-0271
FR-80-7b-1254R-VOL-1 NL

UNCLASSIFIED

NL

The above process provides a generalized procedure for winding fine wire toroidal transformers.

The original requirement for this subtask of the MMT program specifies that the winding be done "under controlled wire tension." Because of machine limitations, dynamic tension controlled winding of fine wire is impossible for toroidal coil winding. Therefore, the controlled tension aspect is covered by the directions to calibrate the slider spring and clean the equipment so that reliable, controlled tension is placed on the wire.

4.4.4 Multi-Filar Wire Winding

There are two principal reasons why multi-filar toroidal winding is used. First, from a design standpoint a bi-filar winding will allow closer coupling between the primary and secondary coils if they are wound side-by-side. Second, from manufacturing considerations, since the tensile strength of wire is proportional to the cross-sectional area of the wire, two, or more, wires wound together should be able to withstand a higher winding tension than a single wire. The essential concern is whether multi-filar winding can be done reliably. This section deals with some of the factors which influence ability to reliably wind multi-filar coils.

The winding of multi-filar toroids is inherently more difficult than winding single wires, because there are more ways to have the wires snag or break. However, if the wires can be grouped together, as in Litz wire, so that they act as a cable, then the winding will become easier than if a single strand of identical wire were wound (but not as easy as if a single strand of wire with an equivalent copper cross-sectional area were wound).

There are three main factors which contribute to multi-filar winding problems. First, if one of the wires in a multi-filar winding is shorter than the rest, all of the winding tension will be placed on it and the wire may be damaged. Second, if multi-filar winding is used to enable the winding of finer sized wires, then there will need to be more interconnections than for a single winding. Third, the operators have a more complicated system to control, due to having two, or more, wires which must be monitored.

For the purposes of this discussion, consider a simple example, such as a toroidal transformer with a turns ratio of 1:3. The transformer can be wound as a four wire multi-filar (quadra-filar) coil, where one of the wires is the primary and the other three wires make up the secondary. The transformer would use 250 cm of AWG 50 copper wire in each of the four strands. The minimum winding tension the machine can use is 15 grams.

If all four wires are exactly the same length and are loaded onto the shuttle exactly parallel and congruent to each other, then they will wind as though they were one AWG 44 strand wire. As a result, the winding tension could be set at 25 grams (for AWG 44) instead of the 7.5 grams required for a single strand of AWG 50 wire. This factor makes it possible to wind the coil, even though the shuttle/slider mechanism cannot wind at tension as low as 7.5 grams.

Unfortunately, in real life, the four wires will not be exactly the same length. One of the wires will always be shorter than any of the others, so the 25 grams winding tension will be applied to that wire, possibly breaking it. The point to consider now is whether or not the multi-filar winding will allow the transformer to be wound.

In order to evaluate the danger that one wire will be sufficiently shorter than the rest of the wires in the quadra-filar bundle, it is necessary to determine how much the wire can stretch, before it is damaged. Current NEMA Standards have a 5 percent minimum elongation requirement before damage occurs to AWG 50 copper wire. Thus, for a 250 cm length of wire, it is permissible to stretch one of the wires as much as 12.5 cm. More to the point, since for typical winding machines there is a minimum of 10 cm of wire between the core and the shuttle/slider, the shortest strand can be as much as 0.5 cm shorter than the longest strand in the quadra-filar bundle. If the shuttle is loaded at 25 grams tension and with the individual wires in the bundle congruent, then none of the wires should be 0.5 cm shorter than the others. Thus, this technique should work for winding AWG 50 wire.

(NOTE: Smaller sizes of wire do not have a NEMA Standard minimum elongation. This should be rectified in order to check whether or not multi-filar winding is safe for them.)

The feasibility of this method requires that the individual strands of wire, in the quadra-filar bundle, act as though they were either one strand or a cable. This can occur with individual strands, as are currently wound, or by using a cable consisting of individually insulated wire strands such as Litz wire.

The second factor which influences the desirability of using multi-filar bundles is the fact that there may be more interconnections in the coil. For the example given above, with a one strand primary and a three strand secondary, there will be six interconnections. This is a 50 percent increase over what would be necessary for a conventionally wound coil.

Since the majority of failures observed in ultra-fine wire transformers occur on the leads and at interconnection points, the increase in interconnections could have a significant, negative effect on reliability. A program of evaluation and improvement in interconnecting techniques is strongly recommended in order to evaluate the risks involved and increase the reliability of ultra-fine wire transformers.

The two factors discussed above indicate that multi-filar winding can provide mixed benefits when winding ultra-fine wire transformers. Multi-filar winding will allow the use of finer wire than can be wound normally. It will also increase the risk for interconnection failures and reduced reliability for the components.

4.4.5 Dynamic Measurement of Wire Damage

During contacts with various toroidal magnetics manufacturing concerns, experienced operators had commented that as the residual ID of the toroid decreases, there was a strong possibility that the shuttle/slider would come into contact with the previously wound turns and damage the wire. Up to now, complete reliance on the operator to detect this occurrence was the only method available. The possibility of detecting such damage electrically needed to be evaluated. To accomplish this it would only

be necessary to ensure that the wire loaded initially on the shuttle would be insulated from it. Then using a continuity detector between the shuttle and the wire as it is being wound on the toroid core, any scraping of the shuttle against the previously wound turns could be detected.

A "black box" damage detector was developed which placed a small current (μA) limited voltage on the wire, grounding the shuttle/slider and detecting any shorts between the two. A schematic is shown in Figure 4-10, and a block diagram in Figure 4-11. The short detector had a response rate fast enough to measure pulse-type shorts at any operating speed of the winding machines available, thus, it would detect any penetration of the insulation by the shuttle/slider.

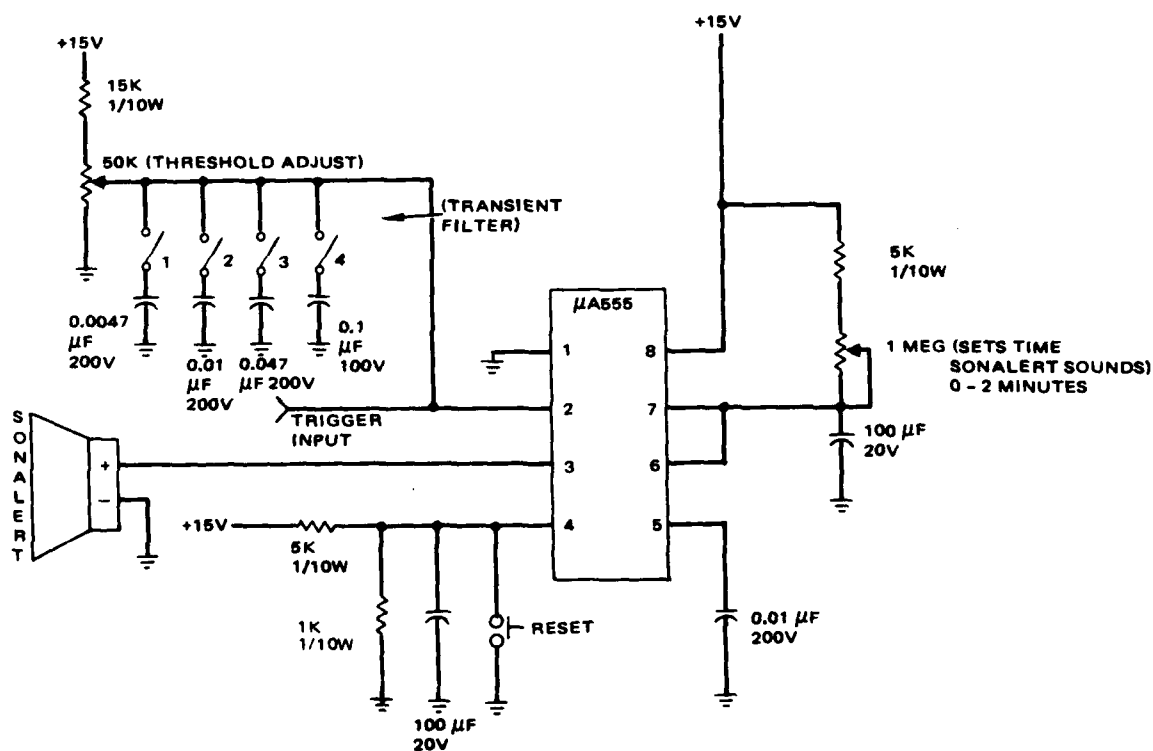


Figure 4-10. Magnet wire insulation damage detector — schematic.

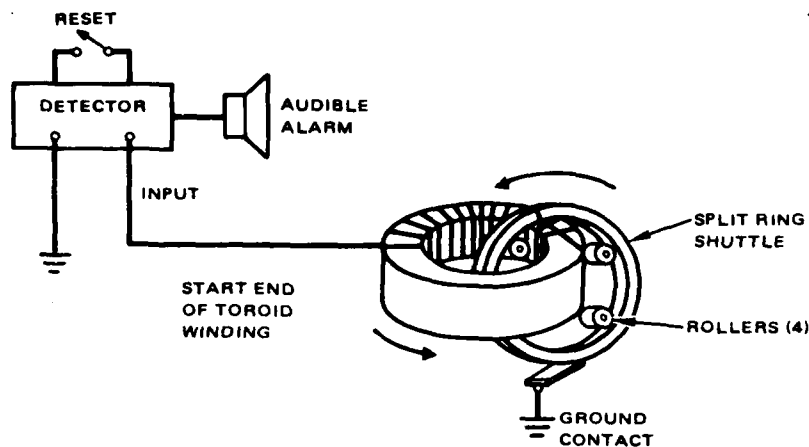


Figure 4-11. Toroidal wire insulation damage detector-block diagram.

After constructing the short detector, several toroidal transformers were wound with AWG 38 wire, with the detector attached. The results of tests confirmed that the slider/shuttle can slice through the insulation of previously wound turns on the toroid. It was so successful that it is recommended that it be used whenever high reliability toroidal magnetics are being wound.

During the course of the investigation two other sources of insulation damage were uncovered. The first unexpected result observed was that the detector indicated shorts to the shuttle/slider at times when there was no contact at all between the wires on the toroid and the shuttle. Considering it might be due to the wire itself, it was discarded and another spool of wire was substituted, which cleared up the problem and did not occur again. The hypothesis which is best supported by the evidence is that the detector probably was picking up pin-holes or thin places in the wire insulation. The frequency of response indicates that the copper was contacting the metal slider through pinholes located at irregular intervals along the wire (averaging approximately one pinhole per 10-20 inches). This fact throws doubt on the reliability of the wire, since less than 10 percent of the surface area of the wire comes into contact with the slider indicating a pinhole in every 1-2 inches of wire. The discarded wire could not be found for microscopic examination to verify the hypothesis.

A capability of detection of wire insulation damage during winding introduces a significant capability for improved quality assurance. Up to now, the only method available to QA to continuously check the insulation integrity of a spool of wire was to wind it from one spool to another, passing it through a conductive fluid. Any holes or missing insulation would thus be detected, but the rewinding procedure would, itself, degrade the quality of the wire, especially in the fine and ultrafine sizes. The only alternative to this, which is normal QA procedure, is to remove a few feet of the wire from the outside of the spool, run the required tests and inspections, and assume that the rest of the wire on the spool is of the same quality. The insulation could be entirely missing in the interior of the spool of wire and would never be detected until the magnetics was in the testing phase. With this detector, it is possible for the insulation integrity of the wire to be monitored during the winding operation without any extra handling of the wire.

The second unexpected result which the detector uncovered is that the wire, which was on the shuttle, was being progressively damaged during winding. This was discovered when intermittent shorts began appearing shortly after winding began and progressed until the shorts became continuous. In some runs this occurred before 50 turns were wound on the core. After all known factors were eliminated as possible causes, the failure mechanism was finally identified as being caused by the shuttle.

The shuttle is constructed as a continuous steel hoop, then cut through the cross-section so that the ends can be sprung apart to insert the core. This cut has very sharp edges, although the edges are designed to interlock to provide smooth interior and exterior surfaces. As the shuttle is rotated during both loading and winding, stress is placed on the opening due to minor misalignment of the shuttle rollers and the radial tension exerted against the inner surface of the shuttle by the roller to drive it. These varying transverse and axial forces on the shuttle causes a small amount of movement

to take place. This movement causes the sharp edges to slice through the thin insulation of the fine wire. The damaged insulation can be seen in the 50X SEM photograph, Figure 4-12. This was located two inches from the end of the wire which was the start of the shuttle loading operation. It is admittedly the worst possible location, being the "first on, last off" section of wire exposed to the most flexures of the shuttle during loading and winding. A closer look at the same region, Figure 4-13 shows that the copper was also nicked. This is verified by the EDAX surveys Figures 4-14, 4-15 and 4-16. The first shows the unbroken insulation as a reference, the second that bare copper is exposed and the third that oil was present from the shuttle.

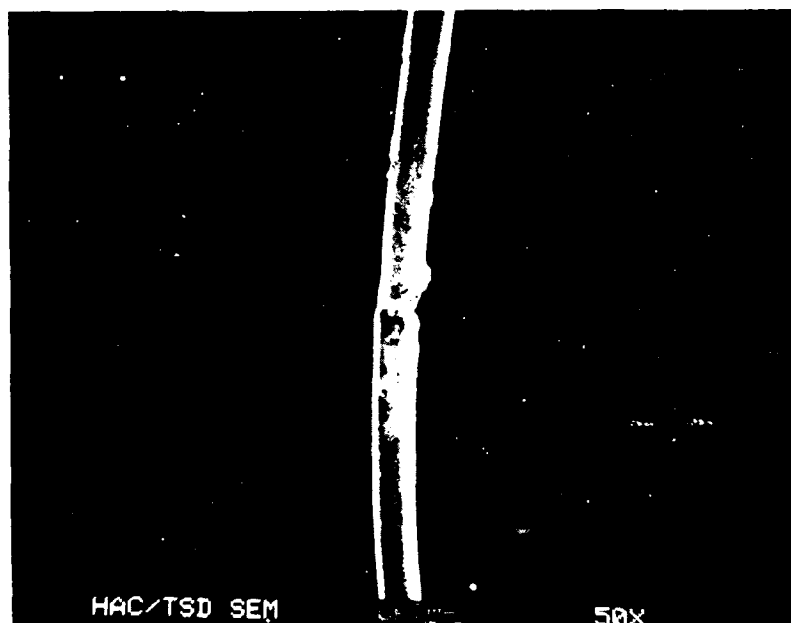


Figure 4-12. Nick in wire, due to shuttle gap flexing and slicing. (50x)

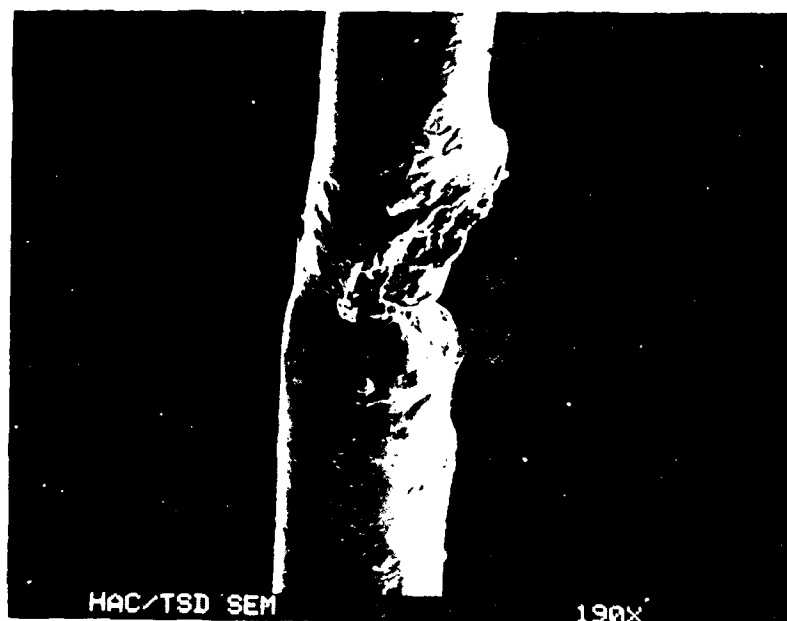


Figure 4-13. Nick in wire , due to shuttle gap flexing and slicing (190x).

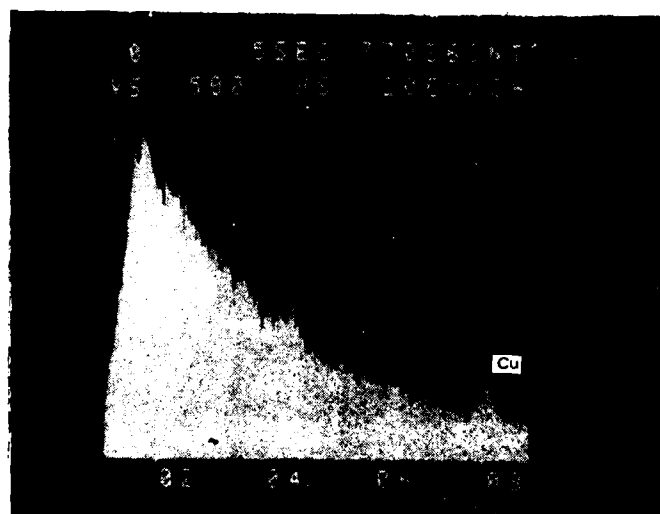


Figure 4-14. EDAX, at point X₁ on Figure 4-12, showing normal light element composition of the insulation material.

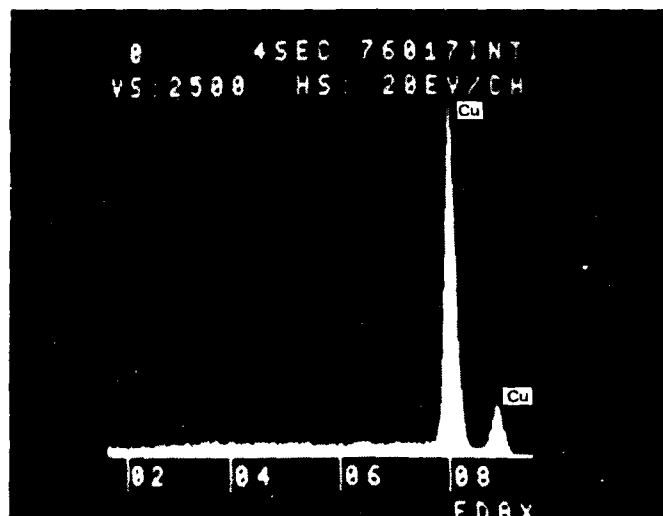


Figure 4-15. EDAX, at point X₂ on Figure 4-12, showing bare copper in the slice.

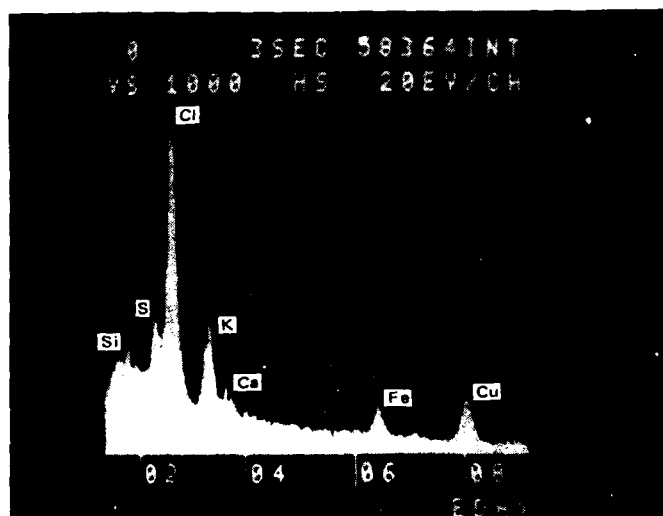


Figure 4-16. EDAX, at point X₃ on Figure 4-12, showing presence of oil (Si, S, Cl, K, Ca, Fe) on the sliced portion of the insulation.

Examination of the wire at multiples of the shuttle perimeter showed similar but usually not as extensive damage. The damage which was done by the shuttle existed on virtually all of the wire which touched the interior edges of the gap. It should be remembered that the damage shown occurred on AWG 38 wire (0.004 inch). This is a long way from ultra-fine wire which is less than half this diameter and accordingly much greater damage would result from the same shuttle gap displacements.

Two ways were investigated to eliminate this wire damage. First, the interior edges of the opening were rounded and smoothed to reduce the possibility of wire damage. Second, a protective shield (such as tape) was placed over the edges, after the core is inserted and before the wire is loaded. It is suggested that both be done to be sure that the problem is eliminated.

An additional improvement was made in the toroidal winder itself. In the models at Hughes Aircraft Company, the toroidal core is held in place and rotated by means of three rubber rollers as sketched in Figure 4-17. Because the roller has a vertical surface, as the core is rotated during the winding operation the core tends to climb away from the roller baseplate. This lets the core change its spacial relationship with the shuttle/slider and eventually may allow the inner part of the winding to come into contact with the rotating shuttle/slider. Operators normally reposition the core by hand before such collisions occur.

If the rollers were constructed with an outward leaning surface (see Figure 4-18), then the core would be automatically positioned in the correct attitude. This modification would eliminate one of the damage modes which normally exist.

4.4.6 Recommendations

There are a few minor changes which can be made on standard toroid winding machines which will increase the operator's control of the winding process and increase reliability. These changes are explained below.

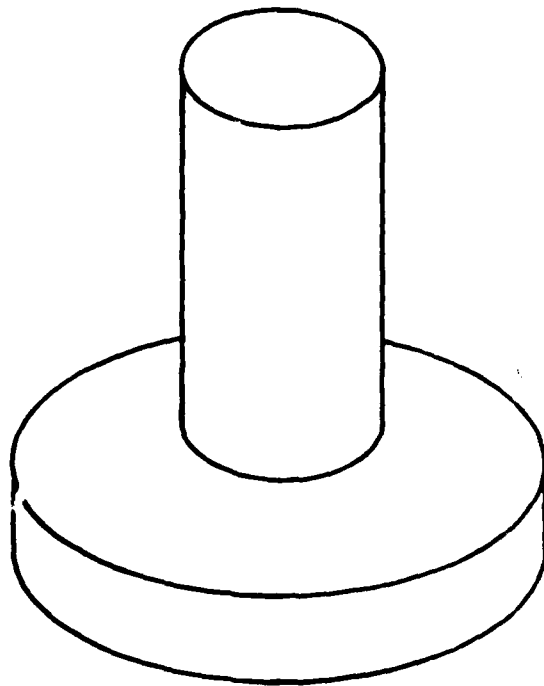


Figure 4.17. Conventional roller configuration.

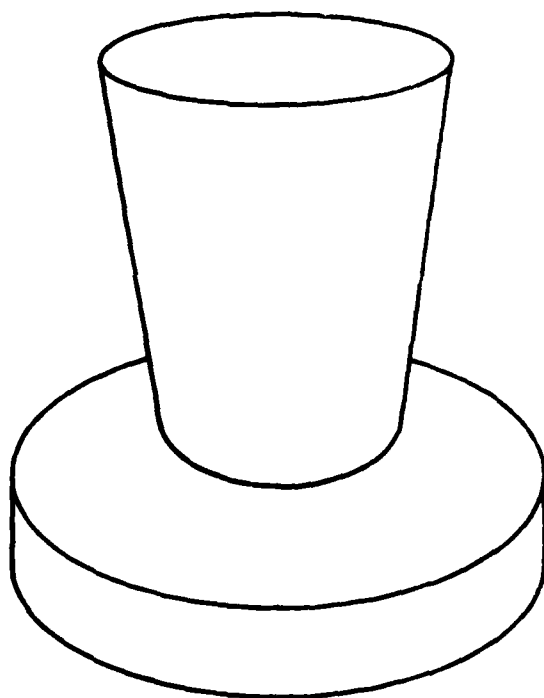


Figure 4-18. Modified roller configuration.

4.4.6.1 Replace Shuttle Loading Tension Devices

One of the major factors influencing the winding of single and multi-filar toroidal transformers is the winding tension of the wire as it is loaded into the shuttle. Loading the shuttle is exactly the same process as winding a coil. The tension must be optimal (maximum allowable tension) in order for subsequent toroidal windings to be reliable. This means that the shuttle should be loaded at the same tension as the toroid is wound.

Currently, the standard practice for controlling wire tension as it is loaded on the shuttle appears to be to load the wire at a reduced and uncalibrated tension. The most commonly used tension device consists of two felt pads with the wire clipped between them. This method is not adequate.

In order to achieve satisfactory wire tension control, the felt pads should be replaced with one of the readily available dynamic tension control devices. (Dynamic, in this sense implies that the tensioning device automatically adjusts the wire tension to a calibrated reliable standard, as described in 4.3.2.2)

4.4.6.2 Remove Sharp Edges

Winding machines often have sharp metal edges which can come into contact with the wire. In particular, the shuttle usually has sharp edges along its rim and on the interior edges of the shuttle opening. Under normal circumstances, these sharp edges can touch the wire and slice through the insulation. Many times through careless handling the shuttle rings also have nicks and scrapes along the O.D. To eliminate this problem, the edges can be sanded and polished smooth, thus greatly reducing the possibility of major wire damage when they do come into contact with the wire. For ultra-fine wire it is better to use a new nick-free shuttle and take extreme care in handling and storing it.

4.4.6.3 Use Calibrated Sliders

During toroidal winding, the slider tension, which controls winding tension, has a considerable influence as to whether the resulting transformer will be reliable. As a result, the operators should be aware that minor

changes in the slider configuration (such as bending, dirt, wrong slider, etc.) can make the winding process extremely unreliable. If the wire tension is not satisfactory (as measured prior to and after winding), the slider should be replaced with one which gives satisfactory tension.

4.4.6.5 Dynamically Detect Wire Damage

Install on all toroidal winders an electronic device to detect damage to the insulation on the wire as the coil is being wound. This technique not only helped to determine damage modes during the Hughes investigation, but it also informs the operator immediately when wire damage or faulty wire is present. If a similar detector is used during winding, wire/insulation damage would be detected immediately.

4.5 INSTALLATION OF INSULATION DAMAGE DETECTOR ON COIL WINDERS

The required modifications of both toroidal coil winders and bobbin/stick winders to accommodate the wire insulation damage detector were investigated, and implemented at Hughes on several toroidal winders. Drawings and photographs are included to show completely the modification procedures. For the bobbin winder, since this has not been implemented yet at Hughes, only sketches of the required modifications are shown.

The circuit for the short detector, shown schematically in Figure 4-10, was fabricated on a universal-type plug-in IC board as shown in Figure 4-19. Since the principal of operation is the same, there should be no difference in the circuit for either the toroidal or bobbin winder applications. The purpose of the transient filter and threshold adjust controls is to provide an input filter which will discriminate between actual shorting contacts of the wire and stray noise pulses which may be present in the manufacturing environment. To minimize noise pickup, shielded wires should be used for the trigger input leads. Further modifications may be made to adapt the circuit to the particular requirements encountered in each company's operation.

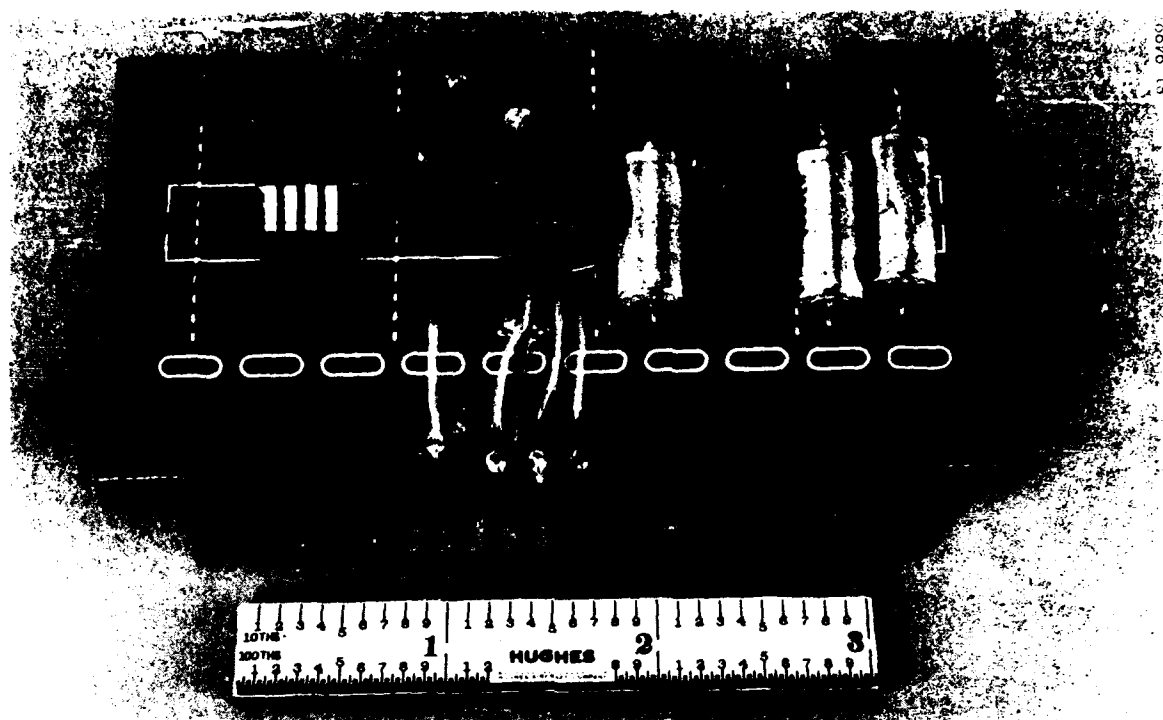


Figure 4-19. Wire damage detector circuit board.

The bobbin winder has an additional requirement for the spool of wire. This is the capability to make an electrical connection to the "start" end of the wire wound on the spool. In present practice this end is not available, especially in the fine and ultrafine wire sizes. In future orders to the wire vendor it could be included into the purchase order as a specification requirement. QA would be then able to check ohmic continuity between the two ends of the wire on the spool.

Because the starts were not available to the technician investigating this method, an alternate approach was devised by drilling a very small hole into the end of the spool at the bottom layer of wire. Careful insertion of a pin resulted in an electrical connection from that point throughout the remainder of the spool to the lead.

This method of connection was also used on the toroidal winder to monitor the wire insulation during the loading operation of the shuttle. It was found to be almost as much trouble to obtain a short-free loading of the shuttle as it was to subsequently wind the toroid. A detection of a short during the loading operation required the scrapping of the winding at that

point, provided one less operation than would be the case if damaged wire was not detected during the winding of the shuttle but was later detected when the toroid was being wound. Thus, it can be seen that if all wire spools were provided by the manufacturer with both ends available, this in-process detection of wire damage would be facilitated. This one step would reduce the cost and enhance the reliability of Hi-Rel components.

4.5.1 Toroidal Winder Modification

A typical modification of a model toroidal winder to incorporate the short detector for both the loading of the shuttle and the winding operations is shown in Figure 4-20, with a closeup of the grounding brush on the shuttle shown in Figure 4-21. Also shown is the clip lead to the shielded input for the input of the detector. If a greater than a 360° pass is required, obviously it is necessary to stop the winding, disconnect the clip lead, and thread the lead through the toroid and reconnect the clip so that the winding can continue. During the loading of the shuttle the clip is connected to the pin in the spool, making contact with the start end wire.

A detailed drawing of the grounding brush is shown in Figure 4-22. The brush, grounding the shuttle ring, was obviously needed in this model of toroidal coil winder which uses 4 insulating rollers to drive the shuttle. Even in coil winders which may use rollers that are metallic or conducting, the use of the grounded brush is still recommended to minimize the introduction of noise caused by varying contacts through the bearings into the short detector.

4.5.2 Bobbin Winder Modification

Although not yet implemented at Hughes, the modification of the bobbin winder to accommodate the short detector is proposed as shown in Figure 4-23. Assuming that the paying out of the wire is over the end of the spool, with the spool stationary, connection to the input of the detector is made to the wire and/or to the driven-in pin modification. The wire is passed through the various tensioning devices and, at either the last pulley, or the metallic wire guide which is used to position the wire on the winding is grounded to provide the complete circuit. Any insulation defects in the

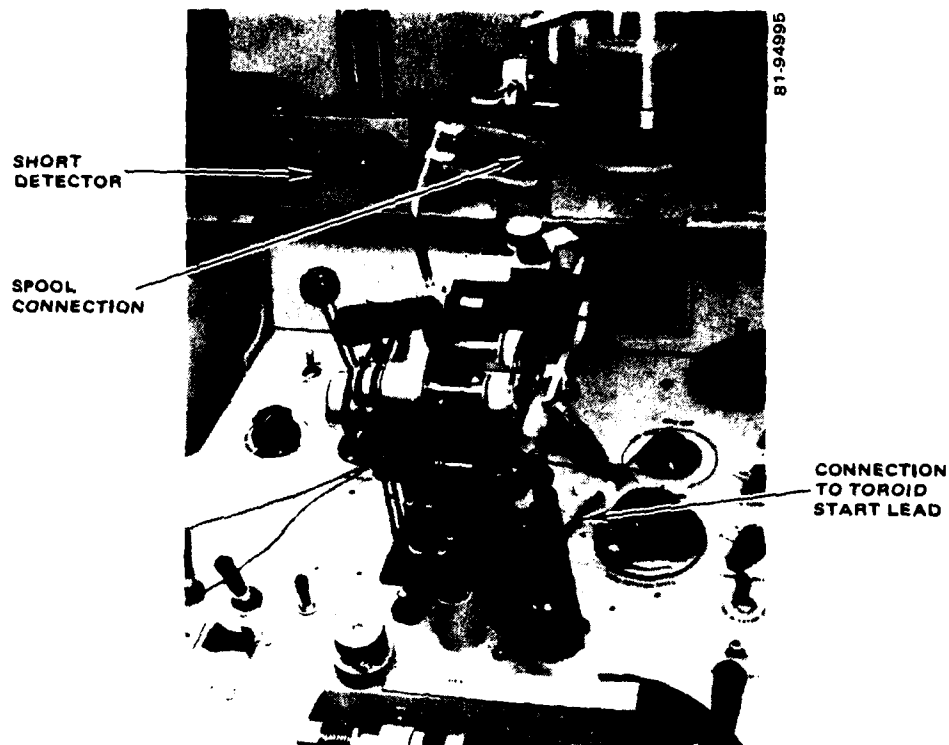


Figure 4-20. Toroidal winder modification.

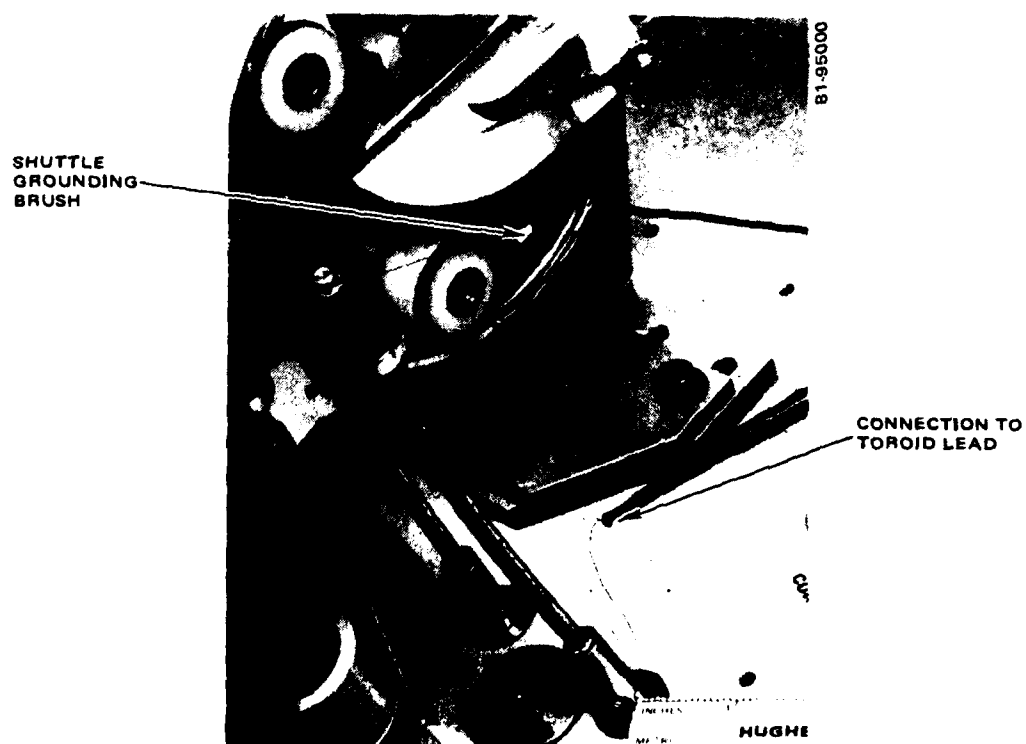


Figure 4-21. Closeup, showing shuttle grounding brush.

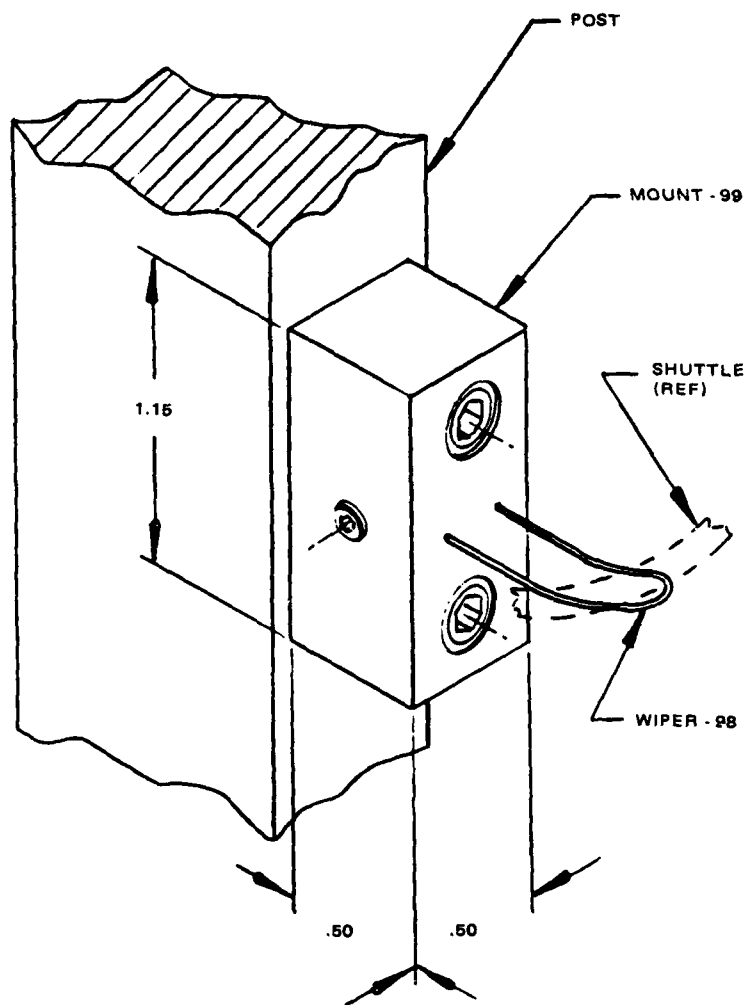


Figure 4-22. Sketch of grounding brush.

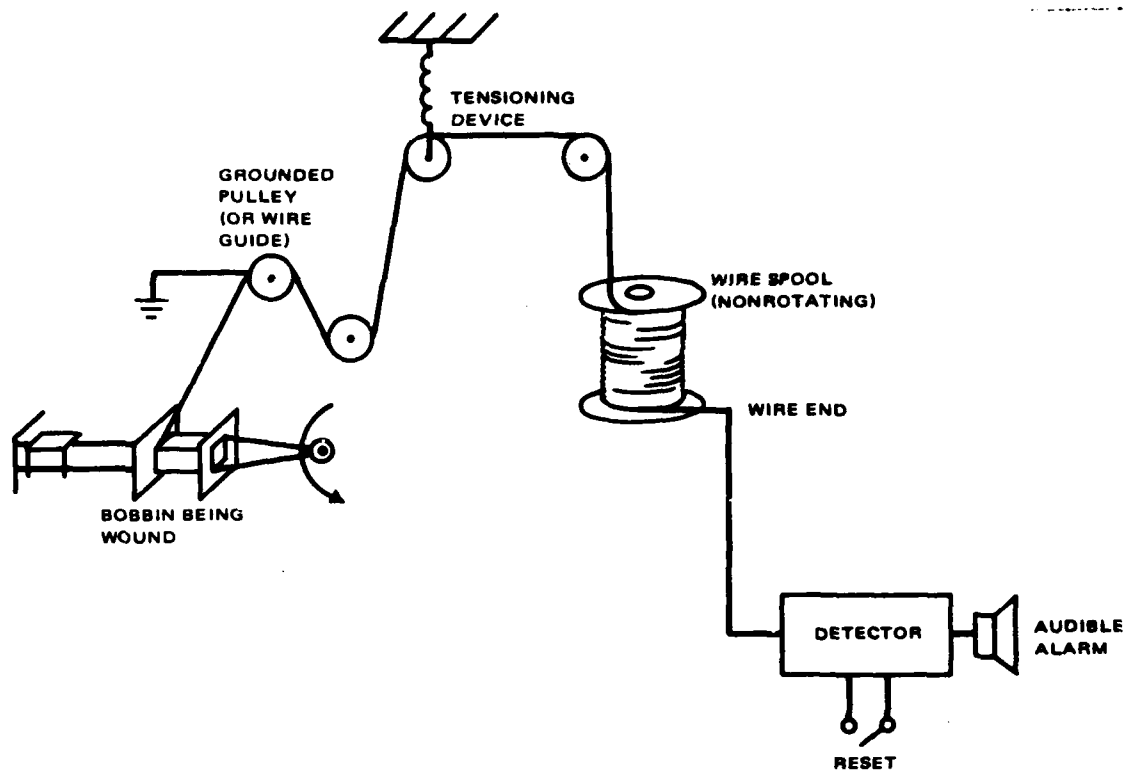


Figure 4-23. Bobbin winder wire damage detector — block diagram.

wire or damage caused by passing through the tensioning device or through the wire guide will thus be detected by the short detector. In the case of a multi-bobbin or stick winder a separate short detector would be required for each winding.

If paying out of the wire requires rotation of the spool, then an insulated commutator ring would be required to be fastened to the end of the spool with a insulated contact available for the input of the short detector.

5.0 REFERENCES, VOLUME I

5. 1. Reference Data for Engineers, 4th Edition, ITT.
5. 2. Dewey, G.H., and Outwater, I.O., "Pressure on Objects Embedded in Rigid Cross-linked Polymers," Modern Plastics, Feb 1960.
5. 3. Isleitson, R.E., and Swanson, F.D., "Embedment Stresses - An Inexpensive and Direct Test Method," paper presented at Fifth Electrical Insulation Conference, Sept 1963.
5. 4. Bunker, E.R., Kloezeiman, W.G., "Embedment Pressures of Various Encapsulation Compounds as a Function of Temperature, Using a Pressure-Calibrated Mercurial Thermometers," Internal report 900-499, 1971, Jet Propulsion Laboratory, Pasadena, CA.
5. 5. Harnwell, G.P., Principles of Electricity and Magnetism, p 40, McGraw Hill, 1938.
5. 6. Stucki, F.F., Fuller, W.D., and Carpenter, R.D., "Measurement of Internal Stresses in Encapsulated Electronic Modules", Lockheed Missiles & Space Company, Palo Alto, California.

6.0 APPENDICES

APPENDIX 6.1



WIRE DEFORMATION IN ULTRA-FINE WIRE COILS

by

John L. Williams
Technology Support Division
Hughes Aircraft Company
Culver City, California

Presented at:

Electrical/Electronics Insulation Conference
Boston, Massachusetts

October 9, 1979

WIRE DEFORMATION IN ULTRA-FINE WIRE COILS

John L. Williams
Hughes Aircraft Company
Culver City, California

ABSTRACT

Analysis of ultra-fine wire coils has shown that the wire is deformed into a hexagonal cross-section during the winding process. As the ultra-fine wire is wound around the corners of a bobbin, internal radial pressure builds up, deforming the wire and eventually causing dislocation of the turns and cold flow of the metal into and through the insulation barriers. This paper presents a quantitative method for determining the internal pressures which develop, and a design change which permits the manufacturing of ultra-fine wire miniature coils without having the internal pressure cause damage to the wire.

INTRODUCTION

The design and manufacture of magnetic components is a tried and true technology. Given a set of electrical, magnetic, and environmental properties, it is relatively easy to design the required components and, for a wide variety of conditions, manufacture the magnetic devices so that they will be effective and reliable. However, as packaging sizes have become miniaturized, the reliability of the components has suffered. One of the major causes of the decrease in reliability in miniature components has been identified as a deformation of the ultra-fine wire used, due to a buildup of internal pressure as the wire is being wound on the coil bobbin.

When the coils from sample transformers have been sliced apart and the wires at the corners of the bobbins examined, several interesting features become immediately obvious:

1. The wire is packed in the closest possible packing order. It is deformed into hexagonal cross-sections, making the closest packing configuration possible.
2. The internal pressure is somewhat relieved by expansion of the bobbin walls and compression of the core materials.
3. The close packed wires exhibit crystal-like slip planes, with straight boundaries, forming equilateral triangles. The fracture pattern is created when the bobbin walls relax and the internal pressure is allowed to act on a slight degree of freedom in movement for the wires.
4. Along the fracture lines between the conglomerates of wire, the individual wires are often greatly deformed, with spikes which stick into the inter-conglomerate spaces and which become points where the coil will fail.

Figure 1 shows the close packed wire and the deformation of the bobbin and core. Figures 2 and 3 show the crystal-like fracture patterns and boundary deformities of the wire.

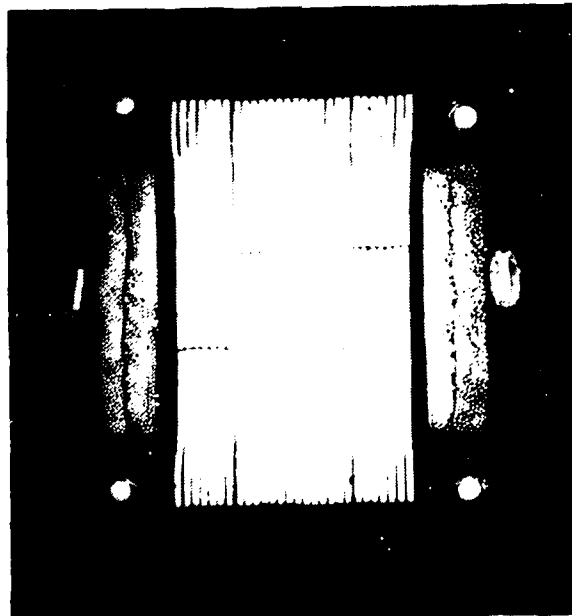


Figure 1. Close packed wire with bobbin and core deformation (9X).

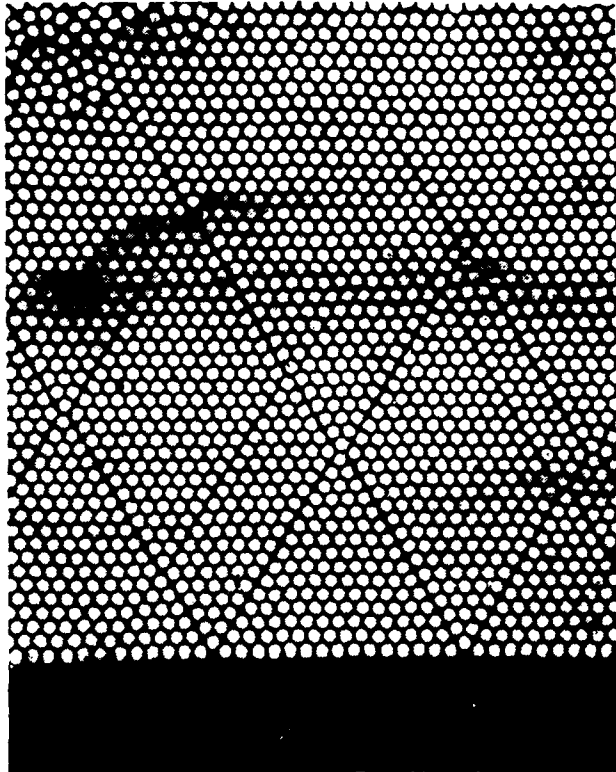


Figure 2. Crystal-like slip planes (100X).

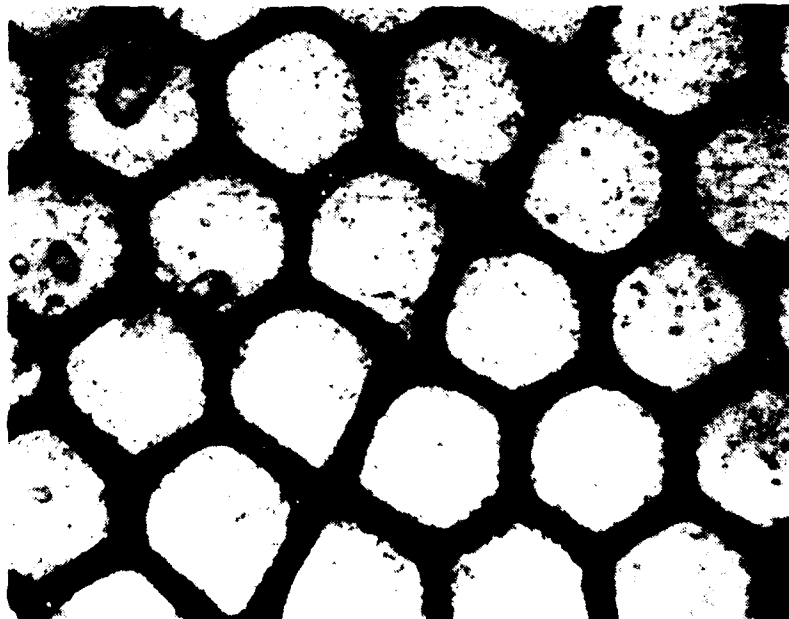


Figure 3. Boundary deformations of the wire (1000X).

This paper is divided into the three major facets of the wire deformation issue. The first section contains the development of a mathematical model for determining the magnitude of the internal radial pressure (IRP) as a function of the winding tension and coil configuration. Section II provides a method for evaluating existing coil designs to determine whether or not the IRP is great enough to cause wire deformation. The last section presents a minor design change which will allow the production of coils with greatly reduced IRP.

I. INTERNAL RADIAL PRESSURE DUE TO THE WINDING PROCESS

The internal radial pressure which develops in coils can be calculated using the methods for determining the internal pressure enhancement of band reinforced pressure containers. As the bands are wound around a pressure tank, the winding tension of the band is translated into an inward radial pressure on the container. The inward pressure is compounded by each additional layer of bands wound. Thus, the pressure is not only placed on the interior of the container, but also on the previously wound interior bands.

By considering each turn of a coil as a band on a pressure container, the IRP can be calculated. The equations, which are used to calculate the IRP, were developed from the work of D. M. Newitt (D. M. Newitt, "The Design of High Pressure Plants and the Properties of Fluids at High Pressure," Oxford University Press, New York 1940). The following equations will hold true, as long as the diameter of the wire is considerably less than the depth of the coil ($r_3 - r_1$ in the equations). (Practical experience suggests that the diameter of the wire should be less than 5 percent of the coil depth for best results.) A cross-sectional diagram of the concentric structure is shown in Figure 4.

In order to calculate the IRP, it is necessary to determine the circumferential forces in the coil. These forces can be determined by manipulating the winding tension and coil configuration. Thus, if the wire is wound at a

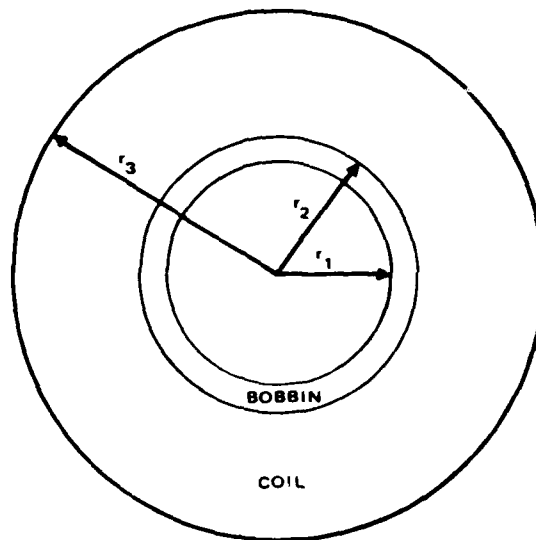


Figure 4. Circular bobbin and coil.

constant tension, σ_w , then the tangential stress, σ_{tc} , at any radius in the coil, due to compression by the layers is:

$$\sigma_{tc} = \sigma_r \left(\frac{r^2 + r_1^2}{r^2 - r_1^2} \right) \quad (1)$$

where

r = radius of the layer in question

r_1 = inner radius of the bobbin

σ_r = the radial stress

Then, the circumferential stress in the completed coil, σ_t , at the radius r , is:

$$\sigma_t = \sigma_w + \sigma_{tc} = \sigma_w + \sigma_r \left(\frac{r^2 + r_1^2}{r^2 - r_1^2} \right) \quad (2)$$

Since the circumferential forces ($2\sigma_t dr$) must be balanced by the net components of the radial forces in the coil, the total forces are:

$$\text{Circumferential force} = 2\sigma_t dr$$

$$\text{Inner surface radial force} = 2r\sigma_r$$

$$\text{Outer surface radial force} = 2(r + dr)(\sigma_r + d\sigma_r)$$

Therefore:

$$-2\sigma_t dr = 2r\sigma_r - 2(r + dr)(\sigma_r + d\sigma_r) \quad (3)$$

When this equation is expanded, and the insignificantly small second order differential, $drd\sigma_r$, is neglected, it reduces to:

$$-\sigma_t + \sigma_r + \left(\frac{rd\sigma_r}{dr}\right) = 0 \quad (4)$$

Then, combining equations (2) and (4), the equation for circumferential stress becomes:

$$\sigma_r + \left(\frac{rd\sigma_r}{dr}\right) = \sigma_t = \sigma_r \left(\frac{r^2 + r_1^2}{r^2 - r_1^2}\right) + \sigma_w \quad (5)$$

Equation (5) may be integrated and evaluated for $\sigma_r = 0$ at $r = r_3$ (refer to Figure 4), yielding:

$$\sigma_r = - \left(\frac{r^2 - r_1^2}{2r^2}\right) \sigma_w \ln \left(\frac{r_3^2 - r_1^2}{r^2 - r_1^2}\right) \quad (6)$$

and

$$\sigma_t = \sigma_w \left\{ 1 - \frac{(r^2 + r_1^2)}{2r^2} \ln \left(\frac{r_3^2 - r_1^2}{r^2 - r_1^2} \right) \right\} \quad (7)$$

Equation (7) gives the stress distribution in the winding when the coil is under zero external pressure. The IRP which is induced in the bobbin (at $r = r_2$) can be calculated as:

$$\text{IRP} = -(\sigma_r)_{r_2} = + \left\{ \frac{r_2^2 - r_1^2}{2r_2^2} \left(\sigma_w \ln \left(\frac{r_3^2 - r_1^2}{r_2^2 - r_1^2} \right) \right) \right\} \quad (8)$$

where:

r_1 = inner radius of the bobbin

r_2 = outer radius of the bobbin = inner radius of the coil

r_3 = outer radius of the coil

σ_w = winding tension

Since typical coils have rectangular bobbins, instead of the circular ones which would exactly fit the preceding equations, it is necessary to make a further approximation. If it is assumed that the radial stress due to winding is zero along the straight sides of the bobbins, where $r_1 = \infty$, then the internal pressure would be the same, at the corners, as if the straight sides were removed (i. e., each corner of the rectangular bobbin contributes one fourth of the stress that a circular bobbin would), as shown in Figure 5.

Figures 6 and 7 show the differences in winding pressure between the corners and the midpoints of the bobbin as evidenced by the packing configuration. This is much tighter at the corners than it is at the midpoints. Thus, the approximation used for the following calculations is valid.

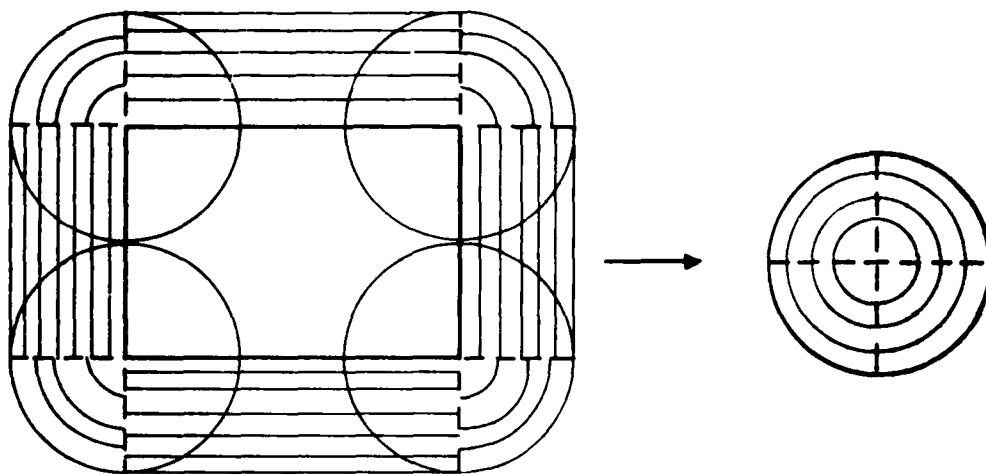


Figure 5. Circular approximation for rectangular coil.

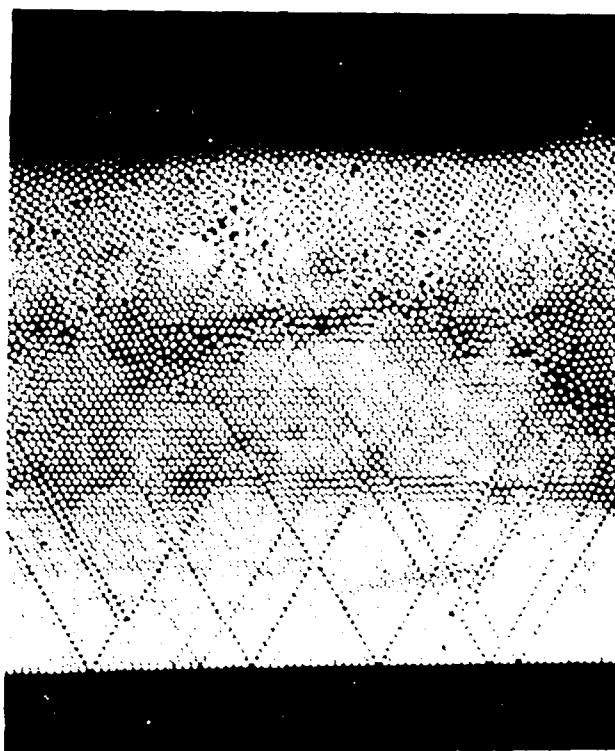


Figure 6. Wire packing at corner of transformer coil (50X).

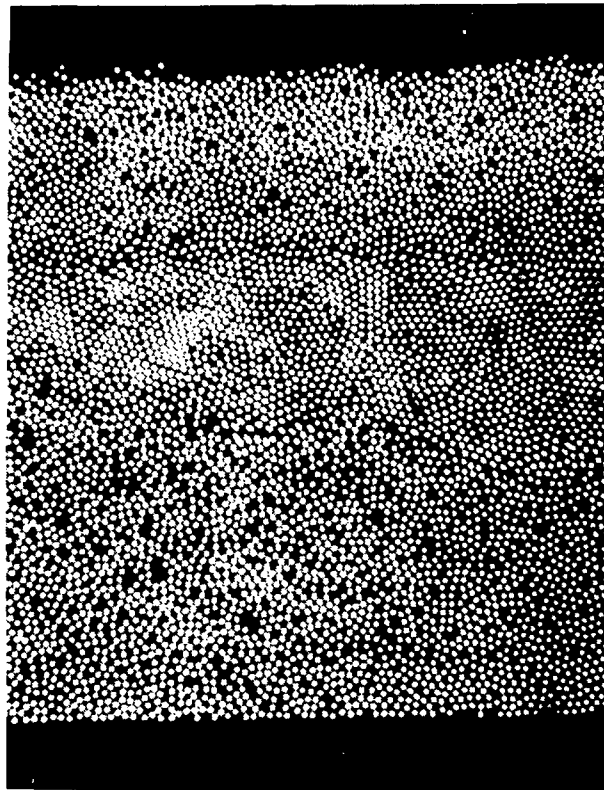


Figure 7. Wire packing at the midpoint between corners of the transformer coil (50X).

For the examined transformers, the measured values for the parameters at the corners of the bobbin are:

$$r_1 = 0$$

$$r_2 = 1.25 \times 10^{-2} \text{ inches} = \text{thickness of bobbin material under the coil}$$

$$r_3 = 8.44 \times 10^{-2} \text{ inches} = r_2 + \text{coil thickness}$$

$$\sigma_w = 1.66 \times 10^4 \text{ psi (recommended winding tension for copper wire)}$$

(A schematic drawing is shown in Figure 8.)

Since $r_1 = 0$, Equation (8) becomes:

$$\text{IRP} = \sigma_w \ln \left(\frac{r_3}{r_2} \right) \quad (9)$$

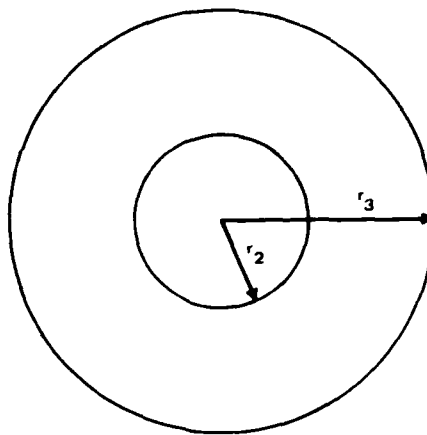


Figure 8. Schematic of round bobbin approximation.

and IRP is found to be:

$$\text{IRP} = 31,440 \text{ psi} = \text{winding pressure in the coil at the bobbin.}$$

Since a pressure of approximately 16,600 psi will cause the wire to become deformed, it is apparent that an IRP of 31,440 psi pressure is not acceptable. As can be seen in Figures 2 and 3, the IRP is great enough to cause cold flow of the copper in the wire of the coil.

II. METHOD FOR EVALUATION OF EXISTING COIL DESIGNS

Once it was realized that IRP causes considerable wire deformation, it became necessary to determine whether or not existing coil designs could be used without causing wire deformation. Equation (9) provides a method for the evaluation of existing coil designs, since the three quantities on the right side of Equation (9) can be determined. Thus, the IRP can be decreased by decreasing the winding tension (σ_w), decreasing the outside radius of the coil (r_3) (putting fewer turns on the coil), or increasing the inner radius of curvature at the corners of the bobbin (r_2). Each of the above factors, including a brief description of their obvious drawbacks, will be discussed below.

The most commonly used method for preventing wire damage due to IRP is to decrease the winding tension (σ_w). Since IRP is directly proportional to σ_w , it is relatively easy to control the pressure for any given values

of r_2 and r_3 . Unfortunately, as σ_w decreases, the coil becomes less tightly wound and at least three major problems can develop. First, the coil can become too large to fit in its allotted volume. Second, the coil may become loose enough to allow upper layers of wire to collapse into the coil and create shorts at the resulting cross-over points. Third, the winding tension may be reduced to the point where it is no longer possible to even wind the coil.

For the example used in this paper, σ_w would need to be reduced to 52 percent of the manufacturer's recommended value in order to bring the IRP down to an acceptable value. Thus, σ_w would become 8632 psi (equivalent to a 3.8 gm load on AWG 49 wire). In this way, the wire deformation could be avoided, but only at the risk of causing the other problems mentioned above.

The second method for controlling wire deformation would be to adjust the thickness of the coil, $r_3 - r_2$. Since IRP is proportional to $\ln(r_3/r_2)$, the coil can be wound safely for any value of r_3 which lets $\ln(r_3/r_2)$ be less than or equal to $2.71828 r_2$ ($e = 2.71828$). The main problem in this approach is that $r_3 - r_2$ is determined by the number of turns required in the coil, and cannot be altered.

In the example used, r_3 would be allowed a maximum value of 3.45×10^{-2} inches. Thus, the bobbin can only safely hold 30 percent of the original turns of wire. This places extreme limitations on any coils which could be made using the existing bobbin.

The remaining way which can be used to reduce IRP is to increase the value of r_2 . If the wire is bent around a larger radius, then IRP will decrease. This solution is a variation of the second method discussed above (i. e., maintain $r_3 \leq 2.71828 r_2$ by increasing r_2). The drawbacks to this method are that it would require a different bobbin design and would result in having at least one of the outside dimensions of the coil become larger. Implementation of this method for reducing IRP to an acceptable level is examined in the following section.

III. BOBBIN DESIGN FOR REDUCED INTERNAL RADIAL PRESSURE

The IRP of a coil can be reduced to an acceptable level (less than 16,600 psi) by increasing the bending radius at the corners of the bobbin. Several ways to do this are possible (including oval, hexagonal or other multi-sided bobbins), but the ideal design would eliminate all corners within the bobbin. This would encourage the use of a round bobbin.

The bobbins used in our samples have cross-sections which are approximately 0.0788 inches by 0.1576 inches at the layers nearest the core. Thus, the cross-sectional area of the core is approximately 0.0124 square inches. A bobbin can be designed with a square hole for the core and a round surface for winding the coil (as in Figure 9). Thus, the radius for the circular portion of the bobbin would be:

$$r = \sqrt{2(L/2)^2} = \sqrt{1/2} L$$

where L is the length of one side of the square core.

Then, for the tested coils,

$$L = 0.1114 \text{ inches}$$

$$r = 0.0788 \text{ inches}$$

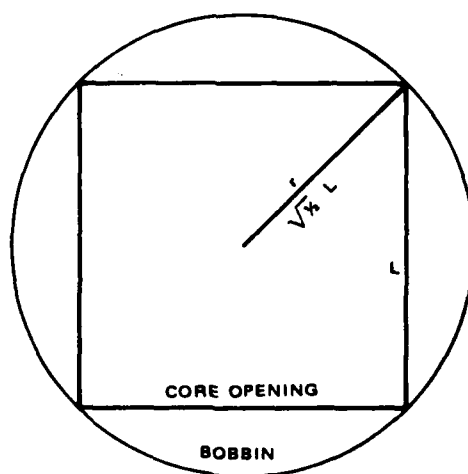


Figure 9. Square core, round bobbin.

Since the thickness of the winding will remain the same, and will equal 0.0717 inches, as in the test coils, the outer diameter for an equivalent circular coil would be $r_3 = 0.1505$ inches, (neglecting rounding errors).

Then,

$$r_1 = 0$$

$$r_2 = 0.0788 \text{ inches}$$

$$r_3 = 0.1505 \text{ inches}$$

$$\sigma_w = 1.66 \times 10^4 \text{ psi}$$

and, using Equation (9),

$$\text{IRP} = 10,700 \text{ psi}$$

This pressure is less than the yield point for copper and therefore should eliminate any wire deformation.

The new dimensions for the coil are defined by $r_3 = 0.1505$ inches. Thus, whereas the existing coil has outside measurements of 0.236 inches by 0.315 inches, the new coil would have a circular cross-section with the diameter equal to $2r_3$ (0.315 inches). The circular coil would have dimensions equal to the largest side of the existing design and it would be 33 percent greater than the smallest side of the existing design.

The losses for the circular coil can be compared to those for the rectangular coil. Looking at an approximation, where the losses are due to the resistance of the coil wire, the efficiency of the two coil types can be calculated. Since resistance will be directly proportional to the length of the wire, the mean length of a turn of wire is significant. Thus, the mean length of a turn of wire on the rectangular coil (LR), is:

$$\text{LR} = 2(0.0788 + 0.1575) + \pi(0.0717) = 0.698 \text{ inches}$$

and the mean length for the circular coil (LC), is:

$$\text{LC} = 2\pi(0.0788 + 0.0359) = 0.721 \text{ inches}$$

Therefore, the circular coil has a mean length of a turn which is 103.3 percent of that for the rectangular coil and the loss for the circular coil is 103.3 percent of that for the rectangular one.

Using the mean length of a turn, the relative efficiency of the two coil configurations can be compared. By assuming an efficiency of 90.0 percent for the rectangular bobbin coil, a set of characteristic values can be determined for both types of coil.

	<u>Rectangular Bobbin</u>	<u>Circular Bobbin</u>
Input Power	50.0 mw	50.0 mw
Output Power	45.0 mw	44.8 mw
Power Losses	5.0 mw	5.2 mw (5.0 x 103.3%)
Efficiency	90.0%	89.6%

The reduction in efficiency, from 90.0 percent to 89.6 percent will not significantly affect the performance of the coils (in most cases). Thus, the circular bobbin design should be a valid substitution for existing designs and eliminate the wire deformation which has previously occurred.

IV. SUMMARY

The existence of wire deformation in ultra-fine wire coils has been a contributing factor in determining the minimum size of reliable magnetic devices. If internal radial pressure is ignored in the design of a coil, then there will be wire deformation, the development of boundary deformities, and subsequent reduction of component reliability.

The mathematical model, developed in the first section of this paper (Equations 8 and 9), provides a quantitative method for evaluating the IRP of both existing and future coil designs. The evaluation results can then be used either to show that IRP is not significant for a particular design or to provide design limitations and changes which will reduce the IRP to acceptable limits.

The use of a round bobbin design can reduce the internal radial pressure, the concomitant wire deformation, and the resulting reliability problem. This design change is not free, since there is a marginal decrease in efficiency and an increase in coil size. However, these drawbacks can be tolerated within most system applications for magnetic components.

This work was supported in part by the U. S. Army Missile Research and Development Command under Contract DAAK 40-78 C-0271.

APPENDIX 6.2

REPORT NO. FR-80-76-866

LOW STRESS POTTING FOR STRESS
SENSITIVE MAGNETIC CORES

by

James R. Arnett,
Earle R. Bunker

Presented at:

Coil Winding Chicago '80
Chicago, Illinois
September 29, 1980

Technology Support Division
Electro-Optical and Data Systems Group
AEROSPACE GROUPS
Hughes Aircraft Company • Culver City, California

INTRODUCTION

It is a recognized problem that magnetic components using toroidal cores of ferrite, powdered iron, and to a lesser extent, Fe-Ni and Si-Fe exhibit inductance changes when the core's normal magnetostrictive motion is restricted by the encapsulation material. Magnetic components employing stacked or cut core laminations are also similarly affected when their cores are subjected to stresses from the encapsulant material. In this latter group, stresses on the core may also change the air gaps in the magnetic circuit. Because of the much higher thermal expansion coefficients of the encapsulants compared to the core materials, stresses on the cores will vary with temperature.

To overcome this problem toroidal cores are placed within an aluminum or plastic protective case to remove the strain from the core. This case adds weight, bulk, and cost to the finished product. Transformers using stacked or cut laminations with bobbin type windings are encapsulated with a teflon insert where the core should be. This insert is removed after curing and the core, either "C" type or stacked, is inserted and strapped in position. This procedure eliminates the pressure upon the core, but the extra manufacturing steps increase the cost.

Our hypothesis was that, if a low stress embedding technique and material were developed, magnetic components with pressure sensitive cores could be more easily fabricated. Several individual soft materials were successfully used. A two step embedding procedure using a soft inner material with a hard outer material was attempted. The decrease in stress was insufficient to classify this technique as a low stress potting procedure.

In order to ascertain the extent of the problem and measure the stresses exerted on the core by the potting material, a convenient, practical method for measuring embedment stresses as a function of temperature was needed. One method, similar to ASTM F135-76, reference 1, using pressure calibrated thermometers, was used on 10 low stress materials. This curve also detected glass transition temperatures for some materials to give a quantitative picture of the stresses generated by the materials on the thermometer over the temperature range of the thermometer. A second method, using small inductors wound on pressure sensitive cores, was developed in an attempt to eliminate two problems associated with the thermometer method: non-electrical output and fragility. This method was not as successful as hoped for use as a pressure gauge, but the technique gave an approximate value for the pressure at which stress sensitive cores were affected, all other parameters held constant. Using this information, those materials having a maximum pressure lower than 200 psi over -40°F to 220°F (-40°C to 105°C) are recommended for low stress potting requirements.

Selection of Materials

Ten prospective potting compounds were chosen from an original field of over forty materials shown in Table 1. The ten selected were: Conap EN-9, EN-9-OZR, EN-11; General Electric RTV-615, RTV-619, RTV-627, RTV-655; Scotchcast 9, 255; Uralane 5753. Hartel 17024 GA was added as a promising material for encapsulation after the work reported in reference 2 was completed. These compounds include urethanes, silicone rubbers, and epoxies. Some of these materials are presently being used for encapsulation and therefore provide a baseline with which to compare the other materials in pressure sensitive core applications. The materials were first evaluated for electrical parameters, followed by a further selection process using the mechanical, thermal and physical parameter data available.

For low embedment stress, the important parameters are: low shrinkage during cure, low glass transition temperature, low hardness and

TABLE I. LIST OF MATERIALS REVIEWED FOR LOW STRESS POTTING MATERIALS

Conathane EN-9*	RTV11/DBT	Eccoseal 63
Conathane EN-10	RTV60/DBT	Stycast 62
Conathane EN-11*	RTV8111	Emerson & Cummings W-67
Conepoxy Y1000/07	RTV619*	Eccoseal 1207
Conepoxy IM1145	RTV615*	Eccoseal 1218
Conepoxy RN1090	RTV655*	GE707
R7521	RTV670	GE702
R7501	RTV627*	Hysol C15-015
Conathane EN-2	Epocast 202	Hysol C60
Conathane EN-902R*	Scotchcast 255*	Hysol HD3561
Epoxy/D230	Scotchcast 235	Hysol E204A/9816
Epoxy/D400	Scotchcast 280	M&T E204A/9652
Epoxy/T403	Scotchcast 281	Uralane 5753*
Epon 825/HV	Scotchcast 5237	Scotchcast 9*

*Denotes materials selected for low stress potting study.

low coefficient of thermal expansion. Some of these properties are in opposition to one another, so that an engineering tradeoff is needed. Although moisture absorption and outgassing parameters were of secondary import, the materials lacking hydrolytic stability were rejected without further study. The thermal requirement for the candidate materials was that each be capable of passing a thermal cycling test of at least ten cycles over a temperature range of -55°C to 130°C . The various parameters given above are to assure this result.

Mechanical requirements for embedment of pressure sensitive core devices are two fold: (1) the material must support and protect the device, (2) the material must not exert sufficient pressure to change the electro-magnetic characteristics of the device over the required temperature range. The requirements of hydrolytic stability, outgassing and moisture absorption provide assurance of physical integrity under adverse environmental conditions.

TEST OF MATERIALS

In order to measure the pressures exerted by the subject encapsulation materials on a device, the device's character must be calibrated as a function of temperature. Previously, several investigators have measured the pressure exerted by the potting compounds on embedded parts by the novel approach of using pressure calibrated mercury thermometers: namely, Dewey and Outwater (reference 3), Isleifson, Swanson (reference 4) and Bunker and Kloeze-man (reference 5). The advantages of the thermometer approach are: simplicity, low cost, inscribed serial numbers, small size of the pressure sensing element (the bulb), extreme linearity of calibration, and elimination of temperature effects by subtraction of thermocouple readings. Disadvantages are fragility, nonelectrical readout and temperature range limitations. Consequently, the unaltered thermometer approach described in references 4 and 5 which is very similar to ASTM F135-76 was selected to evaluate the various low stress embedment materials.

Embedment Pressure Measurement Investigation

This section covers the techniques used to obtain the internal pressures generated by the encapsulating material as a function of temperature. A number of test specimens prepared in accordance with the ASTM as modified were placed in the temperature chamber which had a window in the door as shown in Figure 1. The samples were arranged so that each could be clearly seen through this window. In reference 5, a method of using a Polaroid camera to photograph the readings of the various thermometers through the window, and correcting for parallax to obtain the data at each chamber temperature was discarded in favor of direct visual readings in the interest of simplifying the experimental procedure, since the accuracy of a dead weight tester in the calibration procedure was not available. Because of greater than anticipated spreads of data points in the final analysis it is recommended for future work that the dead-weight tester and photographic readout be reinstated.

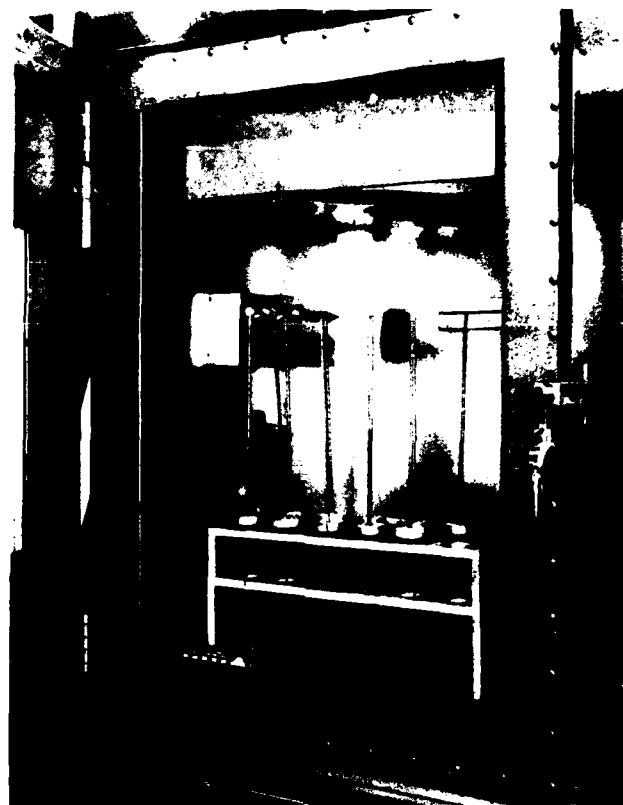


Figure 1. Pressure calibrated thermometers in temperature cycling chamber.

Results of the pressure calibrated thermometer method of measuring the embedment stresses as a function of temperature for selected low stress encapsulation materials are reported in this paper. The parameter which has the most significance for low stress embedment materials is the glass transition temperature. Above this temperature most materials exert average stresses less than 100 psi; below this temperature the stress increases markedly as the material becomes harder and usually more brittle. Obviously, then, low stress materials should have glass transition temperatures lower than the lowest to be encountered by the embedded component. In the plotted curves following, individual points of each run are shown as triangle (Δ), square (\square), or diamond (\diamond), respectively, and the average of the points at a given temperature as circles (O). If the points are close together, then the average points are not shown.

Thermometer Pressure Measurement Results

The differences between the thermocouple readings and the embedded thermometer readings were calculated, and multiplied with the thermometer calibration factor of $67 \text{ psi}/^{\circ}\text{F}$ which was characteristic of nearly all the thermometers used. To show the spread in the data the pressure exerted on the embedded thermometer as a function of temperature by Scotchcast 255 is plotted for three samples separately in Figure 2. First of all, it is obvious that the samples exerted increasingly high stresses as the temperature was decreased. Second, there is an appreciable scatter of points, and third, some of the points are negative, which would appear to show that the material is in tension rather than in compression. Careful analysis and comparison with previous results by one of the authors (Bunker) indicates that the scatter and negative points are due to inaccuracies in the readings. The error in the difference of the two readings is greatly increased when the two numbers are nearly equal. Considering that the scatter is random, then averaging the three sets of points at each temperature should balance out some of the errors. The curve drawn in Figure 2 represents the average.

Extending the tangent to this rapidly rising line back, results in intersection of the x-axis between 85°F and 95°F , which is defined as the glass transition temperature. The value using the Dupont Thermal Analyzer is 35°C , or 95°F . This is remarkable agreement between two totally different determination techniques, providing confidence for the use of thermometers as pressure gauges.

Scotchcast 9 also passes through its glass transition temperature of approximately 60°F , as can be seen from its graph of pressure as a function of temperature in Figure 3.

All of the points from three samples of Uralane 5753 are plotted in Figure 4. Averaging the readings at each temperature and replotting gives the somewhat better picture in Figure 5. The plots indicate that the data was taken appreciably above the glass transition temperature. It appears that a gradual increase is also taking place at the high end, which is also the case with RTV 615, Figure 6, and RTV 655, Figure 7.

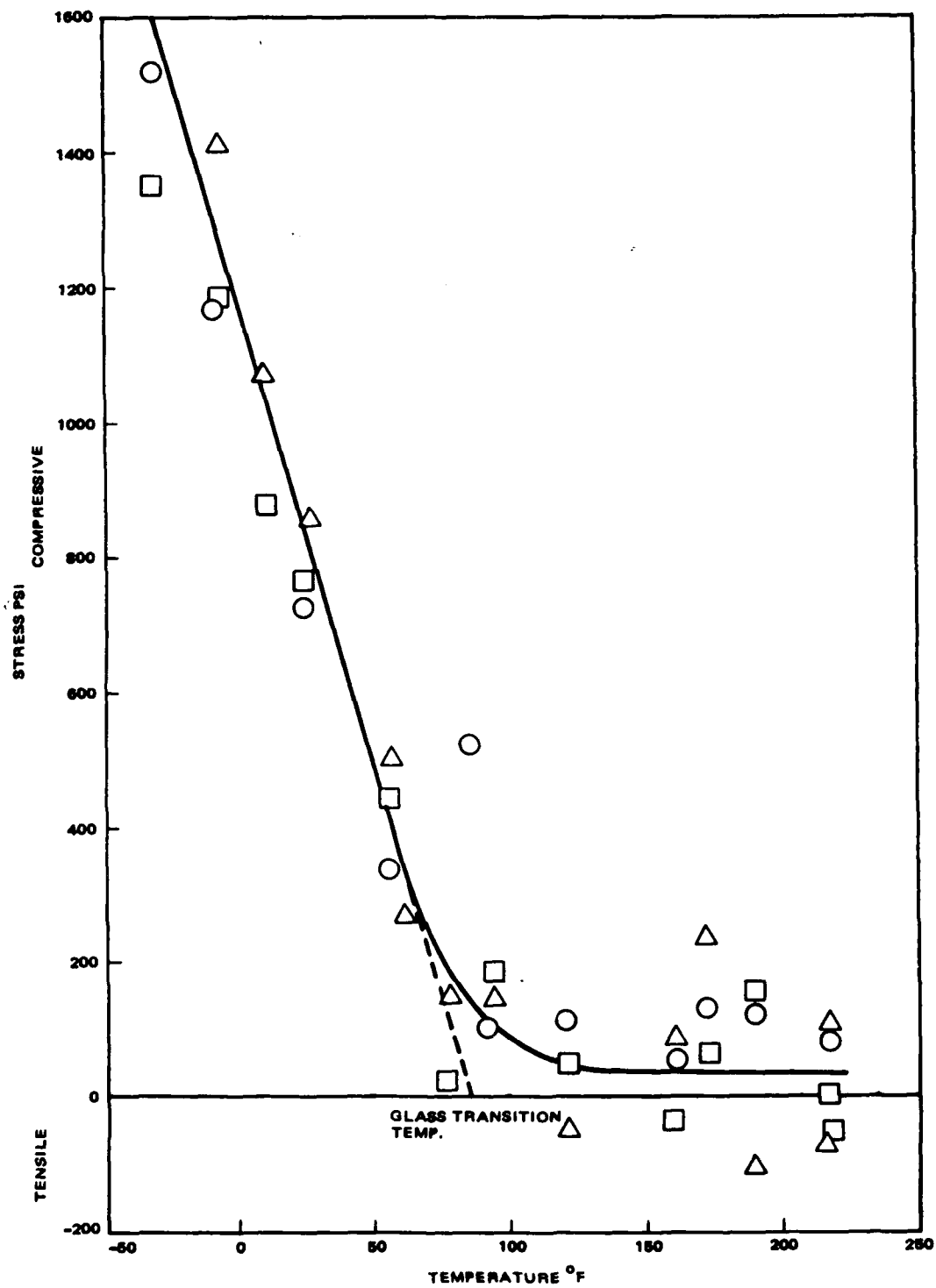


Figure 2. Scotchcast 255 stress vs. temperature, thermometer method.

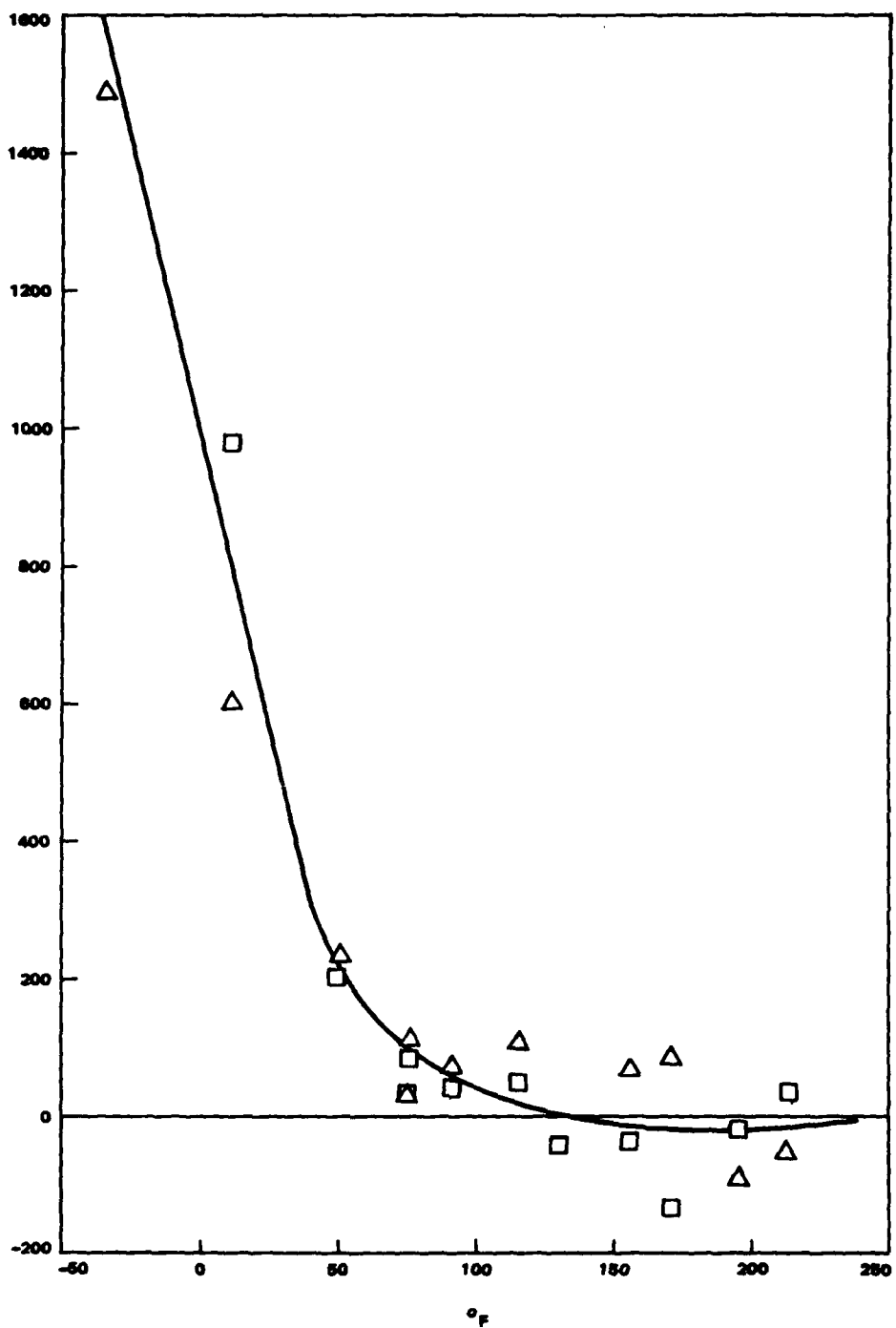


Figure 3. Scotchcast 9 stress vs. temperature, thermometer method.

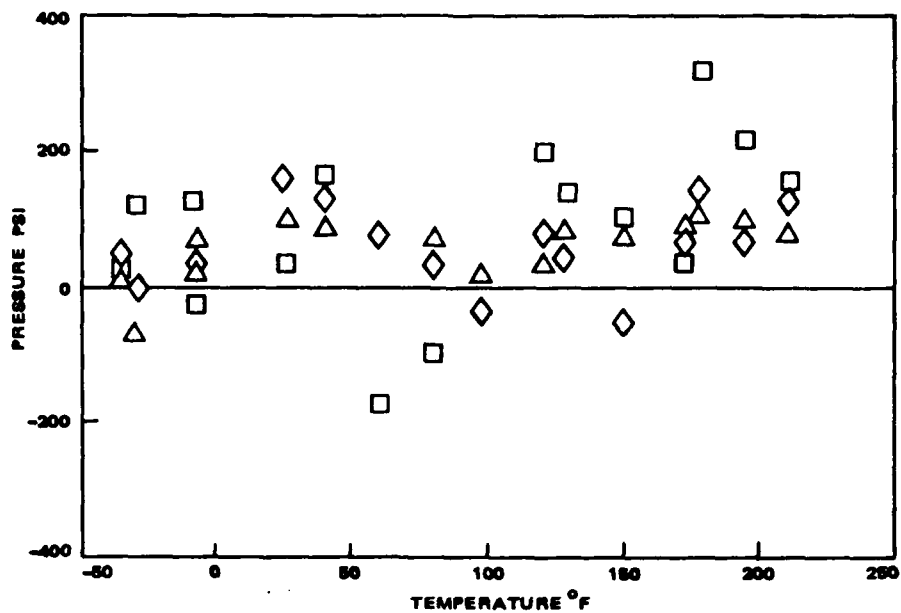


Figure 4. URALANE 5753 stress vs. temperature, thermometer method

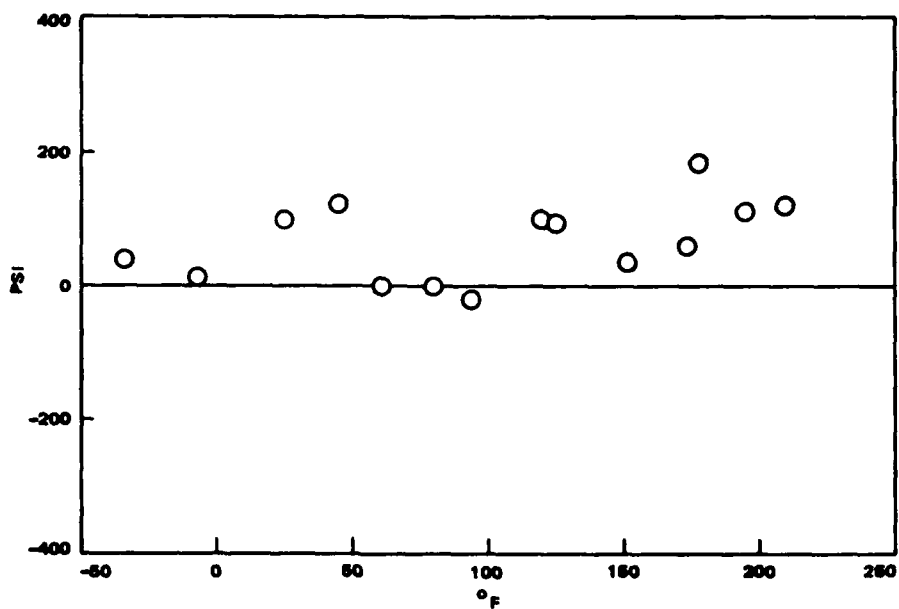


Figure 5. URALANE 5753 stress vs. temperature, thermometer method, average of 3 samples.

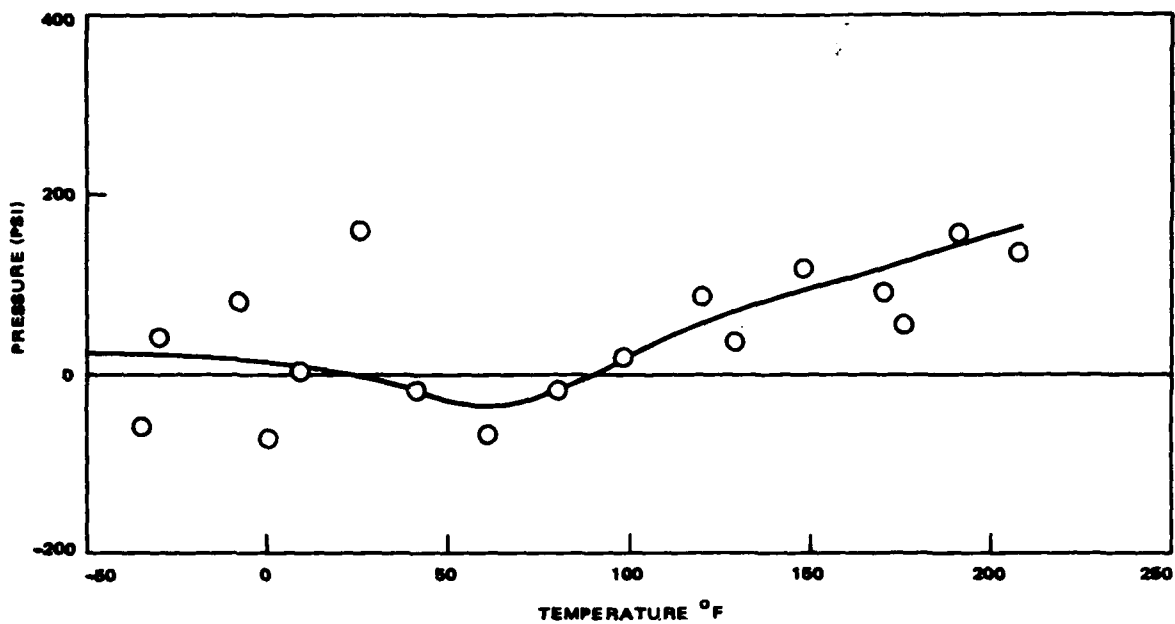


Figure 6. RTV 615 stress vs. temperature, thermometer method.

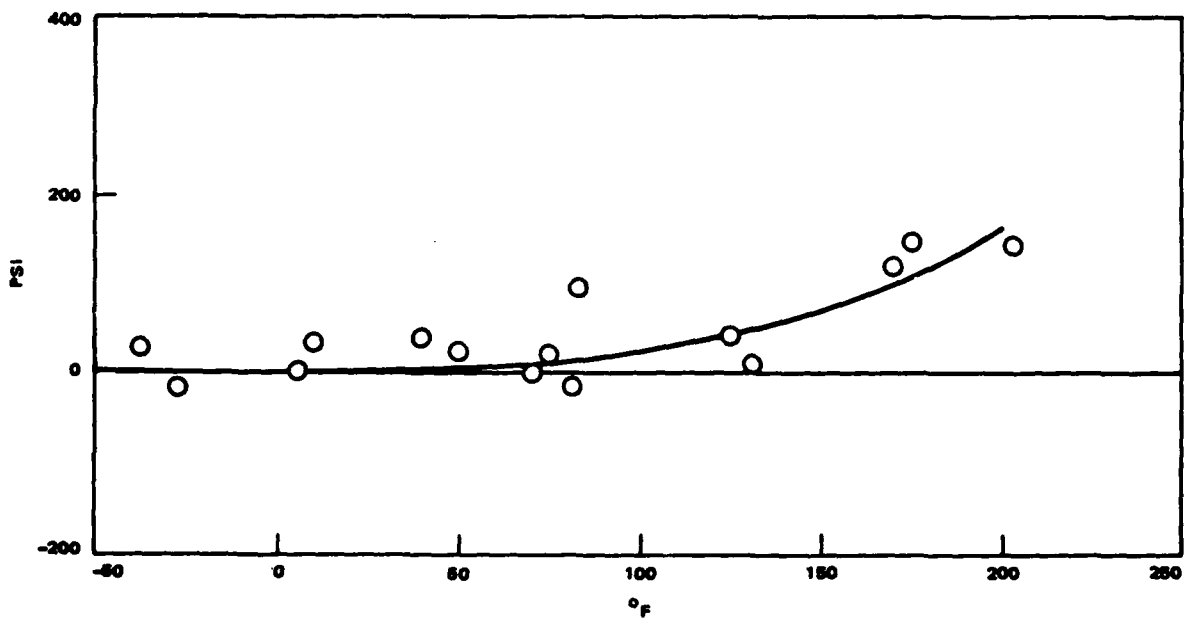


Figure 7. RTV 655 stress vs. temperature, thermometer method.

RTV-627 shows no such rise at either end as plotted in Figure 8. The points are close enough that a plot of the average is not needed to observe the trend. The same is true for RTV 619, Figure 9.

Conap EN-9 and Conap EN-90ZR both show a rise at the low temperature end, Figure 10 and 11 respectively, probably indicating a glass transition point.

From the embedded thermometer tests candidate materials and processes for low stress potting were selected. It was decided that the candidate materials shall have a maximum stress of less than 200 psi. The basis for this figure is somewhat arbitrary, based on the rationale that the percentage change of inductance from 0 psi to 1 K psi is usually less than 1/2 the change from 1 K psi to 2 K psi. Also noted is the experimental observation from hydrostatic testing of transformers that it takes more than 200 psi to note any observable change of inductance value from the zero psi value. The maximum pressures are shown in Table II.

Pressure Sensitive Core Approach

Extensive precautions in manufacture and handling are taken by manufacturers to eliminate stress effects on core materials by coating them with a soft material, or enclosing them in non-magnetic boxes or enclosures. Based on this information, it was proposed that inductors using pressure sensitive cores could be used to directly measure the stresses generated by embedment materials on the core, if they could be suitably calibrated with inductance as a function of pressure. This was to be accomplished with the pressure pot used to calibrate the thermometers shown in Figure 12.

Pressure calibrated inductors could overcome the major disadvantages of the thermometers namely, fragility, limited temperature range, and non-electrical readout. Some of the advantages of the thermometers would still be retained; e. g., low cost, even smaller size. The temperature limits of core magnetic materials range from the Curie point on the high end to cryogenic on the low. A simple inductance bridge would be used as the readout.

Samples of three different types of toroidal core materials considered to be very stress sensitive, some in different sizes, were obtained as listed

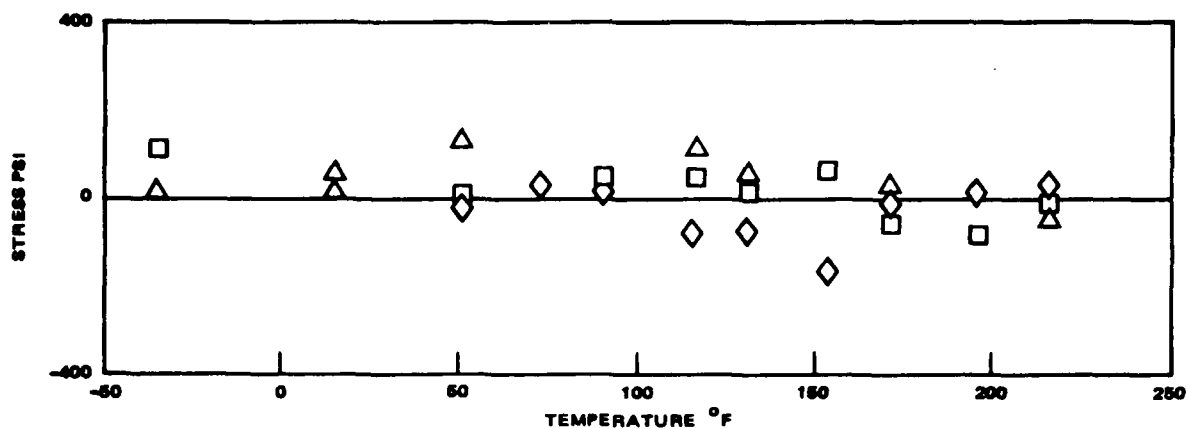


Figure 8. RTV 627 stress vs temperature, thermometer method.

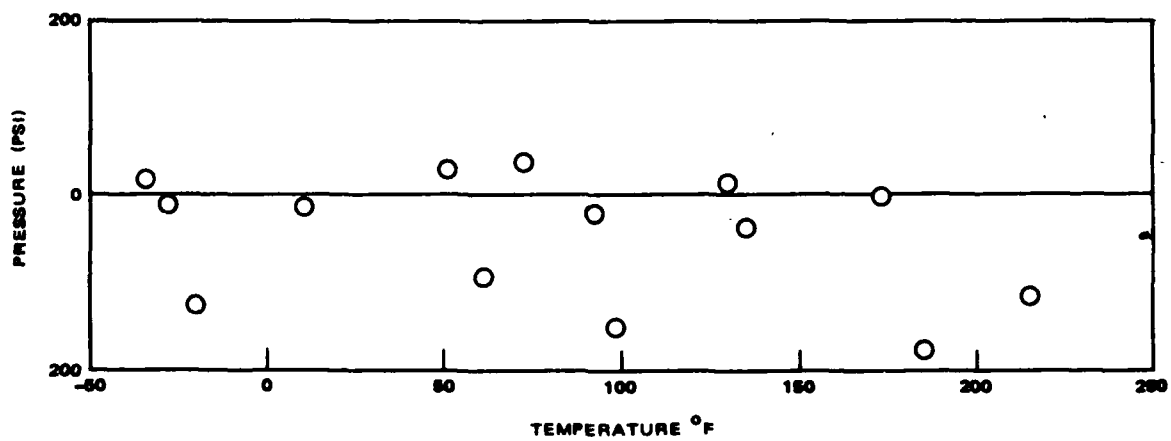


Figure 9. RTV619 stress vs temperature, thermometer method.

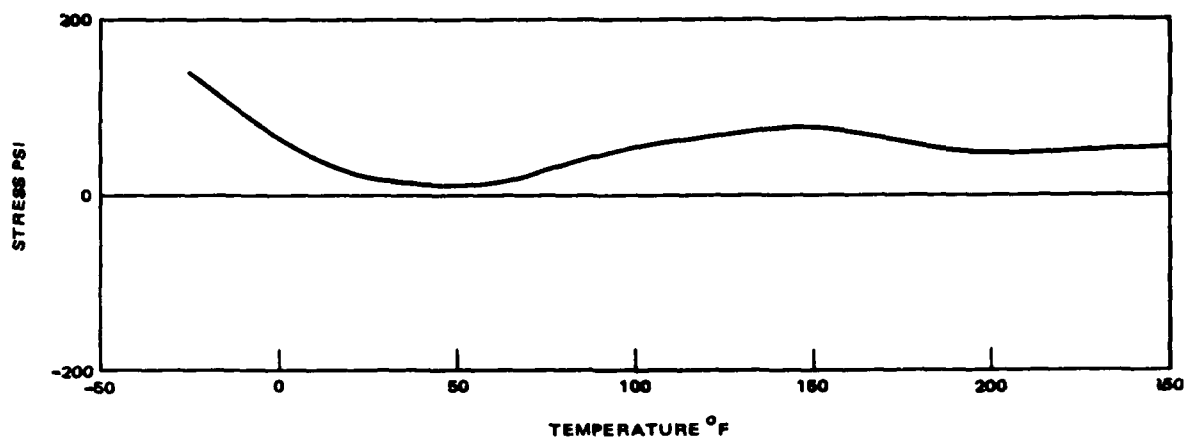


Figure 10. Conap EN-9 stress vs temperature, thermometer method.

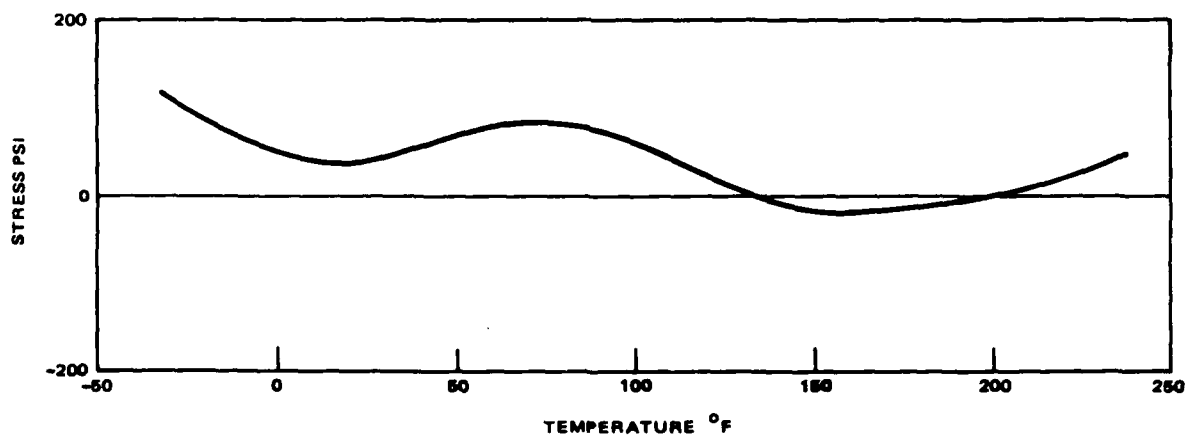


Figure 11. Conap EN-90ZR stress vs temperature, thermometer method.

TABLE II. MAXIMUM PRESSURE FOR SUBJECT MATERIALS

Material	Worst Case Pressure (Average of 3 Samples)	Temperature of Worst Case
Scotchcast 255	1800 psi	-40°F
Scotchcast 9	1600	-40
Conap EN-9	140	-40
Conap EN-9-OZR	110	-40
Conap EN-11	300	-40
Uralane 5753	200	175
Hartel 17024	400	-40
G.E. RTV-615	160	75
G.E. RTV-619	-180	100
G.E. RTV-627	80	75
G.E. RTV-655	150	+205

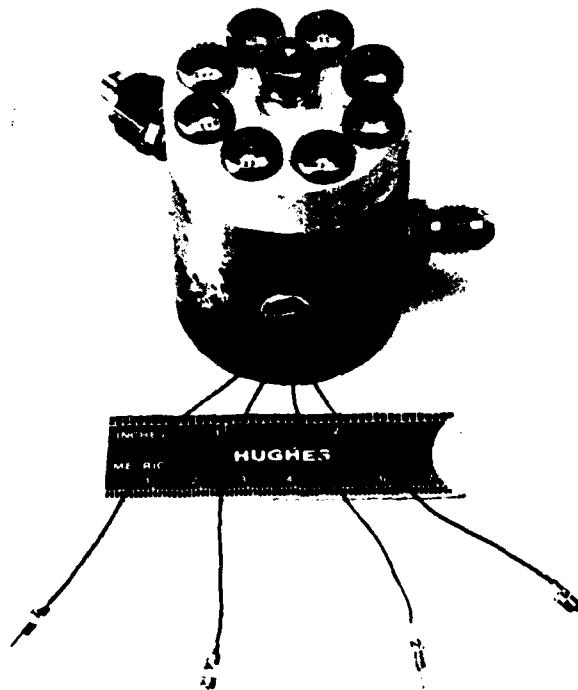


Figure 12. Pressure pot for calibrating inductors.

below in Table III. The only size limitation was that the completed inductor must fit in the 0.55 in. dia hole in the pressure pot.

The plan to use these inductors as stress measuring devices or transducers in various embedment materials was as follows: To calibrate these inductors it is necessary to determine both the pressure-inductance and temperature-inductance curves. Embedding an inductor in a test material, curing it in accordance with applicable specifications, then temperature cycling it and measuring the inductance. The difference between the inductance measured in the test material and the inductance of the unpot-
ted device at that same temperature, should, from the pressure-inductance curve, give the stress being exerted on the test inductors by the material.

In order to determine if the change of inductance with pressure is a function of the inductance itself, two different inductances were wound on the ferrite and Moly Permalloy Powder (MPP) cores using, in all cases, AWG 32 wire. The minimum inductance was one layer, perfect lay, on the cores. The maximum, on the other hand, was winding as many turns as possible on the core by hand, resulting in essentially zero I. D. Because of the larger OD of the Fe-Ni cores, only the minimum inductance was wound, as the larger one would not fit into the pressure pot.

Also, the inductance values are a function of the inductance bridge driving voltage. Measurements of inductance vs driving voltage at 1 kHz were made. It was found that, for all inductors, as the driving voltage was increased from zero, the inductance would increase to a peak value. A further increase in drive voltage would cause the inductance to decrease, and continue decreasing until third harmonic distortion occurred in the drive voltage, as the core saturated. Further increase in drive would cause the inductance curve to flatten out, then, in some cases increase slightly. It was not known at which drive level the inductor would be most sensitive to pressure levels, so runs at different drive voltages were made with the inductors in the pressure pot. Percentage-wise, it was found that there was not much difference, so the sinusoidal drive voltage which gave the peak inductance was used in all cases, since this made it easier to measure with the inductance bridge.

TABLE III. PRESSURE SENSITIVE CORE DATA

Material Type	Mfgr.	Mfgr. Designation	Size			Total Quantity	μ at 25°C	Curie Temp
			ID	OD	Th			
Ferrite Note 1	TDK	H5B2T	2 mm	4 mm	1 mm	4	8,000	136°C
	TDK	H5B2T	3 mm	6 mm	1.5 mm	4	8,000	
	TDK	H5B2T	4 mm	8 mm	2 mm	4	8,000	
MPP (moly - permalloy powder)	Magnetics, Inc.	55031-M4	0.156 in.	0.310 in.	0.125 in.	4	60	460°C
	Magnetics, Inc.	55038-M4	0.200 in.	0.400 in.	0.156 in.	4	160	
Fe-Ni 49 Square-mu wound core Note 2	Magnetic Metals	CC433U4602	0.375 in.	0.438 in.	0.125 in.	15	35,000	480°C
Note 1. Parylene coated								
Note 2. Uncased								

A summary of the inductors wound for the embedment tests reported in inductance values and average changes in inductance with temperature/pressure is shown in Table IV. This table shows several interesting features. The number of turns has no significant effect on the change of inductance with pressure; the percentage change is the same. Ferrite cores show a negative or decreasing inductance with pressure, while the MPP cores have a positive characteristic, although much less. The Fe-Ni cores show no significant change in inductance with pressure. In the case of temperature, MPP cores exhibit zero temperature coefficient simplifying the reduction of data for encapsulated or potted inductors. However, the small percentage change with pressure compared to ferrite imposes more stringent requirements on the measuring equipment.

An unexpected result was the lack of pressure effects on the Fe-Ni coils. This wound core material is from a family of materials considered extremely sensitive to stress; consequently, they are inserted in core boxes by the vendor to prevent any possible stresses during winding and embedment. Perhaps it is unequal or non-isotropic stress that the core is sensitive to as contrasted to the isotropic stresses created by hydrostatic pressures in the pressure pot. In other words, the damping effects of oil at high pressures on the magnetostriction of the iron-nickel cores are not significant.

Inductor Pressure Measurement Results

Using the low stress materials selected from the thermometer tests inductors were potted. Although the responses of the Fe-Ni cores to pressure were disappointing and thought to be due to the isotropic pressure environment, it was thought that these coils might be responsive to non-isotropic stresses in the embedment compounds. Accordingly 11 of these inductors were potted in various materials to be compared with the test results of ferrite or MPP inductors potted with the same materials.

Since Scotchcast 255 is a favorite material, but one with a significant increase in pressure below its glass transition temperature, several test inductors were coated with a softer material, which it was hoped, would provide a cushioning effect that could be evaluated quantitatively. Two of

TABLE IV. TEST INDUCTOR DATA

Core Material	Size	No. Turns AWG 32	Qty	Normal Inductance mH	$\Delta L/10K$ psi avg.	$\Delta L/^{\circ}F$ Avg.			Coil S/N
						-37 $^{\circ}$ to +40 $^{\circ}$	+60 $^{\circ}$ to +160 $^{\circ}$	+200 $^{\circ}$ to +240 $^{\circ}$	
Ferrite	2-4-1	20	2	0.458	-53.8%	+0.28%	-0.054%	-0.41%	1, 2
		36	2	1.66	-50.5%	-0.57%	-0.30%	-0.90%	51, 52
Ferrite	3-6-1.5	34	2	2.21	-30.5%	+0.24%	-0.10%	-1.13%	3, 4
		90	2	15.9	-36.2%	+0.31%	-0.13%	-3.11%	54, 55
Ferrite	4-8-2	44	2	5.25	57.8%	+0.25%	-0.23%	-1.48%	5, 6
		140	2	49.3	-54.1%	+0.27%	-0.071%	-0.12%	55, 56
MPP	031	50	2	0.066	+ 2.3%	No Significant Change			1, 2
	031	120	2	0.367	+ 3.8%				3, 4
MPP	038	64	2	0.350	+10.6%	No Significant Change			5, 6
	038	200	2	3.42	+10.2%				7, 8
Fe-Ni	433	120	14	6.88- 10.0	No Significant Change	Data Very Scattered -0.16%			1-16

these cushioning materials were RTV 619 and RTV 627, previously evaluated in their own right as embedment materials. The third was Epolene C/AC617, a polyethylene wax with a melting point of 250°F.

Plastic potting cups 3/4 in. dia x 3/4 in. H were used for potting the various inductors. In all cases the inductor axis was perpendicular to the cup axis. Materials were mixed and cured in accordance with applicable manufacturers' or Hughes specifications.

The processes used for each embedment were those suggested by the manufacturer, except that all materials requiring a cure were placed in an oven at 190°F overnight. The silicones chosen required only one to two hours at this temperature to cure; however it was convenient to place all of the materials in the oven at the same time and to remove them from the oven at the same time. The two-material potting processes required extra time for the second cure.

After the cures were completed, the potted inductors were temperature cycled between -50°F to +250°F in most cases. At various temperatures, when the samples stabilized, the inductance and Q values were taken at the voltage input to the inductance bridge used before for each group of inductors during calibration.

The data reduction process was relatively straightforward. For each material sample, the temperature vs measured inductance curve was drawn. Referring to the temperature-inductance calibration of the unpotted inductor, the inductance was subtracted from the potted curve. The remaining inductance was then a function of the stress being generated on the inductor by the potting material. Comparing this value for each temperature with the pressure inductance calibration curve gives the pressure being generated on the inductor at that temperature. In the case of the MPP cores, which had essentially zero temperature characteristic, this procedure was greatly simplified, as the values for pressure from the calibration curve can be read directly. The Fe-Ni cores, which showed no pressure effects were included anyway to see if anything would happen.

The results were somewhat confusing as well as disappointing. Following the above procedure for both the ferrite and MPP core resulted in

enormous values of stress, far greater than any material could withstand. Tensile stresses were indicated in temperature regions where compressive stresses would be expected.

The excessive values of stresses were reduced somewhat by the assumption that, at the cure temperature of 200°F (250°F for the Scotchcast 255-Epolene C/AC617 combination) there should be no stress on the embedded inductor. This conclusion follows from the fact that embedment stress is due to the difference between the temperature expansion coefficients of the solid potting material and the inductor core. While the material is liquid, no stress can exist, which is assumed to continue on into the cured material at the cure temperature of 200°F. In all curves plotted, the plotted curve is translated so that the inductances at 200°F are equal; i. e., the difference is zero.

It is recognized that, instead, another mechanism may exist to explain the stresses measured at the cure temperatures; for example, shrinkage of the potting material after curing. A further explanation could be an unnoticed change in the measuring technique or equipment.

Temperature runs of materials with potted Fe-Ni cores showed some change in inductance, so a simple test jig was made to apply non-isotropic stresses to the remaining unpotted inductors. This was done by hanging the inductor on a support, and adding weights to a weight pan to apply a force across it. Knowing the cross-sectional area of the core, the psi value vs inductance can be determined and plotted. Figure 13 shows a sketch of the method.

Reduction of data and comparison of the results of the ferrite cores to the others and to the thermometer method showed unbelievably high pressure values, in some cases 30 K psi and higher. A careful investigation and analysis results in one possible explanation, that the pressure pot method is not an adequate means of pressure calibration of pressure sensitive cores, because of the isotropy of the applied hydraulic stresses. In support of this hypothesis some of the unpotted ferrite cores were stressed on the test jig used on the Fe-Ni inductors described above, with interesting results.

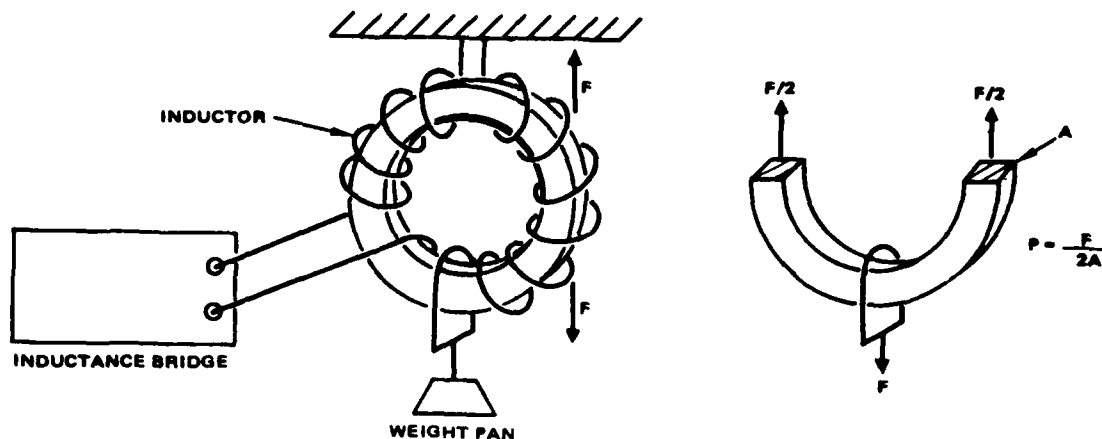


Figure 13. Core tensile stress measurement.

Ferrite core S/N 6, 4 mm x 8 mm x 2 mm, wound with 1 layer of AWG 32 wire had a nominal inductance of 5.45 mH. Applying a force, F , of 850 gms max (1.87 lb) reduced the inductance to 4.72 for a percentage change of

$$\frac{4.72 - 5.45}{5.45} \times 100 = -13.4\%.$$

Taking into account the cross-sectional area over which this force acts, the result is a stress of 151 psi.

Referring to the data for S/N 6 in the pressure pot, there was a -57.8 percent change in inductance at 10 K psi. Assuming a linear relationship then the pressure pot stress to obtain the same percentage change as the tensile stress is

$$\frac{10 \times 13.4\%}{57.8\%} = 2.3 \text{ K psi.}$$

for a ratio of $2.3/0.15 = 15.3$. In other words, an unbalanced tensile stress has a 15.3 times greater effect on the inductance change than the compressive isotropic stress.*

To see what effect occurred with the MPP cores, S/N 8 was exposed to a 900 gm force with absolutely no change in inductance. Since these cores showed an increase in inductance with pressure, this was just opposite to the ferrites. At first this was surprising, but investigation of the method of fabrication of the MPP cores showed that this was reasonable. Great care is taken to select magnetic Permalloy powders with a spectrum of Curie temperatures so that a flat or zero permeability change with temperature is achieved. Since pure Permalloy has a rising temperature coefficient, various powders with different Curie points are employed for core materials. As the temperature is raised, the Curie points of certain mixes are exceeded which results in them becoming non-magnetic, increasing the effective air gaps between the still magnetic particles which offsets their rising permeability values. Hydrostatically stressing an MPP core compresses these air gaps slightly, resulting in a rising inductance curve which was observed. On the other hand, a tensile stress across the core would lengthen some gaps and compress others, resulting in a net zero effect.

A typical inductance vs temperature curve is shown in Figure 14. The curve is for number 51 ferrite core potted and unpotted in Conap EN9 OZR. Taking the difference in inductance, converting it to psi stress from the pressure pot calibration and dividing it by the factor obtained from the tensile test method, the ferrite curve in Figure 15 is obtained. The potted MPP and Fe-Ni temperature vs stress curves are also shown, together with the thermometer for comparison. As can be seen, the ferrite

*At this point in time, an old report (Reference 6) was found in the literature, in which the experimenters reported similarly high stress values using a ferrite core in a specially designed micro pressure transducer, which was calibrated hydrostatically. Having no means of checking such as the thermometer method, they accepted their results at face value.

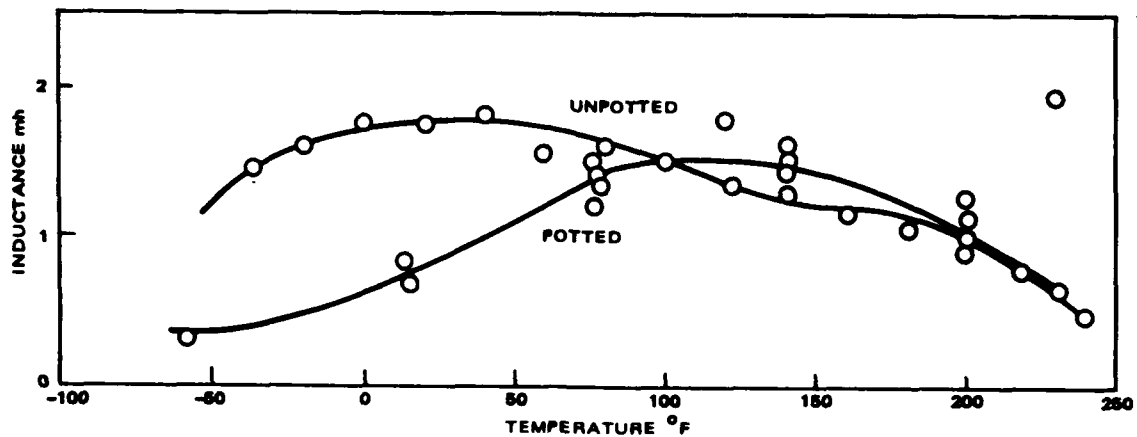


Figure 14. Inductance vs temperature for No. 51 ferrite core, unpotted and potted in Conap EN-90ZR.

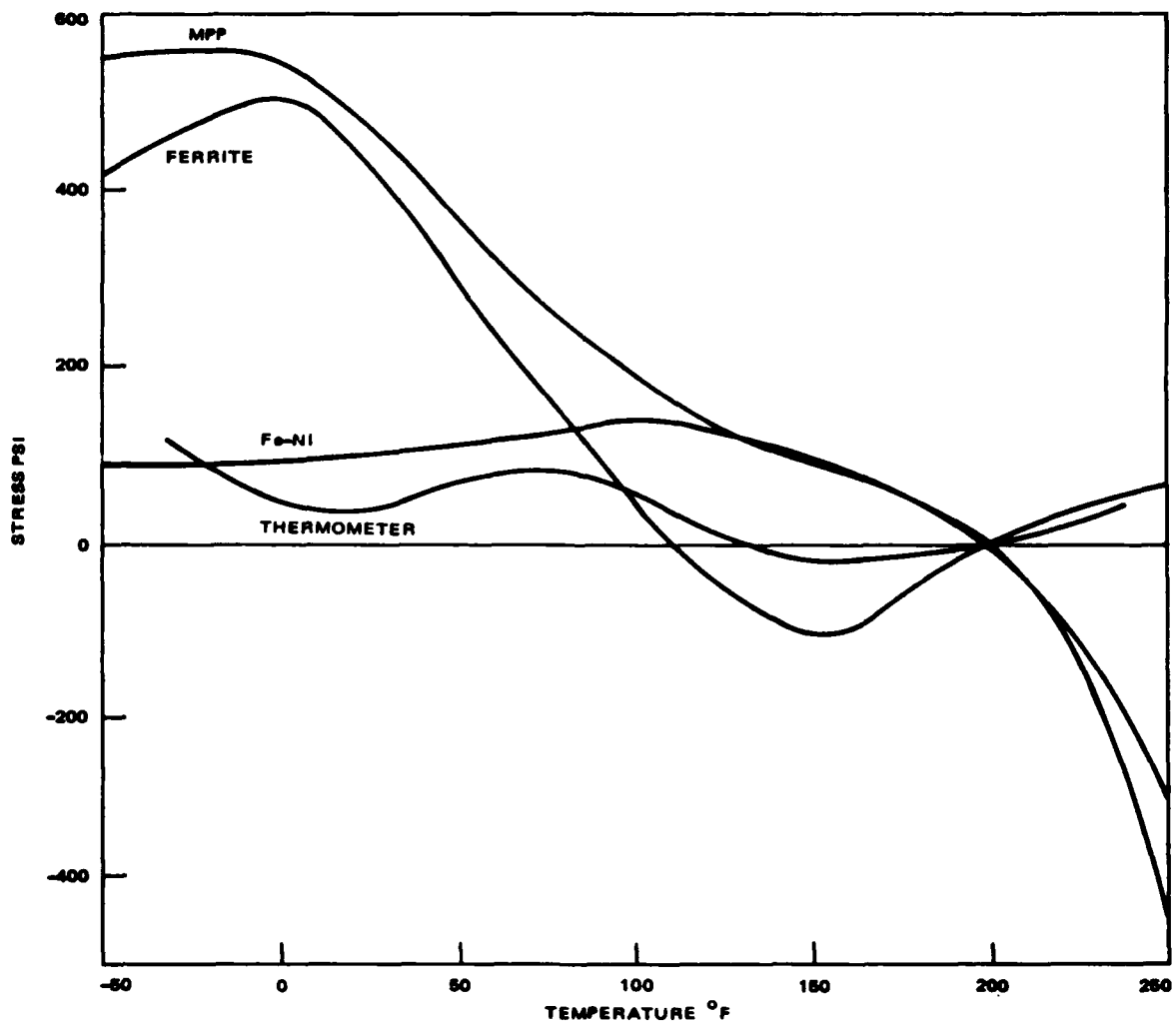


Figure 15. Conap EN-90ZR, stress vs temperature, four sensors.

and Fe-Ni curves show some similarity to the thermometer curve, even to the extent of possibly anticipating a rise in stress due to a possible glass transition point indicated by the thermometer. There is no obvious reason for the MPP curve to take off as it does, and similar curves occur with the other tests.

Table V gives the maximum stress for the toroidal inductors test for each embedding system according to each core type. The results shown in Table V when compared to those in Table II show that the inductor method is not a simple manner in which to measure the stresses on the coils by the potting material. The major problem with the toroidal core method is that there is no suitable calibration technique.

TABLE V. MAXIMUM STRESS FOR SUBJECT MATERIALS AS MEASURED BY TOROIDAL INDUCTORS

Material	Maximum Stress PSI			Temperature °F of Maximum		
	Ferrite*	MPP*	Fe-Ni	Ferrite	MPP	Fe-Ni
Scotchcast 255/RTV619	1000	--	180	0	--	0-100
Scotchcast 255/RTV627	480	--	100	0	--	-50
Scotchcast 255/ Epolene C/AC617	550	--	100	-50	--	-50
Scotchcast 255	1600	--	100	-50	--	-50
Conap EN-90ZR	500	550	100	20	0	-50
Conap EN-9	500	1650	300	0	-50	50
RTV615	--	650	112	--	100	50
RTV619	--	4500	150	--	50	50
RTV627	--	1900	180	--	100	100
RTV655	--	250	217	--	50	-50
Uralane 5753	--	2500	80	--	0	0
*Results have been corrected using 15.3 conversion factor.						

Relative Material Costs

Comparative cost of the various materials have been obtained as of May 1980. Table VI shows unit package cost estimated material and cost for a gallon of mixture.

TABLE VI. MATERIALS COST

	9-1/2 lb	10 lb	12 lb	18 lb	20 lb	22 lb	Cost per Gallon (Est)
EN-9	\$40.15						\$ 40.15
EN-9-OZR	\$42.50						\$ 42.50
EN-11			\$50.55				\$ 33.70
RTV-615		\$137.30					\$109.84
RTV-619		No Longer Made					
RTV-627						\$128.48	\$ 64.24
RTV-655		\$223.30					\$178.64
SC-9					\$117.60		\$ 58.80
SC-255				\$72.72			\$ 40.40
Hartel 17024GA				\$103.60			\$ 51.80

CONCLUSIONS

In order to obtain higher reliability devices using pressure sensitive ferrite, powdered iron and to a lesser extent iron-nickle and iron-silicon cores a lower stress potting system was needed. From forty materials reviewed in Bunker, Arnett and Williams (Ref 2) ten materials were selected. In order to obtain quantitative stress data two methods were utilized: pressure calibrated thermometers and pressure sensitive toroidal core inductors. These parts were calibrated using a hydraulic pressure pot.

1. The thermometer system gave good experimental determinations of the glass transition temperatures for the materials studied. The materials whose glass transition temperatures are below -40°F (-40°C) showed (≤ 200 psi) worst case stresses.
2. The calibrated inductors gave a direct value for the minimum stress which measurably changes the inductance of the coil.
3. The coil results also showed that hydraulic pressure calibration was not a good technique to calibrate the inductors; the coils are much more sensitive to tensile or compressive, non-isostatic stresses.
4. Using the 200 psi threshold stress for changes in inductance of the cores used, Conap EN-9, Conap EN-9-OZR, Uralane 5753, G.E. RTV 615, G.E. RTV 619, G.E. RTV-627, and G.E. RTV-655 all are recommended for potting pressure sensitive core magnetic devices over the temperature range -40°C to 105°C .

ACKNOWLEDGMENT

This work was supported in part by U.S. Army Missile Command under Contract DAAK 40-78-C0271.

REFERENCES

1. American Society for Testing and Materials Test Method F135-76, Vol. 43, pp. 552 to 558, 1977 edition.
2. E. R. Bunker, J. R. Arnett, J. L. Williams, "Manufacturing Methods and Technology for Electromagnetic Components", interim Report, Number FR79-76-1166R, Oct. 1979, U.S. Army Missile Command, Redstone Arsenal, AL. 35809.
3. Dewey, G.H., and Outwater, I.O., "Pressure on Objects Embedded in Rigid Cross-linked Polymers," Modern Plastics, Feb. 1960.
4. Isleitson, R.E., and Swanson, F.D., "Embedment Stresses - An Inexpensive and Direct Test Method," paper presented at Fifth Electrical Insulation Conference, Sept. 1963.
5. Bunker, E.R., Kloezeman, W.G., "Embedment Pressures of Various Encapsulation Compounds as a Function of Temperature, Using a Pressure-Calibrated Mercurial Thermometers," Internal report 900-499, 1971, Jet Propulsion Laboratory, Pasadena, CA.
6. Stucki, F.F., Fuller, W.D., and Carpenter, R.D., "Measurement of Internal Stresses in Encapsulated Electronic Modules", Lockheed Missiles & Space Company, Palo Alto, California.

APPENDIX 6.3

REPORT NO. TP-80-76-542

HIGH RELIABILITY POTTING MATERIALS FOR USE
IN MISSILE SYSTEMS

by

James R. Arnett

Presented at:

Coil Winding Chicago '80
Chicago, Illinois
September 29, 1980

Technology Support Division
Electro-Optical and Data Systems Group
AEROSPACE GROUPS
Hughes Aircraft Company • Culver City, California

SUMMARY

The high reliability transformer design engineer is faced with a vast variety of available embedding resin systems. To make an intelligent choice among the large number of coil embedding and impregnating materials available, a systematic review of material properties is needed. A suggested list of selection parameters is described, and in some cases desired values given. A weighting scheme was chosen for materials to be used in high reliability transformers. The resin systems reviewed in this paper are ranked to the manufacturer's data by this scheme. Obviously, the comparison of the materials is aided if the physical, electrical, processing, and environmental parameters are available in the vendor's literature.

The five materials ranked highest by the weighting scheme were therefore tested using common test conditions. Two low-cost solventless polyester varnishes were added to the original five for comparison. In addition, Scotchcast 255 was substituted for Scotchcast 280 in the original list because vendor data was uncovered showing that 280 was hydrolytically unstable. Subsequent hydrolytic stability tests performed on the remaining materials also showed that two other materials were also unstable.

A quantity of saturable reactors of a typical design were obtained to evaluate the capabilities of the selected embedding materials. A variety of tests were performed on the devices to ascertain which materials performed best. Those potted with Scotchcast 255 and Epon 825/HV were found to be superior to the others tested. As the reactors were not high voltage units, ten high voltage traveling wave tube transformers were also fabricated and electrically tested. These tests showed that Hysol C15-015 and C-60 embedded parts had consistently lower interwinding partial voltage breakdown (corona) values than did the Eccoseal 1218, Scotchcast 255, and Epon 825/HV parts. These last three parts were corona tested at a 50 percent higher voltage level. At this high voltage, the Scotchcast 255 and the Eccoseal 1218 parts had high corona breakdown, while the Epon 825/HV had none. The conclusion is that, of all the materials reviewed, Epon 825/HV is the best material for high reliability, high voltage applications, and Scotchcast 255 is the best material for high reliability, low-to-medium voltage applications.

VENDOR DATA SURVEY

Each vendor contacted sent data on his entire product line of encapsulation materials. From all of these products a sampling of the forty most applicable materials were included in a table of relevant materials and process parameters. These parameters provide a model for comparison of the materials. Table I gives the parameters and in some cases their desired values. It should be noted that many of the parameters have no numerical value but qualitative ratings instead. In other cases a preferred value and a limiting value are given. In still other cases a definite figure is stated. These situations allow latitude for informed engineering judgment.

The assumption made, where a definite figure is stated, is that high voltage or other extreme operational environment is involved. A more benign environment would allow some latitude in these cases also. Certain of the parameters are starred (*); these are important parameters which had sufficient manufacturer's data to be used in the actual selection process. A brief explanation of the parameters follows:

Mix ratio and mix ratio sensitivity. The mix ratio is usually given in the data sheets as a weight ratio of resin to hardener. In most automatic proportioning units, the volume of resin to hardener is needed. This ratio is not on the manufacturer's data sheet, but it can be calculated from resin density at pour temperatures. The mix ratio sensitivity is the precision of component measurement required to obtain quality cured parts.

Pot life. For most applications the pot life (time at resin working temperature needed to double the viscosity) needs to be as long as possible. The longer pot life allows greater care to be taken in the steps after mixing such as degassing and pouring. In the automatic mixing processes, the longer the pot life of the mixed resin the less often the system must be flushed of mixed resin.

TABLE I. MODEL PARAMETERS

Parameter	Value
1. Mix Ratio*	prefer 3:1 maximum 5:1
2. Mix Ratio Sensitivity	proper cure at mix ratios
3. Pot life*	20 minutes minimum
4. Cure cycle	short
5. Viscosity*	1000 maximum at pouring temperature
6. Specific gravity	preference depends on end use
7. Moisture sensitivity	low
8. Ease of Cleanup	uncured resin readily soluble
9. Exotherm of reaction	low as possible
10. Shrinkage*	≤1%
11. Byproduct hazards	few of low severity
12. Dielectric Strength*	≥400 Volts/mil
13. Dielectric Constant*	prefer <4 maximum <6
14. Dissipation Factor*	prefer <0.05 maximum <0.1
15. Volume Resistivity*	<10 ¹² Ω-cm
16. Cured form	semirigid to semiflexible
17. Service temperature range*	-55°C to 125°C or wider
18. Hardness*	80 shore D maximum
19. Mechanical Shock Resistance	>400G
20. Tear resistance	≥15 lb/in
21. Adhesive strength	20 lb/in. width
22. Mechanical Vibration Resistance	≥160G
23. Thermal Shock Resistance	pass 10 cycle -55°C to 130°C
24. Outgassing Resistance	<1% total wt. loss, <.1% Vol. Condens. Mat.
25. Thermal Conductivity*	>3.4 x 10 ⁻⁴ $\frac{\text{gcal}}{\text{sec}} \text{ cm}^2/\text{°C}$
26. Heat Capacity	high
27. Flame Resistance	UL94 V0 or V1 or equivalent
28. Soldering heat resistance	no delamination due to soldering heat
29. Moisture Absorption*	<0.2%/1 day
30. Hydrolytic Stability	<10% hardness decrease at end of test
31. Chemical Solvent Resistance	Cured material must be stable to common cleaning solvents
32. Chemically inert to coil materials	inert
33. Fungus Resistance	non-nutritive
34. Repair Ease	Easy to repair
35. Automatic Mixing	
36. Thermal Expansion (cured)*	≈17.0 x 10 ⁻⁶ /°C maximum 100 x 10 ⁻⁶

Cure cycle. This parameter is a function of curing temperature, the material and the cure time. The cure temperature is dependent on the wire and coil form materials.

Viscosity. The material viscosity at room temperature is most often given in the literature. The viscosity of the mixture at the pouring temperature is more significant.

Specific gravity. The specific gravity of the resins is necessary to convert the mix ratios from parts by weight to parts by volume for use by most automatic equipment.

Moisture sensitivity. This condition is related to tendency of some resins, especially urethanes, not to cure after storage in a humid atmosphere.

Ease of cleanup. This is a subjective parameter related to how readily the uncured mixed resins can be removed using a solvent/air mixture. This is especially important when automatic mixing machinery is used.

Exotherm of reaction. This is the heat released when two chemicals react. The amount of chemicals mixed, the temperature at which the reaction takes place (rate of reaction) and the materials reacting all affect the temperature rise.

Shrinkage. This parameter is related to the structural processes undergone during resin cure. The shrinkage causes one component of the stress generated by the cured plastic on the embedded part. The thermal expansion mismatch between the part and the cured resin causes the other component of embedment stress.

Byproduct hazards. This parameter is to warn the process engineer about safety or environmental hazards associated with the material.

Dielectric strength. This parameter is especially important in high voltage applications. The values are generally measured per ASTM D-149 using a one-tenth inch thick, two inch diameter, disc-shaped sample.

Dielectric constant and dissipation factor. These electrical parameters are related to the atomic and molecular interactions in the dielectric material. Their actual values may vary extensively with frequency and temperature. ASTM D-150 is the standard test method. Care should be taken by the user that these parameters are measured at the operating point.

Volume resistivity. This parameter indicates how much conduction occurs by way of the insulator material. The higher the value, the greater the isolation that exists between otherwise nonconnected conductors. ASTM D-257 is the standard test method.

Cured form. The cured form is determined by the type of resin, the cure cycle and the temperature when the measurement is made.

Service temperature range. This very useful parameter tells the user over what temperatures the cured resin will perform as indicated in the manufacturer's brochure.

Hardness. The hardness indicates that the resin is properly cured.

Mechanical shock resistance. The cured resin should protect the embedded parts from mechanical shock, rather than itself cracking, so that the part can fulfill its intended use.

Tear resistance. This value relates to the cohesive strength of the plastic (how well the material maintains integrity).

Adhesive strength. This parameter measures how well the plastic bonds to other materials.

Mechanical vibration resistance. This relates to the ability of the plastic to protect embedded parts from the effects of mechanical vibration.

Thermal shock resistance. This is the ability of the embedment material to relieve thermal stresses efficiently.

Outgassing resistance. The evaporation of materials and release of gas from the cured resin in a vacuum and high temperature environment is outgassing. The recondensable materials part of the outgassing products are especially important for space applications when optical surfaces are nearby.

Thermal conductivity. This parameter measures how well the cured resin carries heat away from the encapsulated heat source.

Heat capacity. This parameter measures how much heat is necessary to increase the temperature of the material.

Flame resistance. This parameter measures how well the resin extinguishes or impedes the spread of fire.

Soldering heat resistance. The material should not be affected by heat during the soldering operation on a lead wire one-fourth inch (6 mm) away from it.

Moisture absorption. The embedment material should not absorb moisture so that the embedded parts can be protected from corrosion.

Hydrolytic stability. The cured resin should not revert to its previous liquid state due to the presence of heat and humidity so that the parts can have a stable protective environment.

Chemical solvent resistance. The cured resin should not be adversely affected by the solvents used in cleaning and preparation for repair of boards and modules.

Chemically inert to coil materials. The embedment material should not harm nor act as a catalyst for another agent to chemically harm the embedded parts.

Fungus resistance. The cured material should not act as a nutrient for fungus.

Repair ease. The cured resin should be able to be cut open, the part replaced, and new resin poured into the hole without loss of cohesive strength.

Automatic mixing. The resin should be capable of metering, degassing, pouring and curing with automatic equipment.

Thermal expansion in the cured state. The cured resin should expand at nearly the same rate as do the coil materials to minimize thermal expansion mismatch stress.

Table II gives the manufacturer's data for the various material and process parameters. In many cases no data (ND) was given. In many other cases the data was given using differing test methods or conditions. An example of differing test conditions is the dielectric constant and dissipation factor measurements. The frequency used varied from 60 Hz to 1.0 GHz. In many materials the dielectric constant varies significantly over this range of frequencies. Since this wide variation occurs, it is recommended that further testing by the user at the operating frequency be made. The manufacturers of the embedding systems in Table II are found in appendix A.

INITIAL SELECTION OF MATERIALS

The assessment of the relative merit of the various materials was done using the thirteen starred parameters in Table I. These parameters were chosen for two reasons: (1) there was data on these parameters for most of the resin systems; and (2) these parameters seemed to span the types of parameters included in the full list. The true usefulness of the model is that the use of a weighting system allows widely differing end use requirements to be satisfied using the same model by using different weighting schemes. Each starred parameter was given equal weight in the present selection process.

It must be emphasized that comparisons among the material systems apply only to the specific end use. This paper is in no way intended to recommend or defame for all uses any of the products mentioned. Indeed, one of the best lessons taught by this rating scheme is that a material which does not rate as well for one use may indeed be the better material for another use.

Five materials were chosen initially for evaluation of their specific gravity, hardness, thermal conductivity, degradation temperature, glass transition temperature, coefficient of thermal expansion, moisture absorption, shrinkage, dielectric constant, dissipation factor and volume resistivity. Subsequent data from the literature showed that Scotchcast 280 was hydrolytically unstable; consequently, Scotchcast 255 was added to the final list because it ranked very well on the model. At the same time, General Electric 702 and 707, two solventless polyester varnishes, were added to the list because of their low material cost.

ELECTRICAL AND PHYSICAL PARAMETER TESTING

The tests were designed to achieve two goals: (1) test all the materials under the same conditions; and (2) obtain data that was not available from the manufacturers. The materials were cured according to the manufacturer's instruction. The test results are shown in Table III, and comments concerning the test results follow:

1. The specific gravities of all test materials, with the exception of Scotchcast 255 (1.51), ranged from 1.06 to 1.17, and were acceptably close to the manufacturer's values.

TABLE II. MATERIAL EVALUATION OF PROSPECTIVE POTTING
COMPOUNDS BASED ON VENDOR SUPPLIED DATA

Parameter	RTV111/DBT	RTV60/DBT	RTV8111	RTV619	RTV615	RTV655	RTV670	RTV627	Epocast 202	Scotchcast 255
Mix Ratio	500:1	500:1	10:1	10:1	10:1	10:1	10:1	1:1	100:15	2:3
Mix Ratio Sensitivity	High	High	Medium	Medium	Medium	Medium	Medium	Low	Medium	Low
Pot Life	2-4h @ 25°C	2-4h @ 25°C	1.5h @ 35°C	4h @ 25°C	4h @ 25°C	4h @ 25°C	5h @ 25°C	2h @ 25°C	16-20h @ 25°C	4h @ RT
Suggested Cure Time	24-36h @ 25°C	24-36h @ 25°C	12-24h @ 25°C	1h @ 100°C	1h @ 100°C	1h @ 100°C	1h @ 125°C	1h @ 100°C	16h @ 60°C	2h @ 120°C
Viscosity cps Room Temp.	12,000	50,000	12,000	500	3500	4800	5000	1600	4000	23,000
Specific Gravity	1.18	1.47	1.18	0.97	1.02	1.02	1.06	1.39	1.18	1.56
Moisture Sensitivity	ND	ND	ND	ND	ND	ND	ND	ND	Shortens Shelf Life	ND
Ease of Cleanup	MEK, TCE	MEK, TCE	MEK, TCE	MEK, TCE	MEK, TCE	MEK, TCE	MEK, TCE	MEK, TCE	ND	ND
Exotherm of Reaction	0	0	0	0	0	0	0	0	ND	ND
Shrinkage %	0.2 - 0.6	0.2 - 0.6	0.2 - 0.6	0.2 - 0.6	0.2 - 0.6	0.2 - 0.6	0.2 - 0.6	0.2 - 0.6	1.11	ND
Hazards										
Diel. Strength V/mil	500	500	500	500	500	500	500	500	350	375
Diel. Constant	3.6 @ 100 Hz	3.6 @ 100 Hz	3.6 @ 100 Hz	3.0 @ 100 Hz	3.0 @ 100 Hz	3.0 @ 100 Hz	2.8 @ 100 Hz	3.4 @ 100 Hz	4.8 @ 60 Hz	5.9 @ 100 Hz
Diag. Factor	0.019 @ 100 Hz	0.020 @ 100 Hz	0.019 @ 100 Hz	0.001 @ 100 Hz	0.001 @ 100 Hz	0.001 @ 100 Hz	0.001 @ 100 Hz	0.001 @ 100 Hz	0.036 @ 60 Hz	0.05 @ 100 Hz
Volume Resistivity ohm-cm	6×10^{14}	1.3×10^{14}	6×10^{14}	1×10^{15}	1×10^{15}	1×10^{15}	4×10^{15}	1×10^{15}	4.8×10^{14}	1×10^{15}
Cured Form	Rubbery	Rubbery	Rubbery	Gel Like	Rubbery	Rubbery	Rubbery	Rubbery	Semirigid	Semiflex
Service Temp. Range	-60 to 204°C	-60 to 204°C	-60 to 204°C	-60 to 204°C	-60 to 204°C	-115 to 204°C	-60 to 204°C	-60 to 204°C	ND	-55 to 130°C
Hardness, Shore	45(A)	60(A)	45(A)	Penetrates 5 MM	45(A)	45(A)	70(A)	45(A)	85(D)	72(D)

(Continued next page)

(Table II, continued)

Parameter	RTV11/DBT	RTV60/DBT	RTV8111	RTV619	RTV615	RTV614	RTV670	RTV627	Epocast 202	Scotchcast 255
Mech. Shock	ND	ND	ND	ND	ND	ND	ND	ND	ND	7.75 lb
Tear Resist kg/cm	3	7	3	ND	4	4	6	4	ND	ND
Adhesive Strength	Low	Low	Low	Low	Low	Low	Low	Low	ND	High
Mech. Vibration	ND	ND	ND	ND	ND	ND	ND	ND	ND	ND
Thermal Shock	ND	ND	ND	ND	ND	ND	ND	ND	ND	Pass 10 cycles -55 to 130°C
Thermal Conductivity $\times 10^{-4}$ cal/sec cm ² °C	7×10^{-4}	7.4×10^{-4}	7×10^{-4}	4.5×10^{-4}	4.5×10^{-4}	4.5×10^{-4}	4.5×10^{-4}	4.5×10^{-4}	4×10^{-4}	4×10^{-4}
Heat Cap.	ND	ND	ND	ND	ND	ND	ND	ND	ND	ND
Flame Resist	No	No	No	No	No	No	No	Yes	ND	Pass UL-94 (V-0)
Soldering Heat	ND	ND	ND	ND	ND	ND	ND	ND	ND	ND
Moisture Abs.	ND	ND	ND	ND	ND	ND	ND	ND	0.4"/1 day	0.45%/10 day
Hydrolytic Stability	Yes	Yes	Yes	Yes	Yes	Yes	Yes	Yes	ND	Yes
Chemical Solvent	ND	ND	ND	ND	ND	ND	ND	ND	ND	ND
Chem. Inert. to Coil Mat.	ND	ND	ND	ND	ND	ND	ND	ND	ND	ND
Fungus Resist	ND	ND	ND	ND	ND	ND	ND	ND	ND	ND
Repair Ease	ND	ND	ND	ND	ND	ND	ND	ND	ND	ND
Automatic Production	No	No	Yes	Yes	Yes	Yes	Yes	Yes	Yes	Yes
Thermal Exp. cm/cm °C	260×10^{-6}	110×10^{-6}	250×10^{-6}	330×10^{-6}	270×10^{-6}	270×10^{-6}	270×10^{-6}	220×10^{-6}	ND	ND

(Continued next page)

(Table II, continued)

Parameters	Scotchcast 235	Scotchcast 280	Scotchcast 281	Scotchcast 5237	Ecoseal 63	Stycaast 62	Epon 825/(HV)	Ecoseal W-67	Ecoseal 1207	Flooseal 1218
Mix Ratio	1:2	2:3	2:3	3:4	100:1	100:1	100:18	100:85	100:2	100:70
Mix Ratio Sensitivity	Low	Low	Low	Low	High	High	Mod.	Low	High	Low
Pot Life	18 Min @ 120°C	20 min @ 120°C	21 min @ 120°C	15 min @ 60°C	7 day @ 25°C	7 day @ 25°C	25 min @ 67°C	1 month @ 25°C	8h @ 50°C	3h @ 50°C
Sugg. Cure Time	2h @ 120°C	2h @ 120°C	2h @ 120°C	1h @ 95°C	18h @ 85°C	18h @ 85°C	4h @ 125°C	4h @ 125°C + 16h @ 175°C	4h @ 71°C + 1h @ 177°C	12h @ 125°C
Viscosity cps	250 @ 76°C	350 @ 76°C	48,000 @ 23°C	20,000 @ 23°C	ND	ND	4,000 @ 23°C	250 @ 25°C	150 @ 50°C	500 @ 50°C
Specific Gravity	1.1	1.08	1.43	1.35	0.95	1.05	1.15	ND	ND	1.2
Moisture Sensitivity	ND	ND	ND	ND	ND	ND	ND	High	ND	ND
Ease of Cleanup	ND	ND	ND	ND	ND	ND	ND	ND	ND	ND
Exotherm of Reaction	ND	ND	ND	ND	ND	ND	ND	ND	ND	ND
Shrinkage %	ND	ND	ND	ND	ND	ND	ND	ND	ND	ND
Hazards	ND	ND	ND	ND	ND	ND	ND	ND	ND	ND
Diel. Strength V/mil	325	375	375	370	500	500	400-500	450	450	ND
Diel. Constant	4.25 @ 100 Hz	4.07 @ 100 Hz	4.03 @ 100 Hz	5.0 @ 100 Hz	2.4 @ 100 Hz	2.6 @ 100 Hz	3.81 @ 1 KHz	3.3 @ 1 KHz	3.5 @ 1 GHz	3.7 @ 60 Hz
Diag. Factor	0.07 @ 100 Hz	0.008 @ 100 Hz	0.032 @ 100 Hz	0.08 @ 100 Hz	0.005 @ 100 Hz	0.0015 @ 100 Hz	0.004 @ 1 KHz	0.006 @ 1 KHz	0.015 @ 1 GHz	0.025 @ 60 Hz
Volume Resistivity ohm/cm	2.9×10^{14}	10^{15}	10^{15}	10^{15}	10^{16}	10^{16}	3×10^{12}	10^{15}	10^{16}	10^{15}
Cured Form	Semiflex	Semiflex	Semiflex	Semiflex	Semiflex	Semiflex	Semiflex	Semiflex	Semiflex	Semiflex
Service Temp. Range °C	-55 to 125	-55 to 155	-55 to 155	-55 to 125	-55 to 190	-55 to 150	-55 to 125	up to 230	up to 177	-100 to 175
Hardness, Shore	55(D)	65(D)	65(D)	80(D)	ND	ND	80(D)	ND	ND	40(D)

(Continued next page)

(Table II, continued)

Parameters	Scotchcast 235	Scotchcast 280	Scotchcast 281	Scotchcast 5237	Eccoseal 63	Stycast 62	Epon 825/HV	Eccoseal W-67	Eccoseal 1207	Eccoseal 1218
Mech. Shock	7.75 lb ball	7.75 lb ball	7.75 lb ball	5 lb ball	ND	ND	ND	ND	ND	ND
Tear Resist.	ND	ND	ND	ND	ND	ND	ND	ND	ND	ND
Adhesive Strength	ND	ND	ND	ND	ND	ND	ND	ND	ND	ND
Mech. Vibration	ND	ND	ND	ND	ND	ND	ND	ND	ND	ND
Thermal Shock	pass 10 cycle -55 to 130°C	fail, 10 cycle -55 to 130°C	pass, 10 cycle -55 to 130°C	pass, 10 cycle -55 to 130°C	ND	ND	pass, 10 cycle -55 to 130°C	ND	ND	ND
Thermal Conductivity ft. cal. sec cm ² °C	4×10^{-4}	5.3×10^{-4}	12×10^{-4}	ND	ND	ND	ND	ND	ND	5×10^{-4}
Heat Cap.	ND	ND	ND	ND	ND	ND	ND	ND	ND	ND
Flame Resist.	Fails UL-94	ND	ND	Phases UL94-V1	ND	ND	ND	ND	ND	ND
Soldering Heat	ND	ND	ND	ND	ND	ND	ND	ND	ND	ND
Moisture Abs.	0.92%/240h	0.52%/240h	0.32%/240h	0.78%/240h	ND	ND	ND	0.2%/24h	0.2%/24h	0.2%/240h
Hydrolytic Stability	ND	No	No	Yes	ND	ND	Yes	ND	ND	ND
Chem. Solvent	ND	ND	ND	ND	ND	ND	ND	ND	ND	ND
Chem. Inert to Coil Mat.	ND	ND	ND	ND	ND	ND	ND	ND	ND	ND
Fungus Resistant	ND	ND	ND	ND	ND	ND	ND	ND	ND	ND
Repair Ease	ND	ND	ND	ND	ND	ND	ND	ND	ND	ND
Automatic Production	Yes	Yes	Yes	Yes	Yes	Yes	No	Yes	Yes	Yes
Thermal Expansion cm/cm °C	ND	ND	ND	ND	ND	ND	51×10^{-6}	ND	ND	ND

(Continued next page)

(Table II, continued)

Parameters	GE707	GE702	Hysol CI5-015	Hysol C-60	Hysol HD3561	Epocast E204A/9816	Epocast E204A/9652	Uralane 5753	Conathane EN-2	Conathane EN-90ZR
Mix Ratio	100:1	100:1	2:3	2:3	100:30	100:15	100:50	100:20	100:90	100:17.5
Mix Ratio Sensitivity	High	High	Low	Low	Mod	Mod-High	Low	Mod-High	Low	Mod-High
Pot Life	25 min @ 118°C	25 min @ 118°C	90 min @ 90°C	3-9h @ 75°C	35 min @ 25°C	2h @ 65°C	3.5h @ 25°C	35 min @ RT	20 min @ 25°C	30 min @ 25°C
Sugg. Cure Time	1-4h @ 165°C	6-10h @ 180°C	6h @ 125°C	16-24h @ 125°C	3h @ 60°C	2h @ 65°C	3h @ 65°C	8h @ 95°C	4h @ 60°C	24h @ 60°C
Viscosity, cps	1000 @ RT	1000 @ RT	200 @ 90°C	300 @ 75°C	600 @ 25°C	2600 @ 25°C	6000 @ 25°C	ND	ND	ND
Specific Gravity	1.1	1.1	1.15	1.15	1.15	1.1	1.1	ND	1.0	1.0
Moisture Sensitivity	ND	ND	ND	ND	ND	Mod.	Mod.	Mod.	High	High
Ease of Cleanup	ND	ND	ND	ND	ND	ND	ND	ND	Conap S-8	Xylene, MEK TOL
Exotherm of Reaction	ND	ND	90°C/200g	0.0	190°C/200g	ND	ND	ND	0.0	55°C/227g
Shrinkage %	ND	ND	2.8	2.8	0.6	ND	ND	3	0.31	1.0
Hazards	ND	ND	SPICL2	SPICL2	SPICL5	ND	ND	ND	MOCA base	ND
Diel. Strength V/mil	500	500	350	350	ND	395	395	350	645	610
Diel. Constant	1.97 @ 60 Hz	5.4 @ 60 Hz	3.8 @ 100 Hz	4.0 @ 100 Hz	4.96 @ 100 Hz	4.2 @ 100 Hz	4.0 @ 100 Hz	3.6 @ 1 KHz	5.7 @ 100 Hz	3.3 @ 100 Hz
Disa. Factor	0.004 @ 60 Hz	0.03 @ 60 Hz	0.03 @ 100 Hz	0.038 @ 100 Hz	0.007 @ 100 Hz	0.012 @ 100 Hz	0.020 @ 100 Hz	0.021 @ 1 KHz	0.123 @ 100 Hz	0.031 @ 100 Hz
Volume Resistivity ohm-cm	10 ¹¹	10 ⁶	3 x 10 ¹⁴	7 x 10 ¹⁴	4 x 10 ¹⁴	2.6 x 10 ¹⁴	1 x 10 ¹⁴	5 x 10 ¹⁵	3.1 x 10 ¹³	3.4 x 10 ¹⁵
Cured Form	Semirigid	Semiflex	Semiflex	Semiflex	Semiflex	Rigid	Semi-Rigid	Flex	Flex	Flex
Service Temp. Range °C	-55 to 180	-55 to 180	-55 to 125	-55 to 125	-40 to 125	ND	ND	-55 to 125	-65 to 130	-70 to 135
Hardness, Shore	ND	ND	60(D)	60(D)	75(D)	88(D)	75(D)	55-65(A)	69(A)	85(A)

(Continued next page)

(Table II, continued)

Parameters	GE707	GE702	Hysol CT-01	Hysol C-60	Hysol HD350-1	Epo-cast 204A/9M10	Epo-cast 204A/9552	Uralac 5753	Conathane EN-2	Conathane EN-90ZR
Mech. Shock	ND	ND	ND	ND	ND	ND	ND	ND	ND	ND
Tear Resist	ND	ND	ND	ND	ND	ND	ND	110 lb/in	275-310 psi	20 lb/in
Adhesive Strength	ND	ND	ND	ND	20 lb/in	ND	ND	30 lb/in	ND	ND
Mech. Vibration	ND	ND	ND	ND	ND	ND	ND	ND	ND	ND
Thermal Shock	ND	ND	ND	ND	ND	ND	ND	ND	ND	Pass 10 cycles -55 to 130°C
Thermal Conductivity g cal sec cm ² °C	ND	3.4×10^{-4}	4.5×10^{-4}	4.5×10^{-4}	ND	4.8×10^{-4}	4.4×10^{-4}	ND	3.5×10^{-4}	ND
Heat Cap.	ND	ND	ND	ND	ND	ND	ND	ND	ND	ND
Flame Resist.	ND	ND	ND	ND	ND	1.5 in/min	1.1 in/min	ND	ND	No ignition 55 ADC
Soldering Heat	ND	ND	ND	ND	ND	ND	ND	ND	ND	ND
Moisture Abs.	ND	ND	0.51%/7 day	0.84%/7 day	0.43%/1 day	0.16%/1 day	0.31%/1 day	3.0%/1 day	ND	0.5%/24 day
Hydrolytic Stability	ND	ND	ND	ND	ND	ND	ND	ND	ND	ND
Chem. Solvent	ND	ND	ND	ND	ND	ND	ND	ND	ND	ND
Chem. Inert to Coil Mat.	ND	ND	ND	ND	ND	ND	ND	ND	ND	ND
Fungus Resistant	ND	ND	ND	ND	ND	ND	ND	Non Nutrient	ND	Non Nutrient
Repair Ease	ND	ND	ND	ND	ND	ND	ND	ND	ND	ND
Automatic Production	No	No	Yes	Yes	Yes	No	Yes	Yes	Yes	Yes
Thermal Expansion cm/cm °C	ND	220×10^{-6}	190×10^{-6}	ND	54×10^{-6}	98×10^{-6}	140×10^{-6}	250×10^{-6}	ND	ND

(Table II, continued)

Parameters	Conathane EN-9	Conathane EN-10 (11)	Conepoxy Y1000/07	Conepoxy IM1145	Conepoxy RN1600	Epoxy/D400	Epoxy/T403	Epoxy/D230
Mix Ratio	100:17.5	100:37	100:75	1 Component	100:26	100:50	100:40	100:35
Mix Ratio Sensitivity	Med - High	Low	Low	-	Medium	Low	Low	Low - Med
Pot Life	30 min @ 25°C	30 min @ 25°C	105 min	16h @ 60°C	30 min	300 min	320 min	240 min
Sugg. Cure Time	8h @ 100°C	16h @ 80°C	2h @ 60°C	2.3h @ 120°C + 4h @ 155°C	3h @ 140°C	2h @ 90°C + 3h @ 125°C	2h @ 80°C + 3h @ 125°C	2h @ 80°C + 3h @ 125°C
Viscosity, cps	6800 @ 25°C	5500 @ 25°C	3500 @ 25°C	1400 @ 25°C 280 @ 60°C	120,000 @ RT 1600 @ 80°C	500 @ 25°C	1360 @ 25°C	400 @ 25°C
Specific Gravity	1.0	0.97	1.05	1.18	1.7	0.97	0.98	0.95
Moisture Sensitivity	High	High	Moderate	High	Moderate	ND	ND	ND
Ease of Cleanup	Tol, MEK Xylene	Tol, MEK Xylene	ND	ND	ND	Toluene	Toluene	Toluene
Exotherm of Reaction	55°C @ 0.5 lb	55°C @ 0.5 lb	ND	ND	ND	ND	125°C @ 1.0 lb 208°C @ 1.0 lb	208°C @ 1.0 lb
Shrinkage %	1.15	1.19	1.5	2.1	1.4	ND	ND	ND
Hazards	No	No	No	No	No	No	No	No
Diels. Strength V/ml	610	710	ND	ND	375	487	514	479
Diels. Constant	3.03 @ 100 Hz	3.1 @ 100 Hz	3.9 @ 100 Hz	3.8 @ 1 KHz	4.35 note 1	4.01 @ 1 KHz	4.14 @ 1 KHz	4.1 @ 1 KHz
Diss. Factor	0.031 @ 100 Hz	0.027 @ 100 Hz	0.009 @ 100 Hz	0.011 @ 1 KHz	0.020 note 1	0.009 @ 1 KHz	0.011 @ 1 KHz	0.011 @ 1 KHz
Volume Resistivity ohm-cm	3.42 x 10 ¹⁵	4.3 x 10 ¹⁵	3 x 10 ¹³	7.1 x 10 ¹²	2 x 10 ¹⁴	3.0 x 10 ¹⁶	1.7 x 10 ¹⁶	1.6 x 10 ¹⁶
Cured Form	Flexible	Flexible	Semiflex	Semiflex	Semiflex	Semiflex	Rigid	Semiflex
Service Temp. Range, °C	-70 to 135	-70 to 135	to 80	ND	-55 to 155	ND	ND	ND
Hardness, Shore	85(A)	75(A)	60(D)	80(D)	55(D)	80(D)	87(D)	79(D)

ND = No Data

Notes: 1. Test frequency not given.

(Continued next page)

(Table II, concluded)

Parameters	Conathane EN-9	Conathane EN-10 (11)	Conepoxy Y1000/07	Conepoxy IM1145	Conepoxy RN1000	Epoxy/D406	Epoxy/T403	Epoxy/D230
Mech. Shock	ND	ND	ND	ND	ND	ND	ND	ND
Tear Resist.	275-310 psi (Die C)	140-180 psi (Graves)	ND	ND	ND	ND	ND	ND
Adhesive Strength	20 lb/in.	ND	ND	ND	ND	4.7 lb/in.	4.7 lb/in.	5.6 lb/in.
Mech. Vibration	ND	ND	ND	ND	ND	ND	ND	ND
Thermal Shock	Passes 10 cycles -70°C to 135°C	Passes 10 cycles -70°C to 135°C	ND	ND	ND	5 of 10 passed 10 -20°C to 140°C	7 of 10 passed 10 -20°C to 140°C	Passes 10 -20°C to 140°C
Thermal Conductivity	ND	ND	ND	ND	6.5 x 10 ⁻⁴	ND	ND	ND
Heat Cap.	ND	ND	ND	ND	ND	ND	ND	ND
Flame Resist.	No ignition after 55 amp test	ND	ND	ND	Extinguished in 35 sec	ND	ND	ND
Soldering Heat	ND	ND	ND	ND	ND	ND	ND	ND
Moisture Absorption	0.57% - 24 days	ND	0.20% - 1 day	ND	0.17% - 1 day	ND	ND	ND
Hydrolytic Stability	Good	Good	ND	ND	ND	ND	ND	ND
Chemical Solvent	See Cleanup	See Cleanup	Insensitive to solvents	ND	ND	ND	ND	ND
Chem. Inert to Coll. Mils.	ND	ND	ND	ND	ND	ND	ND	ND
Fungus Resistant	Non-nutrient	Non-nutrient	ND	ND	ND	ND	ND	ND
Repair Ease	ND	ND	Not easy to repair	ND	ND	ND	ND	ND
Automatic Production	Difficult	Difficult	Difficult	Possible	Difficult	ND	ND	ND
Thermal Expansion cm/cm/°C	ND	ND	ND	ID	115 x 10 ⁻⁶	ND	ND	ND

TABLE III. ENCAPSULANTS EVALUATION

Test Material	Exposure (hrs.)	Electrical Strength (KV/1/2")	GF (%)	Hydrolysis (100%)	Hydrolysis (250°F)	Scotchcast 250	Scotchcast 280
1. Cure Time (Note 3)	17 hrs. at 120°C (250°F)	16 hrs. at 120°C (250°F)	4 hrs. at 163°C (325°F)	16 hrs. at 70°C (160°F) and 6 hrs. at 120°C (250°F)	17 hrs. at 120°C (250°F)	3 days at 70°C (160°F)	16 hrs. at 70°C (160°F) and 2 hrs. at 120°C (250°F)
2. Specific Gravity (Note 2)	1.10	1.17	1.15	1.17	1.13	1.51	1.10
3. Hardness (Shore D) (Note 4)	10	83	75	55	45	70	55
4. Thermal Conductivity (Cal. cm/sec.cm ² °C) (Note 4)	6.2×10^{-4}	5.9×10^{-4}	4.8×10^{-4}	5.9×10^{-4}	4.8×10^{-4}	9.7×10^{-4}	5.5×10^{-4}
5. Degradation Temperature (°C) (Note 5)	Starts around 250	Starts around 280	Around 225	250 to 300	275 to 300	Around 250	250 to 300
6. Glass Transition Temperature (°C) (Note 5)	15	Near 150	50	40	25	Near 35	35 to 40
7. Coefficient of Thermal Expansion (in/in/°C) (Note 6)	4.33×10^{-6} (15 to 70°C)	172×10^{-6} (150 to 250°C)	204×10^{-6} (75 to 225°C)	249×10^{-6} (50 to 250°C)	246×10^{-6} (25 to 100°C)	172×10^{-6} (55 to 70°C)	246×10^{-6} (50 to 250°C)
8. Moisture Absorption (%) (Note 6)	0.40	0.17	0.27	0.31	0.33	0.12	0.15
9. Shrinkage (%) (Note 7)	1.73	0.37	2.87	0.07	(Note 9)	0.37	1.87
10. Dielectric Constant (Note 8)	3.99	3.98	(Note 10)	3.84	(Note 9)	3.26	3.24
11. Dissipation Factor (Note 8)	0.083	0.011	(Note 10)	0.05	(Note 9)	0.017	0.037
12. Volume Resistivity (Ohm, cm) (Note 8)	1.6×10^{15}	6×10^{15}	(Note 10)	1×10^{15}	(Note 9)	1.3×10^{15}	8×10^{15}

NOTES: 1. Curing of the test materials was performed by Electromagnetic Group

2. Per FED, STD. 406-501
3. Per FED, STD. 406-1083
4. Using Colora Thermoconductometer
5. Using DuPont Thermal Analyzer
6. Per ASTM D570: Modified
7. Per ASTM D570: Modified
8. Refer to report for method and technique
9. Resin material not available at this time
10. Test material did not lend itself to testing (see report)

2. The Epon 825, Hysol C15-015 Scotchcast 255 and Scotchcast 280 test samples' hardness varied from zero to five Shore (D) hardness points from the manufacturer's data. The Hysol C-60 samples' hardness varied fifteen points from the manufacturer's data. The initial hardness values for the hydrolytic stability samples, discussed later, were the same as that found in Table III. The difference between the value shown in Table III and the manufacturer's value may be due to processing problems, but the consistency of the in-house results suggests either material or systematic process variation. In the case of the Eccoseal 1218 test sample hardness discrepancy, the difference appears to be due to a processing error rather than to the material or process. The hydrolytic stability samples for this material cured to an initial hardness of 51 to 52 Shore(D).
3. Eccoseal 1218, Epon 825, Hysol C15-015, Hysol C-60, and Scotchcast 280 test materials showed thermal conductivity values close to the manufacturer's data; Scotchcast 255 test material had a much higher thermal conductivity (9.7×10^{-4} cal cm/sec cm² °C) compared to the manufacturer's specified value (4.5×10^{-4} cal cm/sec cm² °C). The manufacturer of this latter material is possibly using conservative data.
4. All test materials appeared to decompose very readily at approximately 350°C. Starting decomposition temperatures of the test materials are shown in Table III.
5. The glass transition temperature (T_g) of these materials varied from -15°C for Eccoseal 1218 to 250°C for the Epon 825/HV system. The rest of the materials had a T_g between 20°C and 50°C.
6. The Coefficient of Thermal Expansion (CTE) at temperatures lower than the T_g for all the test materials are shown below:

• Eccoseal 1218	89×10^{-6} cm/cm/°C (-175 to -25°C)
• Epon 825/HV	65×10^{-6} cm/cm/°C (+25 to +125°C)
• GE 702	69×10^{-6} cm/cm/°C (-150 to 0°C)
• GE 707	69×10^{-6} cm/cm/°C (-125 to +50°C)
• Hysol C15-015	159×10^{-6} cm/cm/°C (0 to +25°C)
• Hysol C60	91×10^{-6} cm/cm/°C (-125 to +25°C)
• Scotchcast 255	54×10^{-6} cm/cm/°C (-125 to +25°C)
• Scotchcast 280	—
7. All test materials absorbed less than 0.4 percent moisture by weight.
8. The shrinkage during cure was from 0.07 to 2.89 percent.

9. The electrode arrangement used for dielectric constant, dissipation factor, and volume resistivity measurements was a standard air dielectric variable capacitor with its plates fully meshed. Use of these electrode configurations offered several advantages: test specimens are easily produced, the encapsulation is more representative of the end use, the sample is not altered by fabrication to size or electrode processing steps, errors produced in measurement of sample geometry are eliminated, and calculation of dielectric constant is greatly simplified.
10. The dielectric constant was obtained as the ratio of the capacitance after encapsulation to the capacitance before encapsulation. The dissipation factor reported is that associated with the encapsulated capacitance.
11. Using the same sample as was used for the dielectric constant and dissipation factor, the volume resistivity was determined. A volume resistance was measured with a General Radio 1230A DC amplifier and an electrometer. From the capacitance and dielectric constant, an effective electrode geometry term was calculated. The product of the volume resistance and the effective electrode geometry term gave the volume resistivity.

The electrical testing techniques used were not successful with GE 702 and GE 707 resins. These resin systems, which are designed for dip coating applications, produced such an exotherm when cured in the bulk (300 ml) required by the test apparatus that, on cooling, the material cracked severely and meaningful electrical measurements could not be made. Hysol C60 was not available for this portion of the testing program.

The electrical measurements reflect the physical state of the resin system at the time of test under a specific environment. The material's prior history, temperature, test frequency, and many other factors, have an effect on measurements of this type. When the electrical measurements were made here, these factors were known; however, the particular conditions existing during the manufacturer's tests were not known. Variances caused by sample processing, molecular polarizability and test conditions are probable causes for the differences between the manufacturer's data and Table III. In an attempt to resolve the discrepancies, measurements of dielectric strength by ASTM D-149, dielectric constant, and dissipation factor by ASTM D-150, and volume resistivity by ASTM D-257 were performed, and the results tabulated in Table IV for comparison. The two inch diameter, 0.1 thick disc samples were prepared using the manufacturer's instructions or the applicable Hughes Process Specification.

TABLE IV. COMPARISON OF ELECTRICAL PARAMETERS

	Dielectric Strength volt/mil			Dielectric Constant			Dissipation Factor			Volume Resistivity ohm-cm		
	Vendor	1st Test	ASTM D-149	Vendor	1st Test Note 3	ASTM D-150 Note 3	Vendor	1st Test Note 3	ASTM D-150 Note 3	Vendor	1st Test	ASTM D-257
Epon 825	400-500	Note 1	530	3.81 @ 1 KHz	3.98	4.0	0.004 @ 1 KHz	0.011	0.008	3×10^{12}	6×10^{15}	4.3×10^{13}
Hysol C-60	350	Note 1	486	4.0 @ 100 Hz	Note 2	4.4	0.038 @ 100 Hz	Note 2	0.04	7×10^{14}	Note 2	3.9×10^{13}
Hysol C15-015	350	Note 1	496	3.8 @ 100 Hz	3.84	4.1	0.03 @ 100 Hz	0.05	0.054	3×10^{17}	1×10^{15}	3.5×10^{13}
Scotchcast 255	375	Note 1	495	5.9 @ 100 Hz	3.26	3.9	0.05 @ 100 Hz	0.17	0.37	10^{15}	1.3×10^{15}	4×10^{13}
Eccoseal 1218	ND	Note 1	515	3.7 @ 60 Hz	3.99	3.4	0.025 @ 60 Hz	0.083	0.27	10^{15}	1.6×10^{15}	4.9×10^{13}

Note 1: Dielectric strength data not done in 1st test.

Note 2: Material not available in time for test.

Note 3: Dielectric constant and dissipation factor measured at 1 KHz.

A comparison of the vendor's data, first test results and ASTM test results show the following:

1. The dielectric strength vendor data is from 24 to 29 percent lower than the ASTM D-149 values. The difference is probably due to the use of conservative figures by the manufacturers.
2. The locally performed dielectric constant determinations were carried out at 1 KHz while the vendor data was carried out with one exception at either 60 Hz or 100 Hz. This difference in frequency can easily account for a 10% change in dielectric constant. The difference between the vendor data and both sets of locally prepared test data, with the exception of the Scotchcast 255 data, is less than 10%. The Scotchcast 255 vendor data shows a dielectric constant of 5.9 at 100 Hz; the in house data shows the value of 3.9 at 1 KHz.
3. In the dissipation factor data, the percentage differences among the vendor's data, first test and ASTM D-150 data was very large. The probable reason is that the numbers are very small, and small differences in value lead to large percentage changes.
4. In the volume resistivity tests, it would appear that the ASTM D-257 sample holder had surface leakage resistivity which bypassed the sample under test, giving the 10^{13} ohm-cm readings.

After the testing and evaluation of physical parameters was completed, five materials were selected for further study, based on the preferred properties given in Table I. Those materials selected were Hysol C-60, Hysol C15-015, Epon 825/HV, Scotchcast 255 and Eccoseal 1218.

ELECTRICAL AND ENVIRONMENTAL TESTING OF HI-REL CANDIDATE MATERIALS

The electrical and environmental testing of candidate materials and processes seek to determine how well these compounds meet end product and manufacturability requirements. The ideal material was considered at

the beginning as a material that degassed quickly, had a viscosity below 1000 centipoise (cps) at the pouring temperature, had a low surface tension, and cured thoroughly at a relatively low temperature. It also should enable a designer to meet the electrical, material, and environmental end product criteria found in MIL-T-27D, MIL-I-16923G and MIL-S-23586, as appropriate. In the present case, the material must be reliable under extremes of humidity, temperature, vacuum, electric field, and mechanical abuse. This section shows the results of a series of electrical, mechanical and environmental tests. Some of the tests were of short duration, such as resistance to soldering heat. Others were, by nature, of long duration, the most extreme example being the hydrolytic stability tests. Many of the tests described in this paper were conducted in parallel with other tests. For this reason materials eliminated by one test's results are still reported in other subsequently described tests.

Thirteen tests were done using the reactors shown in Figure 1:

1. Hydrolytic stability of electrical parameters.
2. Excess material removal.
3. Visual before and after thermal cycling.
4. Resistance to soldering heat.
5. Corrosion susceptibility before and after temperature cycling.
6. Dielectric strength before and after temperature cycling.
7. Leakage inductance before and after temperature cycling.
8. Inductance, with and without DC bias, before and after temperature cycling.
9. DC resistance before and after temperature cycling.
10. Temperature cycling, +10 cycles, -55°C to 130°C .
11. Adhesion of material to part after temperature cycling.
12. Mechanical shock.
13. Cross section of part to determine extent of voids.

The hydrolytic stability tests were divided into two parts: hydrolytic stability of the high reliability and low stress materials, and electrical parameter testing of the saturable reactor coils undergoing hydrolytic



Figure 1. Saturable reactor used for electrical tests.

stability testing. In both cases, the samples were maintained at an ambient temperature of 71°C and 95 percent relative humidity.

Samples two inches in diameter and about 1/2 inch thick were prepared for the first hydrolytic stability test. The hardness of each sample was measured at the start of the 120-day period, and repeated at various intervals. Two samples of each material were maintained in the humidity chamber and two samples were retained as controls. The results are shown in Table V. The second test utilized saturable reactors as electrical test vehicles. The inductance, leakage inductance, self-resonant frequency, turns ratio and DC resistance were measured at the start, at 30 days, and at 60 days. The results are shown in Table VI.

In the hydrolytic stability tests the following was noted: Hysol C-60 and Eccoseal 1218 reverted to the liquid form. One material, GE 702, had a 33 point hardness reduction, a significant change. No infrared study to detect precursors was performed because this material had been eliminated previously. Only the self-resonant frequency (f_r) of the reactor varied in the parts embedded with material that reverted. Pouring off the liquified compound did not bring the f_r to its previous value due to the surface tension and adhesion of the liquids to the wire. These tests removed Hysol C60 and Eccoseal 1218 from further consideration.

TABLE V. HYDROLYTIC STABILITY OF MATERIALS-TEST RESULTS

Trade Name	GP-7	GF-7	S. of GP-7	S. of GF-7	Specimen Serial Number	RTV-15	RTV-27	Conap EN-9	Conap EN-9-02R		
	1	2	1	2	1	2	1	2	1	2	
75°C, 60% R.H.	Hardness after 6 days exposure	75	75	70	75	35	63	35	35	35	
	Hardness after 24 days exposure	75	80	75	80	35	63	40	35	40	
	Hardness after 50 days exposure	7	77	75	77	37	64	40	35	40	
	Hardness after 84 days exposure	7	75	80	80	35	65	40	35	40	
	Hardness after 120 days exposure	7	75	80	75	40	67	40	35	40	
71°C, 45% R.H.	Specimen Serial Number	3	4	3	4	3	4	3	4	3	4
	Hardness after 6 days exposure	75	75	70	75	37	65	35	35	35	35
	Hardness after 24 days exposure	80	80	65	70	40	63	35	35	34	35
	Hardness after 50 days exposure	80	80	65	70	45	64	35	37	32	31
	Hardness after 84 days exposure	80	80	65	70	47	65	35	35	30	31
Hardness after 120 days exposure	80	80	65	68	47	70	35	35	30	31	

Comments: All initial hardness readings except Uranine 5753 and Conap EN-9 taken 2-15-79.
Part of reversion after 10 days.

(Continued next page)

(Table V, concluded)

Trade Name		Conap EN-11		Epon 825 w/11400		Epon 825 w/T403		Eccoseal 1218		Hysol C60		Hysol C15		Epon 825 w/H.V.		Uralane 5753	
Shore Gauge		"A"		"D"		"D"		"A"		"D"		"D"		"D"		"A"	
Specimen Serial Number		1	2	1	2	1	2	1	2	1	2	1	2	1	2	1	2
Hardness after 0 days exposure		65	63	73	72	65	65	51	52	40	42	55	55	82	80	51	50
Hardness after 28 days exposure		62	62	78	78	80	75	51	53	41	42	60	60	85	80	61	65
Hardness after 56 days exposure		70	70	76	75	75	77	55	55	40	40	57	59	82	81	65	69
Hardness after 84 days exposure		65	67	77	75	75	76	55	55	42	41	58	59	82	83	70	68
Hardness after 120 days exposure		75	75	77	73	75	76					60	60	85	82	75	75
Specimen Serial Number		3	4	3	4	3	4	3	4	3	4	3	4	3	4	3	4
Hardness after 0 days exposure		63	62	75	75	74	70	52	52	40	40	52	53	83	82	50	50
Hardness after 28 days exposure		60	60	70	75	80	80	33	35	32	32	53	55	83	83	67	67
Hardness after 56 days exposure		65	64	75	74	80	80	Reverted		12	13	55	55	81	82	66	66
Hardness after 84 days exposure		60	62	72	73	80	80	—		Reverted		52	54	85	83	65	66
Hardness after 120 days exposure		65	65	72	75	80	80					50	52	83	84	72	72

Comments: All initial hardness readings except Uralane 5753 and Conap EN-9 taken 2-15-79.

* Partial reversion after 60 days.

TABLE VI. HYDROLYTIC STABILITY OF ENCAPSULATED TRANSFORMERS

	Inductance ¹ , μH		Leakage Inductance ² , μH	Self Resonant Frequency ³ , MHz	Ratio	D.C. Resistance, ohms	
	w/20 ADC	w/o ADC				1-2	3-4
EPON/825 w/HV Days							
0	189	207	0.5	38.0 ⁴	0.99774	0.00736	0.0297
30	184	208	0.5	27.4	0.99664	0.00721	0.0290
60	185	211	0.55	26.2	0.99975	0.0083	0.029
Scotchcast 255 Days							
0	187	214	0.58	38.0 ⁴	0.99661	0.00720	0.0287
30	178	203	0.45	27.0	0.99670	0.00713	0.0284
60	180	206	0.55	26.2	0.99890	0.0075	0.028
Eccoseal 1218 Days							
0	188	214	0.53	38.0 ⁴	0.99821	0.00729	0.02920
30	182	207	0.40	29.1	0.99724	0.00713	0.0285
60	182	208	0.55	26.8	0.99955	0.0075	0.029
Hysol C-60 Days							
0	187	216	0.75	33.8 ⁴	0.99697	0.00755	0.02930
30	180	209	0.65	24.2	0.99574	0.00711	0.0286
60	182	212	0.75	22.8	0.99865	0.0074	0.029
Hysol C15-015 Days							
0	190	216	0.60	38.0 ⁴	0.99784	0.00737	0.02942
30	183	212	0.50	28.6	0.99644	0.00719	0.0285
60	185	216	0.62	26.4	0.99865	0.0074	0.029

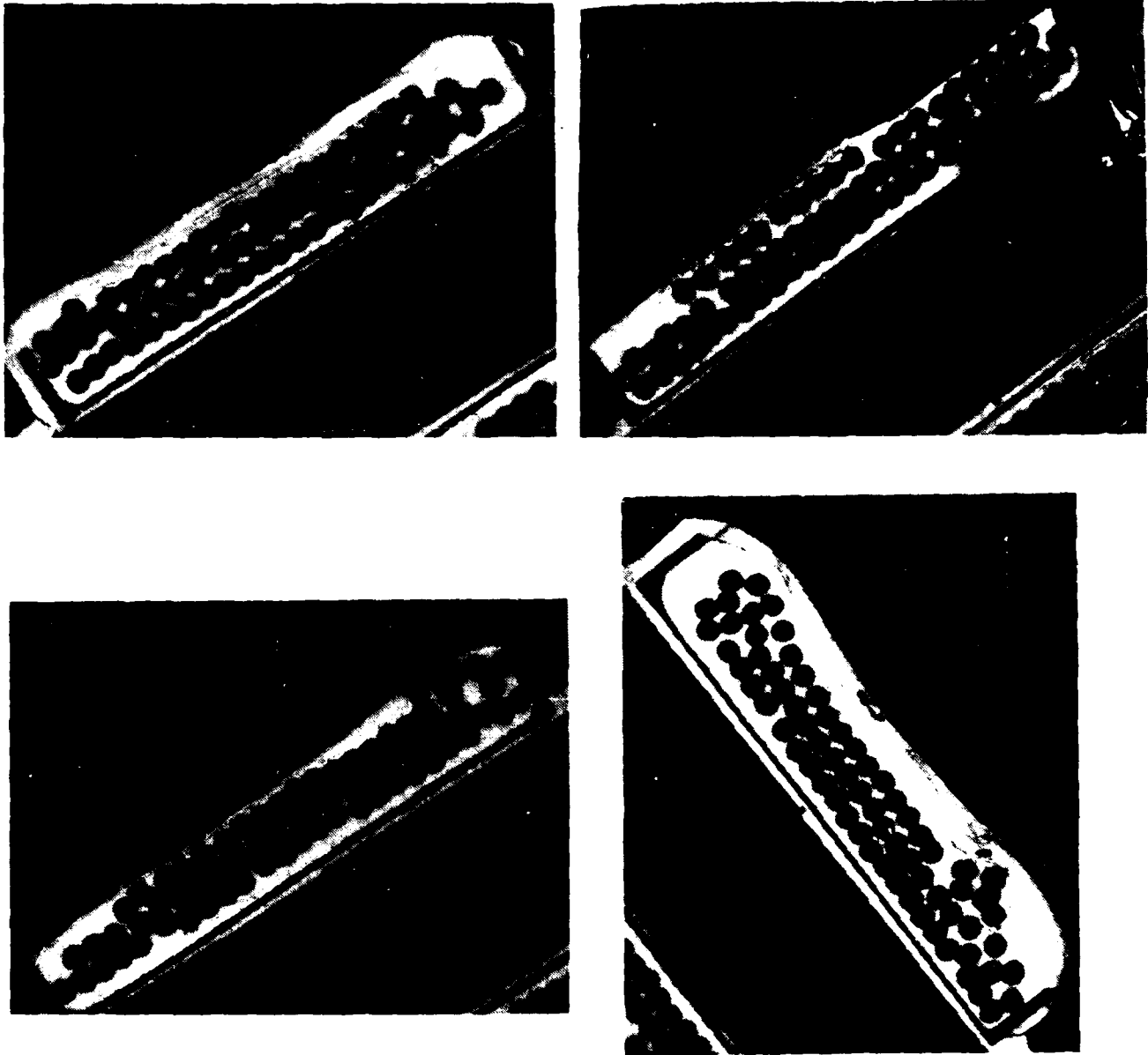
¹ 17 Vrms, 20 kHz, with and without 20 ADC measured across 1-2.² Measured across 3-4 with 1-2 shorted.³ Self resonant frequency with 1-2 shorted.⁴ Self resonant frequency before encapsulation.

Tests of excess material removal, resistance to soldering heat, corrosion susceptibility, adhesion of the material to the parts after corrosion susceptibility, adhesion of the material to the parts after temperature cycling, mechanical shock, and the electrical parameters were made on the reactors in accordance with MIL-T-27. The results of these tests did not differentiate clearly among the materials.

The cross-section of a thermally cycled saturable reactor provided two checks of the resin system: the capability of the resin to provide a void-free encapsulation, and resistance to cracking from thermal shock. The reactors which had been encapsulated with each material were electrically tested and found to meet the design criteria. The parts were then temperature cycled ten times from -55°C to $+125^{\circ}\text{C}$. A second electrical test of the reactors showed that no significant changes occurred during temperature cycling. The parts were then cross-sectioned, polished, and photographed. The longitudinal sections are shown in Figures 2 through 6. The Epon 825, Scotchcast 255 and Eccoseal 1218 embedded parts showed no cracks or voids. The part potted with Hysol C15-015 showed extensive cracking, most probably due to the high coefficient of thermal expansion. The Hysol C60 embedded part shows extensive cracking as well as numerous voids due to the high coefficient of expansion and insufficient degassing. The cross section results removed Hysol C15-015 from consideration.

HIGH VOLTAGE TRANSFORMER MODEL TESTING

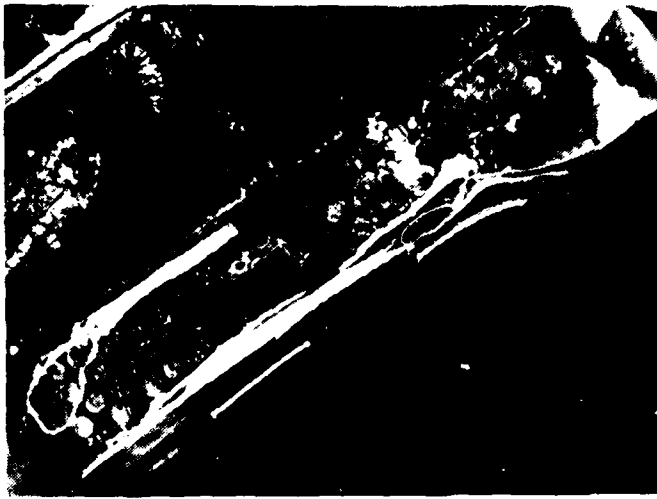
A typical high voltage TWT saturable core transformer design, Figure 7, was used as a test component for the five selected encapsulation materials. Each material was used to encapsulate two parts, so that a material might not be eliminated due to a simple construction error or other nonmaterial related problem. The test criteria included: excitation current, core loss, DC resistance of the windings, dielectric strength, insulation resistance, volt-second support, interwinding insulation, intrawinding insulation and environmental seal. These tests cover the major magnetic and electric characteristics of the transformer.



Magnification: 2.5x

Comments: No voids or cracks
evident

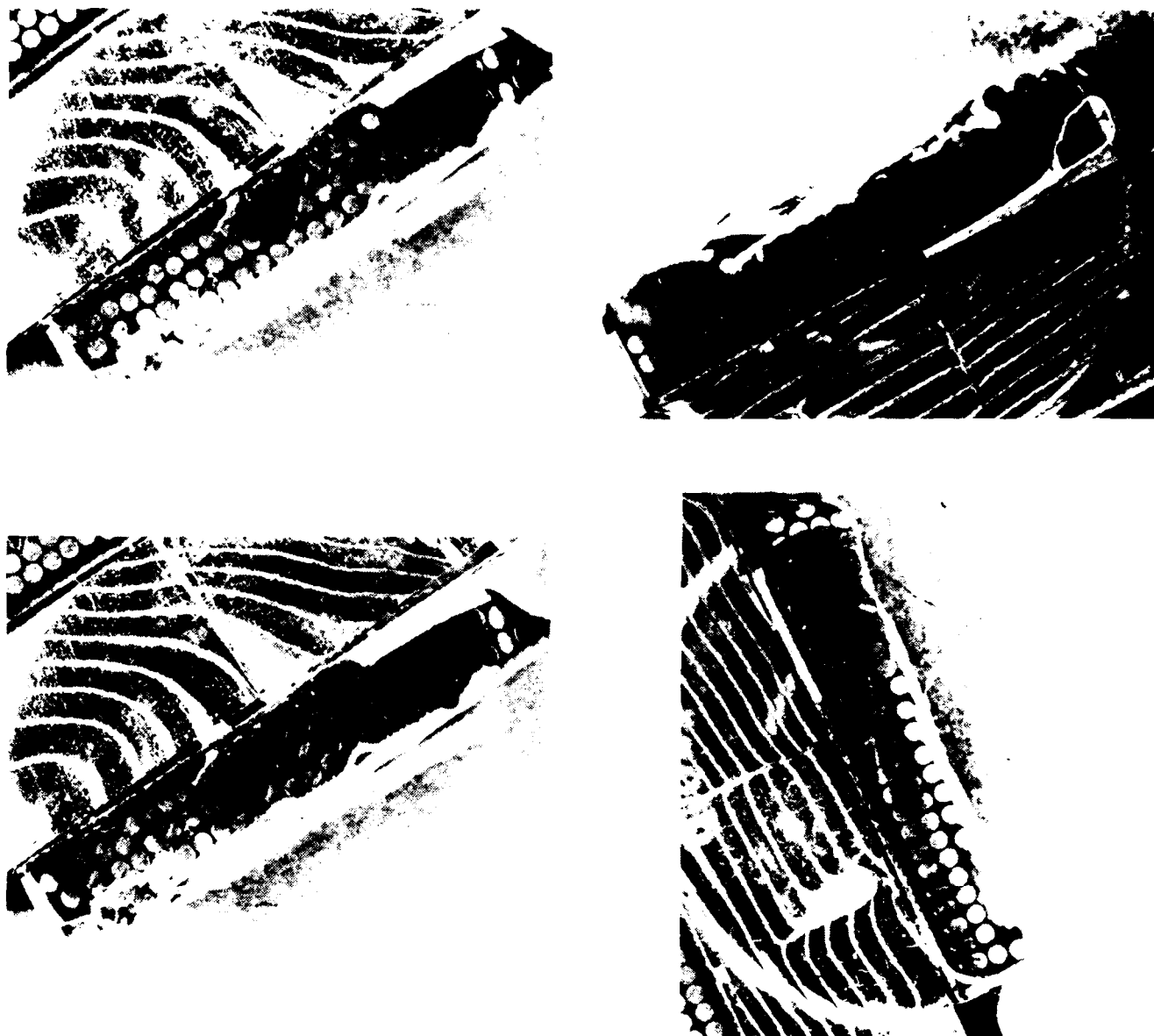
Figure 2. Longitudinal cross sections of part potted with Scotchcast 255.



Magnification: 2.5x

Comments: No voids or cracks
evident

Figure 3. Longitudinal cross sections of part potted with Eccoseal 1218.



Magnification: 2.5x

Comments: No voids or cracks
evident

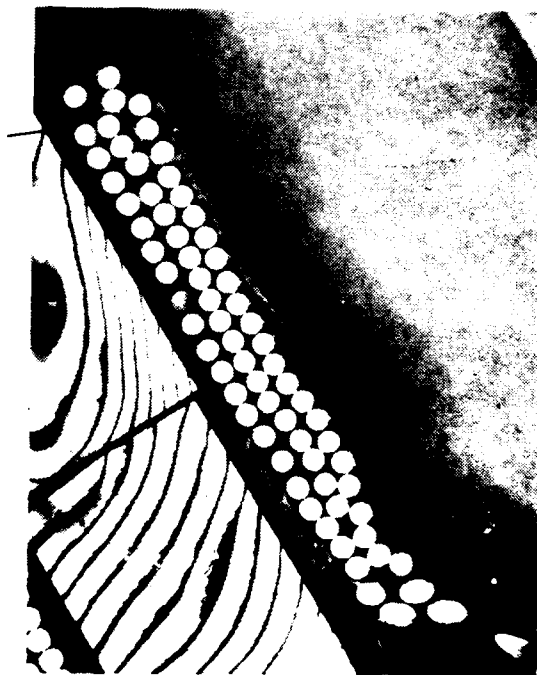
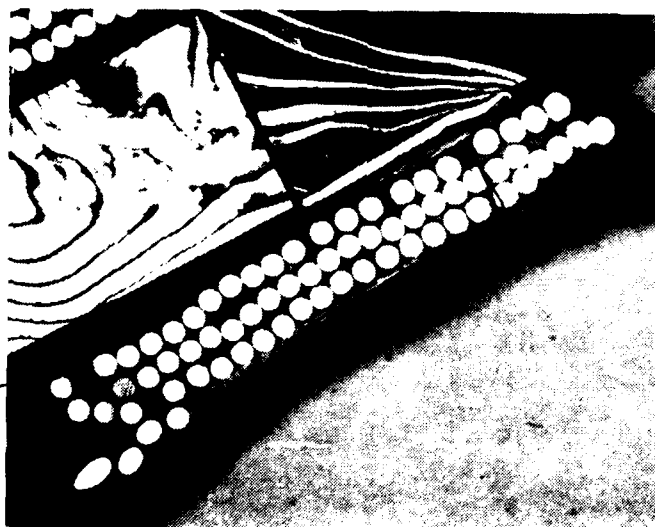
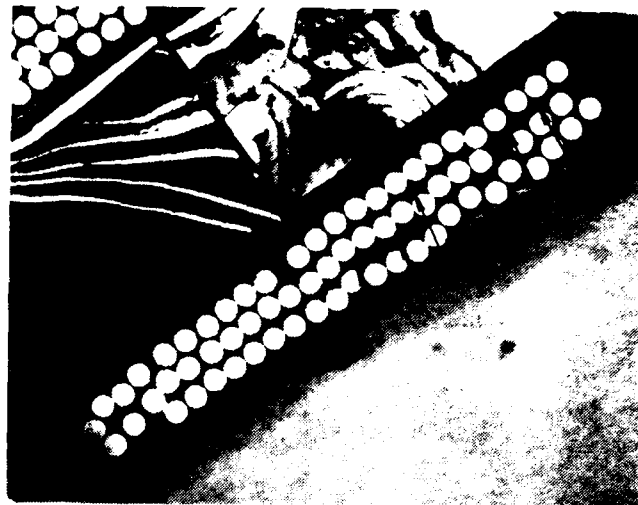
Figure 4. Longitudinal cross sections of part potted with Epon 825.

AD-A098 167 HUGHES AIRCRAFT CO CULVER CITY CA ELECTRO-OPTICAL AN--ETC F/G 9/5
MANUFACTURING METHOOS AND TECHNOLOGY FOR ELECTROMAGNETIC COMPON--ETC(U)
DEC 80 E R BUNKER, J R ARNETT, J L WILLIAMS DAAK40-78-C-0271
UNCLASSIFIED FR-80-76-1254R-VOL-1 NL

Δ Δ



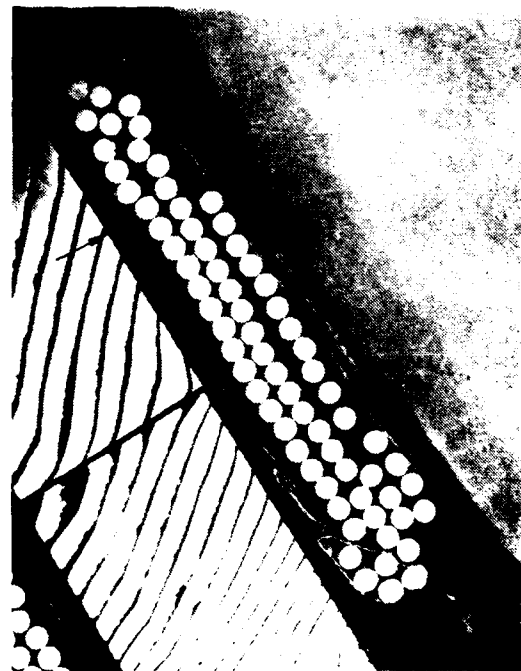
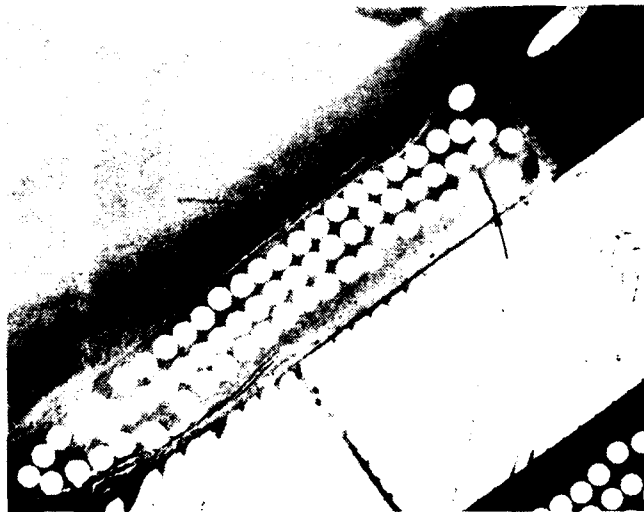
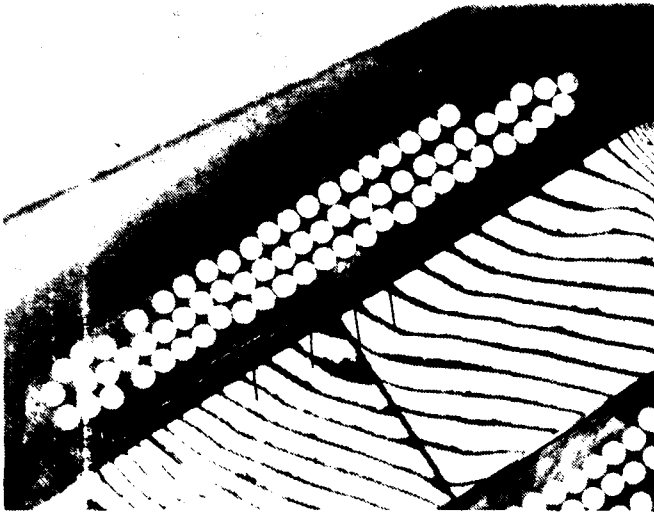
END
DATE
FILMED
3-81
DTIC



Magnification: 2.5x

Comments: Note cracks and voids
in cross sections

Figure 5. Longitudinal cross sections of part potted with Hysol C-60.



Magnification: 2.5x

Comments: No voids in cross section. There is extensive cracking

Figure 6. Longitudinal cross sections of part potted with Hysol C15-015.



Figure 7. TWT high voltage transformer.

The data from these tests are shown in Table VII. The resin viscosity at the pour temperature of the materials used to prepare the parts ranged between 75 and 1500 cps, and it made no difference in the high voltage tests. Some parts that passed the dielectric strength and insulation resistance tests had a high level of corona. Those materials that had no corona also passed the dielectric strength and insulation resistance tests. The inference is that the corona tests should not be eliminated because they can detect incipient problems that the dielectric strength or insulation resistance tests cannot reveal. The corona test of the Hysol C15-015 and Hysol C60 embedded parts detected incipient breakdowns after the parts had passed the dielectric strength and insulation resistance tests.

A further test, an interwinding insulation test, was performed on the transformer at 3300 volts AC at 60 Hz between (7-8) and the other pins. The results of this test are shown below in Table VIII. Only the one good part of each material was available for test. The notable result in Table VIII is that the Epon 825 impregnated part, even at four times the design voltage, had no corona. The Scotchcast 255 and Eccoseal 1218 encapsulated parts definitely showed large quantities of corona.

TABLE VII. HIGH VOLTAGE TRANSFORMER TEST RESULTS

Material Part No.	Excitation Current 5120mA	Core Loss 500W	D. C. Winding Resistance					300 Vrms 60 Hz (1-3) to all Others No Breakdown	300 Vrms 60 Hz (4-6) to all Others No Breakdown	Dielectric Strength 3300 Vrms 60 Hz (7-8) to all Others No Breakdown	2203 Vrms 60 Hz (9-10) to all Others No Breakdown	850 Vrms 60 Hz (11-14) to all Others No Breakdown
			1-3 0.80	4-6 0.30	7-8 25.22	9-10 40.22	11-14 51.12					
Epon 825/HV 1	84mA	27mW	0.450	0.283	223.4	318.30	93.80	OK	OK	OK	OK	OK
Epon 825/HV 2	89	27.1	0.450	0.271	228.0	323.0	95.9	OK	OK	Breakdown 500V	OK	Breakdown
Eccoseal 1218 3	79.8	29	0.641	0.274	220.0	310.2	92.3	OK	OK	OK	OK	OK
Eccoseal 1218 4	81.1	30	0.638	0.265	223.3	312.4	92.1	OK	OK	OK	OK	OK
Hysol C15-015 5	79.9	29	0.647	0.275	223.4	312.4	91.4	OK	OK	OK	OK	OK
Hysol C15-015 6	94.6	31	0.647	0.289	216.4	306.4	92.0	OK	OK	OK	OK	OK
Scotchcast 255 7	47.9	25	0.650	0.279	224.4	302.0	93.3	OK	OK	Breakdown	OK	Breakdown
Scotchcast 255 8	56.0	25	0.647	0.265	221.8	306.8	91.3	OK	OK	OK	OK	OK
Hysol C-60 9	81.9	25	0.642	0.281	226.2	310.8	93.4	OK	OK	OK	OK	OK
Hysol C-60 10	80.0	28	0.644	0.284	223.0	306.1	22.0	OK	OK	OK	OK	OK

(Continued next page)

6-87

Notes: 1. Voltage second support 2. 16 VRMS 800 Hz applied to (1-2)
3. Intrawinding insulation 2), 0 VRMS 1) KHz applied to (1-2)
4. Interwinding insulation: (8-7) to (all others) 1700 VRMS 60 Hz
(2-10) to (all others) 900 VRMS 60 Hz

2. Intrawinding insulation 2). 0 VRMS 11 KHz applied to (1-2)

Interwinding insulation: (8+7) to (all others) 1700 VRMS @ 1 Hz
(2-10) to (all others) 900 VRMS @ 60 Hz

TABLE VIII. INTERWINDING INSULATION TEST

Material	Interwinding Insulation (3300V AC at 60 Hz)				
	2.5 pC Pulse Count	5 pC Pulse Count	10 pC Pulse Count	25 pC Pulse Count	50 pC Pulse Count
Epon 825/HV	0	0	0	0	0
Scotchcast 255	9249	4826	6283	149	4024
Eccoseal 1218	19609	11933	14732	583	9824

CONCLUSION

Among the materials surveyed for use as a high reliability embedding compound, no one material was the best choice under all circumstances. The strengths and weaknesses of each material for each use needs to be considered in a logical systematic manner. Among the materials considered and subsequently tested, Scotchcast 255 is the best material for high reliability, low to medium voltage applications, and Epon 825/HV is the best material for high reliability, high voltage applications.

ACKNOWLEDGMENT

I wish to express appreciation to *Earle R. Bunker* for his suggestions, technical discussions and review of this paper.

This work was supported in part by U. S. Army Missile Command under Contract DAAK 40-78-C-0271.

APPENDIX

<u>Material</u>	<u>Manufacturer</u>
Eccoseal 63, W-67 1207, 1218 Stycast 62	Emerson & Cumming, Inc. Dielectric Materials Division Canton, Mass. 02021
Conathane: EN-2, EN-9(OZR) EN-9, EN-10, EN-11 Conepoxy: Y 1000/07, IM 1145 RN 1600	Conap Incorporated 1405 Buffalo St. Olean, New York 14760
RTV: 11/DBT, 60/DBT 8111, 615, 619, 627 655, 670	Silicone Products Department General Electric Company Waterford, New York 12188
GE: 702, 707	Insulating Materials Department General Electric Company One Campbell Road Schenectady, New York 91749
Scotchcast: 235, 255 280, 281 5237	3 M Company Industrial Electrical Products Division 3 M Center Saint Paul, MN 55101
D 230, D 400, T 403	Jefferson Chemical Company P. O. Box 430 Bellaire, Texas 77401
Hysol C 15-015 C 60 HD 3561	Hysol Division The Dexter Corporation 15051 E. Don Julian Road Industry, CA 91749
Epocast: 202, 204A/9816 204A/9652 Uralane 5753	M & T Chemicals, Incorporated Furane Products Division 5121 San Fernando Road West Los Angeles, CA 90039
Epon 825/HV RFC825	E. V. Roberts & Associates Division EVRA Incorporated P. O. Box 868 Culver City, CA 90230